



# LUND UNIVERSITY

## Microbial Electrochemical System: extracellular electron transfer from photosynthesis and respiration to electrode

Hasan, Kamrul

2016

[Link to publication](#)

*Citation for published version (APA):*

Hasan, K. (2016). *Microbial Electrochemical System: extracellular electron transfer from photosynthesis and respiration to electrode*. Department of Chemistry, Lund University.

*Total number of authors:*

1

### General rights

Unless other specific re-use rights are stated the following general rights apply:

Copyright and moral rights for the publications made accessible in the public portal are retained by the authors and/or other copyright owners and it is a condition of accessing publications that users recognise and abide by the legal requirements associated with these rights.

- Users may download and print one copy of any publication from the public portal for the purpose of private study or research.
- You may not further distribute the material or use it for any profit-making activity or commercial gain
- You may freely distribute the URL identifying the publication in the public portal

Read more about Creative commons licenses: <https://creativecommons.org/licenses/>

### Take down policy

If you believe that this document breaches copyright please contact us providing details, and we will remove access to the work immediately and investigate your claim.

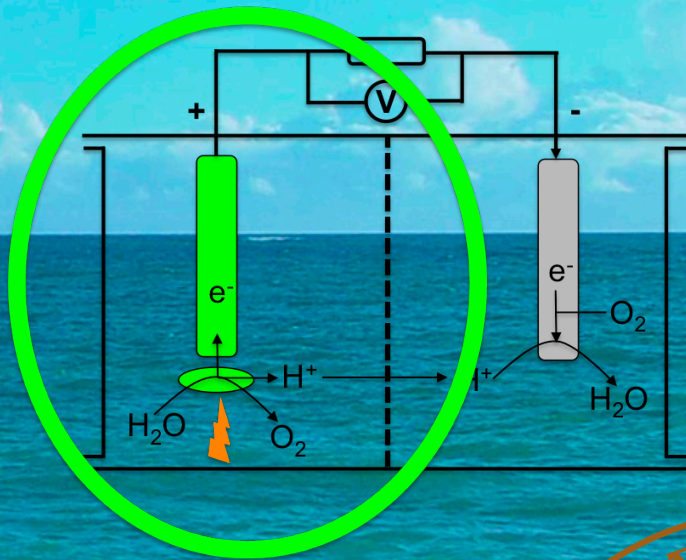
LUND UNIVERSITY

PO Box 117  
221 00 Lund  
+46 46-222 00 00

# Microbial Electrochemical System

Extracellular electron transfer from photosynthesis and respiration to electrode

KAMRUL HASAN | BIOCHEMISTRY AND STRUCTURAL BIOLOGY | LUND UNIVERSITY





# Microbial Electrochemical System

Extracellular electron from photosynthesis and  
respiration to electrode

Kamrul Hasan



**LUND**  
UNIVERSITY

DOCTORAL DISSERTATION

by due permission of the Faculty of Science, Lund University, Sweden.  
To be defended at Chemical center, Lecture hall: A, Naturvetarvägen 14, Lund

Date: 26<sup>th</sup> February 2016, Friday, at 09:15 A.M.

*Faculty opponent*

Professor Christopher Howe  
Department of Biochemistry, University of Cambridge, United Kingdom

The cover picture depicts the abundance of the resources, e.g., solar energy and water, required in photosynthetic energy conversion and a schematic diagram of a biological photovoltaic cell. The background picture is reprinted with permission from [www.zinnovate.se](http://www.zinnovate.se).

**Supervisor:** Professor Lo Gorton  
Lund University, Sweden

**Co-supervisor:** Professor Cecilia Hägerhäll  
Lund University, Sweden

**Examination Committee:** Professor Jenny Emnéus  
Technical University of Denmark, Denmark

Professor Sergey Shleev  
Malmö University, Sweden

Dr. Nikolaos Xafenias  
Chalmers University of Technology, Sweden

Dr. Ed van Niel  
Lund University, Sweden

Cover design by: Kamrul Hasan

Copyright 2016 by Kamrul Hasan. All rights reserved.  
Faculty of Science | Department of Chemistry | Lund University

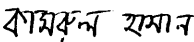
ISBN: 978-91-7422-428-3

Printed in Sweden by Media-Tryck, Lund University  
Lund 2016



Organization Department of Analytical Chemistry /Biochemistry and Structural Biology Lund University P.O. Box 124, SE-22100, Lund, Sweden  Author: Kamrul Hasan	Document name: Doctoral Dissertation	
	Date of issue: 26 <sup>th</sup> February 2016	
	Sponsoring organization: The Swedish Research Council (Project. Nos. 2010-2013, 2010-5031 and 2014-5908)	
Title and subtitle: Microbial Electrochemical System: extracellular electron transfer from photosynthesis and respiration to electrode		
<b>Abstract</b> <p>The electrochemical communication between microorganisms and electrodes has substantial implications both for basic understanding of biological electron transfer as well as in diverse applications, such as, microbial electrochemical system (MES), microbial biosensors and in production of valuable chemicals. In these systems the extracellular electron transfer (EET) from microbial metabolism to electrodes is restricted due to the insulated cellular exterior made of lipid structures. To obtain the electrochemical wiring of biomaterials with electrodes, osmium redox polymers (ORPs) was used as an efficient electron transfer (ET) mediator.</p> <p>In this thesis a systematic study on EET from a variety of biomaterials is demonstrated. The EET from the most metabolically versatile purple bacterium, i.e., <i>Rhodobacter capsulatus</i>, grown under both heterotrophically and photoheterotrophically conditions was studied. <i>Shewanella oneidensis</i> MR-1 is a metal ion reducing bacterium and was highly studied in microbial electrochemical systems (MES) due to its direct ET competence. We have shown that <i>S. oneidensis</i> MR-1 can be coupled with ORP modified graphite electrodes that results in an enhanced current density.</p> <p>A secured supply of cost effective sustainable energy is on of the greatest challenges in the 21<sup>st</sup> century. Biological photovoltaics (BPVs) is emerging as a potential energy generating technology to convert solar energy into electrical energy. To harness solar energy we studied the photo-excited EET from water oxidation via thylakoid membranes, the site of photosynthesis in green plants and algae. In addition three prokaryotic cyanobacteria, two different <i>Leptolyngbya</i> sp., and <i>Chroococcales</i> sp. were photo-electrochemically wired with electrodes. The photo-electrochemical communication of a multicellular eukaryotic alga was assumed to be challenging, since here photosynthesis occurs in a specially designed subcellular organelle called chloroplast. We have shown the photoelectrochemical communication of the eukaryotic alga, <i>Paulschulzia pseudovolvox</i> immobilized on a graphite electrode wired with ORPs.</p> <p>Although a great deal of research is focussed on MES, however, to seek any potential practical application their performance due the low power output and restricted stability need to be improved many folds. Our findings could have substantial implications in MES, such as microbial fuel cells (MFC), microbial biosensors, photosynthetic energy generation and in other light sensitive bioelectrochemical devices.</p>		
Key words: Biological photovoltaics, electron transfer, electrode, <i>Rhodobacter capsulatus</i> , thylakoid membranes, cyanobacteria, algae, photosynthesis, light, photocurrent, electrochemistry		
Classification system and/or index terms (if any)		
Supplementary bibliographical information		Language: English
ISSN and key title		ISBN: 978-91-7422-428-3
Recipient's notes		Number of pages: 204  Price
Security classification		

I, the undersigned, being the copyright owner of the abstract of the above-mentioned dissertation, hereby grant to all reference sources permission to publish and disseminate the abstract of the above-mentioned dissertation.

Signature 

Date 2016-01-20



*Dedicated to my beloved parents: Mobarak Hossain and Khodeja*





# Contents

Popular scientific summary	9
List of publications	10
My contributions to the publications	12
List of abbreviations	15
<b>1. General perspective of the thesis</b>	<b>17</b>
<b>2. Electron transfer (ET) mechanisms</b>	<b>19</b>
2.1. Marcus theory	20
2.2. ET in biological systems	21
2.3. Direct electron transfer (DET)	22
2.4. Mediated electron transfer (MET)	25
2.5. Osmium redox polymers (ORPs)	27
<b>3. Fundamentals of electrochemistry</b>	<b>31</b>
3.1. Convention in electrochemistry	32
3.2. Current	32
3.3. Factors affecting the rate of an electrode reaction	33
3.4. Cell resistance	34
3.5. Electrical double layer (EDL)	35
<b>4. Electrochemical techniques</b>	<b>37</b>
4.1. Cyclic voltammetry (CV)	37
4.2. Chronoamperometry (CA)	40
4.3. Flow injection analysis (FIA)	42

<b>5. Electrode material</b>	<b>45</b>
5.1. Graphite electrode	45
5.2. Gold electrode	47
<b>6. Biomaterials</b>	<b>48</b>
6.1. <i>Rhodobacter capsulatus</i>	48
6.2. <i>Shewanella oneidensis</i> MR-1	49
6.3. Thylakoid membranes (TMs) from spinach	49
6.4. <i>Leptolyngbya</i> sp. (CYN65) (CYN82) and <i>Chroococcales</i> sp. (CYN67)	50
6.5. <i>Paulschulzia pseudovolvox</i> (UKE)	50
<b>7. Bacterial respiration</b>	<b>52</b>
7.1. Glycolysis	52
7.2. Tricarboxylic acid cycle (TCA cycle)	53
7.3. Electron transfer chain (ETC)	53
7.4. ATP synthase (ATP syn)	55
<b>8. Photosynthesis</b>	<b>57</b>
8.1. Interconnecting photosynthetic and respiratory-ETC	57
8.2. Chloroplast	58
8.3. Oxygenic photosynthesis	59
8.4. Light dependent reaction	60
8.5. Light independent reaction	61
8.6. Anoxygenic photosynthesis	62
<b>9. Biological photovoltaics (BPVs)</b>	<b>64</b>
<b>10. Acknowledgements</b>	<b>68</b>
<b>11. References</b>	<b>71</b>

# Popular scientific summary

The global energy consumption is increasing regularly due to the increased population and economic development. In contrast the primary energy sources, fossil fuels, are declining substantially. The combustion of fossil fuels contributes to the global climate change via greenhouse effects. To minimize these negative effects a carbon-neutral energy production is demanded.

To guarantee a secured supply of a cost-effective sustainable clean energy production is one of the greatest challenges in the 21<sup>st</sup> century. Solar energy is the most abundant among all other renewable energy sources such as hydroelectricity, geothermal energy, and wind energy. Solar energy is the most ubiquitous around the world and the largest exploitable renewable energy resource. The amount of solar energy radiating from the sun to the earth in one hour is greater than the entire human annual global energy demand.

Biological photovoltaics (BPVs) is emerging as a potential energy generating technology, where photosynthetic organisms are used to convert solar energy into electrical energy. Photosynthetic organisms in BPVs use solar energy for photolysis of water and provide electrons to the system. They are self-sustainable, inexpensive to maintain their growth culture and stored respiratory metabolites inside the cells could be used to generate electrical energy even in the dark. However, the photo-excited extracellular electron transfer (EET) from photosynthetic organisms to electrodes is one of the great challenges in BPVs.

In this thesis we have studied the photo-electrochemical communication of various photosynthetic materials. We investigated the photo-excited EET from thylakoid membranes (TMs) from spinach, purple bacteria, and cyanobacteria as well as from eukaryotic algae. Besides that we have investigated the electrical wiring of heterotrophic microorganisms to electrodes for possible use in microbial electrochemical systems (MESS).

These findings could have significant impacts in photosynthetic energy conversion, light sensitive bioelectrochemical devices and in biological fuel generation.

# List of publications

- I. **K. Hasan**, S.A. Patil, K. Górecki, D. Leech, C. Hägerhäll, L. Gorton\*  
**Electrochemical communication between heterotrophically grown *Rhodobacter capsulatus* with electrodes mediated by an osmium redox polymer, *Bioelectrochemistry*, 93 (2013) 30-36.**
- II. S. A. Patil\*, **K. Hasan**, D. Leech, C. Hägerhäll, L. Gorton\*  
**Improved microbial electrocatalysis with osmium polymer modified electrodes, *Chemical Communications*, 48 (2012) 10183-10185.**
- III. **K. Hasan\***, K.V.R. Reddy, V. Eßmann, K. Górecki, P.Ó Conghaile, W. Schuhmann, D. Leech, C. Hägerhäll, L. Gorton\*  
**Electrochemical communication between electrodes and *Rhodobacter capsulatus* grown in different metabolic modes, *Electroanalysis*, 27 (2015) 118-127.**
- IV. **K. Hasan**, S.A. Patil, D. Leech, C. Hägerhäll, L. Gorton\*  
**Electrochemical communication between microbial cells and electrodes via osmium redox systems, *Biochemical Society Transactions*, 40 (2012) 1330-1335.**
- V. **K. Hasan\***, Y. Dilgin, S.C. Emek, M. Tavahodi, H.-E. Åkerlund, P.-Å. Albertsson, L. Gorton\*  
**Photoelectrochemical communication between thylakoid membranes and gold electrodes through different quinone derivatives, *ChemElectroChem*, 1 (2014) 131-139.**

- VI. H. Hamidi<sup>†</sup>, **K. Hasan**<sup>\*†</sup>, S.C. Emek, Y. Dilgin, H.-E. Åkerlund, P.-Å. Albertsson, D. Leech, L. Gorton\* (<sup>†</sup> = these authors contributed equally to this work)

**Photocurrent generation from thylakoid membranes on osmium-redox-polymer-modified electrodes, ChemSusChem, 8 (2015) 990-993.**

- VII. **K. Hasan**<sup>\*</sup>, H.B. Yildiz, E. Sperling, P.Ó Conghaile, M.A. Packer, D. Leech, C. Hägerhäll, L. Gorton\*

**Photo-electrochemical communication between cyanobacteria (*Leptolyngbia* sp.) and osmium redox polymer modified electrodes, Physical Chemistry Chemical Physics, 16 (2014) 24676-24680.**

- VIII. **K. Hasan**<sup>\*</sup>, E. Çevik, E. Sperling, M.A. Packer, D. Leech, L. Gorton\*

**Photoelectrochemical wiring of *Paulschulzia pseudovolvox* (algae) to osmium polymer modified electrodes for harnessing solar energy, Advanced Energy Materials, (2015), 5: 1501100. doi: 10.1002/aenm.201501100**

- IX. **K. Hasan**<sup>\*</sup>, V. Grippo, E. Sperling, M.A. Packer, D. Leech, L. Gorton\*

**Comparison of photocurrent generation by cyanobacteria and algae to harness sunlight, submitted**

[\* = Corresponding author]

# My contributions to the publications

- I.** L. Gorton and I designed the experiments. I conducted all experiments, made the data interpretations and evaluations of this paper. S. A. Patil wrote the first draft and I participated in revising and editing the manuscript.
- II.** L. Gorton, S. A. Patil and I designed the experiments. S. A. Patil and I conducted all experiments and made the data interpretations and evaluation of this paper. S. A. Patil wrote the first draft and I participated in revising and editing the manuscript.
- III.** I designed the experiments. I initiated experiments and together with K. V. R. Reddy conducted all experiments. I supervised K. V. R. Reddy to conduct and interpret the experiments. I made all data interpretations and evaluation of this paper. I wrote and revised the manuscript.
- IV.** The editor, Dr. Ed Elloway, of The Biochemical Society Transactions, invited me to write this review. I wrote the first draft and together with L. Gorton and S. A. Patil revised the review.
- V.** I designed, conducted and interpreted the initial experiments. I trained Y. Dilgin to conduct and interpret the experiments and made the data interpretation and evaluation of this paper. Y. Dilgin started the very first draft and I participated in writing, revising, editing and submitted the manuscript.
- VI.** I designed, conducted and interpreted the initial experiments. I trained H. Hamidi to conduct and interpret the experiments and made the data interpretations and evaluation of this paper. H. Hamidi initiated the very first draft and I participated in writing, revising, editing and submitted the manuscript.

- VII.** I designed, conducted and interpreted the initial experiments. I trained H. B. Yildiz to conduct and interpret the experiments. I made the data interpretations and evaluation of this paper. I participated in writing, revising, editing and submitted the manuscript.
- VIII.** I designed, conducted and interpreted the initial the experiments. I trained E. Çevik to conduct and interpret the experiments. I made the data interpretations and evaluation of this paper. I participated in writing, revising, editing and submitted the manuscript.
- IX.** I designed, conducted, and interpreted the initial the experiments. I trained V. Grippo to conduct and interpret the experiments. I made the data interpretations and evaluation of this paper. I participated in writing, revising, and edited the manuscript.



# Other manuscripts not included in the thesis due to the early stage of their preparation

I. **K. Hasan\***, O. Aleksejeva, S.C. Emek, H.-E. Åkerlund, P.-Å. Albertsson,, D. Leech, L. Gorton\*

**Enhanced photoelectrochemical activity of thylakoid membranes via double electron transfer mediator systems**

II. G. Pankratova, **K. Hasan**, D. Leech, L. Hederstedt, L. Gorton

**Electrochemical study of the extracellular electron transfer from *Enterococcus faecalis* to electrodes**

# List of abbreviations

<b>A</b>	Electron acceptor
<b>AR</b>	Aerobic respiration
<b>ATP</b>	Adenosine triphosphate
<b>ATP syn</b>	Adenosine triphosphate synthase
<b>BESs</b>	Bioelectrochemical systems
<b>BPVs</b>	Biological photovoltaics
<b>CA</b>	Chronoamperometry
<b>CE</b>	Counter electrode
<b>CV</b>	Cyclic voltammetry
<b>CM</b>	Cytoplasmic membrane
<b>Cyt <i>c</i></b>	Cytochrome <i>c</i>
<b>Cyt <i>b<sub>6</sub>f</i></b>	Cytochrome <i>b<sub>6</sub>f</i>
<b>FNR</b>	Ferredoxin-NADP-reductase
<b>D</b>	Electron donor
<b>DET</b>	Direct electron transfer
<b>E<sup>0</sup></b>	Standard redox potential
<b>EDL</b>	Electrical double layer
<b>EET</b>	Extracellular electron transfer
<b>ET</b>	Electron transfer
<b>ETC</b>	Electron transfer chain
<b>FAD</b>	Flavin adenine dinucleotide (oxidized)
<b>FADH<sub>2</sub></b>	Flavin adenine dinucleotide (reduced)
<b>FMN</b>	Flavin mononucleotide
<b>Fd</b>	Ferredoxin

<b>FIA</b>	Flow injection analysis
<b>MESs</b>	Microbial electrochemical systems
<b>MET</b>	Mediated electron transfer
<b>MFCs</b>	Microbial fuel cells
<b>NAD<sup>+</sup></b>	Nicotinamide adenine dinucleotide (oxidized)
<b>NADH</b>	Nicotinamide adenine dinucleotide (reduced)
<b>NADP<sup>+</sup></b>	Nicotinamide adenine dinucleotide phosphate (oxidized)
<b>NADPH</b>	Nicotinamide adenine dinucleotide phosphate (reduced)
<b>O</b>	Oxidized form
<b>OEC</b>	Oxygen evolving complex
<b>ORPs</b>	Osmium redox polymers
<b>PC</b>	Plastocyanin
<b>PETC</b>	Photosynthetic electron transfer chain
<b>PMFC</b>	Photosynthetic microbial fuel cell
<b>PSI</b>	Photosystem I
<b>PSII</b>	Photosystem II
<b>PQ</b>	Plastoquinone
<b>PQH<sub>2</sub></b>	Plastoquinol
<b>R</b>	Reduced form
<b>RC</b>	Reaction center
<b>RE</b>	Reference electrode
<b>RETC</b>	Respiratory electron transfer chain
<b>ROS</b>	Reactive oxygen species
<b>TCA-cycle</b>	Tricarboxylic acid cycle
<b>TMs</b>	Thylakoid membranes
<b>TOX</b>	Terminal oxidase
<b>U</b>	Ubiquinone
<b>UQ<sub>2</sub></b>	Ubiquinol
<b>WE</b>	Working electrode

# 1. General perspectives of the thesis

The electrochemical communication between microorganisms and electrodes has very large implications both for the fundamental understanding of biological electron transfer as well as in diverse biotechnological applications, such as electricity production, wastewater treatment, bioremediation and in the production of valuable bio-chemicals, e.g., ethanol and hydrogen. The extracellular electron transfer (EET) from microbial metabolism to electrodes is the greatest challenge in microbial electrochemical systems (MESs), e.g., microbial fuel cells (MFCs), microbial biosensors, biological photovoltaics (BPVs), microbial electrosynthesis, etc.

Microbial metabolism is the way for microorganisms to get necessary nutrients and energy for their survival and maintenance. A series of enzymatic reactions are involved in microbial respiration to convert biochemical energy from nutrients into adenosine triphosphate (ATP), the universal cellular energy molecule. Life on earth depends on photosynthesis. Eukaryot green plants and algae, as well as prokaryot cyanobacteria and purple bacteria perform photosynthesis to convert solar energy into chemical energy.

Although microorganisms developed through evolution, however, they are not adapted for EET to electrodes in MESs. The electron transfer (ET) from the cellular interior is restricted due to the insulated cellular exterior environment made of lipid structures. A thorough and fully detailed mechanism of EET on the molecular level from the microbial metabolism to electrodes is yet to be elucidated even though major breakthroughs have been reached during the last decade. Osmium redox polymers (ORPs) were used as efficient ET-mediators to establish electronic communication between a range of viable cells/membranes and electrodes.

In this thesis an attempt for a systematic study has been pursued on EET from a group of diverse biomaterials. The EET from the most metabolically versatile purple bacteria, i.e., *Rhodobacter capsulatus*, grown both heterotrophically and photoheterotrophically was studied. We investigated one of the most highly studied bacterial species in MESs, i.e., *Shewanella oneidensis* MR-1, a metal ion reducing bacterium also known for mediatorless ET with electrodes. We have

shown *S. oneidensis* MR-1 can be coupled with ORPs modified graphite electrodes resulting in an enhanced current density.

To harness solar energy we studied the photo-excited EET from TMs, the site of photosynthesis in green plants and algae. In addition we studied the photo-excited EET from cyanobacteria, *Leptolyngbya* sp. and *Chroococcales* sp., where photosynthesis takes place in TMs inside the complex membranes system. Photo-electrochemical communication of algae with electrodes is assumed to be challenging, since photosynthesis occurs in a subcellular organelle, the chloroplast. We extended our study to the photo-excited EET from a multicellular eukaryotic green alga, *Paulschulzia pseudovolvox*, to graphite electrodes.

## 2. Electron transfer (ET) mechanisms

ET is one of the fundamental events in chemical, electrochemical, photochemical, biochemical, and biophysical processes. The ubiquity of ET is exciting, however, a comprehensive approach to the understanding of ET is challenging<sup>1</sup>. In living systems, ET across biological membranes is the central process for energy generation in respiration and photosynthesis<sup>2</sup>. The International Union of Pure and Applied Chemistry (IUPAC) defines ET as “the transfer of an electron from one molecular entity to another, or between two localized sites in the same molecular entity”<sup>3</sup>. According to the state of the redox centers and their connectivity, ET has been classified as follows:

- Inner-sphere ET: The two redox centers, i.e., an electron donor (D) and an electron acceptor (A) are covalently linked during the ET reaction. If this link becomes permanent, the ET event is called intramolecular ET. However, in most cases the covalent linkage is temporary prior to the ET and disconnects followed by the ET and is called intermolecular ET. In biological systems intermolecular ET is not common, since redox centers of bulky proteins are insulated by the surrounding molecular structures. Henry Taube discovered inner-sphere ET<sup>4</sup> and was awarded the Nobel prize in chemistry in 1983.
- Outer-sphere ET: No linkage between the redox centers occurs during ET. Rather the electron “hops” through the space between D and A. In this way, electrons are transferred between two different chemical species, however, with no linkage being created between D and A at any time. An electron can also transfer between two identical chemical species varying in oxidation states and such an ET is defined as self-exchange. The chemical species remain separate and intact before, during and after the ET event<sup>3</sup>.
- Heterogeneous ET: An electron moves between the boundaries of two phases, e.g., between chemical species in a solution and a solid-state electrode. In electrochemistry heterogeneous ET is highly studied.

## 2.1. Marcus theory

The generally accepted ET theory commonly known as the Marcus theory was developed by Rudolph A. Marcus to explain the rate of an ET reaction<sup>5</sup>. Initially the theory was based on outer-sphere ET reactions and then it also addressed the inner-sphere ET as well as heterogeneous ET reactions<sup>6</sup>. In 1992, R. A. Marcus was awarded the Noble prize in chemistry “for his contributions to the theory of ET reactions in chemical systems”<sup>7</sup>. The Marcus equation can be written as follows

$$K_{ET} = \frac{2\pi}{\hbar} \frac{H_{DA}^2}{\sqrt{4\pi\lambda RT}} e^{-\frac{(\Delta G^0 + \lambda)^2}{4\lambda RT}} \quad (1)$$

Where  $K_{ET}$  is the ET rate,  $\hbar$  is the reduced Plank constant, R is the universal gas constant, T is the absolute temperature,  $\lambda$  is the nuclear reorganization energy.

The parameters regulate the driving force of the ET reaction related to the change in Gibbs free energy,  $-\Delta G^0$

$$-\Delta G^0 = nF\Delta E^0 \quad (2)$$

Here  $\Delta E^0$  refers to the standard redox potential difference between D and A. Reorganization energy ( $\lambda$ ) is needed for nuclear rearrangement accompanied with ET. The theory describes two-states, i.e., ( $-\Delta G^0 > \lambda$ ), where  $K_{ET}$  increases and ( $-\Delta G^0 < \lambda$ ), where  $K_{ET}$  decreases. The maximum  $K_{ET}$  is obtained when  $-\Delta G^0 = \lambda$ .

The probability of an electron transport through the potential barrier between D and A is defined as  $H_{DA}$ <sup>6c</sup>.  $H_{DA}$  is the electronic coupling between the D and A at the transition state. The potential barrier depends on the distance between the D and A, introducing the distance dependence in ET theory.

A broad range of theoretical approaches have been developed to predict  $H_{DA}$  in protein mediated ET<sup>8</sup>. The simplest one is the square-barrier model, where the protein is considered as an “organic” glass<sup>8b</sup>. It states that  $H_{DA}$  decreases exponentially when the distance between D and A increases linearly and the effectiveness of the protein in mediating ET is given by the tunneling parameter  $\beta$  and expressed as:

$$H_{DA}^2 = (H_{DA}^0)^2 \exp(-\beta \times (r_{DA} - r_0)) \quad (3)$$

Where  $H_{DA}^0$  is the electronic coupling at the van der Waals distance ( $r_0$ ) and  $r_{DA}$  is the distance between D and A. The tunneling parameter,  $\beta$ , ranges between 0.8 – 1.6  $\text{\AA}^{-1}$  depending on the protein structure<sup>9</sup>. Although the Marcus theory was developed using inorganic chemical species, however, it is also valid for biological

materials, i.e., proteins, peptides and the photosynthetic machinery<sup>10</sup>. To summarize, factors determining the rate of ET stated by the Marcus theory can be listed as follows:

- The distance between the D and A;  $K_{ET}$  decreases with an increased distance.
- The reorganization energy,  $\lambda$ , a nuclear rearrangement is needed to accompany the ET. In biological systems,  $\lambda$  reveals the structural rigidity of the redox site in its oxidized and reduced form.
- The thermodynamic driving force,  $\Delta G^0$ , of the ET that arises from the difference in the redox potentials,  $\Delta E^0$  of D and A. In protein electrochemistry,  $\Delta G^0$  is related to  $\Delta E^0$  of the redox active site of the protein and the applied potential of the electrode<sup>11</sup>.

In biological systems ET is carried out by a series of proteins and enzymes comprising the ET-chain (ETC). Biological ET systems are complicated due to the large size and complexity of the proteins in ETC. In biological ET systems individual ET steps vary from single step to multistep and short range to long range. ET in Nature occurs either through a bridge-mediated super-exchange model<sup>12</sup> or an electron hopping model<sup>10</sup>. In the bridge-mediated super-exchange model, the electrons are assumed to tunnel through long distances, i.e., between 14 and 20 Å. In the electron-hopping model, the long-range ET is divided into small multi steps and electron transfers through amino acids, cofactors, and proteins and follows the Marcus theory. Metalloproteins (metal-ion-complex containing proteins) control the long range ET and electrons are transferred by single entities through one or more redox cofactors<sup>8b</sup>. Typically a protein controls the ET by changing its formal potential of its redox active site via regulating the reorganization energy and providing an ET route between the redox centers<sup>13</sup>.

## 2.2. ET in biological systems

The majority of the ET steps in biological systems are performed by cofactors buried inside proteins. These cofactors are either inorganic or organic molecules. The inorganic molecules include metal ions, e.g.,  $\text{Cu}^{2+}$ ,  $\text{Fe}^{2+}$ ,  $\text{Mg}^{2+}$ ,  $\text{Mn}^{2+}$ ,  $\text{Ni}^{2+}$ ,  $\text{Zn}^{2+}$  and metallic complexes, e.g., Fe-S clusters. The organic cofactors can be loosely or strongly bound to the enzyme and include quinones (2  $e^-$ , 2  $\text{H}^+$  centers) e.g., pyrroloquinoline quinone (PQQ), flavins (2  $e^-$ , 2  $\text{H}^+$ ), e.g., flavin adenine dinucleotide (FAD) and flavin mononucleotide (FMN), nicotinamides e.g.,  $\beta$ -nicotinamide adenine dinucleotide ( $\text{NAD}^+$ ) and  $\beta$ -nicotinamide adenine dinucleotide phosphate ( $\text{NADP}^+$ ) (both 2  $e^-$ , 1  $\text{H}^+$  centers), and heme (1  $e^-$ ), which is like the Fe-S clusters, a mixed metal ion-organic molecule. A great deal of research has focused on ET reactions in proteins<sup>8a, 9, 14</sup>, metalloproteins<sup>15</sup>, the distance between redox centers of proteins<sup>16</sup> and long range ET<sup>17</sup> and



heterogeneous ET, where electrons move between the protein in solution and a solid material, e.g., an electrode surface<sup>18</sup>.

Investigations of ET reactions between proteins and electrodes have great implications in different fields, e.g., MESSs, BPVs, biosensors<sup>19</sup>, biofuel cells<sup>20</sup>, bioelectronics<sup>21</sup>, clinical assays and drug screening etc. In this thesis extracellular-ET (EET) from microbial respiration as well as photosynthesis to electrode has been investigated.

### 2.3. Direct electron transfer (DET)

DET stands for the direct transfer coupling between a biological ETC (most commonly the redox cofactor a protein) and an electrode. The requirement of DET can be derived from the Marcus theory<sup>6c, 7</sup> and are controlled by a few factors<sup>18b, 22</sup> listed below:

- The ET-distance and bonding between the redox centers of D and A.
- The thermodynamic driving force, i.e., the redox potential difference between D and A
- The proper association of the redox couple and the protein structure dynamics is coupled with ET

DET provides important information about the intrinsic thermodynamics and kinetic properties of a protein<sup>23</sup> and has significant implications in bioelectrochemical systems (BESS)<sup>24</sup>. DET was originally demonstrated for a key ET component in biological systems, cytochrome *c* (cyt *c*) on solid electrodes<sup>25</sup>. Cytochromes are the most commonly studied small electron transfer proteins in electrochemistry. They contain heme-cofactors and are able to reversibly change the oxidation state of the bound iron ion ( $\text{Fe}^{+2}/\text{Fe}^{3+}$ ) during the ET reaction. The heme-cofactor is made of a conjugated double bond ring structure (porphyrin) surrounding an iron ion and its energy levels are narrowly spaced that facilitate the ET<sup>26</sup>.

Until today DET was shown for about one hundred redox enzymes<sup>27</sup>, e.g., laccase<sup>28</sup>, peroxidase<sup>29</sup> and cellobiose dehydrogenase<sup>30</sup>. DET between redox enzymes and electrodes<sup>31</sup> should in the perfect case be revealed by both of the following characteristics:

- By detecting electrochemical activity of the bound redox cofactor comprising the active site in the absence of substrate (non-turnover conditions)

- By observing a catalytic response in the presence of the enzyme substrate (turnover conditions)

DET is typically exhibited in extrinsic enzymes, where there is a natural redox protein for ET as well as an electron-tunneling pathway between the active site and the enzyme surface. Thus proper orientation of enzymes on the electrode surface is essential so that the active site/built in ET pathway is exposed and the sites of ET-pathways are functioning<sup>27</sup>. Most of the studied enzymes are found in intracellular membranes and participate in biological ET systems. They contain different cofactors either metal compound, e.g., hemes, Fe-S clusters, and copper ions or non-metal compounds, e.g., flavin, PQQ.

Instead, in intrinsic enzymes the catalytic reactions take place in a highly localized assembly of the redox active site and there is no built in ET-pathway to transfer electron from the active site to the enzyme surface to interact with an electrode. Therefore DET in intrinsic enzymes is less feasible and requires either engineering of the enzyme or electrode modification<sup>32</sup>. However, DET was also revealed for some intrinsic enzymes (where the distance between the bound cofactor and enzyme surface is below 20 Å), e.g., horseradish peroxidase (HRP) adsorbed on a graphite electrode<sup>33</sup>.

When it comes to bacteria, documented DET for microorganisms is limited and was mostly demonstrated for metal ion reducing Gram negative bacteria<sup>34</sup>, e.g., *Geobacter sulfurreducens*<sup>35</sup> and *Shewanella putrefaciens*<sup>36</sup>. Electro-active bacteria capable of DET are often referred to as electricigens<sup>37</sup>, or anode respiring bacteria<sup>38</sup>, or exoelectrogenic bacteria<sup>39</sup>. DET of bacterial cells with electrodes occurs via physical contact. DET requires that the microorganisms are supposed to have a membrane bound ET protein relay that will transfer electrons between the inside of the bacterial cell and its outside and then to/from the electrode.

It was reported that outer membrane *c*-type cytochromes<sup>40</sup> and other multi heme proteins are responsible for DET<sup>41</sup> for the bacterial cells, though a detailed mechanism is not yet known. It was revealed that electrically conductive filamentous like pili produced by *G. sulfurreducens*<sup>42</sup> and *Shewanella putrefaciens*<sup>43</sup> increase their EET to metal oxides<sup>44</sup>. Pili are analogous to electrically conductive nanowires and may connect membrane bound cytochromes with electrodes<sup>42</sup>. It was suggested that pili are involved in ET to electrodes for *Geobacter sulfurreducens* cells that are not closely attached onto the electrode surface<sup>37a</sup>. DET was also exhibited for a series of other microorganisms, e.g., the thermophilic Gram positive bacterium *Therminococcus ferriacetis*<sup>45</sup>, Gram negative bacterium *Klebsiella pneumonia*<sup>46</sup> and *Pseudomonas fluorescens*<sup>47</sup> and even one yeast, *Hansenula anomala*<sup>48</sup>, however, any detailed mechanism is yet to be understood. DET provides higher columbic efficiencies<sup>42</sup>, minimizes the over-

potential losses, and simplifies the electrochemical cell design and operation<sup>49</sup>. However, in reality a limited number of microorganisms are capable of DET. The current densities and power output in a pure DET based system are much lower compared to what can be obtained in a well designed mediated-ET (MET) system<sup>50</sup>. A schematic picture of various EET pathways from bacterial cells to electrodes is presented in **Figure 1**.

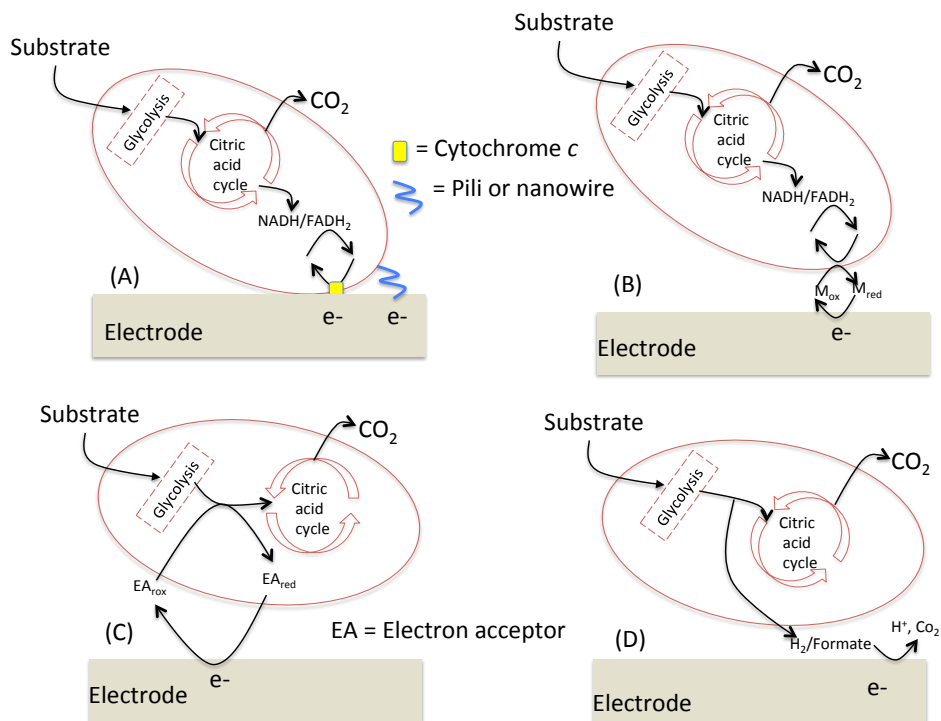


**Figure 1.** A schematic picture of the various EET pathways from bacterial cells to an electrode. (A) DET via membrane bound *c* type cytochromes or nanowires, (B) MET via an artificial ET-mediator (exogenous) (C) MET via primary respiratory metabolites and (D) MET via secondary respiratory metabolites. The term ox and red symbolize the oxidized and reduced forms of the participating redox species. Bacterial cells can use a variety of organic substrates, e.g., lipids, proteins, carbohydrates, as electron donors. Organic substrates are converted through glycolysis and other relevant processes into acetyl-CoA. In aerobic respiration, acetyl-CoA is processed via the tricarboxylic acid cycle (TCA-cycle) and produces energy rich molecules, e.g., NADH and FADH<sub>2</sub>. In anaerobic respiration, acetyl-CoA does not go through the TCA cycle and generates primary metabolites, e.g., sulfate (SO<sub>4</sub><sup>2-</sup>), nitrate (NO<sub>3</sub><sup>-</sup>) and secondary metabolites, e.g., H<sub>2</sub>, formate.

Bacterial cells can use these metabolites as ET-mediators to transfer electrons from their inside to an insoluble electron acceptor.

In this thesis we have focused on oxidation reactions bringing electrons from bacterial cells and membranes to electrode surfaces and emphasis is on anodic ET in the chapters following below. A great deal of research is focused on harnessing solar energy<sup>51</sup> via DET from isolated photosystems, e.g., photosystem I<sup>52</sup> and II<sup>53</sup> (PSI & PSII), photosynthetic membranes, i.e., TMs<sup>54</sup> and also in intact organisms, e.g., prokaryotic cyanobacteria<sup>55</sup> and eukaryotic algae<sup>55b</sup>.

## 2.4. Mediated electron transfer (MET)

The catalytic active site in an intrinsic enzyme is deeply buried inside the three-dimensional (3D) protein structure and consequently the ET between the active site and an electrode is challenging<sup>27</sup>. The primary reason behind this restricted ET is the spatial separation between the redox active site and the electrode. To establish efficient ET with such redox enzymes, exogenous ET mediators can be used that can easily access the active site, pick up charge and transfer it to the electrode. Benzoquinone ( $2e^-$ ,  $2H^+$ ) and potassium ferricyanide<sup>56</sup> ( $1e^-$ , no  $H^+$ ) are examples of such ET mediators<sup>57</sup>.

In this thesis we have studied the EET mostly from microorganisms and hence the following section of ET is focused on microbial EET. Although microorganisms have developed through evolution, however, they were not adapted for EET. Their insulated cellular exterior assembly buries the majority of the redox processes inside the cell and diverting electrons from the microbial metabolism to an electrode is a great challenge. In microbial electrochemical systems (MESs), electrons from the microorganisms are transferred out either via a physical transfer of reduced compounds or through electron hopping across the membranes and through membrane bound redox enzymes. In both cases the ET outside the cell must include a redox active species that is capable of linking electronically the bacterial cells to the electrode. This redox active species can be a soluble redox shuttle, an outer membrane redox protein, or a reduced primary metabolite. Most commonly this species are called ET-mediator<sup>57</sup>. The characteristics of an ideal ET-mediator were demonstrated previously<sup>57-58</sup>.

According to the nature and origin of the ET mediator, they can be classified into the following categories:

**Artificial ET-mediator (exogenous):** Artificial mediators are non-physiological redox compounds that are used to make possible electrochemical communication with microbial cells, which are otherwise unable to properly function as electrons

from the cellular metabolism need these helping molecules be delivered to the electrode<sup>59</sup>. Such mediators need to be deliberately added to the system as soluble compounds or to modify electrodes to make chemically modified electrodes. A large number of compounds have been used as artificial ET mediators. Both organic type  $2e^- H^+$  type acceptors e.g., phenazines, (e.g., neutral red, safranin, phenazine ethosulfate), phenothiazines (e.g., toluidine blue-O, phenothiazinon, thionine, methylene blue), phenoxazines (e.g., resorufin, galloxyanin) and quinones (e.g., 2-hydroxy-1,4-naphthoquinone, anthraquinone-2,6-disulfonate) as well as metal ion complexes  $1e^- no-H^+$  type acceptors, e.g., ferricyanide and ferrocene derivatives, have been frequently used for e.g., *Escherichia coli* (*E. coli*), *Pseudomonas* sp., *Proteus* sp., *Bacillus* sp., *Actinobacillus succinogenes*, and *Proteus vulgaris*<sup>60</sup>.

However, the ability of microorganisms to support their own growth and maintenance in the presence of exogenous mediators is not known in detail. Additionally, the regular additions of these exogenous mediators are practically incompatible, expensive to maintain the desired concentration, may be environmentally unfriendly and toxic for the organism to self-maintenance for a prolonged period of time<sup>37a</sup>. In a mediated system electrons are transferred to a mediator with a higher reduction potential resulting in heat loss<sup>53</sup>. One way to minimize their drawbacks is to use a redox polymer where the mediating functionality is covalently bound but still functioning with microbial cell (see section 2.5).

**Secondary metabolites as ET mediator (endogenous):** When microorganisms grow in thick biofilms, where external ET mediators are not easily accessible, microorganisms may produce some compounds and use them as electron shuttles<sup>61</sup>. Secondary metabolites involved in bacterial EET are phenazine-1-carboxamide, pycocyanine (phenazine) and 2-amino-3-carboxy-1,4-naphthoquinone (ACNQ). Pycocyanin and phenazine-1-carboxamide excreted from *Pseudomonas aeruginosa* are involved in EET<sup>62</sup>. A quinone like redox active small molecule was found to be accountable for long distance EET in *Shewanella oneidensis* MR-1. For a number of bacteria various flavins have also been found to promote EET<sup>63</sup>.

**Primary metabolites as ET mediator (endogenous):** Unlike the secondary metabolites, the primary metabolites are closely associated with oxidative substrate degradation and facilitate EET. In benthic MFCs, sulfate reducing bacteria, i.e., *Desulfovibrio desulfuricans* was shown to use dissolved sulfate as an electron acceptor<sup>64</sup>. Cellulolytic bacteria, i.e., *Clostridium* sp. were demonstrated to use hydrogen, a fermentative product, to transfer electrons from a variety of substrates e.g., cellulose and starch<sup>65</sup>. Besides that the photoheterotrophic bacterium, i.e., *Rhodobacter sphaeroides*<sup>66</sup> and green algae, i.e., *Chlamydomonas*

*reinhardtii*<sup>67</sup> were reported to use photo-biologically produced hydrogen as an ET mediator.

The advantages of using primary metabolites as ET-mediators in BESs are higher current and power output compared to an equivalent DET based system. In addition a great variety of microorganisms and substrates can be exploited in this mode. However, BESs based on primary metabolites experience the formation of electrochemically inactive side products<sup>57</sup>.

To summarize, each ET system has some advantages as well as disadvantages and it is difficult to say which one them is the best in BESs. The nature and metabolic process of a particular microbial species and their capability to utilize a certain substrate should be taken into consideration when evaluating the ET system<sup>57</sup>.

In contrast to the EET from microorganisms to electrodes, the ET from electrodes to microorganisms was also revealed, however, the fundamental mechanism is not known in detail<sup>68</sup>.

## 2.5. Osmium redox polymers (ORPs)

Redox hydrogels are cross linked polymer network structures capable of swelling in water and represent an electron-conducting phase, where water-soluble (bio)molecules can dissolve and diffuse<sup>69</sup>. Redox hydrogels have been widely used to electrically connect the redox centers of enzymes to electrodes and in this way the leaching of electron shuttling diffusional ET-mediators are prevented. Avoiding the leakage of ET mediators is essential in membrane less biofuel cells<sup>70</sup>, in analyzing biochemicals<sup>71</sup> and in subcutaneously implanted biosensors, e.g., glucose sensors for diabetes management<sup>72</sup>. Redox hydrogels form 3D network by surrounding the redox enzymes and electrically wire their reaction centers to electrodes regardless of their spatial orientation. Thus multiple layers of both enzymes and mediator functionalities are immobilized on the electrode surface resulting in higher current densities from bioelectrocatalysis of substrates compared to electrodes covered with only monolayers of enzymes. In addition, the hydrophilic environment of hydrogels provides long-term enzymatic activity and prompt diffusion of substrates and products through the polymer matrix<sup>69</sup>.

Redox hydrogels conduct electrons by self-exchange reactions of electrons through collisions between rapidly reduced and rapidly oxidized centers bound to the backbone of cross-linked polymer networks<sup>73</sup>. Redox centers are required to come close to the electrode so that electrons can cross the distance defined by the Marcus theory<sup>6c</sup>. The rate of ET between those redox centers increases when they are present in equal concentrations. When the concentrations of redox centers are

at unequal concentration the rate of ET decreases. When the hydrogels are poised at close proximity of their redox potential, the ET becomes maximum<sup>74</sup>. The rate of self-exchange of electrons becomes faster when the redox functionalities are bound to cross-linked polymer networks by flexible and long spacers of  $\approx$  8-15 atoms. Instead the rate of self exchange of electrons decreases exponentially with an increased distance between the redox centers<sup>75</sup>.

The Os<sup>2+/3+</sup> comprising electron-conducting redox hydrogels are often referred to as osmium redox polymers (ORPs). The redox potential of hydrogels is mainly defined by the transition metal ion complex and their ligands<sup>76</sup>. Moreover, the concentrations of chloride in hydrogels also influence their  $E^{0'}$ -value. Incorporation of flexible long tethers covalently binding the redox centers to the polymer backbone allows the redox functions at the end of the tethers to swing and exchange electrons, however, the electron diffusion coefficient ( $D_e$ ) increases as the length of the tether becomes longer and decreases with short tethers. The ORPs are highly polycationic thus avoiding partial phase separation with enzymes and bacterial cells that are usually polyanionic at neutral physiological pH. Thus such highly positively charged redox polymers also function as an immobilization matrix for redox enzymes and cells<sup>77</sup>. Heller, who pioneered the use of ORPs in bioelectrochemistry, reported on the synthesis and structure of ORPs in an excellent review<sup>69</sup>.

The majority of the biological components used in bioelectrochemical studies, e.g., enzymes, bacterial cells, are poor in electron conduction, since they are surrounded by an insulated protein shell, e.g., glycoproteins. Heller et al., used ORPs<sup>78</sup> to electrically “wire” the redox centers of enzymes with electrodes for efficient ET between them and electrodes. It was demonstrated that the polycationic ORPs form strong electrostatic interactions with polyanionic enzymes and reduce the ET distance between the redox centers and electrodes. To transfer efficiently electrons from the buried redox centers of enzymes to electrodes, the ORPs are presumed to have the following characteristics:

- They should be water soluble and have hydrophobic, charged or hydrogen binding domains available to bind to enzymes<sup>78a</sup>.
- A tiny part of the ORPs bind with the electrode and most of the remaining parts are available to bind enzymes. These requirements are accomplished when the ORPs are water soluble and are of higher molecular weight<sup>79</sup>.
- Formation of a 3D network that will incorporate a great number of enzyme molecules and for this a cross-linker, e.g., poly-(ethylene glycol)-diglycidyl ether (PEGDGE) is used together with the ORPs to stabilize the redox hydrogels formed initially through electrostatic interactions with covalent linkages making them truly long term stable<sup>80</sup>.

In our group ORPs were extensively used to study enzymes, e.g., horseradish peroxidase<sup>81</sup>, pyranose oxidase<sup>82</sup>, pyranose dehydrogenase<sup>83</sup>, glucose dehydrogenase<sup>84</sup>, cellobiose dehydrogenase<sup>85</sup>, and oligosaccharide dehydrogenase<sup>86</sup>. In addition ORPs were widely used to electrically wire a variety of living bacterial cells, e.g., *Gluconobacter oxydans* and the biocatalytic current was obtained from different substrates such as ethanol, glucose, glycerol. These are typical substrates for membrane bound dehydrogenases<sup>87</sup>. ORPs were also used to accomplish electrochemical communication with the phenol degrading organisms *Pseudomonas putida* and *Pseudomonas fluorescens* and gold electrodes<sup>88</sup>. Moreover, ORPs were reported for stable binding of *Pseudomonas putida* on carbon nanotubes (CNT) and shuttling electrons from redox enzymes in bacterial cells<sup>89</sup>. ORPs were also found to greatly facilitate electrochemical communication of engineered *E. coli*, where cytochromes were inserted into the inner CMs<sup>90</sup>.

All these above mentioned bacterial cells studied with ORPs are gram-negative, where a number of redox enzymes are located inside the inner CMs. However, ORPs were also shown to mediate electrical wiring of gram-positive bacterial cells to electrodes, which was supposed to be difficult, since their cell walls composed of peptidoglycan and teichoic acids are substantially thicker  $\approx 35$  nm than those of the gram-negative bacteria. However, a gram-positive model bacterium, *Bacillus subtilis* was reported to be very efficiently wired with ORPs on electrodes<sup>91</sup>. These studies demonstrate that mediators do not need to pass through the CMs to bring out charge from bacterial respiration. It was hypothesized that conducting structures are present in the thick cell wall of gram-positive bacteria, which are able to transfer electrons from CMs to the outer surface of the cell wall<sup>92</sup>.

In this thesis a series of ORPs of different chemical structures and redox potentials ( $E^{\circ}$ ) ranging from -0.184 V to +0.350 V vs. Ag|AgCl (sat. KCl) at pH 7.0 were studied. The investigated ORPs are presented in Table 1 and their chemical structures are shown in **Figure 2**.

Table 1. The ORPs used in this study, their chemical name, short abbreviation,  $E^{\circ}/V$  vs. Ag|AgCl (sat. KCl), [ $E^{\circ} = 0$  mV vs. Ag|AgCl (sat. KCl) is equivalent to +197 mV vs. SHE]

ORPs chemical name	Abbreviation	$E^{\circ}/V$	Ref.
[Poly(vinylpyridine)-(Os-N,N'-methylated-2,2'-biimidazole) <sub>3</sub> ] <sup>+2+</sup>	[PVP-Os(mbim)]	-0.184	<sup>80b</sup>
[Os(4,4'-dimethoxy-2,2'-bipyridine) <sub>2</sub> (poly-vinylimidazole) <sub>10</sub> Cl] <sup>+2+</sup>	(Os-(dmobpy)PVI (1:9))	-0.069	<sup>93</sup>
[Os(4,4'-dimethyl-2,2'-bipyridine) <sub>2</sub> (poly-vinylimidazole) <sub>10</sub> Cl] <sup>+2+</sup>	(Os-(dmbpy)PVI (1:9))	+0.110	<sup>93</sup>
[Os(2,2'-bipyridine) <sub>2</sub> (poly-vinylimidazole) <sub>10</sub> Cl] <sup>+2+</sup>	(Os-(bpy)PVI)(1:9)	+0.220	<sup>94</sup>
[Os(4,4'-dimethyl-2,2'-bipyridine) <sub>2</sub> (poly-vinylimidazole) <sub>12</sub> Cl <sub>2</sub> ] <sup>+2+</sup>	(Os-(dmbpy)PVI (1:11))	+0.244	<sup>82a</sup>
[Os(4,4-dichloro-2,2'-bipyridine) <sub>2</sub> (PVI) <sub>10</sub> Cl] <sup>+2+</sup>	(Os-(dc(bpy)PVI) (1:9))	+0.350	<sup>95</sup>



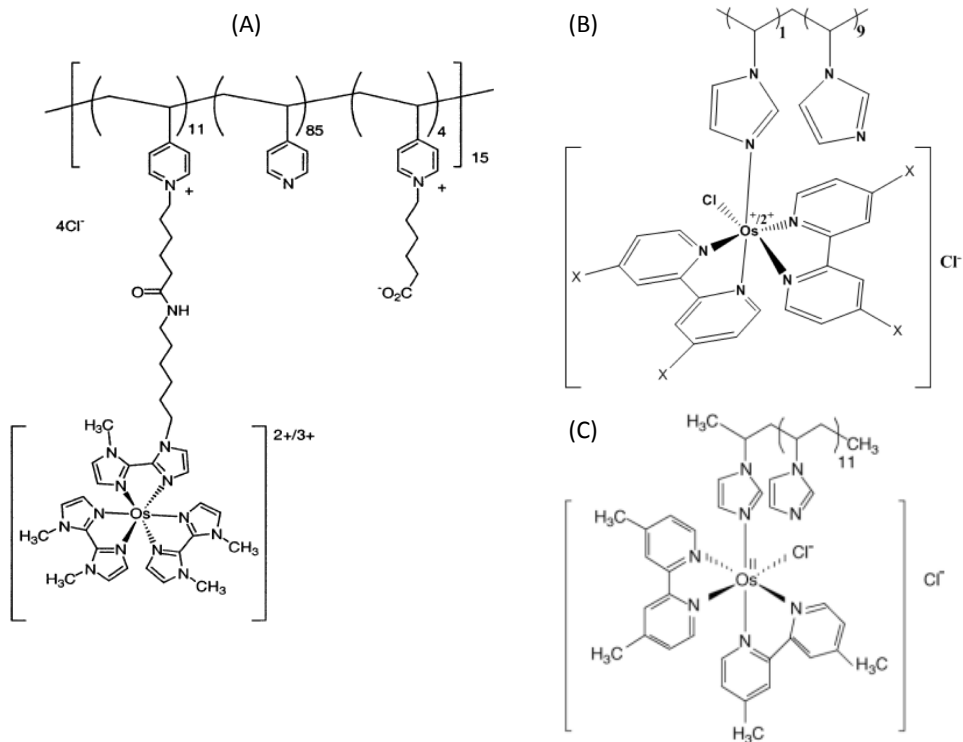


**Figure 2. The chemical structure of the ORPs used in this study, (A) [Poly(vinylpyridine)-(Os-N,N'-methylated-2,2'-biimidazole)<sub>3</sub>]<sup>+2+</sup> [PVP-Os(mbim)] (B) [Os(4,4'-dimethoxy-2,2'-bipyridine)<sub>2</sub>(polyvinylimidazole)<sub>10</sub>Cl]<sup>+2+</sup>, X = OCH<sub>3</sub> (Os-(dmobpy)PVI) (1:9) ; Os(4,4'-dimethyl-2,2'-bipyridine)<sub>2</sub>(polyvinylimidazole)<sub>10</sub>Cl]<sup>+2+</sup>, X = CH<sub>3</sub> (Os-(dmbpy)PVI) (1:9) ; [Os(2,2'-bipyridine)<sub>2</sub>(polyvinylimidazole)<sub>10</sub>Cl]<sup>+2+</sup>, X = H (Os-(bpy)PVI)(1:9); [Os(4,4-dichloro-2,2'-bipyridine)<sub>2</sub>(PVI)<sub>10</sub>Cl]<sup>+2+</sup>, X = Cl Os-(dc(bpy)PVI) (1:9); (C) [Os(4,4'-dimethyl-2,2'-bipyridine)<sub>2</sub>(polyvinylimidazole)<sub>12</sub>Cl<sub>2</sub>]<sup>+2+</sup> (Os-(dmbpy)PVI) (1:11)**

### 3. Fundamentals of electrochemistry

In electrochemistry ET is studied broadly at the interface between a solution and an electrode. In 1800, Alessandro Volta invented the first battery by interchanging stacks of copper and zinc disks separated by paper soaked in acid solutions. In 1835, Michael Faraday defined fundamental elements in electrochemistry, e.g., anode, cathode, electrode, electrolyte, and ion without which any description of electrochemistry is almost impossible. The conventional nomenclature of positive (+) and negative (-) electrical charge is attributed to Benjamin Franklin. The excellent book by Bard and Faulkner: 'Electrochemical Methods: Fundamentals and Applications' is recommended for a deeper understanding of electrochemistry<sup>96</sup>. There are many books<sup>97</sup> explaining the fundamentals and theory of electrochemistry and readers are suggested to 'The Handbook of Electrochemistry' edited by Cynthia G. Zoski<sup>98</sup> for electrochemical information explained in a very comprehensive way. Bioelectrochemistry is a branch of electrochemistry and biophysical chemistry concerned with electrophysiological topics like cell electron-proton transport, cell membrane potentials and electrode reactions related to biological ET<sup>2</sup>.

A basic electrochemical reaction can be written as:



Where O is the oxidized species, R is the reduced species, and n is number of electrons transferred between O and R. The potential of the electrode can be related to the standard potential of the redox reaction and the activities of the species involved in the conversion by the Nernst equation

$$E = E^{0'} + \frac{RT}{nF} \ln \frac{a_O}{a_R} \quad (5)$$

Here  $E^{0'}$  is the formal potential of the redox reaction, R is the universal gas constant ( $8.3145 \text{ J mol}^{-1} \text{ K}^{-1}$ ) and T is the absolute temperature (K), F is the Faraday constant ( $96485 \text{ C/mol}$ )  $a_O$  and  $a_R$  is the chemical activities of the species involved in the reaction.

### 3.1. Convention in electrochemistry

In an electrochemical half-cell the reaction of interest takes place on the working electrode (WE). The conventional RE is the standard hydrogen electrode (SHE) and by definition its potential is equal to 0.000 V at all temperatures. The potential of a cell is measured as the difference between the potential of the cathode and the potential of the anode. Usually SHE is not used as a typical RE because of its difficulties on operation. Commonly used REs are the either saturated calomel electrode (SCE) or the silver|silver chloride electrode (Ag|AgCl). Traditionally, the potential of a cell that utilizes standard conditions is as follows:

$$E^0_{\text{cell}} = E^0_{\text{cathode}} - E^0_{\text{anode}} \quad (6)$$

Here,  $E^0_{\text{cathode}}$  and  $E^0_{\text{anode}}$  refer to the  $E^0$  of the cathode and the anode, respectively.

Conventionally the anode is defined as the electrode where an oxidation occurs and the cathode as the electrode where a reduction occurs. There are two basic classifications of electrochemical cell:

- I. Galvanic cell: Electrical energy is produced from spontaneous reactions occurring at the anode and cathode when connected via a conductor.
- II. Electrolytic cell: The reactions are non-spontaneous and an external source is used to apply a potential difference across the cell to force the electrochemical reactions to take place.

In this thesis all cells are electrolytic cell and the graphical depiction of a voltammogram, i.e., a potential vs. current plot is expressed according to the European convention. According to this convention a positive potential (oxidation potential) and a positive current (anodic current) are to the right of the origin and vice versa.

### 3.2. Current

To understand what is happening at the electrode solution interface, i.e., the electrochemical reaction, the origin of the current and how the current changes with the applied potential is important. The current is equal to the change of charge with time and can be expressed as:

$$I = \frac{dQ}{dt} \quad (7)$$

Where  $I$  (A) is the faradic current, i.e., the redox process involved in the charge transfer reaction,  $t$  (s) is time and  $Q$  (C) is the charge given by Faraday's law:

$$Q = nFN \quad (8)$$

Here,  $F$  is the Faraday's constant =  $96,485.3 \text{ C mol}^{-1}$ ,  $n$  is the number of electrons transferred per mole of product,  $N$ . So, in order to reduce one mole of reactant from oxidant ( $O + ne^- \rightarrow R$ ), where  $n = 1$ , the total charge pass through the cell is  $9.65 \times 10^4 \text{ C}$ .

Chemical reactions can be either homogenous or heterogeneous. A homogeneous reaction occurs in a single phase and the reaction rate is uniform. Heterogeneous reactions are common in electrochemistry and take place at the electrode-solution interface. The rate of a heterogeneous reaction in which a charge is transferred between the two phases (an electrochemical reaction) can be expressed as follows:

$$\text{Rate (mol sec}^{-1} \text{ cm}^{-2}) = \frac{i}{nFA} = \frac{j}{nF} \quad (9)$$

Here  $j$  is the current density ( $\text{A cm}^{-2}$ ).

### 3.3. Factors affecting the rate of an electrode reaction

The four major factors govern the reaction rate at the electrode surface are listed below:

- I. Mass-transfer to/from the electrode surface.
- II. Kinetics of the ET.
- III. Chemical reactions preceding or following the ET.
- IV. Surface reactions, i.e., adsorption, desorption.

The above-mentioned factors are important to study in electrochemistry. Both kinetics and mass transfer control electrochemical systems. In kinetically controlled systems, the rate of ET is restricted. However, in a mass transfer controlled system, the heterogeneous ET rate is not the limiting factor but rather the rate with which the chemical species involved move through the bulk solution towards or away from the electrical double layer (EDL) at the electrode surface. Mass transfer is accomplished by three different modes:

- I. Migration: movement of charged particles in an electrical field.
- II. Diffusion: movement of species along a concentration gradient.
- III. Convection: movement of species persuaded by e.g., stirring.

In electroanalytical chemistry, control of the electrochemical system is of outmost importance and as migration cannot really be controlled in contrast to diffusion and convection, migration is largely suppressed as a means for mass transfer at the electrode/solution interface by the addition of a rather high concentration of supporting electrolyte. If we consider the simple reaction:  $O + ne^- \rightleftharpoons R$  where O is converted to R. The ET process at the electrode-solution interface is shown in **Figure 3**. The reaction may be considered as a set of equilibria that are involved, e.g. convection/diffusion of O from the bulk solution to the electrode surface, chemical reaction at the electrode surface that results in an ET to or from the electrode and convection/diffusion of R away from the electrode surface.

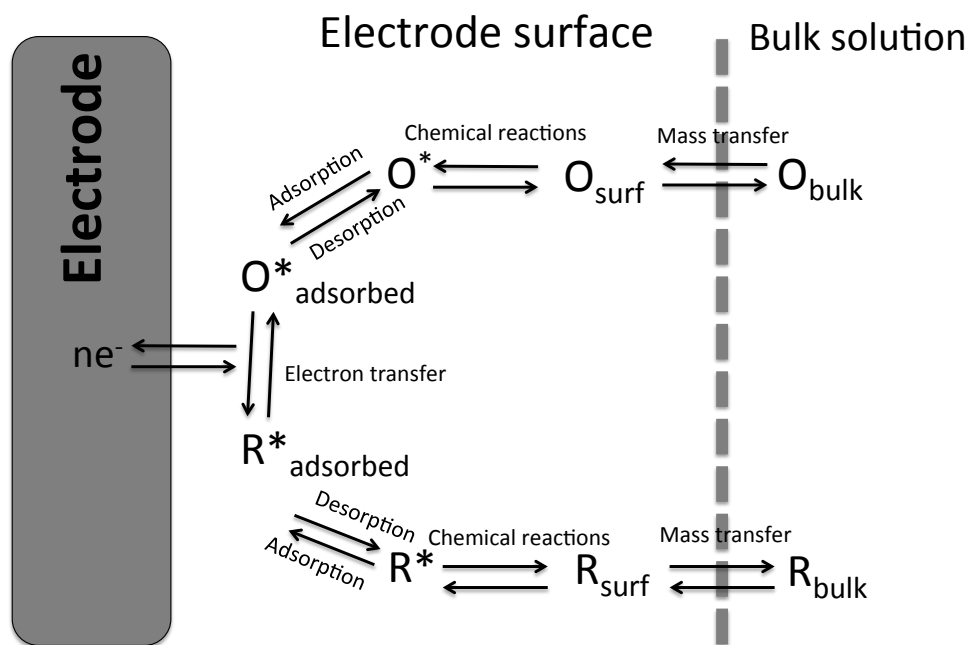


**Figure 3.** The ET process at the electrode-solution interface

### 3.4. Cell resistance

There are two types of current flows in an electrochemical cell, i.e., faradic current, and non-faradic current. All contributions to the current generated from oxidation or reduction reactions at the electrode-solution interface are defined as faradic current and are described by the following equation:

$$\frac{dQ}{dt} = \frac{d}{dt} (nFN) = nF \frac{dN}{dt} \text{ (i.e., } Q = nFN) \quad (10)$$

Where Q (C) is the charge, t (s) is the time, n is the number of electrons transferred, and F is the Faraday's constant. Current associated with the movement of electrolyte ions, reorientation of solvent dipoles, adsorption and desorption of ions, etc. at the electrode-electrolyte interface is considered as non-faradic current. All current follow Ohm's law:

$$I = \frac{V}{R} = \frac{V}{Z} \quad (11)$$

Here, I (A) is current, V (V) is potential, R ( $\Omega$ ) is the resistance. Z ( $\Omega$ ) is the impedance that includes resistance and capacitance arising from EDL.

### 3.5. Electrical double layer (EDL)

The heterogeneous ET occurs at the electrode-solution interface where the EDL<sup>99</sup> is developed. When an electrode is submerged into an electrolyte solution, as a consequence of non-identical surroundings mobile charge carriers (in the electrode; electrons, in the solution; ions) will spontaneously move to/from the interface to form an electrical double layer, EDL. This flow of charge is identical to a current and is denoted charging current. When the potential of the electrode is changed by the potentiostat or the composition of the solution is changed, a charging current (non-faradic) pass through the cell to compensate for the change. The EDL is composed of two different sub-layers (**Figure 4**).

The first layer contains solvent molecules and specifically adsorbed ions due to chemical interactions. The center of this electrical layer is called inner Helmholtz plane (IHP). The second layer consists of highly oriented solvent molecules and solvated ions located at the closest distance from the electrode, electrostatically interacting with electrode. The center of this 2<sup>nd</sup> electrical layer is called the outer Helmholtz plane (OHP). A schematic graphical presentation of the EDL is shown in **Figure 4**. The IHP and the OHP make up the compact double layer, in which the potential drop is virtually linear. Outside the OHP some organization of the solution is still at hand but less than within the compact double layer. This part is denoted the diffusive double layer and within this layer the potential drop is exponential. If the ionic strength of the electrolyte is sufficiently high there will only be a compact double layer and thus bulk properties will range all the way through the solution until the OHP.

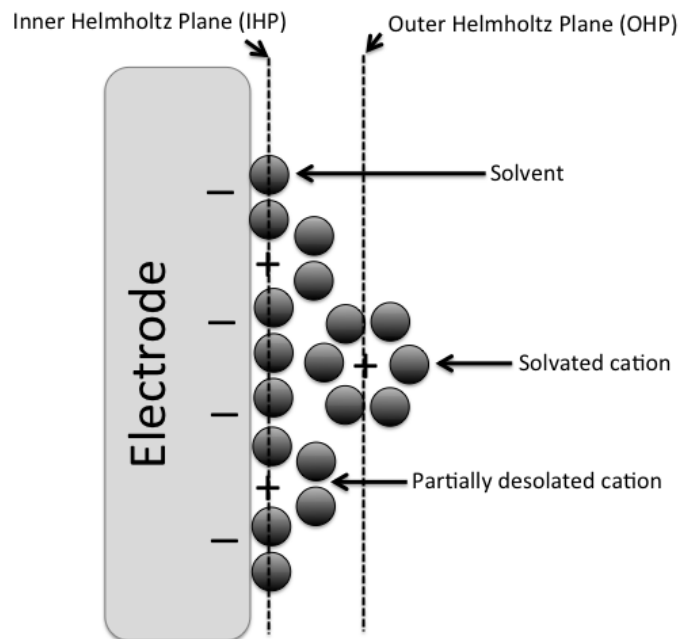


Figure 4. A schematic diagram of the electrical double layer (EDL).

## 4. Electrochemical techniques

The most commonly used electrochemical techniques can be classified into two major groups, i.e., static when  $I = 0$  and dynamic when  $I \neq 0$ . Potentiometry is the static method where equilibrium potential vs. time is measured. The most widely used potentiometric applications are pH measurements with a glass electrode and the use of other ion selective electrodes. The dynamic method includes cyclic voltammetry (CV), chronoamperometry (CA) and CA in combination with flow injection analysis (FIA). These techniques are extensively used in this thesis.

### 4.1. Cyclic voltammetry (CV)

CV<sup>100</sup> is the most versatile and broadly used electrochemical technique, where the potential is changed linearly with time and the current vs. potential<sup>96, 101</sup> is recorded. The rate at which the potential is scanned with time is called scan or sweep rate ( $\text{Vs}^{-1}$ ). In CV, the potential is scanned at a constant rate between two values, i.e., the initial potential ( $V_1$ ) and the switching potential ( $V_2$ ). The potential starts to scan from  $V_1$  and reaches  $V_2$ , and then the scan is reversed back to  $V_1$  (**Figure 5 A**). In a typical CV, the potential waveform is triangular. If we consider a redox couple ( $\text{Fe}^{2+}/\text{Fe}^{3+}$ ) then the following CV will represent its electrochemical properties (**Figure 5 B**).

In the beginning before the potential approaches the potential, where oxidation starts there is no faradaic current, however, as the applied potential is constantly and linearly changed there is a constant contribution from the charging current (**Figure 5 B**). During the potential scan from  $V_1$  to  $V_2$ , the equilibrium position between the O and R forms of the redox couple shifts from the fully reduced ( $\text{Fe}^{2+}$ ) at  $V_1$  to the fully oxidized form ( $\text{Fe}^{3+}$ ) at  $V_2$ . When the potential reaches a more oxidizing potential, the equilibrium starts to shift to generate more of the O form and the anodic current begins to flow. At some point the anodic current reaches a peak value, where the surface concentration of O at the electrode surface drops down to nearly zero due to mass transfer limitations as the Nernst diffusion layer has been depleted of O. In this situation the anodic current starts to drop down following the Cottrell<sup>102</sup> equation. The electron transfer in  $\text{Fe}^{2+} \rightleftharpoons \text{Fe}^{3+} + e^-$  is faster than the voltage scan rate. During the voltage scan an equilibrium is established at



the electrode surface obeying the Nernst equation. For an electrochemically reversible reaction E is always in equilibrium with the surface concentrations,  $[O]_{x=0}$  and  $[R]_{x=0}$ .

$$E_{\text{appl}} = E^0 + \frac{RT}{nF} \ln \frac{[O]_{x=0}}{[R]_{x=0}} \quad (12)$$

The reversed scan ( $V_2$  to  $V_1$ ) moves in a similar but reverse way and completes the CV. A graphical presentation of a typical CV is shown in **Figure 5 B**.

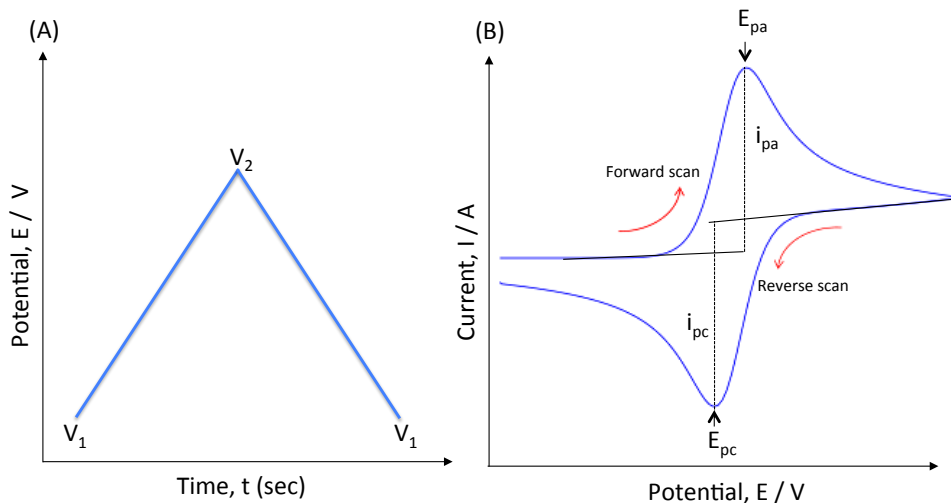


**Figure 5.** A graphical presentation of a CV. (A) the potential waveform and (B) a typical CV of an electrochemically reversible reaction.  $E_{pa}$  and  $E_{pc}$  indicate the anodic peak potential and the cathodic peak potential,  $i_{pa}$  and  $i_{pc}$  indicate the anodic peak current and the cathodic peak current.

**Parameters in CV:** In an electrochemically reversible reaction, where the reaction kinetics are fast the current is limited by the diffusion of O and R to or from the electrode. For an electrochemically reversible reaction the CV has some distinct characteristics, which are listed below:

**Peak potential:** The potential at which the peak current is reached its maximum value is called the peak potential. The peak potentials at maximum anodic current and maximum cathodic current are referred to as  $E_{pa}$  and  $E_{pc}$ , respectively. The formal potential ( $E^{0'}$ ) of a redox couple is determined by averaging the  $E_{pa}$  and  $E_{pc}$ .

$$E^{0'} = \frac{E_{pa} + E_{pc}}{2} \quad (13)$$

The difference in peak potentials ( $\Delta E_p$ ) is used to determine the electrochemical reversibility. For an electrochemically reversible reaction,  $\Delta E_p$  does not change with scan rate,

$$\Delta E_p = E_{pa} - E_{pc} = \frac{59}{n} \text{ mV [at 298 K]} \quad (14)$$

whereas for a quasireversible and an irreversible reaction  $\Delta E_p$  changes with an increased scan rate.

**Ratio of peak current:** The ratio of the anodic peak current ( $i_{pa}$ ) and the cathodic peak current ( $i_{pc}$ ) for an electrochemically reversible reaction is equal to one.

$$\frac{i_{pa}}{i_{pc}} = 1 \quad (15)$$

**Peak current depends on scan rate:** In an electrochemically reversible system,  $i_p$  increases linearly with the square root of the scan rate. During the scan the diffusion layer of the analyte grows further away from the electrode, initially the concentration gradient increases and results in a higher current. However, at some potential the surface concentration of O,  $[O]_{X=0}$  equals 0, and thereafter the current will decrease as a result of a that the concentration gradient will continuously become less and less and as a consequence the current will continuously decrease. In a diffusion controlled reversible system, the peak current depends not only on the analyte concentration and diffusion coefficient but also on scan rate as expressed by the Randles-Sevcik equation<sup>103</sup>.

$$i_p = 0.4463 nFAC \left( \frac{nFvD}{RT} \right)^{1/2} \quad (16)$$

Here, A is the area of working electrode ( $\text{cm}^2$ ), D is the diffusion coefficient of analyte ( $\text{cm}^2 \text{s}^{-1}$ ), C is the analyte concentration ( $\text{mol cm}^{-3}$ ) and  $v$  is the scan rate ( $\text{Vs}^{-1}$ ). The symbols within  $nFRT$  have their regular values stated above. When the solution is at 25 °C equation (20) can be expressed as follows:

$$i_p = (2.69 \times 10^5) n^{3/2} A D^{1/2} C^{1/2} v^{1/2} \quad (17)$$

Therefore, peak current increases linearly as a function of the square root of the scan rate of a reversible system. A plot of  $i_p$  and  $v^{1/2}$  should be linear and pass through origin and thus the diffusion coefficient (D) can be calculated from the slope.

$$i_p \propto \sqrt{v} \quad (18)$$

To characterize the electrochemical reversibility an  $i_p$  vs.  $\sqrt{v}$  plot can be used. A deviation from the linearity indicates kinetic restrictions in the ET system. However, if the redox species are immobilized on the electrode surface either by physical adsorption or covalent bonding, the diffusion coefficient ( $D$ ) will no longer control  $i_p$ . In this situation  $i_p$  is directly proportional to the surface coverage ( $\Gamma$ ) and the scan rate ( $v$ ) rather than the square root of the scan rate ( $\sqrt{v}$ )<sup>104</sup>.

$$i_p = \frac{n^2 F^2 \Gamma A v}{4RT} \quad (19)$$

The surface coverage ( $\Gamma$ ) of the electro-active species on the electrode surface can be calculated from Faraday's law<sup>105</sup>.

$$Q = nFA\Gamma \quad (20)$$

Here  $Q$  is the electrical charge involved in the reaction.

In bioelectrochemistry, CV has been extensively used to study EET of microorganisms to the electrodes<sup>57, 106</sup>, their electrochemical activity<sup>107</sup> in biological fuel cells<sup>108</sup>, in microbial biosensors<sup>19a</sup>, in photo-bioelectrochemical system to harnessing solar energy<sup>109</sup>.

## 4.2. Chronoamperometry (CA)

In CA either a single constant applied potential or various potential steps are used and the output is plotted as current vs. time. CA can be performed either in a stagnant solution and then mass transfer of electroactive species to/from the electrode is diffusion controlled or one can combine constant convection with diffusion in e.g., a flow system with a constant flow and with the WE located in an electrochemical flow through system or with the use of a rotating disk electrode.

For the case when a stagnant solution is used the following description explains how the current will vary with time. If we consider  $R$  as an electroactive species and thermodynamically unfavorable to be oxidized at the initial applied potential,  $E_1$ . Then the potential is stepped to  $E_2$ , where  $R$  is oxidized to  $O$ .  $E_2$  is selected so that the  $[R]_{x=0}$  is 0 (**Figure 6 A**). In the beginning ( $t_1$ ) the concentration of  $R$  close to the electrode surface is high and as a consequence results in a steep slope of the concentration profile and thus a high current. The slope gradually decreases with time, see  $t_2$  and  $t_3$  (**Figure 6 B**). The current (**Figure 6 C**) is a result of the diffusion of  $R$  from the bulk to the electrode surface (and out diffusion of  $O$  from the electrode surface to the bulk). In the beginning, the current reaches the highest level due to the high concentration of  $R$  near the electrode surface, see the

concentration profile. As the reaction occurs with time, the concentration of R decreases with time and at the end, the current (**Figure 6 C**) reaches zero, since the diffusion layer is totally depleted of O.

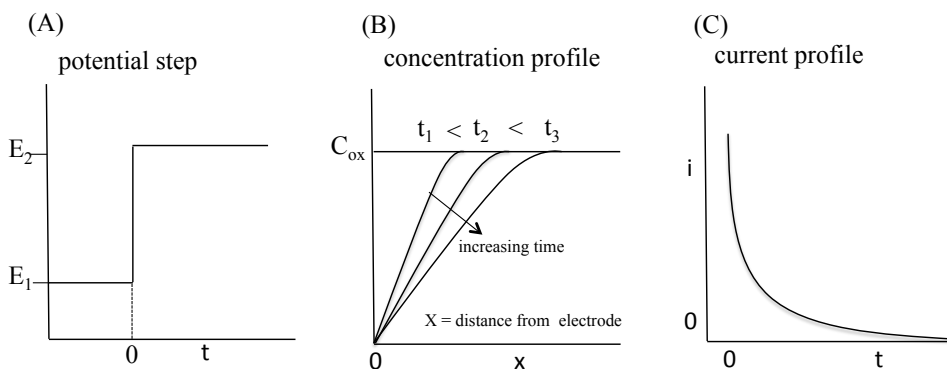


**Figure 6.** Potential step experiment in CA where  $E_2 > E_1$ ; (A) potential waveform (B) concentration profile adjacent to the electrode with increasing time ( $t$ ) and (c) current ( $i$ ) vs. time ( $t$ ).

In CA, the Cottrell equation<sup>102</sup> for the strongly anodic case,  $C_{R,X=0} = 0$ , is the most useful expression that describes the variation of current followed by a large potential step for a reversible redox reaction on a planar electrode with time.

$$i = \frac{nFAC_R\sqrt{D_R}}{\sqrt{\pi t}} \quad (21)$$

Here,  $i$  is current,  $n$  is the number of electron transferred in the reaction;  $F$  is Faraday's constant,  $A$  is the area of the planar electrode ( $\text{cm}^2$ ),  $C_R$  is the initial concentration of the electroactive species ( $\text{mol cm}^{-3}$ ),  $D_R$  is the diffusion coefficient of the electroactive species ( $\text{cm}^2 \text{sec}^{-1}$ ) and  $t$  is time (sec).

This is the general Cottrell equation valid for a planar electrode. Besides that further derivations of this equation can be found for electrodes of other geometries. To test if a redox reaction is diffusion controlled,  $i$  vs.  $\sqrt{t}$  is plotted and the graph will presumably be linear. This equation can also be used to measure the electroactive surface area of the electrode ( $A$ ) by using a redox couple of known values of  $n$  and  $D$  as well as of the concentration of the electroactive species.

### 4.3. Flow injection analysis (FIA)

CA in combination with FIA<sup>110</sup> is a very simple but very useful electrochemical technique, where a constant potential is applied to the WE and the current is measured with time. The applied potential is selected from CV measurement, where the  $E^{0'}$  of the redox couple is determined. If we consider the basic reaction,  $O + ne^- \rightleftharpoons R$  and  $E^{0'}$  of this particular redox couple is 0 mV vs. Ag|AgCl (sat. KCl). If the oxidation reaction is of interest to follow then a sufficient positive potential ( $> E^{0'}$ ) is to be applied on the WE and vice versa. The applied potential also depends on electrochemical reversibility.

To control the mass transfer of the analyte either to or from the electrode, two strategies can be considered and these are listed below:

- I. Moving the electrode with respect to the electrolyte, i.e., rotating disk electrode, where an electrode moves during the experiment to induce the flux of analyte to the electrode.
- II. Moving the electrolyte with respect to the electrode, e.g., in the wall-jet configuration<sup>111</sup>, where the electrolyte flows to the electrode by means of a pump.

A device for hydrodynamic voltammetry is the wall-jet cell, where a controlled flow of electrolyte to a disk electrode is provided<sup>112</sup>. In 1975, Růžička and Hansen pioneered the idea of FIA and discussed the influence of the sample volume, tubing dimensions and the flow rate on the detector response<sup>113</sup>. FIA<sup>114</sup> has been extensively used in different electro-analytical applications in agriculture, food industry, biochemical, clinical and environmental processes<sup>115</sup>, e.g., determination of glycerol in biodiesel<sup>116</sup> amperometric detection of  $Cu^{2+}$  in yeast biosensor<sup>117</sup> and glucose biosensing<sup>118</sup>.

FIA is based on the injection of a liquid sample into a moving, non-segmented continuous carrier stream of an electrolyte. The injected sample forming a zone is subsequently carried to a detector that continuously records one of a series of possible variables, e.g., absorbance, current, potential, or other physical parameters<sup>110</sup>. A demonstration of the FIA system would be helpful for a better understanding of how FIA system works<sup>119</sup>. The simplest FIA system consists of a pump that continuously pumps the carrier solution, most commonly an aqueous based buffer solution, an injector with which a well-defined and highly reproducible sample volume is injected into the carrier solution, a flow through detector that is able to detect a particular parameter of interest, e.g., current, and a recorder to record continuously any changes registered by the detector, see Figure 7. The details of the construction of the FIA system used in this thesis was reported earlier<sup>120</sup>.

There are a number of different flow through electrochemical detector designs and among those the thin-layer and the wall jet cells are the most commonly used<sup>121</sup>. Throughout the work done in this thesis only a wall jet cell has been used. In the wall-jet arrangement the flow enters the cell perpendicular to the electrode surface and the jet flow very efficiently spreads the solution onto the electrode surface<sup>111</sup>. **Figure 7** shows the various parts of the wall-jet cell. The WE is located in the upper part, the CE made of a Pt thread circulates the bottom of the circular cell, and the RE is located in a separate lower part, which is in contact with the upper part through four small holes surrounding the inlet flow preventing the mixing of the carrier solution and solution (0.1 M KCl) in the chamber for the RE. These two parts are screwed together to adjust the distance of the WE from the inlet of the carrier solution (around 1-2 mm). The RE is an Ag|AgCl (0.1 M KCl), where the KCl solution is saturated with Ag<sup>+</sup> to maintain a constant [Cl] and thus a constant applied potential. The mass transfer limited current in a wall-jet type cell is given below:

$$i_{lim} = 0.89nFCD^{2/3}v^{-5/12}a^{-1/2}A^{3/8}U^{3/4} \quad (22)$$

Here,  $i_{lim}$  is the mass transfer limited current  $v$  is kinematic viscosity (for water at 20 °C,  $v = 0.01 \text{ cm}^2 \text{ sec}^{-1}$ ),  $a$  is the diameter of the inlet tube,  $A$  is the electrode surface area and  $U$  is the volumetric flow rate.

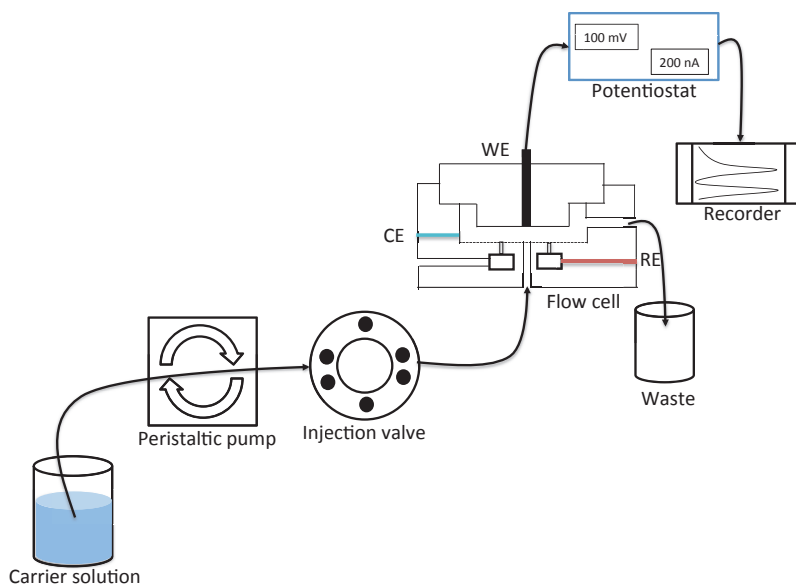


**Figure 7.** A schematic presentation of a FIA system.

**Dispersion in FIA:** When a sample is injected into the carrier solution it will disperse before reaching the detector and the dispersion depends basically on the volume of the injected sample, the geometry of the inlet tubing (i.e., diameter and length), the flow rate of the carrier, and the design of the flow through detector. To correlate the original injected sample concentration with the detector response it is important to know the dispersion factor of the system. The dispersion coefficient (Dc) is the ratio of the analytical read out by the sample concentration before and after the dispersion process has taken place in the carrier solution<sup>110</sup>. A sample having been subjected to dispersion during its way to the detector will generate a lower response. In amperometric detection, the dispersion coefficient is measured by using a fast redox couple, e.g., (ferricyanide/ferrocyanide) and can be expressed as follows:

$$Dc = \frac{\text{Steady state current when the sample itself is passed to the detector (Iss)}}{\text{Peak current when sample moves to the electrode via the carrier solution (Ip)}} \quad (23)$$

From eqn. 27 it follows that D is  $\geq 1$ .

The advantages of using FIA are fast, precise, accurate, a low volume of sample is required for analysis, offers the possibility to control any drift in the background current of the WE with time, a low signal to noise ratio, quantitative, highly reproducible and tremendously versatile, simple in operation and cheap<sup>110</sup>.

## 5. Electrode material

The electrode material is a key component in (bio)electrochemistry. The most commonly used electrode materials are based on inert conducting materials such as platinum, gold and a whole variety of carbon-based electrodes. Especially carbon based electrodes are commonly used in (bio)electrochemistry<sup>122</sup>. The good conductivity, wide electrochemical potential range, availability, versatility, easy handling and low cost of carbon materials make them widely used<sup>123</sup>. The most common form of carbon materials used in electrode materials is based on  $sp^2$  hybridized carbon atoms that form a variety of microstructures including highly ordered pyrolytic graphite (HOPG) to more polymer like structures<sup>124</sup>.

### 5.1. Graphite electrode

The carbon atoms of the electrode surface can be exposed as basal plane or edge plane. In basal plane electrodes a single graphene layer is exposed at the surface. In edge plane electrodes many graphene layers are exposed at the surface. The surface chemistry of the edge plane is complex and it reacts with atmospheric oxygen and forms a variety of oxygen containing functional groups on the surface<sup>123, 125</sup>, e.g., carbonyl, phenolic, hydroxyl, keto, quinone and carboxyl groups. These functional groups are the sites of ET processes<sup>126</sup> and often react with other molecules<sup>127</sup>. A schematic representation of a HOPG electrode surface and their oxygen containing functionalities are shown in **Figure 8**.



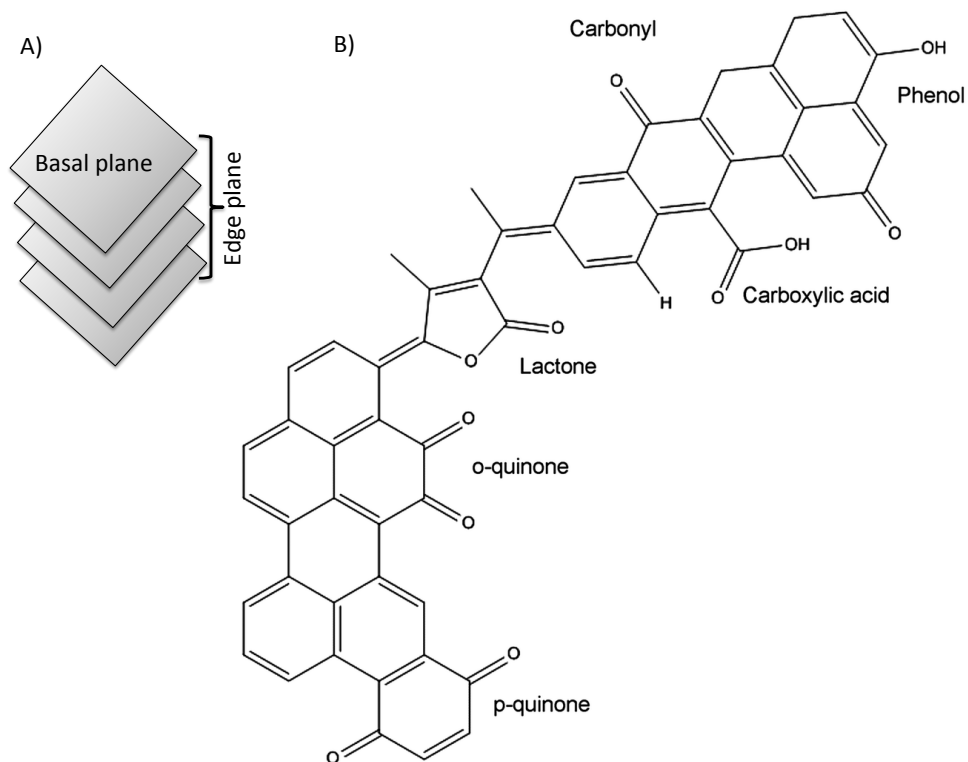


**Figure 8.** (A) A schematic picture of a HOPG electrode surface exhibiting the basal plane and the edge plane and (B) possible oxygen containing functionalities on an edge plane surface (adapted from <sup>127</sup>).

These functional groups contribute to interfering faradic currents and may result in an additional background current<sup>128</sup>. As these oxygen functional groups are immobilized on the electrode surface the current from their redox conversion obeys a linear relation between current and scan rate just like the capacitive current and therefore their contribution is usually denoted as pseudocapacitance. In this thesis spectroscopic graphite electrodes have been mostly used, where the structure consists of a random mixture of basal and edge planes. Spectroscopic graphite is pure, highly porous and generates a high charging current<sup>129</sup>. The most easily detectable electrochemically active functionality, surface confined quinones<sup>130</sup>, on a HOPG electrode can act as an electron shuttle for enzymes and catalyze the oxidation of NADH<sup>131</sup>. Reproducible preparations of graphite electrodes are challenging due to the uncontrolled formation of these functional groups<sup>124</sup>.

## 5.2. Gold electrode

The electrochemical characteristics of electrodes made of noble metals such as gold, platinum or silver are very well defined<sup>132</sup>. The ET-kinetics for many redox systems on metal electrodes is faster and the anodic potential window is wider compared to that of the carbon based electrodes. Gold electrodes can come either in bulk form or as a thin film form, where a few hundred nanometers of gold is deposited on a suitable substrate such as glass, silicon and mica. The cathodic potential of metal electrodes is limited due to hydrogen evolution<sup>132</sup>. The formation and reduction of surface oxides and adsorption and desorption of H<sup>+</sup> and other ions may lead to a high background current that may affect the kinetics of the studied electrode reaction. The chemical properties of gold electrodes are highly stable. Gold electrodes are easily obtainable and conveniently manufactured<sup>133</sup>.

Gold atoms form many possible crystal planes on the electroactive surface. In this thesis only polycrystalline gold electrodes containing a combination of all possible crystalline planes were used. The immobilization of biomaterials on a bare gold electrode surface may cause denaturation due to the somewhat hydrophobic characteristics of gold<sup>133</sup>. To improve the situation, gold electrodes are modified with self-assembled-monolayers (SAMs)<sup>134</sup> of thiol compounds to enhance the biocompatibility and to establish beneficial hydrophilic/hydrophobic/electrostatic interactions between biomaterials and the SAM on the electrodes.

# 6. Biomaterials

## 6.1. *Rhodobacter capsulatus*

*R. capsulatus* is a gram-negative, purple non-sulfur, prokaryotic  $\alpha$ -proteobacterium<sup>135</sup>. It is one of the most metabolically versatile bacteria and can grow under diverse metabolic conditions<sup>136</sup>, e.g., photosynthetic, aerobic respiring, anaerobic respiring and chemolithotrophic. *R. capsulatus* can also grow photoauto- or photoheterotrophically, where an inorganic or an organic electron donor is supplied, respectively, and light is used as an extra energy source<sup>135b</sup>. *Rhodobacter* can synthesize a variety of substrates e.g., organic acids, fatty acids, amino acids, alcohols, carbohydrates and aromatic compounds<sup>135b</sup>. The photosynthetic growth of *R. capsulatus* requires both light and anoxic conditions usually found in lakes, ponds, and in other aquatic environments<sup>135b</sup>.

Photosynthesis in *R. capsulatus* is considerably simpler compared to the corresponding system in cyanobacteria and eukaryotic organisms. In *R. capsulatus*, photosynthesis occurs in their intracellular membrane, whereas in eukaryotic organisms it is located in a subcellular organelle called chloroplast. *Rhodobacter* contains one photosystem and cannot split water. Thus when grown photoheterotrophically, *R. capsulatus* cells require to be provided with an electron donor, e.g., an organic substrate. The ET system in *Rhodobacter* is cyclic, whereas in cyanobacteria and eukaryotic organisms it is non-cyclic, see below. The growth of *R. capsulatus* is complicated and depends on the quality and intensity of light, anoxic condition, pH, and temperature<sup>135b</sup>.

*Rhodobacter* is used as a common tool to study photosynthesis and classical biochemical events and its genetic information is known<sup>135b</sup>. Previously *R. capsulatus* was also reported for bio-hydrogen production<sup>137</sup>. However, very few electrochemical studies on *R. capsulatus* have been reported in the literature<sup>138</sup>.

In this thesis we studied the EET from *R. capsulatus* grown in both aerobic heterotrophic conditions<sup>139</sup> as well as in anaerobic photoheterotrophic conditions<sup>140</sup>. The feasibility of using *R. capsulatus* as a microbial catalyst in BESs has been demonstrated.

## 6.2. *Shewanella oneidensis* MR-1

*S. oneidensis* MR-1 is a dissimilatory metal ion-reducing bacterium and is widely studied in BESs. It is a gram-negative, facultative anaerobic, electrogenic and metabolically versatile<sup>36</sup> bacterium. It can use a diverse range of metal ions as electron acceptors, e.g., manganese (IV), iron (III) and has its own electron conduit system in the outer membrane. It is one of the few bacteria having a well documented DET competence through its outer membrane bound cytochromes<sup>43</sup>. In addition pilus-like electrically conductive appendages “nanowires” attached to the outer membrane in *S. oneidensis* MR-1 are capable of transferring electrons over a multiple cell length distance of ( $\approx 50 \mu\text{m}$ ) to an insoluble electron acceptor. It can produce nanowires while exposed to an environment with limited oxygen availability<sup>43</sup>.

Studies indicated that EET in *S. oneidensis* occurs via membrane-associated cyt *c*. In *S. oneidensis* electrons are transferred from quinones bound in the inner membrane, then through the periplasm and to the outer membrane<sup>141</sup>. Electrons are then subsequently transferred to the extracellular environment either by direct electrical contact with insoluble metal oxides or shuttled by excreted flavins, which in turn can transfer the electrons to an electron acceptor at a further distance<sup>141</sup>. Both riboflavin (vitamin B2) and flavin mononucleotide (FMN) are documented as endogenous mediators and are able to contribute in EET. It was demonstrated that flavins in *S. oneidensis* are responsible for 75% of its entire EET activities<sup>142</sup>. In the absence of O<sub>2</sub> or any other soluble electron acceptor, *S. oneidensis* MR-1 forms a 3D biofilm<sup>143</sup> on insoluble electron acceptors and when grown on electrodes this results in a higher catalytic current<sup>38</sup>.

We studied the enhanced current density when *S. oneidensis* MR-1 were immobilized on (Os-(bpy)PVI)(1:9) modified graphite electrodes. These findings suggest that the inherent EET of this exoelectrogen can be further coupled with the ORPs to result in a several fold higher current density<sup>144</sup>.

## 6.3. Thylakoid membranes (TMs) from spinach

TMs are the site of photosynthesis in green plants and algae. They are the most abundant of the biological membranes and are unique for their distinguished chemical structure and composition. The quantum efficiency of TMs is nearly 100% that make them a potential candidate to use in photosynthetic electrochemical cells. In electrochemical applications there are several advantages of using TMs compared with isolated photosystems. TMs are relatively stable, since the photosynthetic protein complexes e.g., PSI, PSII and Cyt *b<sub>6</sub>f* remain in their native environment. There are multiple photosynthetic ET routes in TMs

compared to their isolated counterparts. The electrochemical immobilization of TMs on electrode surfaces is fairly simple compared with the immobilization of the isolated photosystems. Substantial efforts have been made on TMs to harness solar energy<sup>51, 54a</sup>.

In this thesis we have studied the photoelectrochemical communication of TMs with gold electrodes via a series of quinone derivatives<sup>145</sup>. In addition we investigated the photocurrent generation from TMs immobilized on ORPs modified graphite electrodes<sup>54d</sup>.

#### 6.4. *Leptolyngbya* sp. (CYN65) (CYN82) and *Chroococcales* sp. (CYN67)

CYN65, CYN67 and CYN82 are benthic prokaryotic cyanobacteria organisms. CYN65 and CYN67 are from Antarctica and CYN82 is from New Zealand. Benthic organisms can grow on surfaces and are considered to have a greater electrogenic activity compared to their planktonic counterparts such as *Synechocystis* sp., *Spirulina* sp., and *Anabaena* sp.<sup>146</sup>. Benthic cyanobacterial species become positively buoyant, detach from the growth surface and form floating mats during their growth cycle. This self-harvesting characteristic of benthic species is considered to have potential advantages in large-scale commercial applications of BPVs, since this will minimize the dewatering costs<sup>147</sup>.

Moreover, prokaryotic cyanobacteria are considered as the superior photosynthetic organisms in BPVs, due to their simpler physiology and lower energy requirements compared to their eukaryotic counterparts. Cyanobacteria are able to grow in almost all environmental conditions that will provide them to harness solar energy in a versatile global area. In cyanobacteria photosynthesis occurs in TMs and respiration occurs in CMs inside the complex membrane system and PETC and RETC are interconnected and share electrons<sup>51a, 51b</sup>.

In this thesis we have investigated the photosynthetic electrogenic activity of CYN65, CYN67 and CYN82<sup>148</sup> and compared their EET competence for photocurrent generation<sup>149</sup>.

#### 6.5. *Paulschulzia pseudovolvox* (UKE)

UKE is a eukaryotic multicellular green alga collected from Lake Tikitapu, New Zealand. UKE is demonstrated to have a greater photosynthetic electrogenic activity compared to cyanobacteria under identical conditions in PMFC. UKE is a strong benthic organism and grows in both low and high salt media.<sup>146</sup> Algae are photosynthetic organisms and account for 50% of the overall photosynthesis and

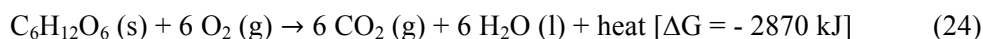
CO<sub>2</sub> fixation on earth. The photosynthetic events in eukaryotic algae and in plants are identical. Eukaryotic algae are preferable in BPVs, since they can be used to feed heterotrophic organisms when grown in a mixed culture<sup>150</sup>. In addition autotrophic organisms can be used to produce hydrogen as an alternative source of energy<sup>151</sup>. Moreover, algae were demonstrated for biodiesel production due to their efficient light absorption and conversion into chemical energy<sup>152</sup>.

In this thesis we have studied the photoelectrochemical communication of UKE immobilized on graphite electrodes and ORPs modified graphite electrodes<sup>153</sup>. In addition we have compared the photocurrent generation by UKE with three cyanobacterial species (CYN65, CYN67 and CYN82)<sup>149</sup>.

# 7. Bacterial respiration

In BESs<sup>24</sup>, microbial respiration is used to convert chemical energy into electrical energy<sup>37a</sup>. The chosen electrode material in BESs is used as final electron acceptor. In 1911, Potter reported “the disintegration of organic compounds by microorganisms is accompanied by the liberation of electrical energy”<sup>154</sup>. Bacterial respiration<sup>155</sup> is the key way for bacterial cells to gain useful energy for their growth and maintenance. A series of metabolic processes are used in bacterial respiration to convert biochemical energy from nutrients, e.g., organic carbon, into highly energetic compounds such as NAD(H) and adenosine triphosphate (ATP), the universal cellular energy. In this chapter emphasis is given on aerobic respiration (AR), since the bacterial cells used in this study, e.g. *Shewanella oneidensis* MR-1 and heterotrophic *Rhodobacter capsulatus* were grown under aerobic conditions.

In AR, O<sub>2</sub> is used as terminal electron acceptor to generate ATP by oxidizing energy rich substrates. The typical nutrients used by the microorganisms are carbohydrates, fats and proteins. In AR, CO<sub>2</sub> and H<sub>2</sub>O are released. The simplified reaction for AR can be written as follows:



The negative sign of  $\Delta\text{G}$  indicates a spontaneous reaction. The energy released during this process is used to drive thermodynamically unfavorable reactions in catabolic reactions. AR is considered efficient than that of anaerobic respiration since in this process organic substrates are completely oxidized into CO<sub>2</sub>. AR. The overall process of bacterial respiration is shown in **Figure 9**. The initial step of bacterial respiration is glycolysis.

## 7.1. Glycolysis

Glycolysis is the metabolic process that converts glucose (C<sub>6</sub>H<sub>12</sub>O<sub>6</sub>) into pyruvate (CH<sub>3</sub>COCOOH) by a series of enzyme catalyzed reactions and intermediate metabolites<sup>156</sup>. The free energy released in this process is used to form ATP and reduced nicotinamide adenine dinucleotide (NADH)<sup>156</sup>. Glycolysis is an oxygen independent process, where atmospheric oxygen, O<sub>2</sub>, is not used<sup>157</sup>. However, in

AR, the glycolytic products, i.e., pyruvate and NADH are catalyzed by atmospheric molecular  $O_2$  as the terminal electron acceptor. Instead, in anaerobic respiration,  $O_2$  is not used for the catalysis of the glycolytic products. Therefore, glycolysis is a universal processes in most organisms irrespective of aerobic or anaerobic respiration. In the majority of all organisms, glycolysis occurs in the cytosol, also called the intracellular fluid or the cytoplasmic matrix. Most common glycolytic processes follow the Embden-Meyerhof-Parnas (EMP) pathway<sup>157</sup>. Inhibiting or activating the involved enzymes in glycolysis results in slowing down or speeding up those reactions regulating glycolysis. An overview of glucose oxidation is presented in **Figure 9**.

## 7.2. Tricarboxylic acid cycle (TCA-cycle)

In aerobic respiration pyruvate is transferred by pyruvate decarboxylation into acetyl-CoA (and  $CO_2$ ), the entry point in the TCA cycle<sup>158</sup>. The TCA cycle is also known as the citric acid cycle or the Krebs's cycle. In bacterial cells this cycle takes place in the cytosol. The TCA-cycle is the metabolic hub in aerobic respiration and the collective pathway for the oxidation of carbon fuels, e.g., amino acids, fatty acids, and carbohydrates. Acetyl-CoA is further oxidized into  $CO_2$  and generates the energy rich electron carriers, i.e., NADH and reduced flavin adenine dinucleotide ( $FADH_2$ ). This cycle is considered as highly energy efficient, since a limited number of molecules in Nature are able to generate NADH and  $FADH_2$ . The TCA-cycle together with oxidative phosphorylation, where NADH and  $FADH_2$  are used to generate ATP, provide the majority of the energy needed for aerobic organisms. The TCA-cycle is regulated by the substrate availability and product inhibition. The TCA cycle in bacterial respiration is presented in **Figure 9**.

## 7.3. Electron transfer chain (ETC)

In the ETC<sup>159</sup>, electrons are transferred from electron donors to electron acceptors via a series of enzymatic reactions. Electrons are transferred from lower electronegative molecules to higher ones and the process continues until the electrons reach the maximum electronegative molecule ( $O_2$ ) in the ETC. In eukaryotic cells the ETC is located in the mitochondrial inner membrane, whereas in bacterial cells it is located in the cytoplasmic membranes. The ETC in the bacterial cell is versatile, since these cells are able to grow in a variety of growth conditions<sup>160</sup> using different substrates<sup>161</sup>. The ETC in bacterial cells is similar to that in mitochondria<sup>2</sup>. In the ETC, electrons are transferred from NADH and  $FADH_2$  to  $O_2$ .



There are four membrane bound multiunit protein complexes in the ETC. Complex I, NADH dehydrogenase, is the most complex and largest protein in the ETC<sup>162</sup>. It transfers two electrons from NADH to ubiquinone (Q), a lipid soluble electron carrier, and forms ubiquinol (QH<sub>2</sub>) that can freely diffuse through the membrane. Together with ET, complex I translocates four protons (H<sup>+</sup>) across the membrane for each NADH molecule that is oxidized. It is the site of premature electron leakage to O<sub>2</sub> and results in the formation of reactive oxygen species (ROS)<sup>163</sup>.

Complex II, succinate ubiquinone oxidoreductase, is the only protein complex that participates in both the TCA cycle and in the ETC<sup>164</sup>. It transfers electrons from FADH<sub>2</sub> to Q generating QH<sub>2</sub>. Complex II also oxidizes succinate produced in the TCA cycle. Unlike complex I, complex II does not pump H<sup>+</sup> across the membrane and is considered as a less energy efficient complex. QH<sub>2</sub> transfers electrons to the Q-cycle.

Complex III, cytochrome *bc*<sub>1</sub> complex<sup>165</sup>, transfers electrons from QH<sub>2</sub> (produced by complex I & II), to cytochrome *c* (cyt *c*) via the Q-cycle<sup>166</sup>. Cyt *c* is known as a highly water soluble protein on membrane surface. The reaction mechanism of complex III is known as the Q-cycle, where two QH<sub>2</sub> are oxidized to Q and one Q is reduced back to QH<sub>2</sub>. In doing so complex III pumps out four H<sup>+</sup> equivalents from the inside to the outside of the membrane and only two H<sup>+</sup> equivalents are received from the inside that results in a H<sup>+</sup> gradient across the membrane. Electrons can leak out from the ETC in the Q-cycle and result in formation of ROS that are highly toxic for the cell<sup>167</sup>.

In complex IV, cytochrome *c* oxidase<sup>168</sup>, four electrons are transferred from four molecules of cyt *c* (one at a time) to O<sub>2</sub> and produce two molecules of H<sub>2</sub>O. It is the final protein complex in the ETC. In the process it binds with four H<sup>+</sup> equivalents inside the membrane to produce H<sub>2</sub>O. At the same time it translocates four H<sup>+</sup> equivalents across the membrane and results in the electrochemical H<sup>+</sup> gradient, which in turn is used by ATP synthase to generate ATP<sup>169</sup>. All these complexes are linked by Q, and cyt *c*<sup>170</sup>. They contain several prosthetic groups that are organized in a way that ET occurs in an ordered fashion. Complex I-IV are summarized in **Table 2**.

**Table 2.** The four protein complexes in the ETC.

Complex	Redox centers	Comments	Ref
I. NADH dehydrogenase	Flavin mononeocleotide (FMN) Fe-S clusters, quinones	Transmembrane, pumps H <sup>+</sup>	171
II. Succinate quinone oxidoreductase	Flavin adenine dinucleotide (FAD)	Membrane bound, does not pump H <sup>+</sup>	172
III. Cytochrome <i>bc</i> <sub>1</sub> complex	Fe-S cluster, Heme <i>b</i>	Transmembrane, pumps H <sup>+</sup>	173
IV. Cytochrome <i>c</i> oxidase	Heme <i>c</i> , Fe-S cluster, Heme <i>a</i> , Cu	Transmembrane, pumps H <sup>+</sup>	174

#### 7.4. ATP synthase (ATP syn)

ATP syn<sup>175</sup> is a membrane bound enzyme found in all living organisms. In bacterial cells ATP syn is located in the CM. The electrochemical  $H^+$  gradient generated in the ETC is used by this enzyme to synthesize ATP from adenosine diphosphate (ADP) and inorganic phosphate (iP). In most of the organisms ATP is the universal energy molecule to drive cellular activities. ATP syn is a large protein complex comprised of two different multi-subunit portions. The hydrophobic domain ( $F_o$ ) is embedded inside the membrane and makes  $H^+$  translocation. The hydrophilic domain ( $F_1$ ) protrudes above the membrane and synthesizes ATP. The  $F_o$  domain uses the energy from the  $H^+$  gradient and forces the  $F_1$  domain to generate ATP. It is considered as the most efficient molecular motor and nano-scale machine.

A simplified illustration of the glucose metabolism in bacterial respiration and the  $E^{0'}$ -values of some important molecules in the ETC are presented in **Figure 9**.

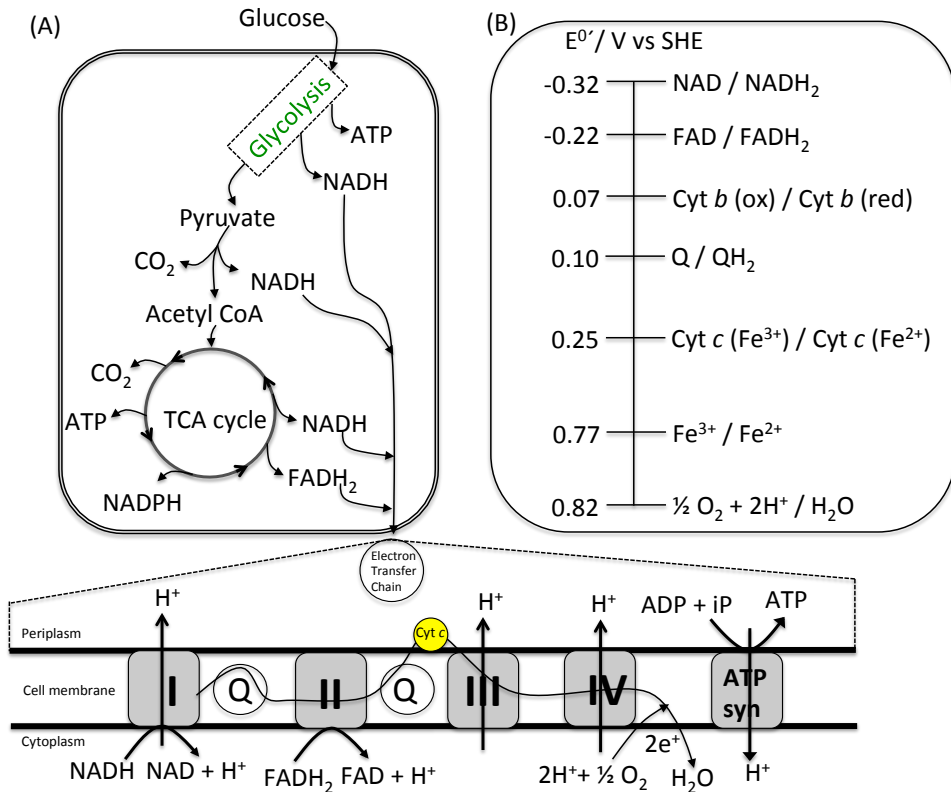


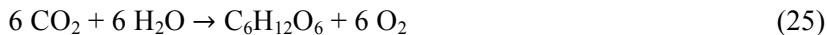
**Figure 9. A simplified schematic presentation of bacterial respiration.**

(A) The primary energy source, glucose, is initially converted by glycolysis into pyruvate and subsequently to acetyl CoA, the entry point in the TCA-cycle. In a series of reactions acetyl CoA is converted into CO<sub>2</sub>. Through these processes ATP is formed and the reducing equivalents, i.e., NADH<sub>2</sub>, FADH<sub>2</sub>, transfer electrons to molecular oxygen, O<sub>2</sub> via ETC. Complex I, III, and IV pump out H<sup>+</sup> across the membrane and generate an electrochemical H<sup>+</sup> gradient that is used to synthesize ATP. (B) The standard redox potentials  $E^{\circ}$  (at pH 7.0 and 25 °C) of some important molecules in the ETC.

# 8. Photosynthesis

Life depends on photosynthesis. Higher plants, algae and some bacteria perform photosynthesis to convert solar energy into chemical energy. In plants and algae photosynthesis occurs in a specialized organelle called chloroplast, whereas in cyanobacteria photosynthesis occurs in a special membrane. All these organisms use water as the sole electron donor, which is split and oxidized to form molecular oxygen, thus this process is called oxygenic photosynthesis. In contrast, in photosynthetic purple bacteria this process occurs in the CM and they are not able to oxidize water but rather require inorganic or organic substrates, e.g., malate, acetate, or sulfur compounds, e.g., hydrogen sulfide, as electron donor and the process is called anoxygenic photosynthesis<sup>176</sup>.

The overall reaction of oxygenic photosynthesis can be written as follows:



## 8.1. Interconnecting photosynthetic and respiratory-ETC

Cyanobacteria are prokaryotic, gram-negative organisms and perform oxygenic photosynthesis. In cyanobacteria both the photosynthetic and respiratory-ETC can be shared<sup>177</sup>. These unique characteristics of cyanobacteria give them the possibility to exist in almost all environments on earth<sup>177c</sup>. The cytoplasmic membrane separates the cytoplasm from the intermembrane space (**Figure 10A**). In most of the cyanobacteria photosynthesis occurs in TMs and respiratory electron flow occurs in both the TMs and in the cytoplasmic membrane.

The shared events of photosynthesis and respiration in cyanobacteria are presented in **Figure 10B**, where it is shown that photosystem II (PSII) uses light to oxidize water and the gained electrons are transferred to reduce the plastoquinone (PQ) pool, which in turn is followed by reduction of cytochrome *b<sub>6</sub>f* (Cyt *b<sub>6</sub>f*) and plastocyanin (PC)<sup>178</sup>. Electrons are then transferred to photosystem I (PSI) and by light excitation electrons are transferred via ferredoxin (Fd) to finally reduce nicotinamide adenine dinucleotide phosphate (NADP<sup>+</sup>) to form NADPH. Electrons are also transferred via the respiratory complexes, NADPH dehydrogenase (NDH-1) and succinate dehydrogenase (SDH)<sup>179</sup> to the PQ pool.

Terminal oxidase (TOX) transfers the excess electrons generated in PSII to  $O_2$  and thus prevents overreduction of the PQ pool. Some components, e.g., PQ, Cyt  $b_6f$  and PC are shared in both photosynthesis and respiration<sup>177a</sup>. In cyanobacteria the abundance of PSI is higher than that of PSII that results in a rather oxidized PQ pool that in turn eventually protects cyanobacteria from photodamage<sup>180</sup>.

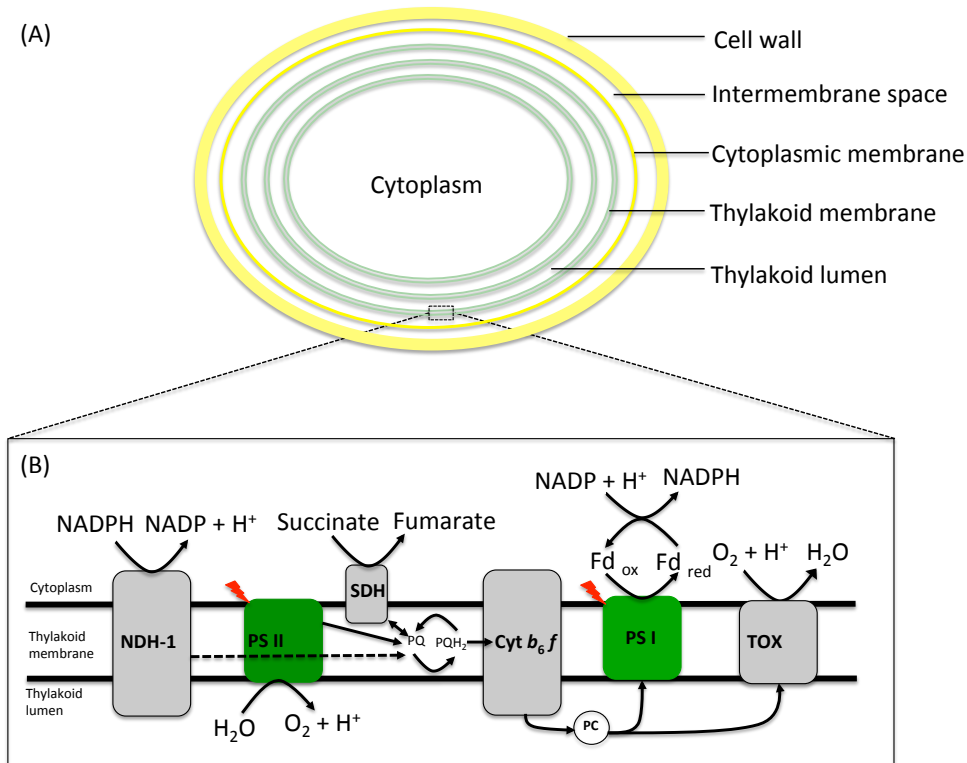


**Figure 10.** (A) An outline of the cyanobacterial membrane compartments. (B) A schematic presentation of the interconnecting ET of the photosynthetic and respiratory electron conduits in cyanobacteria. The photosynthetic complexes, PSI and PSII are colored in green. The respiratory complexes, NDH-1, SDH, TOX are colored in gray. The oxidized and reduced forms of Fd are shown as  $Fd_{ox}$  and  $Fd_{red}$ .

## 8.2. Chloroplast

The photosynthetic events in plants are identical to those in cyanobacteria, however, they occur in a special organelle, the chloroplast, which is thought to originate from cyanobacteria. Unlike cyanobacteria there is no connection between the TMs and the respiratory membrane (cytoplasmic membrane in cyanobacteria) in chloroplasts<sup>181</sup>. A typical chloroplast in a plant cell consists of an inner membrane surrounded by an outer membrane and in between there is an

intermembrane space. These membranes are composed of phospholipids and galactolipids. The inner membrane is filled with a gelatinous aqueous fluid called stroma, which comprises the membrane bound disk like structures called thylakoids, the site of photosynthesis. The thylakoid membranes (TMs) are the most abundant biological membranes in Nature and are distinguished for their unique structure and composition. Thylakoids often form stacks of disks referred to as grana and are connected by lamellae. The TMs are surrounded by an aqueous phase called lumen. During the light dependent reaction  $H^+$  are pumped out across the TMs into the lumen<sup>182</sup>. The basic structure of a chloroplast is presented in **Figure 11**.

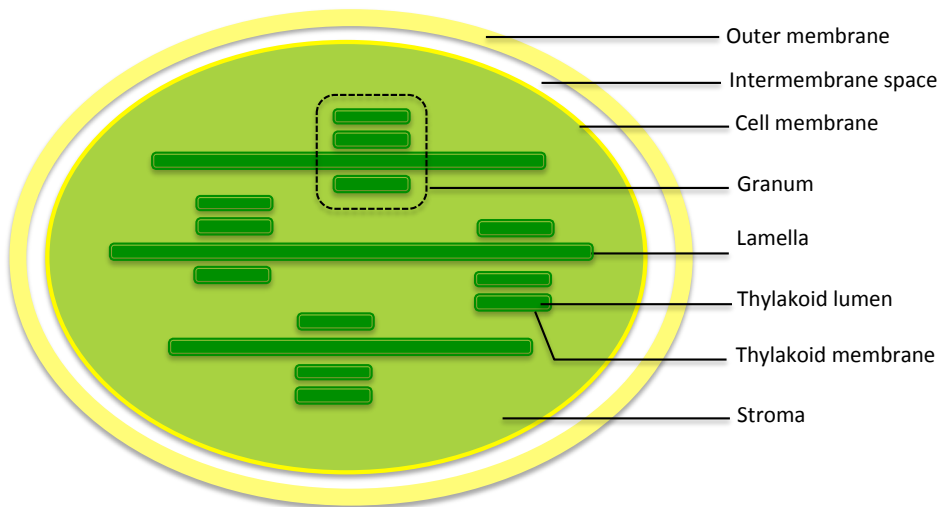


**Figure 11. A schematic picture of the structure of a chloroplast in a typical plant cell.**

### 8.3. Oxygenic photosynthesis

In general photosynthesis is the reverse of respiration, where glucose is oxidized to form carbon dioxide and water by using cellular energy. Instead in photosynthesis carbon dioxide is reduced to glucose via photolysis of water and energy obtained from light<sup>183</sup>. Photosynthesis involves two reactions:

- I. The light dependent reaction often called the light reaction, which occurs in the TMs
- II. The light independent reaction, which occurs in the stroma, the aqueous fluid containing the open space inside the chloroplast<sup>184</sup>.

The TMs contain light-absorbing pigments, i.e., primarily chlorophylls but also other accessory pigments, e.g., carotenoids. These pigments are embedded in the light harvesting complexes and are highly tuned to work together and referred to as the photosystem (PS). The PS is a network of chlorophylls, accessory pigments and associated proteins held within a protein matrix on the surface of the TMs. The PS consists of a series of chlorophyll molecules associated together, called the antenna complex and the reaction center (RC). Light is absorbed in the antenna complex and the excitation energy is transferred from one chlorophyll pigment molecule to adjacent pigments and subsequently to the RC<sup>176a</sup>.

Photosynthesis is not supported by all wavelengths of light. The photosynthetic action spectrum depends on the pigments. In green plants, algae, and cyanobacteria the action spectrum is within the visible light that ranges between 400-700 nm, often called the photosynthetic active radiation (PAR). Chlorophyll *a* is the primary photosynthetic pigment and chlorophyll *b* is the secondary or accessory pigment. Chlorophyll *b* increases light harvesting by supplementing the light absorption region. However, carotenoids are other accessory pigments absorbing light that is not efficiently absorbed by the chlorophylls. The photosynthetic-ETC (PETC) comprises three major protein complexes, such as, PSII, PSI and Cyt *b*<sub>6</sub>*f*<sup>185</sup> and are presented in **Figure 12A**. In photosynthetic purple bacteria the spectral region is extended and the maximum absorption of light is at 870 nm<sup>186</sup>.

#### 8.4. Light dependent reaction

Light absorption by the RC of PSII (P680) excites the energy level of an electron to a higher state (P680\*). The excited PSII gets relaxed by taking electrons from water oxidation mediated by the oxygen evolving complex (OEC) and releases oxygen. This photoexcited electron is coupled with H<sup>+</sup> generation and accumulated in the thylakoid lumen. This photoexcited electron is then shuttled via a series of electron carriers such as pheophytin (phe), quinone-A (Q<sub>A</sub>), quinone-B (Q<sub>B</sub>) and subsequently reduces PQ to PQH<sub>2</sub>. The PQH<sub>2</sub> is a strong electron donor and passes light energized electrons to Cyt *b*<sub>6</sub>*f* to pump H<sup>+</sup> from the stroma into the lumen. A small water-soluble electron carrier, PC, then carries electrons to PSI<sup>184</sup>. A schematic photosynthetic-ET is presented in **Figure 12 A**.

Similarly light absorption of the RC of PSI (P700) stimulates the energy level of an electron to a higher state (P700\*). PSI accepts electrons from PC and transfers it to Fd. The reduced Fd carries high potential electrons, which eventually reduce NADP<sup>+</sup> to NADPH via a membrane bound enzyme called ferredoxin-NADP-reductase (FNR). This long way of photoexcited ET from H<sub>2</sub>O to NADPH is coupled with a H<sup>+</sup> gradient across the TMs. This electrochemical H<sup>+</sup> gradient

through the TMs is used by ATP syn to generate ATP<sup>176a, 182</sup>. A schematic picture of PETC is shown in **Figure 12A** and the photosynthetic Z-scheme with a standard redox potential scale is shown in **Figure 12B**.

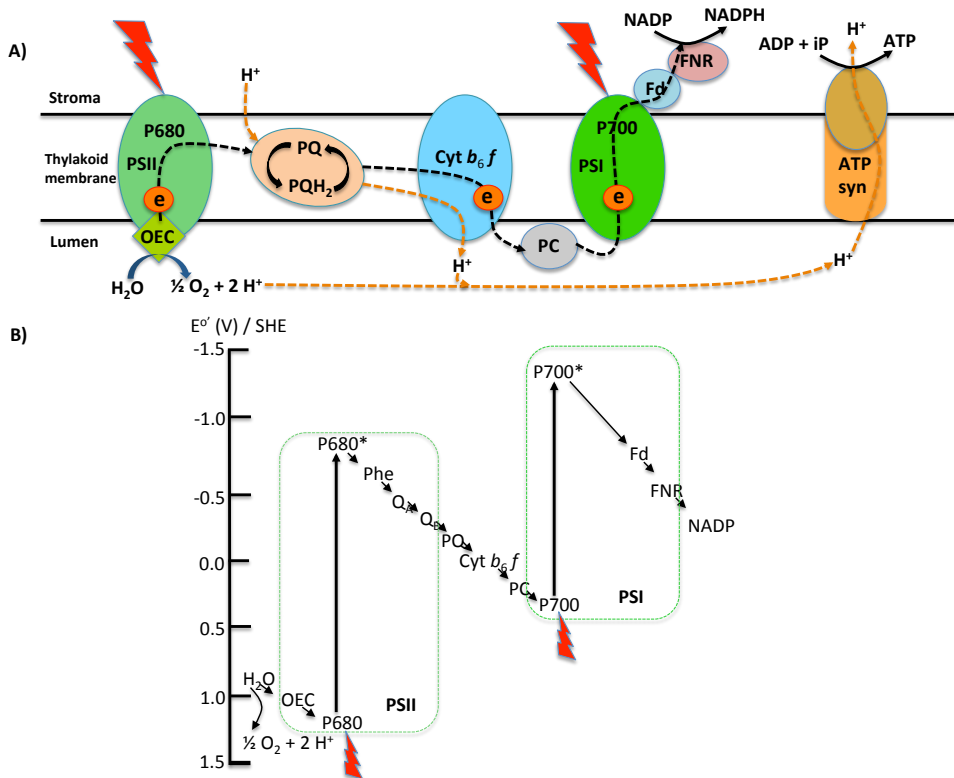


**Figure 12.** (A) A schematic picture of the PETC. The absorption of light by P680 excites its electron, which in turn is transferred via PQ, Cyt *b*<sub>6</sub> *f* complex and followed by PC to PSI. The light absorption at P700 excites again the electron, which eventually is transferred via Fd and FNR to reduce NADP<sup>+</sup> to NADPH. The ET is coupled with formation of a H<sup>+</sup> gradient across the TMs, the energy of which is used by ATP syn to generate ATP. The black dashed arrows indicate ET and the purple dashed ones indicate H<sup>+</sup> transfer. (B) The photosynthetic Z-scheme shows the sequential performance of PSII and PSI. Initially the light absorption of P680 excites it to a high energy level, P680\*. The electron then passes through Phe, Q<sub>A</sub>, Q<sub>B</sub> and leaves PSII at the PQ pool. This ejected electron subsequently transfers through Cyt *b*<sub>6</sub> *f*, PC to PSI. When P700 absorbs light, its electron gets excited (P700\*) and subsequently such energized electrons are used to form NADPH. The standard redox potential, E<sup>0'</sup> (at pH 7.0 and 25 °C) scale of the PETC is presented.

### 8.5. Light independent reaction

In the light independent reaction atmospheric CO<sub>2</sub> is reduced primarily to glucose by using ATP and NAD(P)H produced in the light dependent reaction, a process called the Calvin cycle<sup>187</sup>. ATP provides endergonic energy and NADPH provides



the necessary reducing input to reduce CO<sub>2</sub> into organic molecules. CO<sub>2</sub> diffuses into the stroma and binds with a five-carbon sugar, ribulose-1,5-bisphosphate to form three-carbon molecules of phosphoglycerate. The key carbon-fixing enzyme in photosynthesis, ribulose bisphosphate carboxylase/oxygenase is usually called RuBisCO and mediates this reaction. Then a series of enzymatic reactions transform phosphoglycerate into glucose and other metabolic precursors<sup>184</sup>.

## 8.6. Anoxygenic photosynthesis

In photosynthetic purple bacteria, there is only one photosystem and the light dependent reaction is cyclic<sup>188</sup>. Cyclic-PETC produces ATP in the light dependent reaction and the reducing equivalent, NADPH in light independent reaction. Moreover in cyclic-PETC, water is not used as electron donor and hence oxygen is not released as a byproduct. Purple bacteria require anoxic conditions for photosynthesis, since bacteriochlorophyll (Bchl) is repressed in the presence of oxygen<sup>135a, 189</sup>.

The cyclic-PETC of purple bacteria is presented in **Figure 13** showing light absorption at P870 resulting in the excitation of one electron to a higher level (P870\*) that then passes through a series of electron carriers down the PETC, i.e., bacteriochlorophyll (Bchl), bacteriopheophytin (Bph), Q<sub>A</sub>, Q<sub>B</sub>, Q-pool, Cyt *bc*<sub>1</sub>, Cyt *c*<sub>2</sub>. The photoexcited electron eventually flows back to P870 and is used again when excited. This photo induced ET is combined with H<sup>+</sup> pumping across the CM and is used to produce ATP<sup>190</sup>. Since the photo-excited electron goes back to the system, purple bacteria require inorganic, e.g., H<sub>2</sub>S or organic substrates, e.g., malate, as a reducing equivalent to drive the Calvin cycle for carbon fixation<sup>191</sup>. The electron generated from the oxidation of these substrates enters into the system via Q-pool. The E<sup>0'</sup> of quinone (+0.10 V) is higher than that of the NADP<sup>+</sup>/NADPH couple (- 0.32 V). Thus a reverse electron flow is required to reduce NADP<sup>+</sup> to NADPH. The reverse electron flow uses ATP generated in light dependent reaction to do this work.

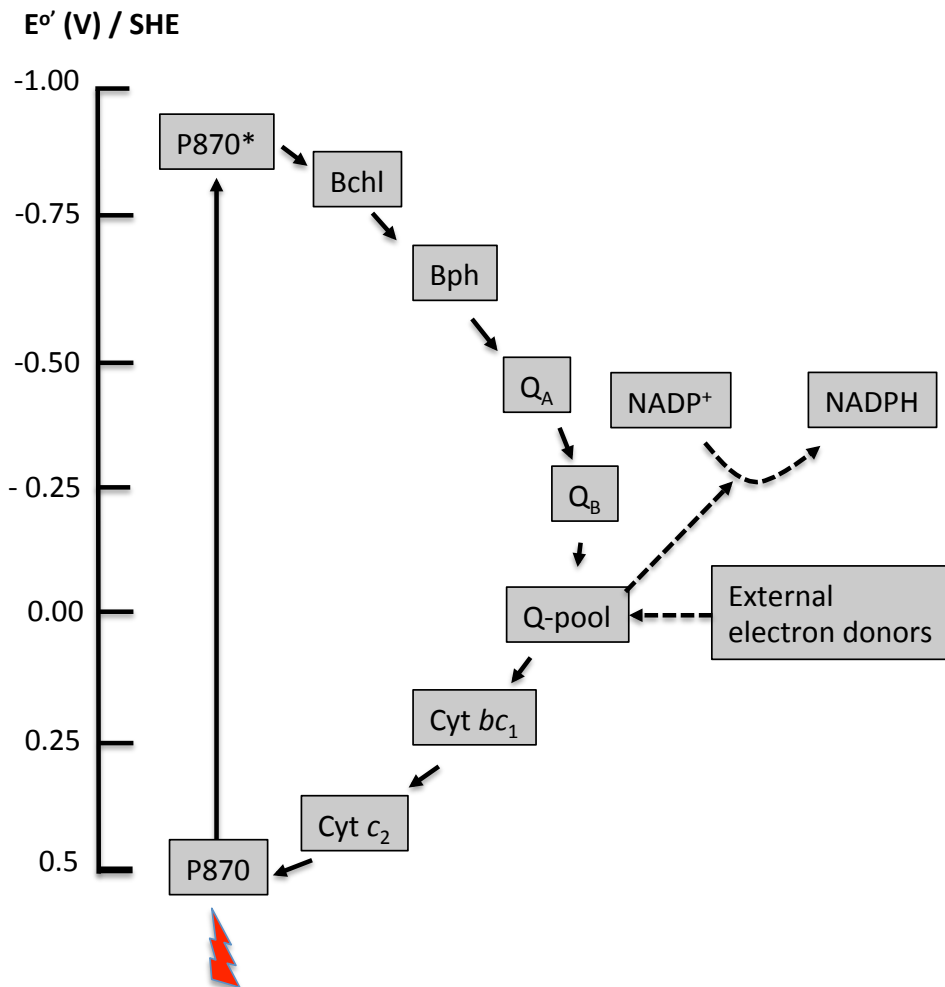


**Figure 13.** A scheme of the cyclic-PETC in purple bacteria. Light absorption at P870 excites its electron to a higher energy level (P870\*) that then passes through a series of electron carriers down the PETC and returns back to the photosystem from where it originates. The standard redox potential,  $E^\circ$  (at pH 7.0 and 25 °C) scale is also presented.

## 9. Biological photovoltaics (BPVs)

Global energy consumption is increasing regularly due to an increased population and economic growth while the primary energy resources, i.e., fossil fuels, are decreasing substantially. The combustion of fossil fuels greatly contributes to the global climate change via the greenhouse effect that in turn demands a change into a carbon-neutral energy production. The secured supply of cost-effective clean energy is one of the greatest challenges in the 21<sup>st</sup> century<sup>176b</sup>. Among all renewable energy sources such as hydroelectricity, geothermal energy, and wind energy, solar energy is the most abundant around the world and the largest exploitable energy resource. The amount of solar energy radiating from the sun to the earth in one hour is greater than the entire annual global energy demand<sup>192</sup>.

However, currently the technology available for solar energy conversion, i.e., photovoltaics is based on silicon-based solar panels. The photovoltaics are highly expensive and their efficiency is restricted by the inherent chemical structure of such materials. The quantum efficiency of charge separation in photosynthesis is nearly 100%, whereas the maximum internal quantum efficiency in silicon based photovoltaics is around 34%. Moreover, the charge carrier recombination time in photosynthesis is shorter than that of the highest performed silicon based photovoltaics. Besides that artificial systems mimicking natural photosynthesis were constructed to convert solar energy into electricity<sup>109c, 193</sup>. Furthermore any photosynthetic light independent reaction that can reduce atmospheric CO<sub>2</sub> to form an organic molecule is yet to be achieved by any of the existing photovoltaics<sup>194</sup>.

A great deal of research is focused on converting photosynthetic energy into renewable, self-sustainable and environmentally friendly energy<sup>51b, 176b, 194-195</sup>. Biological photovoltaics (BPVs)<sup>196</sup> is emerging as a potential energy generating technology, where photosynthetic organisms are used to convert sunlight into electrical energy<sup>51a</sup>. BPVs is also referred to as photosynthetic microbial fuel cells (PMFCs)<sup>51b</sup>. In this chapter BPVs is the name to be preferred to be used, since the current established technology for solar energy harvesting is called photovoltaics, accordingly it is convenient to refer to its biological counterpart as BPVs.

Photosynthetic organisms in BPVs use sunlight for photolysis of water and provide electrons to the system. Instead of a regular supply of organic substances as electron donors, which is required to run a typical microbial fuel cell cell

(MFC) yielding the end product  $\text{CO}_2^{20}$ , most photosynthetic organisms are self-sustainable as they use water as electron donor and the growth culture is inexpensive to maintain. Moreover, during photosynthesis these organisms store respiratory metabolites inside the cell that can in principle be used to generate electrical power even in a dark period<sup>151</sup>. These diverse properties of photosynthetic organisms offer BPVs a greater prospect over typical silicon based solar panels<sup>51a</sup>. However, BPVs with intact organisms suffer from intrinsic metabolic loss and intracellular competition for energy<sup>150</sup>. A schematic diagram of a BPV is presented in **Figure 14**.

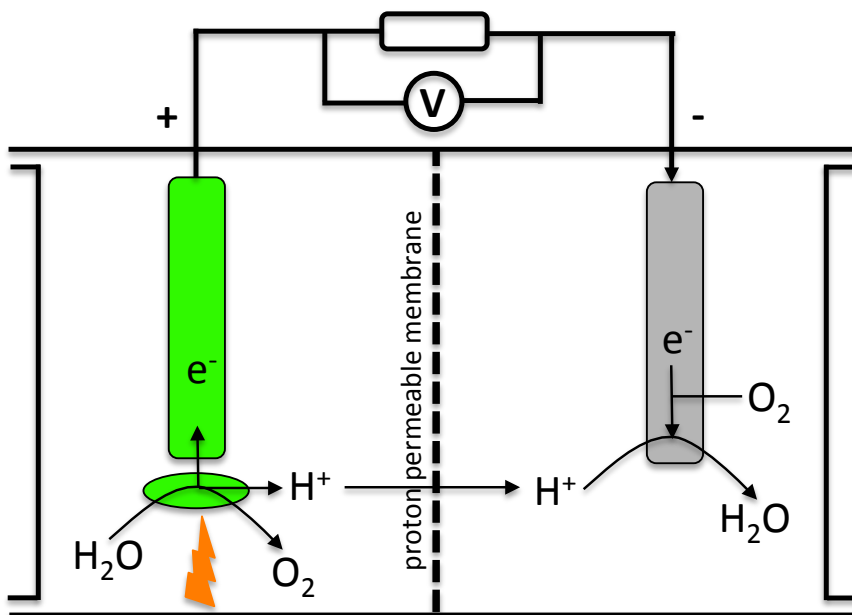


**Figure 14.** A schematic presentation of a BPV cell. In the anodic (+) part photosynthetic organisms perform photolysis of water in the presence of sunlight. In the cathodic (-) part an oxygen reducing enzyme, i.e., bilirubin oxidase (BOx)<sup>197</sup> directly reduces oxygen into water. When this circuit is closed with a certain load it generates electrical power.

A great variety of biological components have been studied in BPVs including isolated photosynthetic pigments, e.g., PSI<sup>198</sup> and PSII<sup>199</sup> as well as isolated TMs<sup>54b, 200</sup>, and chloroplasts<sup>201</sup>. Mershin et al. reported the greatest photocurrent density of  $362 \mu\text{A cm}^{-2}$  in the literature from self assembled PSI onto a zinc-oxide nanostructured semiconductor<sup>202</sup>. The immobilization of PSII onto ORPs modified gold electrodes produces a significant photocurrent density of  $45 \mu\text{A cm}^{-2}$ <sup>203</sup>. When TMs were immobilized on an electrode modified with multi-walled carbon

nanotubes (MWCNT), the maximum photocurrent density was  $68 \mu\text{A cm}^{-254c}$ . Although the photocurrent generation from these photosynthetic machineries was relatively high, however, it is yet unlikely for large-scale photosynthetic energy conversion due to the following reasons<sup>194</sup>:

- I. Expensive, time-consuming and laborious extraction and purification processes.
- II. A prerequisite of a particular environmental condition, e.g., pH, temperature and a particular electrolyte to keep them functioning.
- III. Inability to self-maintenance in an artificial environment and subsequently unstable for long-term electrical power generation

These above-mentioned limitations can be overcome by using intact photosynthetic whole cell organisms in BPVs<sup>51a</sup>. For this purpose a diverse range of intact organisms have been investigated in BPVs that include purple bacteria<sup>138</sup>, cyanobacteria<sup>55c, 195b, 204</sup> as well as algae<sup>67</sup>. Purple bacteria requires a supply of organic substances e.g., malate, succinate, or acetate as electron donor, since they are unable to oxidize water. In algae the EET from PETC is limited because the photosynthetic apparatus is located inside a specially designed subcellular organelle, the chloroplast that is insulated by a thick cell wall<sup>146</sup>.

In contrast cyanobacteria are robust and their physiology is simpler and requires lower energy for cellular activities compared to that of algae. The PETC and RETC in cyanobacteria can communicate inside the TMs<sup>177a, 177b, 200b</sup>. They have their own mechanism to be protected from photo-damage at high light intensity. In addition, they are able to survive at diverse atmospheric conditions, e.g., irregular CO<sub>2</sub> concentration, unusual light intensity, and dryness<sup>205</sup>. Therefore, cyanobacteria have the practical potential to harness solar energy in a versatile global area. A variety of cyanobacterial species such as *Synechococcus elongatus*, *Synechocystis* sp., *Nostoc* sp., *Anabaena variabilis* and *Spirulina platensis* have been studied in BPVs<sup>194</sup>.

Photosynthetic energy conversion could be used to power remote electrical instruments, handy electronic devices, and photo fuel production. However, to explore the BPVs commercially, their efficiency due to quantum conversion, power output and stability need to be substantially improved. Therefore, it is of great importance to deeply understand how Nature performs photosynthesis to explore its applications.

The key feature for future development should consider the photosynthetic electron exit and their extended viability and stability. A superior electrode material that would provide a natural environment to the photosynthetic organisms with a maximized surface area while minimizing the distance between the

organisms and the electrode could improve the performance of the BPVs. The immobilization of cyanobacteria on such advanced electrode materials, e.g., polypyrrole<sup>55c</sup>, indium tin oxide<sup>55b</sup>, was shown to enhance the photocurrent density. E.g., the immobilization of cyanobacteria on carbon nanotubes generates a photocurrent density of 25  $\mu\text{A cm}^{-255a}$  and on a polyaniline modified electrode the photocurrent density was 150  $\mu\text{A cm}^{-2206}$ . A microfluidic-miniaturized BPV without using any ET-mediator or membrane was reported for cyanobacteria to produce 100  $\text{mW m}^{-2}$ , the highest power density reported of until today<sup>207</sup>.

The theoretical power output from BPVs is estimated to be 700-7700  $\text{mW m}^{-2}$ , whereas the present maximum power output is reported to be 100  $\text{mW m}^{-251a, 207}$ . Although research on BPVs is progressing regularly, the present power output for commercial applications is much too low. The EET from photosynthetic organisms in BPVs is one of the major challenges<sup>51b</sup>. The EET from photosynthetic organisms in BPVs is relatively low compared to that of the dissimilar metal reducing bacteria in MFCs<sup>208</sup>. Although photosynthetic organisms have developed through evolutionary time, they did not evolve for EET to electrodes in BPVs.

With the use of modern technologies available in genetic engineering and molecular biology, photosynthetic organisms should be able to be engineered for enhanced EET. The electrogenic activity of *Synechocystis* sp. PCC 6803 in BPVs was shown to improve significantly by deleting respiratory TOX<sup>209</sup>. Recently, the EET ability from *Geobacter* sp. was expressed in *Synechococcus elongatus* PCC 7942 and as a consequence a nine-fold higher photocurrent generation was recorded compared to that of its wild type species<sup>210</sup>. Photosynthetic organisms could also be engineered to extend the light absorption region by combining the absorption spectrum of purple bacteria with that of cyanobacteria<sup>211</sup>.

The understanding of how photoexcited electrons are transferred out of the organisms is the key to improve the performance of BPVs<sup>150</sup>. In this thesis a systematic study of EET from photosynthetic biomaterials to electrodes in BPVs was conducted. For this purpose we have investigated the EET from a prokaryotic photosynthetic purple non-sulfur bacterium, *R. capsulatus*<sup>140</sup>, TMs from spinach<sup>54d, 145</sup>, a prokaryotic cyanobacterium, *Leptolyngbya* sp.<sup>148</sup> and a eukaryotic algae, *Paulschulzia pseudovolvox*<sup>153</sup>.

At present the photosynthetic energy conversion research is at an early stage of development that seeks attention from diverse groups of the research community for any effective practical application. The combined efforts from multidisciplinary fields such as bioelectrochemistry, surface engineering, molecular biology, biotechnology and genetic engineering are required to make a paradigm shift in this field.

# 10. Acknowledgements

It was 21<sup>st</sup> of August 2008; I came to Sweden to pursue a Masters program on Biotechnology at Lund University. That was the first time I came outside of my home country, Bangladesh. I would like to express my cordial gratitude to Anna Carlqvist, then coordinator at the international admission office of LTH, for helping me during the admission time and after my arrival at Lund.

In the beginning life was challenging for me to adjust in the new Swedish education system as well as in the new environment here. I cordially acknowledge to my then Khulna University folks who lived in Lund. They were Subrata Paul (Kelu ☺), Polash vai, Kausar Alom, Millu BT, Rod mama (the tallest BD guy in Sweden) for helping me enormously to familiarize me in Lund and finding me a work in the Indian restaurants at Malmö. The guy who showed me the greatest kindness at that very vital time was Azad vai from Niribili. It is impossible for me forget his kind support.

By this time I found Prof. Per Olof Larsson (P-O) as my mentor and one of the greatest teachers in my entire educational life. My memory is still fresh of that night that I was sitting for Enzyme Technology exam in his office. Thank you Christian Nilsson, Staffan Nilsson, Leif Bülow, Rickard, Loy, and Curt Reimann for your support during my master thesis at Pure and Applied Chemistry department.

One day I was reading research activities of many group leaders and found Lo Gorton's research very interesting. I was getting more curious to meet him face to face. After several days of trying to meet Lo, one day I have found him in his office. Well, I was a bit confused that was it Lo whom I was looking for or it was someone else? I tried to get some courage in my heart and asked him, "are you Professor Lo Gorton?" He replied, "yes I am and what's wrong with me?" I said, 'no no, nothing wrong'. I introduce myself and told him that I am interested in his research work. I asked him if there is any opportunity for me to work in his group. Lo said, ok let me think and visit me another day.

I visited him again and found him about to leave for Malmö. I was also scheduled to go to Malmö and we went together. When he got me off from his car beside the restaurant where I used to work, I asked him, where will you go now? I might not ask such a private question (Poor me!). He replied me that he will go to a sex (!!!)

party in Turning Torso? I am not really sure if I was surprised so much in my entire life ever. I could not understand that he was joking with me. Everyday I was surprised of your wonderful sense of humour, Lo.

I do not know if my English vocabulary is rich enough to express my heartfelt gratitude to you. Lo, you are a non-aging personality. I have never met such a person who I can share my mind like an open book. Now you are my best friend. I think you know how to get the best out of me scientifically. I did not know there is something called 'Electrochemistry' before meeting you. You entered me in this very fascinating research field; teach me like a baby by keeping hand on hand.

I wonder how could someone be so much cheerful always. We used to discuss many different aspects of life outside lab. I understand that you have great interest in languages, history, and liberal on religious affairs. You inspired me a lot in both socially and scientifically. I think it is a great blessing for my life. You always tried to insert some German genes in me. But I do not how much German I am currently ☺. I always think 'Lo in Lund' might be the best combination to get best out of me. Love you, Lo.

Cecilia Hägerhäll, my co-supervisor. I can't forget your words when I visited you to sign on my PhD agreement paper. You told me 'Kamrul, don't worry, I would not die before your PhD dissertation'. You are always in my heart. I see you walking around me. You suggest me in my dream to do these and those experiments and I tried to do that during my PhD period. Wish you rest in peace.

By this time I had very nice time with so many good people around the world. I would like to thank, Nadeem, Najat, Behnaz, Ioana, Beatrice, Peter, Somayyeh, Kati, Francesca, Ali (Ali Baba), Andrea.

I would like to convey my gratitude to Sunil Patil. You teach me 'publish or perish'. Thank you Roberto (nano rob) for helping me during the Electrochemistry course, in everyday laboration and off course we had lots of fun outside lab. Christopher, you were my mentor in the beginning of my PhD program, you are a storehouse of innovative ideas, a great scientific thinker, very precise on work and a pleasant personality. On top of that you are one of my true friends nowadays. My well wishes will follow you always. Thank you Galina and Masha from Russia. You are very a social and enjoyable personality. I have found your presence amiable always. I am delighted to have you as my colleagues and nowadays we are very good friends.

Kamil and Eva, I am cordially grateful to you for your kind help and patience in lab. I have learnt a lot from you by this time. Ga'bor, thank you. You are my Origin (software) guru and it is impossible to forget your support. Thank you Aniko, always a smiling face. Keep it up. Vera Eßmann, thank you for teaching me how to teach. You were the first graduate student who I supervised (although



it's a serious word!) and found it pleasant to teach. Kesava, believe on your great skills, knowledge and efficiency. I always believe that you could do something great. Valentina, you are simply a very good company both scientifically and socially. Olga, I wondered on you superb performance while you worked as a project student with me. Laleh, take time and you will make it happen.

Thank you Yusuf Turk, Husseyin Bekir Yeldiz, Emre Çevik. I have enjoyed to work together with you and off course we had lots of fun inside and outside of lab. Hassan Hamidi, I have learnt a lot from you while you were here in Lund. Thank you. Sumaya, salam, salam satta salam to you.

I worked as a laboratory assistant for the Electrochemistry and Analytical Chemistry courses. Thank you all students who I taught. By teaching I learnt 'the best way of learning is teaching'. Thank you Maggan for giving me the opportunity to teach. I am thankful to all collaborators in my PhD project. Thank you Dónal for providing me these polymers and for your great scientific input in my PhD project. Thank you Mike Packer for successful collaboration and support. Thank you Sinan, Per-Åke and Hans-Erik for fruitful collaboration.

I am cordially acknowledged to the Swedish Research Council and Biochemistry Department for financial support. Thank you all present and past members of CMPS. It is really a wonderful working environment here. Thank you Gert (former technician in the department) for happily repairing our instruments. Thank you Adine for purchasing lots of chemicals on time. Please excuse me if I forget to mention you whom I should acknowledge.

I am thankful to the Bangladeshi community in Lund and Malmö. You people have made my life cheerful. Thank you Lund Summer Cricket (Jhijhipoka) and Bangladesh Cultural Association in Skåne (BCAS) to organize lots of events. I enjoyed these events a lot and appreciate your great effort.

It would be impossible for me to come in my present stage without the never-ending support from my family members. You have supported me whatever I wanted to do in my life. No thankful words are sufficient to express my gratitude to you. It is only my mother, who knows, whom I was and how difficult was it to raise me. My father did not hesitate to sacrifice his last belongings for my higher education. My brothers sacrifice enormously for me that usually brothers do not do. My wife is always very much patient and welcoming on my passionate. Love you and best of luck. On 3<sup>rd</sup> of June 2015 I have been blessed with a baby girl, Bella Nawaz Hasan. Your smiles make me happy everyday. Love you BURI MA.

# 11. References

1. (a) A. M. Kuznetsov and J. Ulstrup, *Electron Transfer in Chemistry and Biology: An Introduction to The Theory*, John Wiley & Sons Ltd., Chichester, 1999; (b) S. F. Nelsen, in *Electron Transfer in Chemistry*, Wiley-VCH Verlag GmbH, Berlin, 2008, pp. 342-392.
2. P. N. Bartlett, in *Bioelectrochemistry*, John Wiley & Sons, Ltd, Chichester, 2008, pp. 1-37.
3. A. D. McNaught and A. D. McNaught, *Compendium of Chemical Terminology*, Blackwell Science, Oxford, 1997.
4. H. Taube, H. Myers and R. L. Rich, *Journal of the American Chemical Society*, 1953, 75, 4118.
5. (a) R. A. Marcus, *The Journal of Chemical Physics*, 1956, 24, 966; (b) R. A. Marcus, *The Journal of Chemical Physics*, 1956, 24, 979.
6. (a) R. Marcus, *Annual Review of Physical Chemistry*, 1964, 15, 155; (b) R. A. Marcus, *The Journal of Chemical Physics*, 1965, 43, 679; (c) R. A. Marcus and N. Sutin, *Biochimica et Biophysica Acta (BBA)-Reviews on Bioenergetics*, 1985, 811, 265.
7. R. A. Marcus, *Angewandte Chemie International Edition*, 1993, 32, 1111.
8. (a) G. W. Canters and M. van de Kamp, *Current Opinion in Structural Biology*, 1992, 2, 859; (b) C. C. Moser, J. M. Keske, K. Warncke, R. S. Farid and P. L. Dutton, *Nature*, 1992, 355, 796; (c) M. L. Jones, I. V. Kurnikov and D. N. Beratan, *Journal of Physical Chemistry A*, 2002, 106, 2002.
9. H. B. Gray and J. R. Winkler, *Annual Review of Biochemistry*, 1996, 65, 537.
10. M. Cordes and B. Giese, *Chemical Society Reviews*, 2009, 38, 892.
11. (a) J. A. Cracknell, K. A. Vincent and F. A. Armstrong, *Chemical Reviews*, 2008, 108, 2439; (b) U. Wollenberger, R. Spricigo, S. Leimkühler and K. Schröder, in *Biosensing for the 21st Century*, Springer, Berlin, 2008, pp. 19-64.
12. H. B. Gray and J. R. Winkler, *Quarterly Reviews of Biophysics*, 2003, 36, 341.
13. H. Yue and D. H. Waldeck, *Current Opinion in Solid State and Materials Science*, 2005, 9, 28.
14. C. C. Page, C. C. Moser and P. L. Dutton, *Current Opinion in Chemical Biology*, 2003, 7, 551.
15. H. B. Gray and J. R. Winkler, in *Electron Transfer in Chemistry*, Wiley-VCH Verlag GmbH, Weinheim, 2008, pp. 2-23.
16. C. C. Page, C. C. Moser, X. Chen and P. L. Dutton, *Nature*, 1999, 402, 47.

17. H. B. Gray and J. R. Winkler, *Proceedings of the National Academy of Sciences of the United States of America*, 2005, 102, 3534.
18. (a) X. de Hemptinne, *Bulletin des Sociétés Chimiques Belges*, 1968, 77, 21; (b) L. J. C. Jeuken, *Biochimica et Biophysica Acta (BBA)-Bioenergetics*, 2003, 1604, 67.
19. (a) L. Su, W. Jia, C. Hou and Y. Lei, *Biosensors and Bioelectronics*, 2011, 26, 1788; (b) J. Frew, H. Hill and J. Thomas, *Philosophical Transactions of the Royal Society B: Biological Sciences*, 1987, 316, 95; (c) K. Habermüller, M. Mosbach and W. Schuhmann, *Fresenius Journal of Analytical Chemistry*, 2000, 366, 560.
20. K. Rabaey and W. Verstraete, *Trends in Biotechnology*, 2005, 23, 291.
21. C. J. McNeil, D. Athey and W. O. Ho, *Biosensors and Bioelectronics*, 1995, 10, 75.
22. A. Bond, *Inorganica Chimica Acta*, 1994, 226, 293.
23. F. A. Armstrong, H. A. O. Hill and N. J. Walton, *Accounts of Chemical Research*, 1988, 21, 407.
24. K. Rabaey, *Bioelectrochemical Systems: From Extracellular Electron Transfer to Biotechnological Application*, IWA publishing, London, 2010.
25. (a) P. Yeh and T. Kuwana, *Chemistry Letters*, 1977, 6, 1145; (b) M. J. Eddowes and H. A. O. Hill, *Journal of the Chemical Society, Chemical Communications*, 1977, 771b.
26. C. J. Reedy and B. R. Gibney, *Chemical Reviews*, 2004, 104, 617.
27. E. E. Ferapontova, S. Shleev, T. Ruzgas, L. Stoica, A. Christenson, J. Tkac, A. I. Yaropolov and L. Gorton, in *Perspectives in Bioanalysis*, eds. F. S. Emil Paleček and J. Wang, Elsevier, Oxford, 2005, pp. 517-598.
28. M. R. Tarasevich, A. I. Yaropolov, V. A. Bogdanovskaya and S. D. Varfolomeev, *Bioelectrochemistry and Bioenergetics*, 1979, 6, 393.
29. A. Iaropolov, V. Malovik, S. Varfolomeev and I. Berezin, *Doklady Akademii Nauk SSSR*, 1979, 249, 1399.
30. (a) L. Stoica, T. Ruzgas, R. Ludwig, D. Haltrich and L. Gorton, *Langmuir*, 2006, 22, 10801; (b) C. Léger and P. Bertrand, *Chemical Reviews*, 2008, 108, 2379.
31. H. Hill and N. Hunt, *Methods in Enzymology*, 1992, 227, 501.
32. L.-H. Guo and H. A. O. Hill, *Advanced Inorganic Chemistry*, 1991, 36, 341.
33. T. Ruzgas, E. Csöregi, J. Ennéus, L. Gorton and G. Marko-Varga, *Analytica Chimica Acta*, 1996, 330, 123.
34. F. Kracke, I. Vassilev and J. O. Krömer, *Frontiers in Microbiology*, 2015, 6, 575.
35. D. R. Lovley, J. F. Stolz, G. L. Nord and E. J. P. Phillips, *Nature*, 1987, 330, 252.
36. C. R. Myers and K. H. Nealon, *Science*, 1988, 240, 1319.
37. (a) D. R. Lovley, *Nature Reviews Microbiology*, 2006, 4, 497; (b) C. I. Torres, A. K. Marcus, H. S. Lee, P. Parameswaran, R. Krajmalnik-Brown and B. E. Rittmann, *FEMS Microbiology Reviews*, 2010, 34, 3.
38. B. E. Logan, *Nature Reviews Microbiology*, 2009, 7, 375.
39. D. R. Lovley, *Environmental Microbiology Reports*, 2011, 3, 27.

40. J. P. Busalmen, A. Esteve-Núñez, A. Berná and J. M. Feliu, *Angewandte Chemie International Edition*, 2008, 47, 4874.
41. O. Bretschger, A. Obratsova, C. A. Sturm, S. C. In, Y. A. Gorby, S. B. Reed, D. E. Culley, C. L. Reardon, S. Barua, M. F. Romine, J. Zhou, A. S. Beliaev, R. Bouhenni, D. Saffarini, F. Mansfeld, B. H. Kim, J. K. Fredrickson and K. H. Nealson, *Applied and Environmental Microbiology*, 2007, 73, 7003.
42. G. Reguera, K. D. McCarthy, T. Mehta, J. S. Nicoll, M. T. Tuominen and D. R. Lovley, *Nature*, 2005, 435, 1098.
43. Y. A. Gorby, S. Yanina, J. S. McLean, K. M. Rosso, D. Moyles, A. Dohnalkova, T. J. Beveridge, I. S. Chang, B. H. Kim, K. S. Kim, D. E. Culley, S. B. Reed, M. F. Romine, D. A. Saffarini, E. A. Hill, L. Shi, D. A. Elias, D. W. Kennedy, G. Pinchuk, K. Watanabe, S. Ishii, B. Logan, K. H. Nealson and J. K. Fredrickson, *Proceedings of the National Academy of Sciences of the United States of America*, 2006, 103, 11358.
44. S. M. Strycharz-Glaven, R. M. Snider, A. Guiseppi-Elie and L. M. Tender, *Energy & Environmental Science*, 2011, 4, 4366.
45. C. W. Marshall and H. D. May, *Energy & Environmental Science*, 2009, 2, 699.
46. L. Zhang, S. Zhou, L. Zhuang, W. Li, J. Zhang, N. Lu and L. Deng, *Electrochemistry Communications*, 2008, 10, 1641.
47. W. Ghach, M. Etienne, V. Urbanova, F. P. Jorand and A. Walcarius, *Electrochemistry Communications*, 2014, 38, 71.
48. D. Prasad, S. Arun, M. Murugesan, S. Padmanaban, R. S. Satyanarayanan, S. Berchmans and V. Yegnaraman, *Biosensors and Bioelectronics*, 2007, 22, 2604.
49. B. E. Logan, B. Hamelers, R. Rozendal, U. Schröder, J. Keller, S. Freguia, P. Aelterman, W. Verstraete and K. Rabaey, *Environmental Science and Technology*, 2006, 40, 5181.
50. G. Reguera, K. P. Nevin, J. S. Nicoll, S. F. Covalla, T. L. Woodard and D. R. Lovley, *Applied and Environmental Microbiology*, 2006, 72, 7345.
51. (a) A. J. McCormick, P. Bombelli, R. W. Bradley, R. Thorne, T. Wenzel and C. J. Howe, *Energy & Environmental Science*, 2015, 8, 1092; (b) N. Sekar and R. P. Ramasamy, *Journal of Photochemistry and Photobiology C: Photochemistry Reviews*, 2015, 22, 19; (c) C. F. Meunier, J. C. Rooke, A. Léonard, H. Xie and B. L. Su, *Chemical Communications*, 2010, 46, 3843.
52. B. Munge, S. K. Das, R. Ilagan, Z. Pendon, J. Yang, H. A. Frank and J. F. Rusling, *Journal of the American Chemical Society*, 2003, 125, 12457.
53. M. Kato, T. Cardona, A. W. Rutherford and E. Reisner, *Journal of the American Chemical Society*, 2012, 134, 8332.
54. (a) R. Carpentier, S. Lemieux, M. Mimeault, M. Purcell and D. C. Goetze, *Bioelectrochemistry and Bioenergetics*, 1989, 22, 391; (b) M. Rasmussen and S. D. Minteer, *Electrochimica Acta*, 2013, 126, 68; (c) J. O. Calkins, Y. Umasankar, H. O'Neill and R. P. Ramasamy, *Energy & Environmental Science*, 2013, 6, 1891; (d) H. Hamidi, K. Hasan, S. C. Emek, Y. Dilgin, H.-E. Åkerlund, P.-Å. Albertsson, D. Leech and L. Gorton, *ChemSusChem*, 2015, 8, 990.

55. (a) N. Sekar, Y. Umasankar and R. P. Ramasamy, *Physical Chemistry Chemical Physics*, 2014, 16, 7862; (b) A. J. McCormick, P. Bombelli, A. M. Scott, A. J. Philips, A. G. Smith, A. C. Fisher and C. J. Howe, *Energy & Environmental Science*, 2011, 4, 4699; (c) J. M. Pisciotta, Y. Zou and I. V. Baskakov, *PLoS ONE*, 2010, 5, e10821.
56. R. M. Allen and H. P. Bennetto, *Applied Biochemistry and Biotechnology*, 1993, 39, 27.
57. U. Schröder, *Physical Chemistry Chemical Physics*, 2007, 9, 2619.
58. Y. Qiao, S.-J. Bao and C. M. Li, *Energy & Environmental Science*, 2010, 3, 544.
59. W. Vielstich, A. Lamm and H. A. Gasteiger, eds., *Handook of Fuel Cells-Fundamentals, Technology, and Application*, John Wiley & Sons, Ltd., Chichester, 2003.
60. (a) D. H. Park and J. G. Zeikus, *Applied and Environmental Microbiology*, 2000, 66, 1292; (b) *Biotechnology and Bioengineering*, 2003, 81, 348; (c) H. P. Bennetto, G. M. Delaney, J. R. Mason, S. D. Roller, J. L. Stirling and C. F. Thurston, *Biotechnology Letters*, 1985, 7, 699.
61. M. E. Hernandez and D. K. Newman, *Cellular and Molecular Life Sciences*, 2001, 58, 1562.
62. K. Rabaey, N. Boon, M. Höfte and W. Verstraete, *Environmental Science & Technology*, 2005, 39, 3401.
63. D. K. Newman and R. Kolter, *Nature*, 2000, 405, 94.
64. L. M. Tender, S. A. Gray, E. Groveman, D. A. Lowy, P. Kauffman, J. Melhado, R. C. Tyce, D. Flynn, R. Petrecca and J. Dobarro, *Journal of Power Sources*, 2008, 179, 571.
65. (a) J. Niessen, U. Schröder, F. Harnisch and F. Scholz, *Letters in Applied Microbiology*, 2005, 41, 286; (b) J. Niessen, U. Schröder and F. Scholz, *Electrochemistry Communications*, 2004, 6, 955.
66. M. Rosenbaum, U. Schröder and F. Scholz, *Environmental Science & Technology*, 2005, 39, 6328.
67. M. Rosenbaum, U. Schröder and F. Scholz, *Applied Microbiology and Biotechnology*, 2005, 68, 753.
68. M. Rosenbaum, F. Aulenta, M. Villano and L. T. Angenent, *Bioresource Technology*, 2011, 102, 324.
69. A. Heller, *Current Opinion in Chemical Biology*, 2006, 10, 664.
70. I. G. Gazaryan, L. Gorton, T. Ruzgas, E. Csoregi, W. Schuhmann, L. M. Lagrimini, D. M. Khushpul'yan and V. I. Tishkov, *Journal of Analytical Chemistry*, 2005, 60, 558.
71. R. Kurita, N. Yabumoto and O. Niwa, *Biosensors and Bioelectronics*, 2006, 21, 1649.
72. A. Heller, in *Annual Review of Biomedical Engineering*, 1999, pp. 153-175.
73. A. Aoki and A. Heller, *The Journal of Physical Chemistry*, 1993, 97, 11014.

74. P. Pickup, W. Kutner, C. Leidner and R. W. Murray, *Journal of the American Chemical Society*, 1984, 106, 1991.
75. V. Soukharev, N. Mano and A. Heller, *Journal of the American Chemical Society*, 2004, 126, 8368.
76. A. B. P. Lever, *Inorganic Chemistry*, 1990, 29, 1271.
77. K. Hasan, S. A. Patil, D. Leech, C. Hägerhäll and L. Gorton, *Biochemical Society Transactions*, 2012, 40, 1330.
78. (a) Y. Degani and A. Heller, *Journal of the American Chemical Society*, 1989, 111, 2357; (b) A. Heller, *Journal of Physical Chemistry*, 1992, 96, 3579.
79. M. Pishko, I. Katakis, S.-E. Lindquist, L. Ye, B. Gregg and A. Heller, *Angewandte Chemie International Edition*, 1990, 102, 109.
80. (a) B. A. Gregg and A. Heller, *Analytical Chemistry*, 1990, 62, 258; (b) F. Mao, N. Mano and A. Heller, *Journal of the American Chemical Society*, 2003, 125, 4951.
81. A. Belay, A. Collins, T. Ruzgas, P. T. Kissinger, L. Gorton and E. Csöregi, *Journal of Pharmaceutical and Biomedical Analysis*, 1999, 19, 93.
82. (a) S. Timur, Y. Yigzaw and L. Gorton, *Sensors and Actuators B: Chemical*, 2006, 113, 684; (b) F. Tasca, S. Timur, R. Ludwig, D. Haltrich, J. Volc, R. Antiochia and L. Gorton, *Electroanalysis*, 2007, 19, 294.
83. (a) M. N. Zafar, F. Tasca, S. Boland, M. Kujawa, I. Patel, C. K. Peterbauer, D. Leech and L. Gorton, *Bioelectrochemistry*, 2010, 80, 38; (b) A. Killyéni, M. E. Yakovleva, D. MacAodha, P. Ó. Conghaile, C. Gonaus, R. Ortiz, D. Leech, I. C. Popescu, C. K. Peterbauer and L. Gorton, *Electrochimica Acta*, 2014, 126, 61.
84. (a) M. N. Zafar, X. Wang, C. Sygmund, R. Ludwig, D. Leech and L. Gorton, *Analytical Chemistry*, 2011, 84, 334; (b) M. Zafar, N. Beden, D. Leech, C. Sygmund, R. Ludwig and L. Gorton, *Analytical and Bioanalytical Chemistry*, 2012, 402, 2069.
85. R. Ludwig, R. Ortiz, C. Schulz, W. Harreither, C. Sygmund and L. Gorton, *Analytical and Bioanalytical Chemistry*, 2013, 405, 3637.
86. M. Tessema, E. Csöregi, T. Ruzgas, G. Kenausis, T. Solomon and L. Gorton, *Analytical Chemistry*, 1997, 69, 4039.
87. I. Vostiar, E. E. Ferapontova and L. Gorton, *Electrochemistry Communications*, 2004, 6, 621.
88. S. Timur, B. Haghighi, J. Tkac, N. Pazarlioglu, A. Telefoncu and L. Gorton, *Bioelectrochemistry*, 2007, 71, 38.
89. S. Timur, U. Anik, D. Odaci and L. Gorton, *Electrochemistry Communications*, 2007, 9, 1810.
90. S. Alferov, V. Coman, T. Gustavsson, A. Reshetilov, C. von Wachenfeldt, C. Hägerhäll and L. Gorton, *Electrochimica Acta*, 2009, 54, 4979.
91. V. Coman, T. Gustavsson, A. Finkelsteinas, C. Von Wachenfeldt, C. Hägerhäll and L. Gorton, *Journal of the American Chemical Society*, 2009, 131, 16171.
92. H. L. Ehrlich, *Geobiology*, 2008, 6, 220.
93. P. Kavanagh, S. Boland, P. Jenkins and D. Leech, *Fuel Cells*, 2009, 9, 79.

94. E. M. Kober, J. V. Caspar, B. P. Sullivan and T. J. Meyer, *Inorganic Chemistry*, 1988, 27, 4587.
95. H.-H. Kim, N. Mano, Y. Zhang and A. Heller, *Journal of The Electrochemical Society*, 2003, 150, A209.
96. A. J. Bard and L. R. Faulkner, *Electrochemical Methods: Fundamentals and Applications*, Wiley New York, 1980.
97. (a) C. Lefrou, P. Fabry and J.-C. Poignet, *Electrochemistry: The Basics*, with Examples, Springer Science & Business Media, Berlin, 2012; (b) C. H. Hamann, A. Hamnett and W. Vielstich, *Electrochemistry*, 2nd, Wiley VCH, Weinheim, 2007.
98. C. G. Zoski, in *Handbook of Electrochemistry*, ed. C. G. Zoski, Elsevier, Amsterdam, 2007, pp. 1-876.
99. H. Helmholtz, *Annalen der Physik*, 1853, 165, 211.
100. L. A. Matheson and N. Nichols, *Trans. Electrochem. Soc.*, 1938, 138.
101. (a) M. Ciobanu, J. P. Wilburn, M. L. Krim and D. E. Cliffler, in *Handbook of Electrochemistry*, ed. C. G. Zoski, Elsevier, Amsterdam, 2007, pp. 3-29; (b) G. A. Mabbott, *Journal of Chemical Education*, 1983, 60, 697; (c) B. Speiser, in *Encyclopedia of Electrochemistry*, Wiley-VCH Verlag GmbH & Co. KGaA, Weinheim, 2007.
102. F. G. Cottrell, *Zeitschrift für Physikalische Chemie*, 1903, 42, p. 385.
103. (a) P. Zanello, *Inorganic Electrochemistry: Theory, Practice and Applications*, Royal Society of Chemistry, Cambridge, 2003; (b) J. E. B. Randles, *Transactions of the Faraday Society*, 1948, 44, 327; (c) A. Ševčík, *Collection of Czechoslovak Chemical Communications*, 1948, 13, 349.
104. (a) M. I. Prodromidis, A. B. Flown, S. M. Tzouwara-Karayanni and M. I. Karayannis, *Electroanalysis*, 2000, 12, 1498; (b) A. K. Yagati, M. Jung, S. U. Kim, J. Min and J. W. Choi, *Thin Solid Films*, 2009, 518, 634.
105. X. Lu, Q. Zhang, L. Zhang and J. Li, *Electrochemistry Communications*, 2006, 8, 874.
106. (a) H. J. Kim, H. S. Park, M. S. Hyun, I. S. Chang, M. Kim and B. H. Kim, *Enzyme and Microbial Technology*, 2002, 30, 145; (b) H. Liu, S. Cheng and B. E. Logan, *Environmental Science & Technology*, 2005, 39, 658.
107. K. Rabaey, N. Boon, S. D. Siciliano, M. Verhaege and W. Verstraete, *Applied and Environmental Microbiology*, 2004, 70, 5373.
108. A. Shukla, P. Suresh, S. Berchmans and A. Rajendran, *Current Science*, 2004, 87, 455.
109. (a) C. F. Meunier, J. C. Rooke, A. Le'onard, H. Xie and B. L. Su, *Chemical Communications*, 2010, 46, 3843; (b) O. Yehezkeli, R. Tel-Vered, J. Wasserman, A. Trifonov, D. Michaeli, R. Nechushtai and I. Willner, *Nature Communications*, 2012, 3; (c) I. McConnell, G. Li and G. W. Brudvig, *Chemistry & Biology*, 2010, 17, 434.
110. J. Ružicka and E. H. Hansen, in *Flow Injection Analysis*, John Wiley & Sons, New York, 1988.
111. M. Glauert, *Journal of Fluid Mechanics*, 1956, 1, 625.

112. J. Yamada and H. Matsuda, *Journal of Electroanalytical Chemistry and Interfacial Electrochemistry*, 1973, 44, 189.
113. (a) J. Růžička and E. Hansen, *Analytica Chimica Acta*, 1975, 78, 145; (b) J. Růžička and J. Stewart, *Analytica Chimica Acta*, 1975, 79, 79; (c) C. B. Ranger, *Analytical Chemistry*, 1981, 53, 20A.
114. J. Růžička and E. H. Hansen, *Trends in Analytical Chemistry*, 2008, 27, 390.
115. B. Rocks and C. Riley, *Clinical Chemistry*, 1982, 28, 409.
116. F. A. Vega, C. G. Núñez, B. Weigel, B. Hitzmann and J. C. D. Ricci, *Analytica Chimica Acta*, 1998, 373, 57.
117. K. Tag, K. Riedel, H.-J. Bauer, G. Hanke, K. H. R. Baronian and G. Kunze, *Sensors and Actuators B: Chemical*, 2007, 122, 403.
118. J. S. Y. Chia, M. T. Tan, P. S. Khiew, J. K. Chin and C. W. Siong, *Sensors and Actuators B: Chemical*, 2015, 210, 558.
119. B. Karlberg and G. E. Pacey, *Flow Injection Analysis: a Practical Guide*, Elsevier, Amsterdam, 1989.
120. R. Appelqvist, G. Marko-Varga, L. Gorton, A. Torstensson and G. Johansson, *Analytica Chimica Acta*, 1985, 169, 237.
121. K. Stulik and V. Pacakova, *Electroanalytical Measurements in Flowing Liquids*, John Wiley and Sons, New York, 1987.
122. (a) C. E. Banks and R. G. Compton, *Analytical Sciences*, 2005, 21, 1263; (b) K. Kalcher, I. Svancara, R. Metelka, K. Vytras and A. Walcarius, *Encyclopedia of Sensors*, 2006, 4, 283.
123. G. G. Wildgoose, P. Abiman and R. G. Compton, *Journal of Materials Chemistry*, 2009, 19, 4875.
124. R. L. McCreery, *Chemical Reviews*, 2008, 108, 2646.
125. C. A. Thorogood, G. G. Wildgoose, J. H. Jones and R. G. Compton, *New Journal of Chemistry*, 2007, 31, 958.
126. X. Ji, C. E. Banks, A. Crossley and R. G. Compton, *ChemPhysChem*, 2006, 7, 1337.
127. R. L. McCreery, *Electroanalytical Chemistry*, 1991, 17, 221.
128. K. Okajima, K. Ohta and M. Sudoh, *Electrochimica Acta*, 2005, 50, 2227.
129. L. A. Coury and W. R. Heineman, *Journal of Electroanalytical Chemistry and Interfacial Electrochemistry*, 1988, 256, 327.
130. J. F. Evans and T. Kuwana, *Analytical Chemistry*, 1977, 49, 1632.
131. L. Gorton and P. Bartlett, *Bioelectrochemistry: Fundamentals, Experimental Techniques and Applications*, 2008, 157.
132. G. M. Swain, in *Handbook of Electrochemistry*, ed. C. G. Zoski, Elsevier, Amsterdam, 2007, pp. 111-153.
133. G. Li and P. Miao, in *Electrochemical Analysis of Proteins and Cells*, Springer, Berlin, 2013, pp. 5-18.
134. C.-J. Zhong and M. D. Porter, *Analytical Chemistry*, 1995, 67, 709A.



135. (a) P. Weaver, J. Wall and H. Gest, *Archives of Microbiology*, 1975, 105, 207; (b) M. Madigan and D. Jung, in *The Purple Phototrophic Bacteria*, eds. C. N. Hunter, F. Daldal, M. Thurnauer and J. T. Beatty, Springer, Amsterdam, 2009, pp. 1-15.
136. S. J. Ferguson, J. B. Jackson and A. G. McEwan, *FEMS Microbiology Letters*, 1987, 46, 117.
137. (a) J. Gebicki, M. Modigell, M. Schumacher, J. Van Der Burg and E. Roebroek, *Journal of Cleaner Production*, 2010, 18, S36; (b) A. A. Tsygankov, Y. Hirata, M. Miyake, Y. Asada and J. Miyake, *Journal of Fermentation and Bioengineering*, 1994, 77, 575.
138. Y. K. Cho, T. J. Donohue, I. Tejedor, M. A. Anderson, K. D. McMahon and D. R. Noguera, *Journal of Applied Microbiology*, 2008, 104, 640.
139. K. Hasan, S. A. Patil, K. Go'recki, D. Leech, C. Hägerhäll and L. Gorton, *Bioelectrochemistry*, 2013, 93, 30.
140. K. Hasan, K. V. R. Reddy, V. Eßmann, K. Górecki, P. Ó. Conghaile, W. Schuhmann, D. Leech, C. Hägerhäll and L. Gorton, *Electroanalysis*, 2015, 27, 118.
141. J. K. Fredrickson, M. F. Romine, A. S. Beliaev, J. M. Auchtung, M. E. Driscoll, T. S. Gardner, K. H. Nealson, A. L. Osterman, G. Pinchuk, J. L. Reed, D. A. Rodionov, J. L. M. Rodrigues, D. A. Saffarini, M. H. Serres, A. M. Spormann, I. B. Zhulin and J. M. Tiedje, *Natural Reviews Microbiology*, 2008, 6, 592.
142. N. J. Kotloski and J. A. Gralnick, *MBio*, 2013, 4, e00553.
143. K. M. Thormann, S. Duttler, R. M. Saville, M. Hyodo, S. Shukla, Y. Hayakawa and A. M. Spormann, *Journal of Bacteriology*, 2006, 188, 2681.
144. S. A. Patil, K. Hasan, D. Leech, C. Hägerhäll and L. Gorton, *Chemical Communications*, 2012, 48, 10183.
145. K. Hasan, Y. Dilgin, S. C. Emek, M. Tavahodi, H.-E. Åkerlund, P.-Å. Albertsson and L. Gorton, *ChemElectroChem*, 2014, 1, 131.
146. V. Luimstra, S.-J. Kennedy, J. Güttler, S. Wood, D. Williams and M. Packer, *Journal of Applied Phycology*, 2014, 26, 15.
147. D. Esson, S. Wood and M. Packer, *AMB Express*, 2011, 1, 1.
148. K. Hasan, H. B. Yildiz, E. Sperling, P. Ó. Conghaile, M. A. Packer, D. Leech, C. Hägerhäll and L. Gorton, *Physical Chemistry Chemical Physics*, 2014, 16, 24676.
149. K. Hasan, V. Grippo, E. Sperling, M. A. Packer, D. Leech and L. Gorton, Comparison of photocurrent generation by cyanobacteria and algae to harness sunlight, 2016, (submitted).
150. R. W. Bradley, P. Bombelli, S. J. L. Rowden and C. J. Howe, *Biochemical Society Transactions*, 2012, 40, 1302.
151. M. Rosenbaum and U. Schröder, *Electroanalysis*, 2010, 22, 844.
152. J. V. Moroney and R. A. Ynalvez, in *eLS*, John Wiley & Sons, Ltd, Chichester, 2001, <http://www.els.net> [doi: 10.1002/9780470015902.a0000322.pub2]
153. K. Hasan, E. Çevik, E. Sperling, M. A. Packer, D. Leech and L. Gorton, *Advanced Energy Materials*, 2015, DOI: 10.1002/aenm.201501100.

154. M. C. Potter, *Proceedings of the Royal Society of London. Series B, Containing Papers of a Biological Character*, 1911, 84, 260.
155. B. A. Haddock and C. W. Jones, *Bacteriological Reviews*, 1977, 41, 47.
156. J. M. Berg, J. L. Tymoczko and L. Stryer, in *Biochemistry*. 5th edition, W H Freeman, New York, 2002.
157. B. H. Kim and G. M. Gadd, *Bacterial Physiology and Metabolism*, Cambridge University Press, New York, 2008.
158. H. Krebs and J. Lowenstein, *Metabolic Pathways*, 1960, 1, 129.
159. Y. Anraku, *Annual Review of Biochemistry*, 1988, 57, 101.
160. W. Ingledew and R. Poole, *Microbiological Reviews*, 1984, 48, 222.
161. K. H. Nealson, *Origins of Life and Evolution of the Biosphere*, 1999, 29, 73.
162. U. Brandt, *Annual Review of Biochemistry*, 2006, 75, 69.
163. M. Murphy, *Biochemistry Journal*, 2009, 417, 1.
164. K. S. Oyedotun and B. D. Lemire, *Journal of Biological Chemistry*, 2004, 279, 9424.
165. A. R. Crofts, *Annual Review of Physiology*, 2004, 66, 689.
166. D. M. Kramer, A. G. Roberts, F. Muller, J. Cape and M. K. Bowman, in *Methods in Enzymology*, Academic Press, Cambridge, 2004, pp. 21-45.
167. F. L. Muller, M. S. Lustgarten, Y. Jang, A. Richardson and H. Van Remmen, *Free Radical Biology and Medicine*, 2007, 43, 477.
168. S. Yoshikawa, A. Shimada and K. Shinzawa-Itoh, in *Sustaining Life on Planet Earth: Metalloenzymes Mastering Dioxygen and Other Chewy Gases*, eds. P. M. H. Kroneck and M. E. Sosa Torres, Springer International Publishing, Cham, 2015, pp. 89-130.
169. M. P. Spector, in *Encyclopedia of Microbiology (Third Edition)*, ed. M. Schaechter, Academic Press, Oxford, 2009, pp. 242-264.
170. F. S. Mathews, *Progress in Biophysics and Molecular Biology*, 1985, 45, 1.
171. L. A. Sazanov and P. Hinchliffe, *Science*, 2006, 311, 1430.
172. G. Cecchini, *Annual Review of Biochemistry*, 2003, 72, 77.
173. A. R. Crofts, *Annual Review of Physiology*, 2004, 66, 689.
174. M. W. Calhoun, J. W. Thomas and R. B. Gennis, *Trends in Biochemical Sciences*, 1994, 19, 325.
175. P. D. Boyer, *Annual Review of Biochemistry*, 1997, 66, 717.
176. (a) R. E. Blankenship, *Molecular Mechanisms of Photosynthesis*, John Wiley & Sons, Chichester, 2013; (b) O. Kruse, J. Rupprecht, J. H. Mussgnug, G. C. Dismukes and B. Hankamer, *Photochemical and Photobiological Sciences*, 2005, 4, 957.
177. (a) W. F. J. Vermaas, in *eLS*, John Wiley & Sons, Ltd, Chichester, 2001, <http://www.els.net> [doi: 10.1038/npg.els.0001670]; (b) C. W. Mullineaux, *Biochimica et Biophysica Acta (BBA)-Bioenergetics*, 2014, 1837, 503; (c) D. J. Lea-Smith, P. Bombelli, R. Vasudevan and C. J. Howe, *Biochimica et Biophysica Acta (BBA)-Bioenergetics*, <http://dx.doi.org/10.1016/j.bbabi.2015.10.007>.

178. D. J. Vinyard, G. M. Ananyev and G. Charles Dismukes, *Annual Review of Biochemistry*, 2013, 82, 577.
179. J. W. Cooley and W. F. Vermaas, *Journal of Bacteriology*, 2001, 183, 4251.
180. I. Vass, *Biochimica et Biophysica Acta (BBA)-Bioenergetics*, 2012, 1817, 209.
181. U. C. Vothknecht and P. Westhoff, *Biochimica et Biophysica Acta (BBA)-Molecular Cell Research*, 2001, 1541, 91.
182. N. Nelson and A. Ben-Shem, *Nature Reviews Molecular Cell Biology*, 2004, 5, 971.
183. J. Stenesh, *Biochemistry: Solutions Manual*, Springer, New York, 1998.
184. D. Ort and C. Yocum, in *Oxygenic Photosynthesis: The Light Reactions*, Springer, Houten, 1996, pp. 1-9.
185. D. S. Bendall, in *eLS*, John Wiley & Sons Ltd, Chichester, 2006, p. doi:10.1038/npg.els.0001311.
186. K. J. McCree, *Agricultural Meteorology*, 1972, 9, 191.
187. J. A. Bassham, A. A. Benson and M. Calvin, *Journal of Biological Chemistry*, 1950, 185, 781.
188. A. B. Melandri and D. Zannoni, *Journal of Bioenergetics and Biomembranes*, 1978, 10, 109.
189. M. T. Madigan and H. Gest, *Journal of Bacteriology*, 1979, 137, 524.
190. C. Wraight and M. Gunner, in *The Purple Phototrophic Bacteria*, eds. C. N. Hunter, F. Daldal, M. Thurnauer and J. T. Beatty, Springer, Amsterdam, 2009, pp. 379-405.
191. D. D. Androga, E. Özgür, I. Eroglu, M. Yücel and U. Gündüz, in *Hydrogen Energy - Challenges and Perspectives* ed. D. Minic, Intech Open Access Publisher, Rijeka, 2012, pp. 77-120.
192. N. S. Lewis and D. G. Nocera, *Proceedings of the National Academy of Sciences of the United States of America*, 2006, 103, 15729.
193. S. E. Canton, K. S. Kjær, G. Vankó, T. B. van Driel, S.-i. Adachi, A. Bordage, C. Bressler, P. Chabera, M. Christensen, A. O. Dohn, A. Galler, W. Gawelda, D. Gosztola, K. Haldrup, T. Harlang, Y. Liu, K. B. Møller, Z. Németh, S. Nozawa, M. Pápai, T. Sato, T. Sato, K. Suarez-Alcantara, T. Togashi, K. Tono, J. Uhlig, D. A. Vithanage, K. Wärnmark, M. Yabashi, J. Zhang, V. Sundström and M. M. Nielsen, *Nature Communications*, 2015, 6, doi:10.1038/ncomms7359.
194. N. Sekar and R. P. Ramasamy, *Electrochemical Society Interface*, 2015, 24, 67.
195. (a) S. K. Ravi and S. C. Tan, *Energy & Environmental Science*, 2015, 8, 2551; (b) M. Rosenbaum, Z. He and L. T. Angenent, *Current Opinion in Biotechnology*, 2010, 21, 259.
196. P. Bombelli, M. Zarrouati, R. J. Thorne, K. Schneider, S. J. Rowden, A. Ali, K. Yunus, P. J. Cameron, A. C. Fisher and D. I. Wilson, *Physical Chemistry Chemical Physics*, 2012, 14, 12221.
197. M. Falk, Z. Blum and S. Shleev, *Electrochimica Acta*, 2012, 82, 191.

198. (a) O. Yehezkeli, O. I. Wilner, R. Tel-Vered, D. Roizman-Sade, R. Nechushtai and I. Willner, *The Journal of Physical Chemistry B*, 2010, 114, 14383; (b) D. Yu, M. Wang, G. Zhu, B. Ge, S. Liu and F. Huang, *Scientific Reports*, 2015, 5, doi:10.1038/srep09375.
199. O. Yehezkeli, R. Tel-Vered, J. Wasserman, A. Trifonov, D. Michaeli, R. Nechushtai and I. Willner, *Nature Communications*, 2012, 3, 742.
200. (a) C. F. Meunier, P. Van Cutsem, Y. U. Kwon and B. L. Su, *Journal of Materials Chemistry*, 2009, 19, 1535; (b) A. Agostiano, D. C. Goetze and R. Carpentier, *Photochemistry and Photobiology*, 1992, 55, 449; (c) N. D. Kirchhofer, M. A. Rasmussen, F. W. Dahlquist, S. D. Minter and G. C. Bazan, *Energy & Environmental Science*, 2015, 8, 2698.
201. R. Carpentier, C. Loranger, J. Chartrand and M. Purcell, *Analytica Chimica Acta*, 1991, 249, 55.
202. A. Mershin, K. Matsumoto, L. Kaiser, D. Yu, M. Vaughn, M. K. Nazeeruddin, B. D. Bruce, M. Graetzel and S. Zhang, *Scientific Reports*, 2012, 2, 1.
203. A. Badura, D. Guschin, B. Esper, T. Kothe, S. Neugebauer, W. Schuhmann and M. Rögner, *Electroanalysis*, 2008, 20, 1043.
204. J. M. Pisciotta, Y. Zou and I. V. Baskakov, *Applied Microbiology and Biotechnol*, 2011, 91, 377.
205. W. Adams Iii, C. R. Zarter, K. Mueh, V. e. Amiard and B. Demmig-Adams, in *Photoprotection, Photoinhibition, Gene Regulation, and Environment*, eds. B. Demmig-Adams, W. Adams, III and A. Mattoo, Springer, Amsterdam, 2006, pp. 49-64.
206. F. Yuji, M. Takeyuki and M. Keisuke, *Journal of Micromechanics and Microengineering*, 2006, 16, S220.
207. P. Bombelli, T. Müller, T. W. Herling, C. J. Howe and T. P. Knowles, *Advanced Energy Materials*, 2015, 5, DOI: 10.1002/aenm.201401299.
208. D. R. Lovley, *Current Opinion in Biotechnology*, 2008, 19, 564.
209. R. W. Bradley, P. Bombelli, D. J. Lea-Smith and C. J. Howe, *Physical Chemistry Chemical Physics*, 2013, 15, 13611.
210. N. Sekar, R. Jain, Y. Yan and R. P. Ramasamy, *Biotechnology and Bioengineering*, 2015, DOI: 10.1002/bit.25829.
211. R. E. Blankenship, D. M. Tiede, J. Barber, G. W. Brudvig, G. Fleming, M. Ghirardi, M. R. Gunner, W. Junge, D. M. Kramer, A. Melis, T. A. Moore, C. C. Moser, D. G. Nocera, A. J. Nozik, D. R. Ort, W. W. Parson, R. C. Prince and R. T. Sayre, *Science*, 2011, 332, 805.



# Paper I





## Electrochemical communication between heterotrophically grown *Rhodobacter capsulatus* with electrodes mediated by an osmium redox polymer

Kamrul Hasan<sup>a</sup>, Sunil A. Patil<sup>a</sup>, Kamil Górecki<sup>a</sup>, Dónal Leech<sup>b</sup>, Cecilia Hägerhäll<sup>a</sup>, Lo Gorton<sup>a,\*</sup>

<sup>a</sup> Department of Biochemistry and Structural Biology, Lund University, P.O. Box 124, SE-22100 Lund, Sweden

<sup>b</sup> School of Chemistry, National University of Ireland Galway, University Road, Galway, Ireland

### ARTICLE INFO

#### Article history:

Received 16 December 2011

Received in revised form 24 April 2012

Accepted 17 May 2012

Available online 15 June 2012

#### Keywords:

*Rhodobacter capsulatus*

Osmium redox polymer

Mediated electron transfer

Microbial biosensor

Biofuel cell

### ABSTRACT

The metabolically versatile purple bacteria *Rhodobacter capsulatus* was investigated to check its possible applicability in biofuel cells and electrochemical microbial biosensors. The wild type strain ATCC 17015 and mutant strain 37b4 lacking the lipopolysaccharide capsule was compared for their ability to communicate with electrodes modified with an osmium redox polymer. In this work, aerobic heterotrophically grown *R. capsulatus* were used to screen for efficient cell–electrode communication for later implementation using photoheterotrophically grown bacteria. The bacterial cells embedded in the osmium polymer matrix demonstrated efficient electrical “wiring” with the electrodes and were able to generate a noticeable current with succinate as substrate. Interestingly, at 2 mM succinate the wild type strain showed much better bioelectrocatalytic current generation (4.25  $\mu\text{A}/\text{cm}^2$ ) than the strain lacking capsule (1.55  $\mu\text{A}/\text{cm}^2$ ). The wild type strain also exhibited a stable current response for longer time, demonstrating that the bacterial lipopolysaccharide in fact enhances the stability of the polymer matrix layer of the modified electrode. Control experiments with *R. capsulatus* without any mediator did not show any current irrespective of the capsule presence. This demonstrates that development of photosensors and other light driven bioelectrochemical devices could be feasible using *R. capsulatus* and will be at focus for future studies.

© 2012 Elsevier B.V. All rights reserved.

### 1. Introduction

The growing interest in microbial fuel cells (MFCs), for both electricity generation and a wide range of other applications [1] and electrochemical microbial biosensors [2], has during the last decade led to an increased attention in “wiring” microbial cells to electrodes to facilitate the electrochemical communication [3–7]. The bacteria are able to transfer electrons to an electrode mainly by the use of various redox mediators (artificial or produced by bacteria) or using direct electron transfer (DET) via cytochrome rich membranes, electrically conductive pili, or nanowires produced by the bacteria [8,9]. Limited bacterial groups such as *Geobacteraceae* [10,11] and *Shewanellaceae* [12–14] possess the ability to communicate electrochemically with the electrodes without any mediator, thanks to the metabolism and electron conducting structures evolved for use in their natural habitat. These bacteria may, however, not be the most suitable for many applications. Consequently, bacteria that are unable to communicate with the electrodes by themselves have been the focus of research during the last decade [2,7,15,16]. Many attempts have been made to enhance the electron transfer by exploring genetic engineering to provide the bacteria with better electron conducting structures or

other enhanced metabolic features [6,17–19]. In addition, research on various other influential factors like anode materials, inoculum sources, substrates, separators, cathode, design, operational parameters etc. have resulted into several advancements, increased performance and widened application range for MFC technology [20–25].

In addition to pure microbial cultures MFC research mainly employs electrochemically enriched biofilms of mixed culture or *G. sulfurreducens* from different inoculum sources [5,11,26]. Amongst the widely used bacteria for MFC research, very few like *Shewanella* sp. possess metabolic diversity and facultative oxidant tolerance [27,28]. Furthermore, although research has been conducted with different mixed microbial inoculum sources and pure cultures, very few reports introduced new metabolically versatile microbial catalysts for MFCs and whole cell biosensors [5,26]. Moreover, most of the organisms investigated in MFCs so far, are strictly anaerobic [5], which limits their applicability. Therefore, to speed up the development of MFCs and whole cell electrochemical biosensors, there is a necessity to explore alternative versatile bacteria that might increase the types of microorganisms that can be used as possible catalysts at the bioanode or as biocathode [4].

In this work we have investigated the metabolically versatile  $\alpha$ -proteobacterium *Rhodobacter capsulatus* [29,30] and tested its capability as a microbial catalyst for MFC and microbial biosensor. *R. capsulatus* is amongst the most nutritionally versatile non-sulfur purple bacteria [31], which have the capacity to grow rapidly under

\* Corresponding author. Tel.: +46 46 222 758; fax: +46 46 222 45 44.  
E-mail address: [Lo.Gorton@biochemistry.lu.se](mailto:Lo.Gorton@biochemistry.lu.se) (L. Gorton).



either anaerobic photosynthetic conditions or aerobic dark conditions [30,32]. *R. capsulatus* has previously been utilized for anoxygenic hydrogen production [33,34], but this bacterium has never been tried in any electrochemical application. In this study, we used heterotrophically grown *R. capsulatus* under aerobic conditions and tested its ability to communicate electrochemically with osmium (Os) redox polymer modified electrodes. *R. capsulatus* is a Gram-negative organism with an outer and an inner membrane, with a thin peptidoglycan cell wall in between. In addition, wild type *R. capsulatus* possesses an outer capsule of slimy lipopolysaccharides [35,36]. The exact composition of the lipopolysaccharide layer varies among different *R. capsulatus* strains [37], but the capsule presence as such may interfere with the polymer used for communication with the electrode and increase the distance from the outer membrane surface to the electrode surface. Therefore, the mutant strain 37b4 that does not produce any lipopolysaccharide capsule [38] was compared to the wild type *R. capsulatus*.

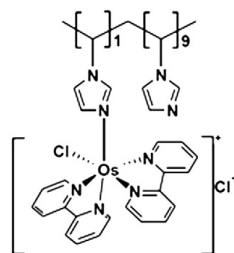
The use of flexible Os redox polymers in biofuel cells (BFCs) or biosensors has gained attention due to the efficient electron shuttling properties, polymeric structure, a stable adsorption in addition to the possibility to lead to the formation of multiple layers of both immobilized enzymes and microbial cells on the electrode surface [6,39–41]. Our earlier studies with such polymeric mediators showed an enhanced electron transfer between different microbial cells and electrodes [7,15,17,18]. Therefore, the current research is a logical continuation of previous work from our group involving the electrochemical communication between different bacteria and electrodes using Os polymers. For this study, an Os polymer with a high positive redox potential (0.176 V vs. SCE; 0.221 V vs. Ag/AgCl, sat. KCl) was chosen, because of its proven ability of efficient wiring of enzymes to electrodes [42,43]. This Os polymer has a high redox potential and a short length of the side chains, where the Os<sup>3+/2+</sup> functionalities are located at their ends. In addition, the advantage of using high redox potential polymers is that they efficiently compete with O<sub>2</sub> as electron acceptor [18].

Herein, the electrochemical communication of the wild type and capsule lacking mutant strains of *R. capsulatus* with Os redox polymer modified electrodes was investigated using cyclic voltammetry (CV) measurements. Additionally, the current response characteristics of the bacterial cell modified Os polymer graphite electrodes were evaluated for succinate as substrate in flow analysis mode. Succinate was chosen as this substrate can be used both for heterotrophic and phototrophic *R. capsulatus* cells. The succinate:quinone oxidoreductase enzyme has not been biochemically characterized in *R. capsulatus*, but primary sequence comparison reveal it to be similar to that of *Paracoccus denitrificans* [44] and thus belonging to class 1 [45]. Furthermore, the ability of *R. capsulatus* to communicate with the electrode by itself through a DET mode was also investigated in potentiostatically controlled half-cell set-ups. Besides, the electron transfer efficiency of the Os polymer was compared with that of a soluble mediator, hexacyanoferrate. The stability of the current response for *R. capsulatus* with Os polymer modified electrodes was carefully considered throughout the experiments. Both gold electrodes protected by a thiol based self assembled monolayer as well as graphite electrodes were used in line with previous investigations [7,18].

## 2. Experimental

### 2.1. Chemicals

[Os(2,2'-bipyridine)<sub>2</sub>-poly(N-vinylimidazole)<sub>10</sub>Cl]<sup>2+/+</sup> (poly[Os(bpy)<sub>2</sub>(PVI)<sub>10</sub>Cl]<sup>2+/+</sup>) of E° equal to +176 mV vs. SCE (sat. KCl)/+221 mV vs. Ag/AgCl (sat. KCl) ("Scheme 1") was synthesized as reported in [46]. The weight-average molecular weight of the poly(vinylimidazole) as determined by viscometry in ethanol was 10,000 g/mol [47]. All chemicals were purchased from Sigma–Aldrich/Merck and were of either research or analytical grade. All aqueous solutions were prepared



Scheme 1. Structural representation of the osmium redox polymer.

by using water purified and deionized (18 MΩ) with a Milli-Q system (Millipore, Bedford, MA, USA).

### 2.2. Microbial growth conditions and inoculum preparation

*R. capsulatus* strains, ATCC 17015 (wild type) and 37b4 (capsule lacking mutant) were purchased from DSMZ – Deutsche Sammlung von Mikroorganismen und Zellkulturen GmbH (Braunschweig, Germany). These strains were grown and maintained on minimal peptone yeast extract medium (MPYE) agar plates [29]. A single, well isolated colony was used for inoculum preparation throughout the study. For inoculum preparation, the bacterial cells were grown aerobically in 10 mL of MPYE broth (in 50 mL baffled E-flasks at 200 rpm) for 20 h at 30 ± 2 °C by transferring 1 mL of cell suspension prepared by suspending an isolated colony into the saline (0.85% NaCl). The cells grown in MPYE were harvested in the early stationary growth phase by centrifuging the broth at 4000 rpm for 10 min. Further, the cells were washed once in 20 mM MOPS (3-morpholinopropanesulfonic acid) buffer (pH 7.4), centrifuged again as before, resuspended in the same buffer to adjust cell density to 1 g/mL (wet weight) [48] and used immediately for electrochemical experiments (CV and amperometric flow mode measurements).

For batch mode chronoamperometry (CA) experiments the cells harvested from the growth medium were transferred to 200 mL of synthetic medium composed of PIPES buffer 15.1 g/L; NaOH 3.0 g/L; NH<sub>4</sub>Cl 1.5 g/L; KCl 0.1 g/L; NaH<sub>2</sub>PO<sub>4</sub>·H<sub>2</sub>O 0.6 g/L; NaCl 5.8 g/L; mineral solution 10 mL/L; vitamin solution 10 mL/L; amino acid solution 10 mL/L [49]. The substrate used was 10 mM succinate (disodium salt). After incubation of flasks at 30 ± 2 °C (500 mL baffled E-flasks, aerobically while shaking at 200 rpm for 72 h) the cells were harvested and used as an inoculum in potentiostatic half-cell set ups hosting a similar synthetic medium. These experiments were performed to check the capability of *R. capsulatus* to communicate with an electrode without any mediator.

### 2.3. Preparation of the electrodes modified with bacteria

Either gold (BAS, West Lafayette, IN, USA) or spectrographic graphite rods (Ringsdorf Werke GmbH, Bonn, Germany, type RW001, 3.05 mm diameter and 13% porosity) were used as working electrodes. The procedure explained by Coman et al. [18] was followed to prepare the modified working electrodes. Polycrystalline gold electrodes (projected surface area; 0.02 cm<sup>2</sup>) were electrochemically cleaned by cycling in 0.1 M NaOH between 0 and –1000 mV vs. NHE, followed by mechanical polishing on Microcloth (Buehler, Lake Bluff, IL) in an aqueous alumina UF slurry (1 and 0.1 μm, Struers, Copenhagen, Denmark). The electrodes were rinsed with water, ultrasonicated for 5 min in Milli-Q water, followed by cycling in 0.5 M H<sub>2</sub>SO<sub>4</sub> between 0 and +1950 mV vs. NHE, and finally rinsed with Milli-Q water. Formation of a self-assembled monolayer (SAM) of aldrithiol at the electrode surface was done by immersing the electrode in a saturated aqueous solution of

the thiol for 2 h (at room temperature). In the following step, a 5  $\mu\text{L}$  portion of Os redox polymer solution (10 mg/mL in Milli-Q water) was spread over the surface of the modified gold electrode and water was allowed to evaporate at room temperature for 30 min. Finally, a 5  $\mu\text{L}$  portion of *R. capsulatus* suspension in 20 mM MOPS buffer (pH 7.4) was placed on the modified electrode surface. The droplet was allowed to gently dry at room temperature. Before use, a dialysis membrane (Spectrum Laboratories Inc., Rancho Dominguez, CA, USA, molecular mass cutoff: 6000–8000) was used to trap the bacterial cells onto the surface to prepare a permselective membrane electrode [50]. The dialysis membrane (presoaked in buffer) was pressed onto the electrode and fixed tightly to the electrode with a rubber O-ring and Parafilm.

In case of graphite electrodes, the material was polished on wet emery paper (Tufbak, Durite, P1200) and subsequently carefully rinsed with Milli-Q water and dried. Then 5  $\mu\text{L}$  of Os polymer solution (10 mg/mL in Milli-Q water) was spread onto the entire active surface of the electrode (0.0731  $\text{cm}^2$ ). The electrode was dried at room temperature for 10–15 min and then 5  $\mu\text{L}$  of the cell suspension was spread onto the surface and further gently dried until a layer was formed on the surface (10–15 min).

#### 2.4. Measurement set-ups

The amperometric measurements were done in flow modes at room temperature ( $22 \pm 2^\circ\text{C}$ ) with disodium succinate as electron donor for the *R. capsulatus* modified electrode mounted in a standard three electrode flow through electrochemical wall jet cell containing the working electrode (graphite electrode modified with Os polymer and cells) as well as a Pt counter and an Ag|AgCl (0.1 M KCl) (Beta Sensor AB, Södra Sandby, Sweden) reference electrode controlled with a small potentiostat (Zäta Elektronik, Höör, Sweden). The procedure explained elsewhere was followed to perform flow mode experiments [18]. The modified electrode was press fitted into a Teflon holder and inserted into the wall jet cell and kept at a constant distance (ca. 1 mm) from the inlet nozzle. The flow rate of the solutions was maintained at 0.5 mL/min with a peristaltic pump Minipuls 2 (Gilson, Villiers-le-Bel, France). The response currents were recorded on a strip chart recorder (Kipp & Zonen, Delft, The Netherlands). The injector was an electrically controlled six-port valve (Rheodyne, Cotati, CA, USA), and the injection loop volume was 50  $\mu\text{L}$ . The MOPS buffer (20 mM MOPS, 0.1 M KCl; pH 7.4) used as electrolyte throughout the study, was carefully degassed under vacuum prior to experiments. The reported results are based on three equivalently prepared electrodes and the relative standard deviation was always less than 10%.

To test the competition theory, the efficiency of the Os polymer was also compared with a freely diffusing mediator, hexacyanoferrate (III) (0.236 V vs. Ag|AgCl; sat. KCl) by continuously pumping 2 mM hexacyanoferrate (III) solution prepared in 20 mM MOPS buffer with 2 mM succinate into the flow cell. Furthermore, the stability of the Os polymer modified graphite electrode with the *R. capsulatus* cells was checked by monitoring the current response with continuous pumping of 2 mM succinate with flow buffer (20 mM MOPS) for a few hours through the flow cell.

CV measurements were performed using an AUTOLAB PGSTAT 30 (EcoChemie, Utrecht, The Netherlands) equipped with GPES 4.9 software with a three-electrode configuration using an Ag|AgCl reference electrode (sat. KCl, Sensortechnik Meinsberg, Germany) and a counter electrode made of a platinum foil. These experiments were performed with both gold and graphite as working electrodes. In case of modified gold electrodes, a SCE (sat. KCl) was used as reference electrode. If not stated otherwise, these measurements were performed at a scan rate of  $2 \text{ mV s}^{-1}$ . All CV experiments were performed under anoxic conditions (to exclude possible competition by  $\text{O}_2$  as electron acceptor), which were achieved by sparging argon for 20 min in the buffer solution. Furthermore, the headspace of the

solution was also sparged with argon during the CV measurements. All reported data are based on at least three independent replicates of each experiment.

Batch mode CA experiments with succinate were performed to check the ability of *R. capsulatus* to communicate with the electrode by itself without the use of any mediator/Os polymer using optimum growth temperature of  $30 \pm 2^\circ\text{C}$  at anoxic conditions. These experiments were executed with a three-electrode configuration using bare graphite rods as working as well as counter electrodes and an Ag|AgCl reference electrode (sat. KCl). The working electrode was constantly polarized at positive potential of  $+0.2 \text{ V}$  (vs. Ag|AgCl) to check the ability of the bacteria to utilize the electrode as an electron acceptor. The sealed, water jacketed glass vessels, connected to a thermostat (Paratherm U2 electronic, Julabo, Schwarzwald, Germany) were employed as electrochemical cells that allowed maintenance of strictly anoxic conditions as well as temperature control. These CA experiments performed with bare graphite electrode demonstrated the incompetence of *R. capsulatus* to communicate with the electrode without any mediator (data not shown).

### 3. Results and discussion

The electrochemical behavior of the used Os polymer was characterized using CV. The CV response of the Os polymer adsorbed on the surface of an aldrithiol modified gold electrode obtained in 20 mM MOPS buffer at pH 7.4 with and without bacterial cells is depicted in Fig. 1. As can be seen in the CV (Fig. 1A), the Os polymer shows a pair of well-defined redox peak for the Os redox center in the polymer. The  $E^\circ$ -value of the Os polymer was evaluated by taking the mean value of the anodic and cathodic peak potentials of the CV and was found to be  $+180 \text{ mV}$  vs. SCE (sat. KCl), a value in close agreement with previous results [43,46]. In comparison to the electrode modified with only Os polymer, the adsorption of bacterial cells into the polymer matrix retards the redox response of the Os center of the polymer as displayed by the drastic decrease in the peak current values in the CV (Fig. 1B). The decrease in the current response in the presence of bacterial cells is attributed to the fact that the cationic Os polymers form strong electrostatic complexes with the anionic cell wall coating of the viable bacterial cells. As a consequence, the mobility of the individual redox units get hampered that leads to the lowering of the current response, which is well in accordance with previous investigations with bacterial cells and redox enzymes [18,43]. Furthermore, it is also reasonable that the interaction between bacterial cells and Os polymer reduces the mobility of the segments of

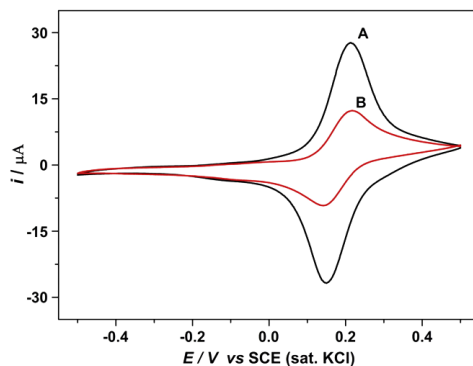


Fig. 1. Cyclic voltammograms of the Os polymer adsorbed on an aldrithiol modified gold electrode, in the (A) absence and (B) presence of bacterial cells. Experiments were performed in a 20 mM MOPS buffer (0.1 M KCl) at pH 7.4. The scan rate was  $50 \text{ mV s}^{-1}$ .

the Os polymer and thus the flow of electrons between the  $\text{Os}^{3+/2+}$  redox centers (electron self-exchange) of the polymer resulting in lowering of current response as observed in the CV. However, as can be seen in Fig. 1B, the bacterial cells do not influence the redox potential of the Os polymer.

Further CV measurements with Os polymer modified graphite electrodes exhibited similar electrochemical behavior with and without wild type *R. capsulatus* cells (Fig. 2B and C). Fig. 2 depicts the comparative CVs with bare graphite (A), Os polymer modified graphite (B), Os polymer + cell modified graphite (C) in 20 mM MOPS buffer and Os polymer + cell modified graphite in 20 mM MOPS buffer with 2 mM succinate (D) at 2 mV/s scan rate. In comparison to the CV response observed in previous studies with *Gluconobacter* sp. and *Pseudomonas* sp. [7,15], the response was not pronounced for *R. capsulatus* in the presence of substrate, which might be due to the mass transfer and/or kinetic limitations. However, at a constant applied potential the wild type *R. capsulatus* with the Os polymer modified graphite electrode showed steady state current generation at different substrate concentrations (Figs. 3A & 4A). The increased (although lower than previously observed with other bacteria) current response in presence of substrate (as can be seen in CV in Fig. 2D) in comparison to the CV obtained in absence of substrate (Fig. 2C) and steady state current generation at constant potential (Fig. 3A inset) indicates the bioelectrocatalytic activity and thus the electrochemical communication between viable *R. capsulatus* with the Os polymer modified graphite electrode.

The electrical wiring of *R. capsulatus* with electrodes is due to the strong electrostatic interactions between the negatively charged bacterial cells and the positively charged adsorbed Os polymer matrix. Therefore, the electron transfer can be attributed to the sequential electrical conduit starting from intracellular redox proteins to external Os redox centers at the polymer matrix and finally towards the electrode surface (as illustrated in "Scheme 2"). *R. capsulatus* lacking the capsule also exhibited similar electrochemical behavior with CV measurements (data not shown). Control experiments with an electrode only modified with wild type *R. capsulatus* cells in a solution containing succinate did not reveal any current generation (data not shown) indicating the necessity of Os-polymer for successful bioelectrocatalysis.

The quantitative evaluation of the electron transfer efficiency and thus, bioelectrocatalytic performance of *R. capsulatus* was investigated with amperometric measurements by applying a constant potential. For the Os polymer modified electrodes, a +300 mV vs. Ag/AgCl

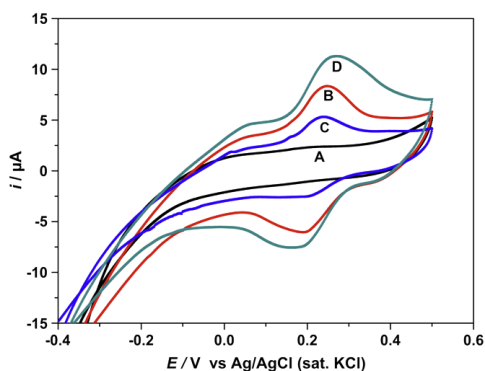


Fig. 2. Cyclic voltammograms of the (A) bare graphite (B) Os polymer modified graphite (C) Os polymer modified graphite in the presence of cells in only 20 mM MOPS buffer (0.1 M KCl) at pH 7.4 and (D) Os polymer modified graphite in the presence of cells with 2 mM succinate in 20 mM MOPS buffer. The scan rate was 2 mV s<sup>-1</sup>. The measurements were conducted with wild type *R. capsulatus*.

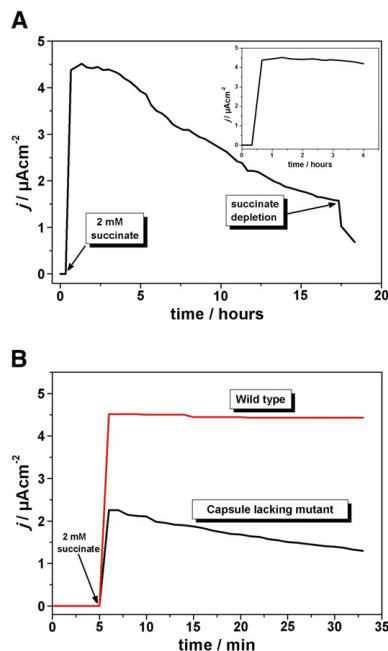
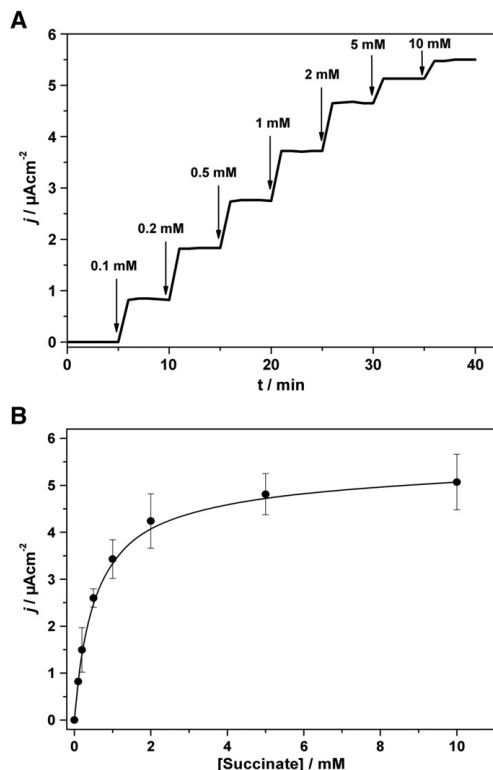


Fig. 3. (A) Stability characteristics (current density vs. time) for wild type *R. capsulatus* cells on osmium redox polymer modified electrode. Measurements were performed in flow mode (0.5 ml/min). Inset figure shows the stable current generation for approximately 4 h. (B) Comparison between current density responses of intact wild type and capsule lacking *R. capsulatus* cells mediated by osmium redox polymer ( $E_{app} = +300$  mV vs. Ag/AgCl, 0.1 M KCl) adsorbed on graphite electrode. Measurements were performed in flow analysis mode after removing oxygen from the solution.

(0.1 M KCl) potential was applied (a potential value sufficiently more positive than the  $E^{0'}$  value of the polymer, to guarantee a potential independent response). The viability and stability of the cells trapped at the Os polymer modified electrode surface is a critical issue. Therefore, the operational stability of the Os polymer modified graphite electrodes with both *R. capsulatus* strains in the flow cells was investigated by monitoring the current response of the system with 2 mM succinate. After initial adjustment of the flow system for a stable baseline (for 30–45 min) with only buffer, the system was continuously fed with succinate. We observed a stable current generation ( $\sim 4.25$   $\mu\text{A}/\text{cm}^2$ ) for about 4 h with wild type *R. capsulatus* (Fig. 3A inset). Afterwards, a continuous decrease in current response was observed with time and reached approximately 35% of the initial response after 18 h (Fig. 3). The decrease in current response can be attributed to the lowering of the microbial substrate oxidation. This is due to a gradual decrease in the number of active cells on the electrode surface. As we provide only carbon source but no other nutrients in the flow buffer, the cells do not multiply as they do naturally in presence of complete growth medium. Therefore the cell number continues decreasing with time. Also there is detachment or washout of the cells from the electrode, in particular with mutant cells. In order to check the role of the continuous supply of succinate on the generated current the pump was stopped after approximately 18 h, which resulted in a drastic decrease in the current response. It is well known that the lipopolysaccharide capsule layer helps many organisms to adhere to the substratum very firmly and lead to biofilm formation [51]. Thus, the stability of wild type *R. capsulatus*



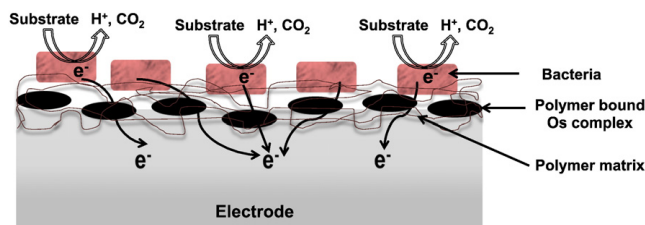
**Fig. 4.** (A) Current density response of intact wild type *R. capsulatus* cells mediated by osmium redox polymer ( $E_{app} = +300$  mV vs. Ag|AgCl, 0.1 M KCl) on graphite electrode at different concentrations of succinate (indicated by arrows) in 20 mM MOPS buffer. Measurements were performed in flow analysis mode. (B) Dependence of the bioelectrocatalytic current densities on the succinate concentration. The data are derived by depicting the steady state current from experiments analogue to those presented in panel A.

can be attributed to the outer capsule layer, which helps the biofilm to remain intact and thus stable for a long time at the Os polymer matrix adsorbed on the electrode. In comparison, with the capsule lacking *R. capsulatus* the current response was stable for less than 1 h and reached approximately 10% of the initial response after 3 h (data not shown). This indicates the wash out/detachment of physically adsorbed capsule lacking bacterial cells from the graphite electrode during continuous flow operation. As a consequence, with regard to

the stability observations all flow mode experiments were planned and executed within 1 h and 4 h (after a stable baseline was obtained) for capsule lacking and wild type strains respectively. Furthermore, as can be seen from Fig. 3B, the wild type strain ( $\sim 4.25 \mu\text{A}/\text{cm}^2$ ) exhibited almost a 3.5 times higher bioelectrocatalytic current generation than the capsule lacking strain ( $\sim 1.55 \mu\text{A}/\text{cm}^2$ ) with 2 mM succinate in flow mode measurements. The superior current response with wild type compared to capsule lacking *R. capsulatus* can be attributed to their stability and conductive capsule – polymer matrix. Although Os polymers exhibit excellent communication with the electrode, these findings raise the concerns about their stability as mediators and their applicability in BFCs. We anticipate that the use of some non-toxic cross-linking agents may increase the long term stability of the Os polymer electrodes.

Fig. 4A shows the dependence of the bioelectrocatalytic current generation on the substrate concentration. After adjustment of the flow cell to continuous flow conditions with only buffer, the system was exposed to a stepwise increase in the succinate concentration after every 5 min interval. It can be clearly seen that the current density increases with increasing substrate concentration up to 10 mM. The subsequent pumping of  $\geq 10$  mM succinate in the system resulted in a slight decrease in the current response (data not shown). The decrease in the current signal at high substrate concentrations could be attributed either to product inhibition or pH changes inside the cell. The maximum bioelectrocatalytic activity ( $\sim 5.5 \mu\text{A}/\text{cm}^2$ ) was achieved at 10 mM succinate. Fig. 4B summarizes the results of experiments similar to those shown in Fig. 4A by depicting the succinate concentration dependence of the steady state current densities. Furthermore, one can also see the linear dependence of the current response on the succinate concentration at low range (up to 2 mM). A similar kind of a linear dependence of the current response on the succinate concentration in the  $\mu\text{M}$  (5–200) range was observed for capsule lacking *R. capsulatus* (data not shown) and also have been reported by Coman et al. for *Bacillus subtilis* [18].

The efficiency of the Os polymer was also compared to that of a freely diffusing mediator, hexacyanoferrate (III). In this case, the system was polarized at a potential of +300 mV for the Os polymer modified electrode and the results were compared (Fig. 5). Once a stable baseline was obtained with only buffer, a 2 mM succinate containing buffer was continuously pumped into the system. Immediately after a stable current response with 2 mM succinate for approximately 10 min was obtained, a flow buffer containing 2 mM hexacyanoferrate (III) in addition to 2 mM succinate was pumped to the system. As expected, the low molecular weight and freely diffusing monomeric hexacyanoferrate (III) proved to be a more efficient mediator compared with the Os polymer. As can be clearly deduced from Fig. 5, approximately a five times increased current was observed with hexacyanoferrate (III), when using 2 mM succinate as substrate with capsule lacking *R. capsulatus* cells. A similar hexacyanoferrate (III) effect was observed with wild type *R. capsulatus* (data not shown). Furthermore, the observations are well in agreement to the previously obtained results with *Gluconobacter oxydans* [7] and with engineered *Bacillus subtilis* [18].



**Scheme 2.** Proposed extracellular electron transfer from the viable bacteria to the electrode mediated by an osmium redox polymer.

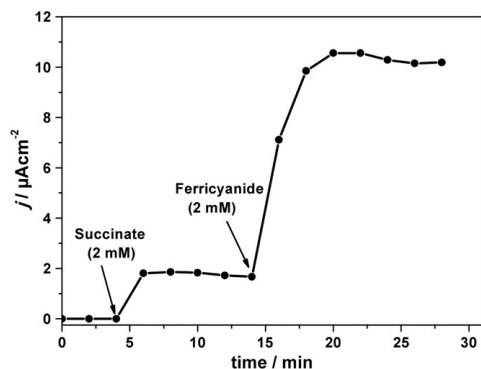


Fig. 5. The effect of ferricyanide on the current density generated by the osmium polymer mediated capsule lacking *R. capsulatus* cells modified graphite electrode. The applied potential was +300 mV vs. Ag/AgCl (0.1 M KCl) and the rest of the conditions were similar as mentioned before.

Here it has to be stressed that the *R. capsulatus* cells used within this study were directly harvested from the MPYE medium without pre-adjustment of the cells to succinate as substrate. Any prior supplementation of substrate into the MPYE during inoculum preparation might considerably increase the response of the bacteria with respect to that substrate. The immobilization of the bacteria/mediator on the electrode and ensuring an efficient electron transfer from the enzyme/bacteria to the electrode via the mediator are decisive features of mediated electrochemical biosensors. Based on these results and our previous research, we anticipate that the use of Os polymers as electron shuttles in whole cell biosensors and MFCs can enable the possibility of exploration of wide range of microbial catalysts for both anode and biocathode applications. With further investigations, we also assume that the use of Os polymer modified electrodes may simplify the design and the use of electrochemical microbial biosensors, particularly for on-site applications and for flow systems.

#### 4. Conclusion

In this study we have demonstrated the possibility to "wire" heterotrophically grown *R. capsulatus* to both gold and graphite electrodes with the aid of an Os redox polymer. Wild type *R. capsulatus* cells embedded in the Os polymer matrix demonstrated their ability to generate a significant current with succinate as substrate. The study further showed the linear dependence of the current response on substrate concentration (in the  $\mu\text{M}$  range). Although stability is a main concern, the results of this study are encouraging for the possible exploitation of non-oxoelectrogens as biocatalysts in microbial biosensors and BFCs with Os polymers. Further work is in progress to exploit photoheterotrophically grown *R. capsulatus* at anoxic conditions for phototrophic MFCs.

#### Acknowledgments

The authors thank – The European Commission ("Chebana" FP7-PEOPLE-2010-ITN-264772), a Charles Parsons Energy Research Award through Science Foundation Ireland, and The Swedish Research Council (projects: 2010–5031, 2010–2013) for the financial support.

#### References

[1] K. Rabaey, R.A. Rozendal, Microbial electrosynthesis – revisiting the electrical route for microbial production, *Nat. Rev. Microbiol.* 8 (2010) 706–716.

[2] L. Su, W. Jia, C. Hou, Y. Lei, Microbial biosensors: a review, *Biosens. Bioelectron.* 26 (2011) 1788–1799.

[3] S. Timur, U. Anik, D. Odaci, L. Gorton, Development of a microbial biosensor based on carbon nanotube (CNT) modified electrodes, *Electrochem. Commun.* 9 (2007) 1810–1815.

[4] F.J. Rawson, D.J. Garrett, D. Leech, A.J. Downard, K.H.R. Baronian, Electron transfer from *Proteus vulgaris* to a covalently assembled, single walled carbon nanotube electrode functionalised with osmium bipyridine complex: application to a whole cell biosensor, *Biosens. Bioelectron.* 26 (2011) 2383–2389.

[5] V. Sharma, P.P. Kundu, Biocatalysts in microbial fuel cells, *Enzyme Microb. Technol.* 47 (2010) 179–188.

[6] H. Shkil, A. Schulte, D.A. Guschin, W. Schuhmann, Electron transfer between genetically modified *Hansenula polymorpha* yeast cells and electrode surfaces via os-complex modified redox polymers, *Chemphyschem* 12 (2011) 806–813.

[7] I. Vostiar, E.E. Ferapontova, L. Gorton, Electrical "wiring" of viable *Gluconobacter oxydans* cells with a flexible osmium-redox polyelectrolyte, *Electrochem. Commun.* 6 (2004) 621–626.

[8] U. Schröder, Anodic electron transfer mechanisms in microbial fuel cells and their energy efficiency, *Phys. Chem. Chem. Phys.* 9 (2007) 2619–2629.

[9] Y. Qiao, S.J. Bao, C.M. Li, Electro-catalysis in microbial fuel cells-from electrode material to direct electrochemistry, *Energy Environ. Sci.* 3 (2010) 544–553.

[10] D.R. Lovley, Powering microbes with electricity: direct electron transfer from electrodes to microbes, *Environ. Microbiol. Rep.* 3 (2011) 27–35.

[11] F. Harnisch, C. Koch, S.A. Patil, T. Hubschmann, S. Muller, U. Schroder, Revealing the electrochemically driven selection in natural community derived microbial biofilms using flow-cytometry, *Energy Environ. Sci.* 4 (2011) 1265–1267.

[12] A.A. Carmona-Martinez, F. Harnisch, L.A. Fitzgerald, J.C. Biffinger, B.R. Ringseisen, U. Schroder, Cyclic voltammetric analysis of the electron transfer of *Shewanella oneidensis* MR-1 and nanofilament and cytochrome knock-out mutants, *Bioelectrochemistry* 81 (2011) 74–80.

[13] A. Okamoto, R. Nakamura, K. Hashimoto, In-vivo identification of direct electron transfer from *Shewanella oneidensis* MR-1 to electrodes via outer-membrane OmcA-MtrCAB protein complexes, *Electrochim. Acta* 56 (2011) 5526–5531.

[14] M.Y. El-Naggar, G. Wanger, K.M. Leung, T.D. Yuzvinsky, G. Southam, J. Yang, W.M. Lau, K.H. Nealon, Y.A. Gorby, Electrical transport along bacterial nanowires from *Shewanella oneidensis* MR-1, *Proc. Natl. Acad. Sci. U. S. A.* 107 (2010) 18127–18131.

[15] S. Timur, B. Haghghi, J. Tkac, N. Pazarlioglu, A. Telefoncu, L. Gorton, Electrical wiring of *Pseudomonas putida* and *Pseudomonas fluorescens* with osmium redox polymers, *Bioelectrochemistry* 71 (2007) 38–45.

[16] Y. Yuan, Q. Chen, S. Zhou, L. Zhuang, P. Hu, Bioelectricity generation and microcystins removal in a blue-green algae powered microbial fuel cell, *J. Hazard. Mater.* 187 (2011) 591–595.

[17] S. Alferov, V. Coman, T. Gustavsson, A. Reshetilov, C. von Wachenfeldt, C. Hagerhall, L. Gorton, Electrical communication of cytochrome enriched *Escherichia coli* JM109 cells with graphite electrodes, *Electrochim. Acta* 54 (2009) 4979–4984.

[18] V. Coman, T. Gustavsson, A. Finkelstein, C. Von Wachenfeldt, C. Hagerhall, L. Gorton, Electrical wiring of live, metabolically enhanced *Bacillus subtilis* cells with flexible osmium-redox polymers, *J. Am. Chem. Soc.* 131 (2009) 16171–16176.

[19] H.M. Jensen, A.E. Albers, K.R. Malley, Y.Y. Londer, B.E. Cohen, B.A. Helms, P. Weigele, J.T. Groves, C.M. Ajo-Franklin, Engineering of a synthetic electron conduit in living cells, *Proc. Natl. Acad. Sci. U. S. A.* 107 (2010) 19213–19218.

[20] K. Rabaey, L. Angenent, U. Schröder, J. Keller, Bioelectrochemical systems: from extracellular electron transfer to biotechnological applications, in: P. Lens (Ed.), *Integrated Environmental Technology Series*, IWA Publishing, London, New York, 2010.

[21] S. Chen, H. Hou, F. Harnisch, S.A. Patil, A.A. Carmona-Martinez, S. Agarwal, Y. Zhang, S. Sinha-Ray, A.L. Yarin, A. Greiner, U. Schröder, Electrospun and solution blown three-dimensional carbon fiber nonwovens for application as electrodes in microbial fuel cells, *Energy Environ. Sci.* 4 (2011) 1417–1421.

[22] D.R. Lovley, K.P. Nevin, A shift in the current: new applications and concepts for microbe-electrode electron exchange, *Curr. Opin. Biotechnol.* 22 (2011) 441–448.

[23] S. Patil, F. Harnisch, U. Schröder, Toxicity response of electroactive microbial biofilms—a decisive feature for potential biosensor and power source applications, *Chemphyschem* 11 (2010) 2834–2837.

[24] S.A. Patil, F. Harnisch, B. Kapadnis, U. Schröder, Electroactive mixed culture biofilms in microbial bioelectrochemical systems: the role of temperature for biofilm formation and performance, *Biosens. Bioelectron.* 26 (2010) 803–808.

[25] S.A. Patil, F. Harnisch, C. Koch, T. Hubschmann, I. Fetzer, A.A. Carmona-Martinez, S. Muller, U. Schröder, Electroactive mixed culture derived biofilms in microbial bioelectrochemical systems: the role of pH on biofilm formation, performance and composition, *Bioresour. Technol.* 102 (2011) 9683–9690.

[26] M.H. Osman, A.A. Shah, F.C. Walsh, Recent progress and continuing challenges in bio-fuel cells. Part II: Microbial, *Biosens. Bioelectron.* 26 (2010) 953–963.

[27] J.K. Fredrickson, M.F. Romine, A.S. Beliaev, J.M. Auchtung, M.E. Driscoll, T.S. Gardner, K.H. Nealon, A.L. Osterman, G. Pinchuk, J.L. Reed, D.A. Rodionov, J.L.M. Rodrigues, D.A. Saffarini, M.H. Serres, A.M. Spormann, I.B. Zhulin, J.M. Tiedje, Towards environmental systems biology of *Shewanella*, *Nat. Rev. Microbiol.* 6 (2008) 592–603.

[28] H.H. Hau, J.A. Gralnick, Ecology and biotechnology of the genus *Shewanella*, *Annual Review of Microbiology, Annual Reviews, Palo Alto*, 2007, pp. 237–258.

[29] P.F. Weaver, J.D. Wall, H. Gest, Characterization of *Rhodospseudomonas capsulata*, *Arch. Microbiol.* 105 (1975) 207–216.

[30] M.T. Madigan, D.O. Jund, An overview of purple bacteria: systematics, physiology, and habitats, in: C.N. Hunter, F. Daldal, M.C. Thurnauer, J.T. Beatty (Eds.), *The Purple Phototrophic Bacteria*, Springer Netherlands, Amsterdam, 2008, pp. 1–15.

- [31] R. Tabita, The Biochemistry and Metabolic Regulation of Carbon Metabolism and CO<sub>2</sub> Fixation in Purple Bacteria, Anoxygenic Photosynthetic Bacteria, Kluwer Academic Publishing, Dordrecht, 1995, pp. 885–914.
- [32] S.J. Ferguson, J.B. Jackson, A.G. McEwan, Anaerobic respiration in the *Rhodospirillaceae* – characterization of pathways and evaluation of roles in redox balancing during photosynthesis, *FEMS Microbiol. Rev.* 46 (1987) 117–143.
- [33] A.A. Tsygankov, Y. Hirata, M. Miyake, Y. Asada, J. Miyake, Photobioreactor with photosynthetic bacteria immobilized on porous-glass for hydrogen photo-production, *J. Ferment. Bioeng.* 77 (1994) 575–578.
- [34] J. Gebicki, M. Modigell, M. Schumacher, J. van der Burg, E. Roebroek, Comparison of two reactor concepts for anoxygenic H<sub>2</sub> production by *Rhodobacter capsulatus*, *J. Cleaner Prod.* 18 (2010) S36–S42.
- [35] J. Weckesser, G. Drews, I. Fromme, Chemical-analysis of and degradation studies on cell-wall lipopolysaccharide of *Rhodopseudomonas-capsulata*, *J. Bacteriol.* 109 (1972) 1106–1113.
- [36] E. Bräutigam, F. Fiedler, D. Woitzik, H.T. Flammann, J. Weckesser, Capsule polysaccharide-protein-peptidoglycan complex in the cell-envelope of *Rhodobacter-capsulatus*, *Arch. Microbiol.* 150 (1988) 567–573.
- [37] A.S. Omar, H.T. Flammann, D. Borowiak, J. Weckesser, Lipopolysaccharides of 2 strains of the phototropic bacterium *Rhodopseudomonas-capsulata*, *Arch. Microbiol.* 134 (1983) 212–216.
- [38] J. Weckesser, G. Drews, R. Ladwig, Localization and biological and physicochemical properties of cell-wall lipopolysaccharide of *Rhodopseudomonas-capsulata*, *J. Bacteriol.* 110 (1972) 346–353.
- [39] A. Heller, Electron-conducting redox hydrogels: design, characteristics and synthesis, *Curr. Opin. Chem. Biol.* 10 (2006) 664–672.
- [40] A. Heller, B. Feldman, Electrochemical glucose sensors and their applications in diabetes management, *Chem. Rev.* 108 (2008) 2482–2505.
- [41] S. Timur, Y. Yigzaw, L. Gorton, Electrical wiring of pyranose oxidase with osmium redox polymers, *Sens. Actuators B Chem.* 113 (2006) 684–691.
- [42] M.N. Zafar, F. Tasca, S. Boland, M. Kujawa, I. Patel, C.K. Peterbauer, D. Leech, L. Gorton, Wiring of pyranose dehydrogenase with osmium polymers of different redox potentials, *Bioelectrochemistry* 80 (2010) 38–42.
- [43] M.N. Zafar, X.J. Wang, C. Sygmund, R. Ludwig, D. Leech, L. Gorton, Electron-transfer studies with a new flavin adenine dinucleotide dependent glucose dehydrogenase and osmium polymers of different redox potentials, *Anal. Chem.* 84 (2012) 334–341.
- [44] J.D. Pennoyer, T. Ohnishi, B.L. Trumpower, Purification and properties of succinate-ubiquinone oxidoreductase complex from *Paracoccus-denitrificans*, *Biochim. Biophys. Acta* 935 (1988) 195–207.
- [45] C. Hägerhäll, Succinate: quinone oxidoreductases – variations on a conserved theme, *Biochim. Biophys. Acta, Bioenerg.* 1320 (1997) 107–141.
- [46] S. Boland, Doctoral Thesis, National University of Ireland, Galway, 2008.
- [47] F. Barrière, P. Kavanagh, D. Leech, A laccase–glucose oxidase biofuel cell prototype operating in a physiological buffer, *Electrochim. Acta* 51 (2006) 5187–5192.
- [48] M.B. Hansen, S.E. Nielsen, K. Berg, Re-examination and further development of a precise and rapid dye method for measuring cell growth/cell kill, *J. Immunol. Methods* 119 (1989) 203–210.
- [49] R.M. Atlas, *Handbook of Microbiological Media*, third edition CRC Press LLC, New York, 2004.
- [50] J. Haladjian, P. Bianco, F. Nunzi, M. Bruschi, A permselective-membrane electrode for the electrochemical study of redox proteins – application to cytochrome *c*<sub>552</sub> from *Thiobacillus ferrooxidans*, *Anal. Chim. Acta* 289 (1994) 15–20.
- [51] H.C. Flemming, J. Wingender, The biofilm matrix, *Nat. Rev. Microbiol.* 8 (2010) 623–633.



# Paper II





## Improved microbial electrocatalysis with osmium polymer modified electrodes†

Sunil A. Patil,<sup>\*a</sup> Kamrul Hasan,<sup>a</sup> Dónal Leech,<sup>b</sup> Cecilia Hägerhäll<sup>a</sup> and Lo Gorton<sup>\*a</sup>

Received 9th July 2012, Accepted 26th August 2012

DOI: 10.1039/c2cc34903e

Using the well-known exoelectrogen *Shewanella oneidensis* MR-1, an osmium redox polymer modified anode exhibited ca. 4-fold increase in current generation. Additionally, a significant decrease in the start-up time for electrocatalysis was observed. The findings suggest that the inherent extracellular electron transfer capabilities of electrogens coupled with such polymers could enhance electrocatalysis.

Microbial electrocatalysis at electrodes is the decisive aspect of all microbe–electrode interaction based systems. Microbial bioelectrochemical systems (BESs) like microbial fuel cells (MFCs) exploit the ability of exoelectrogens to donate electrons to an anode.<sup>1</sup> The extracellular electron transfer occurs mainly by two mechanisms: direct *via* outer membrane cytochromes and conductive pili (widely referred to as nanowires), and mediated *via* exogenous or endogenous electron shuttles.<sup>2–4</sup> In addition to the electricity generation from various pure substrates and wastewaters,<sup>5</sup> the application range of BESs has widened due to possible electrical current driven biochemical/fuel production (referred to as microbial electrosynthesis).<sup>6</sup> However, inefficient electron transfer (ET) from bacteria to electrodes and/or limited extraction of microbially produced electrons at electrodes restrict performance of these systems and limits their feasible large-scale implementation.<sup>7</sup> Therefore, in addition to the exploration and improvement of microorganisms, development of the electrode materials is considered as an important task to enhance the ET rates to electrodes.<sup>2</sup> Research efforts have consequently focused electrode surface modification and fabrication of conductive polymeric electrode materials to overcome limitations of slow ET and to facilitate maximum bacterial growth and proliferation.<sup>8–17</sup> Recently, the strategy of exoelectrogen immobilization in the conductive polypyrrole matrix

has been successfully tried, which resulted in an enhanced current generation.<sup>18</sup> The use of polymeric mediators such as osmium (Os) redox polymers instead of monomeric mediators has gained substantial interest for electrochemically “wiring” enzymes to electrodes for biofuel cell and biosensor applications.<sup>19,20</sup> The success in enzyme-based fuel cells encouraged their application in establishing electrochemical communication between non-exoelectrogens (includes both bacteria and yeasts) during the last few years.<sup>21–25</sup> The main goal in most of these studies was to extract electrons from microbes and facilitate ET to electrodes with the aid of Os-based redox polymers.<sup>26</sup> However, combinations of these polymers with exoelectrogens have not been studied so far. Therefore, considering their efficient electron shuttling properties, reversibility and polymeric nature,<sup>26</sup> the objective of this study is to investigate the ability of such polymers to improve the ET from the exoelectrogen *S. oneidensis* MR-1 to electrodes.

An Os polymer (Fig. 1A) with a positive redox potential ( $E^{\circ}$ ) of 0.221 V (vs. Ag/AgCl, sat. KCl)<sup>27</sup> was used because of its proven ability in wiring non-exoelectrogens to electrodes.<sup>22,28</sup> With polymer-modified anodes (PMAs), two different approaches for microbial culture addition were attempted. In the first approach (*PMA-1*), the microbial inoculum was added to the growth medium and a natural electrochemical growth of electrogens at the anode was allowed. In the second approach (*PMA-2*) the microbial inoculum was directly adsorbed on the polymer-modified electrode and trapped with the use of a permselective membrane (referred to as artificial immobilization). During start-up, consistency in the microbial inoculum size and the amount of Os polymer used to modify the electrodes was maintained (see details in ESI†).

A gradual increase in the current generation with lactate (substrate) was observed after initial lag time with both polymer-modified and unmodified anodes (*control*). The start-up time of current generation with the PMAs (with both approaches) was shorter than that of the unmodified anode (Fig. 1C). The decrease in start-up time for current generation is attributed to the contribution of the Os-redox centres embedded in the polymer matrix in facilitation of ET from bacterial cells to the electrode. Amongst the two different approaches that were investigated, *PMA-2* showed an immediate current response (Fig. 1C). This might be attributed to the instant bioelectrocatalytic activity of immobilized bacterial cells at PMA. The *PMA-1* exhibited ca. 4-fold increase in

<sup>a</sup> Department of Biochemistry and Structural Biology, Lund University, P.O. Box 124, SE-22100 Lund, Sweden.  
E-mail: Sunil.Patil@biochemistry.lu.se,  
Lo.Gorton@biochemistry.lu.se; Fax: +46 46 222 4116

<sup>b</sup> School of Chemistry, National University of Ireland Galway, University Road, Galway, Ireland

† Electronic supplementary information (ESI) available: Detailed experimental section; representative semi-batch CA experiments showing current generation with a bare electrode and PMA-1; CVs of *S. oneidensis* MR-1 during turnover and non-turnover conditions at the graphite electrode; CVs of polymer-modified electrodes after two fed-batch cycles; SEM images of enriched biofilms at bare and polymer-modified electrodes. See DOI: 10.1039/c2cc34903e

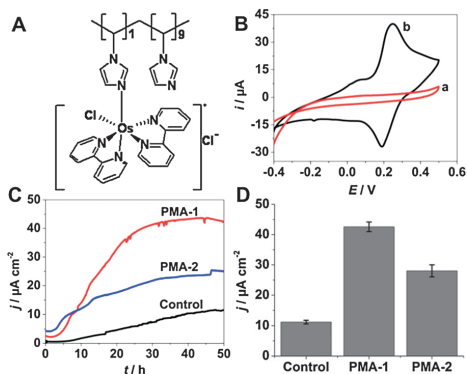


**Fig. 1** (A) Structural representation of the used Os polymer. (B) CV curve of unmodified (a) and Os redox polymer modified graphite electrode (b) in 50 mM PIPES buffer (pH 7.0). The scan rate was 2 mV s<sup>-1</sup>. (C) Chronoamperometric (CA) measurements showing start-up time of current generation with unmodified anode (control) and PMAs (both approaches) by *S. oneidensis* MR-1. The substrate was 18 mM sodium lactate. (D) Steady state maximum current densities achieved with control and PMAs. The data are derived from at least three independent CA experiments with all electrodes.

maximum current density compared to the unmodified anode (Fig. 1D) under a similar set of experimental conditions. Although a decrease in start-up time was observed with *PMA-2*, the maximum current (26 μA cm<sup>-2</sup>) was lower than that achieved with *PMA-1* (42 μA cm<sup>-2</sup>) with both approaches providing current signals much better than the *control* experiments with an unmodified electrode (11 μA cm<sup>-2</sup>), with all current densities displaying maximum relative standard deviation less than 10%. The representative semi-batch CA experiments with a bare electrode and *PMA-1* are shown in Fig. S1 in ESI†. With *PMA-2*, the artificial immobilization of cells at PMA most probably limits their growth as well as the natural enrichment capabilities that ultimately affect the maximum current generation. The cells in close proximity to the polymer-modified electrode surface in this case dominate the current generation. Individual *Shewanella* cells suspended in the medium also contribute to the current generation, as they can produce flavins in the medium.<sup>4</sup> However, the enhanced current generation is principally due to the role of the Os polymer adsorbed at the electrode. Furthermore, the enhanced bioelectrocatalysis was observed without any cross-linker or stabilizer. The use of non-toxic cross-linking molecules to increase the stability of such polymers could further improve the bioelectrocatalysis.

To clarify the role of Os-redox centres in the ET process, CV measurements were conducted. In the case of an unmodified electrode, CV curves acquired during turnover and non-turnover conditions are in accordance with studies conducted with wild type *S. oneidensis* strain (see Fig. S2 in ESI†). The CV recorded during substrate turnover and non-turnover conditions with *PMA-1* (depicted in Fig. 2I) clearly show a pair of well-defined redox peaks that closely resemble the redox peaks and *E*<sup>0</sup>-value of the polymer (see Fig. 1B(b)). Furthermore, the CV measurements after more than two fed batch cycles with PMAs showed a similar behavior (see Fig. S3 in ESI†) and

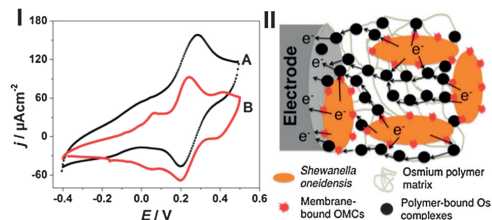


**Fig. 2** (I) Representative CV curves obtained with *PMA-1* during substrate turnover (A) and non-turnover conditions (B). (II) Hypothesized scheme to support enhanced ET from *Shewanella* cells to the electrode by inherent direct and mediated via Os-redox complexes (embedded in the polymer matrix) mechanisms. It also shows possible long-distance ET to electrodes.

confirmed the stability of the Os polymer on the anode. The Os polymer-modified electrodes (without bacterial cells) in the presence of substrates showed negligible electrocatalysis compared to *PMA-1*/*PMA-2* in control experiments. In general, current generation can be attributed to the natural extracellular ET abilities of the *S. oneidensis* via flavins, cell bound cytochromes and/or nanowires.<sup>3,4,29</sup> However, the enhanced current generation in the case of PMAs can be reasonably attributed to the Os-redox centres embedded in the polymer matrix. Hence, we attribute the improved electron exchange process to the cell bound cytochromes at the cell–electrode and the cell–polymer–electrode interface (as proposed in Fig. 2II). Moreover, the improved ET can also be attributed to the formation/existence of a long-distance electron channeling/self-exchange by Os-redox centres that mediate the ET from distant cells to electrodes (Fig. 2II). A better cell adherence and thus biofilm formation on the PMAs might also have contributed to the improved current generation as well as helped the polymer to remain intact and stable on the electrode surface.

Electrode surface modifiers result in augmentation of surface area and thus are considered as one of the reasons for improved bioelectrocatalysis.<sup>15,30</sup> In order to check whether the Os polymer matrix amends the electrode area for microbial colonization, we examined bare graphite and polymer-modified graphite by SEM (Fig. 3). SEM was further used to characterize the architecture of the biofilm and confirm its formation on the unmodified and PMAs. As can be seen from Fig. 3A and B, the difference in SEM images of bare and Os polymer-modified graphite is slight, possibly due to complete adsorption of the Os polymer into the rough and porous graphite surface. The presence of rod shaped (2–3 μm long) structures embedded at the electrode surface that resembles the normal size of *S. oneidensis* cells at both bare and *PMA-1* (Fig. 3C and D) indicates biofilm formation and further confirms biofilm associated current generation. The cell density on the bare anode is relatively low and less homogenous than that of the biofilm grown at *PMA-1* (Fig. S4 in ESI†). The improved electrocatalysis with PMAs could thus be attributed to the ET promoting effect of the Os-redox complexes embedded in the polymer matrix and the high density of cells at these electrodes.

Immobilization of monomeric mediators on electrodes has been tried using chemical reactions or polymers to increase the performance of MFCs.<sup>13,31,32</sup> Such research findings

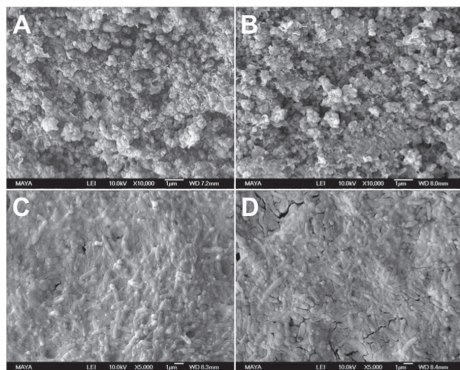


**Fig. 3** SEM images of (A) bare graphite, (B) Os-polymer modified graphite, enriched electroactive biofilms at (C) bare anode and at (D) PMA-1.

encourage the idea of employing mediators with exoelectrogens to enhance the ET rates at electrodes. However, in comparison to monomeric mediators the simple physical adsorption of polymeric Os mediators on electrodes, their ability to form electrostatic complexes with the cells and multilayer scaffolds while retaining electrochemical reversibility makes the exploitation of this approach easy to improve bioelectrocatalysis in BESs. Recent research with 3D porous anode materials has revealed enhanced current generation in comparison to traditional carbon-based materials.<sup>8,33</sup> It would be interesting to modify such porous materials with Os polymers to further boost current generation. Future work will focus on investigating a wide range of Os-redox polymers, particularly those with redox potentials more negative than the Os polymer selected in this work so as to increase effective MFC voltages for electrode surface modifications. The understanding of the molecular mechanisms of electrochemical communication between bacteria and electrodes *via* Os polymers will be a prerequisite for improving their applications.

In conclusion, natural electrogen growth at PMAs is a strategy to achieve enhanced current compared to artificial electrogen immobilization at such electrodes. We anticipate that the strategy of natural growth or artificial immobilization of electrogens like *Shewanella oneidensis*, *Geobacter sulfurreducens* etc. at Os polymer modified highly porous carbon-based electrode materials can improve the electrocatalysis many-fold.

The authors acknowledge the financial support from The European Commission (“Chebana” FP7- 462 PEOPLE-2010-ITN-264772), The Swedish Research Council (projects: 2010–5031, 2010–2013), nmc@LU and the Charles Parsons Energy Research Award through Science Foundation Ireland. We thank Domhnall MacAodha and Peter Connolly (NUI, Galway) for synthesis of the Os polymer.

## Notes and references

- Bioelectrochemical Systems: From extracellular electron transfer to biotechnological application*, ed. K. Rabaey, L. Angenent, U. Schröder and J. Keller, IWA Publishing, London, 2010.

- Y. Qiao, S.-J. Bao and C. M. Li, *Energy Environ. Sci.*, 2010, **3**, 544–553.
- Y. A. Gorby, S. Yanina, J. S. McLean, K. M. Rosso, D. Moyles, A. Dohnalkova, T. J. Beveridge, I. S. Chang, B. H. Kim, K. S. Kim, D. E. Culley, S. B. Reed, M. F. Romine, D. A. Saffarini, E. A. Hill, L. Shi, D. A. Elias, D. W. Kennedy, G. Pinchuk, K. Watanabe, S. Ishii, B. Logan, K. H. Nealson and J. K. Fredrickson, *Proc. Natl. Acad. Sci. U. S. A.*, 2006, **103**, 11358–11363.
- E. Marsili, D. B. Baron, I. D. Shikhare, D. Coursolle, J. A. Gralnick and D. R. Bond, *Proc. Natl. Acad. Sci. U. S. A.*, 2008, **105**, 3968–3973.
- D. Pant, G. Van Bogaert, L. Diels and K. Vanbroekhoven, *Bioresour. Technol.*, 2010, **101**, 1533–1543.
- K. Rabaey and R. A. Rozendal, *Nat. Rev. Microbiol.*, 2010, **8**, 706–716.
- B. Logan, *Appl. Microbiol. Biotechnol.*, 2010, **85**, 1665–1671.
- S. Chen, H. Hou, F. Harnisch, S. A. Patil, A. A. Carmona-Martinez, S. Agarwal, Y. Zhang, S. Sinha-Ray, A. L. Yarin, A. Greiner and U. Schröder, *Energy Environ. Sci.*, 2011, **4**, 1417–1421.
- Y.-X. Huang, X.-W. Liu, J.-F. Xie, G.-P. Sheng, G.-Y. Wang, Y.-Y. Zhang, A.-W. Xu and H.-Q. Yu, *Chem. Commun.*, 2011, **47**, 5795–5797.
- J. R. Kim, H. C. Boghani, N. Amini, K.-F. Aguey-Zinsou, I. Michie, R. M. Dinsdale, A. J. Guwy, Z. X. Guo and G. C. Premier, *J. Power Sources*, 2012, **213**, 382–390.
- N. Zhu, X. Chen, T. Zhang, P. Wu, P. Li and J. Wu, *Bioresour. Technol.*, 2011, **102**, 422–426.
- Y. Zhao, S. Nakanishi, K. Watanabe and K. Hashimoto, *J. Biosci. Bioeng.*, 2011, **112**, 63–66.
- K. Wang, Y. Liu and S. Chen, *J. Power Sources*, 2011, **196**, 164–168.
- M. Picot, L. Lapinonnière, M. Rothballer and F. Barrière, *Biosens. Bioelectron.*, 2011, **28**, 181–188.
- C. Li, L. Zhang, L. Ding, H. Ren and H. Cui, *Biosens. Bioelectron.*, 2011, **26**, 4169–4176.
- B. Lai, X. Tang, H. Li, Z. Du, X. Liu and Q. Zhang, *Biosens. Bioelectron.*, 2011, **28**, 373–377.
- B. Cercado-Quezada, M.-L. Delia and A. Bergel, *Electrochem. Commun.*, 2011, **47**, 12825–12827.
- Y.-Y. Yu, H.-I. Chen, Y.-C. Yong, D.-H. Kim and H. Song, *Chem. Commun.*, 2011, **47**, 12825–12827.
- D. Guschin, J. Castillo, N. Dimcheva and W. Schuhmann, *Anal. Bioanal. Chem.*, 2010, **398**, 1661–1673.
- A. Heller, *Curr. Opin. Chem. Biol.*, 2006, **10**, 664–672.
- H. Shkil, A. Schulte, D. A. Guschin and W. Schuhmann, *ChemPhysChem*, 2011, **12**, 806–813.
- V. Coman, T. Gustavsson, A. Finkelsteinas, C. von Wachenfeldt, C. Hägerhäll and L. Gorton, *J. Am. Chem. Soc.*, 2009, **131**, 16171–16176.
- S. Timur, B. Haghighi, J. Tkac, N. Pazarlıoğlu, A. Telefoncu and L. Gorton, *Bioelectrochemistry*, 2007, **71**, 38–45.
- F. J. Rawson, A. J. Gross, D. J. Garrett, A. J. Downard and K. H. R. Baronian, *Electrochem. Commun.*, 2012, **15**, 85–87.
- F. J. Rawson, D. J. Garrett, D. Leech, A. J. Downard and K. H. R. Baronian, *Biosens. Bioelectron.*, 2011, **26**, 2383–2389.
- K. Hasan, S. A. Patil, D. Leech, C. Hägerhäll and L. Gorton, *Biochem. Soc. Trans.*, 2012, in press.
- F. Barrière, Y. Ferry, D. Rochefort and D. Leech, *Electrochem. Commun.*, 2004, **4**, 237–241.
- K. Hasan, S. A. Patil, K. Görecki, D. Leech, C. Hägerhäll and L. Gorton, *Bioelectrochemistry*, 2012, DOI: 10.1016/j.bioelechem.2012.05.004.
- A. Okamoto, Y. Ferry, D. Hashimoto and R. Nakamura, *Bioelectrochemistry*, 2012, **85**, 61–65.
- M. Zhou, M. Chi, J. Luo, H. He and T. Jin, *J. Power Sources*, 2011, **196**, 4427–4435.
- M. Adachi, T. Shimomura, M. Komatsu, H. Yakuwa and A. Miya, *Chem. Commun.*, 2008, 2055–2057.
- D. A. Lowy, L. M. Tender, J. G. Zeikus, D. H. Park and D. R. Lovley, *Biosens. Bioelectron.*, 2006, **21**, 2058–2063.
- K. Katuri, M. L. Ferrer, M. C. Gutierrez, R. Jimenez, F. del Monte and D. Leech, *Energy Environ. Sci.*, 2011, **4**, 4201–4210.



## Electronic Supplementary Information (ESI)†

### Improved microbial electrocatalysis with osmium polymer modified electrodes

Sunil A. Patil,<sup>\*a</sup> Kamrul Hasan,<sup>a</sup> Dónal Leech,<sup>b</sup> Cecilia Hägerhäll<sup>a</sup> and Lo Gorton<sup>\*a</sup>

<sup>a</sup>Department of Biochemistry and Structural Biology, Lund University, P.O. Box 124, SE-22100 Lund, Sweden

<sup>b</sup>School of Chemistry, National University of Ireland Galway, University Road, Galway, Ireland

\*E-mail: Sunil.Patil@biochemistry.lu.se; Lo.Gorton@biochemistry.lu.se

#### 1. Detailed experimental section

##### 1.1 Chemicals and general conditions

[Os(2,2'-bipyridine)<sub>2</sub>-poly(N-vinylimidazole)<sub>10</sub>Cl]<sup>2+/+</sup> (poly[Os(bpy)<sub>2</sub>(PVD)<sub>10</sub>Cl]<sup>2+/+</sup>) with an E° equal to +221 mV vs. Ag|AgCl (sat. KCl) was synthesized as reported.<sup>1</sup> The weight-average molecular weight of the poly(vinylimidazole) as determined by viscometry in ethanol was 10,000 g/mol.<sup>2</sup> All chemicals were purchased from Sigma-Aldrich/Merck and were of either research or analytical grade. All aqueous solutions were prepared by using water purified and deionized (18 MΩ) with a Milli-Q system (Millipore, Bedford, MA). If not stated otherwise, all potentials provided in this article refer to the Ag|AgCl (sat. KCl) reference electrode. All electrochemical experiments were performed under strictly sterile and anoxic conditions.

##### 1.2. Microbial growth conditions and inoculum preparation

*Shewanella oneidensis* MR-1 (LMG 19005/ATCC 700550) was obtained from Belgian Coordinated Collections of Microorganisms/Laboratorium voor Microbiologie (BCCM<sup>TM</sup>/LMG, Ghent University, Belgium). The strain was grown and maintained on tryptone soya agar. For inoculum preparation, a single, well-isolated colony was transferred to 15 mL of LB broth (in 50 mL tubes) and incubated aerobically at 30±2° C while shaking at 150 rpm (Universal shaker SM 30 A, Edmund Bühler GmbH, Germany) for 24 h. Then the cells grown in LB broth were harvested by centrifuging the broth at 4000 rpm for 10 min. Further, the cells were washed once in 50 mM PIPES buffer (pH 7.4) and once in minimal (M1) medium by centrifuging as before. Subsequently, the cells were transferred to 200 mL of minimal growth medium containing sodium lactate 18 mM/L, PIPES buffer 15.1 g/L; NaOH 3.0 g/L; NH<sub>4</sub>Cl 1.5 g/L; KCl 0.1 g/L; NaH<sub>2</sub>PO<sub>4</sub>·H<sub>2</sub>O 0.6 g/L; NaCl 5.8 g/L; mineral solution 10 mL/L; vitamin solution 10 mL/L and amino acid solution 10 mL/L.<sup>3, 4</sup> After incubation at 30±2° C (500 mL baffled E-flasks, aerobically while shaking at 150 rpm for 72 h) the cells were harvested and used either as an inoculum in potentiostatic half-cell set ups hosting a similar minimal growth medium or for further inoculum preparation.

### 1.3. Preparation of the osmium polymer-modified electrodes

Spectrographic graphite rods (Ringsdorff Werke GmbH, Bonn, Germany) were used as working electrodes. The procedure explained by Coman et al.<sup>5</sup> was followed to prepare the osmium (Os) polymer modified working electrodes. The material was polished on wet emery paper (Tufbak, Durite, P1200) and subsequently carefully rinsed with Milli-Q water and dried. Then 20  $\mu\text{L}$  of Os polymer solution (10 mg/mL in Milli-Q water) was spread onto the entire active surface of the electrode (**projected surface area; 0.282 cm<sup>2</sup>**). The electrode was dried at room temperature for 10-15 min and was used for further bioelectrochemical experiments.

### 1.4. Measurement set-ups and bioelectrochemical experiments

All experiments were conducted using either AUTOLAB PGSTAT 30 (EcoChemie, Utrecht, The Netherlands) or PalmSens (Palm Instruments BV, The Netherlands) with a three-electrode configuration—an Ag|AgCl reference electrode (sat. KCl, Sensortechnik Meinsberg, Germany), a bare/polymer modified graphite as a working and bare graphite as a counter electrode. The sealed, water-jacketed glass vessels connected to a thermostat (Paratherm U2 electronic, Julabo, Schwarzwald, Germany) were employed as electrochemical cells that allowed maintenance of temperature control. All experiments were performed under anoxic conditions, which were achieved by sparging argon for 20 min in the buffer solution/growth medium before use. Furthermore, the headspace of the solution was also sparged with argon during the CV measurements.

With polymer-modified anodes (PMAs), two different approaches for microbial culture addition were investigated. In the first approach (PMA-1), the microbial inoculum was added to the growth medium and natural electrochemical **growth** of electrogens at the anode was allowed. While in the second approach (PMA-2) the microbial inoculum was directly adsorbed on to the polymer-modified electrode and trapped with the use of a dialysis membrane (Spectrum Laboratories Inc., Rancho Dominguez, CA, molecular mass cutoff: 6000-8000) to prepare a permselective membrane electrode<sup>6</sup> (referred to as artificial immobilization). The semi-batch chronoamperometric (CA) experiments were performed with PMAs (both approaches) at an applied potential of +0.350 V (vs. Ag|AgCl) with regular medium replenishments. Similar experiments were also performed with unmodified anodes as controls. In this case, a bare graphite electrode was used as the anode and the cells were directly inoculated to the medium. All reported data are based on at least three independent replicates of each experiment. In all cases, cyclic voltammetry (CV) was recorded during turnover conditions, i.e. at the bioelectrocatalytic substrate consumption, and during non-turnover, i.e. substrate deprived conditions at a scan rate of 2 mV s<sup>-1</sup>.

### 1.5. Scanning electron microscopy

Clean and bare graphite, Os polymer-modified graphite, enriched biofilm at bare graphite and at polymer-modified graphite (both PMA-1 and PMA-2) were analyzed with SEM (JEOL JSM-6700F). The samples with bacterial cells were fixed overnight using 2.5% glutaraldehyde (prepared in 0.1 M phosphate buffer, pH 7.0) and then washed with phosphate buffer (pH 7.0). Before SEM observation, all samples were dried and coated with Au/Pd.

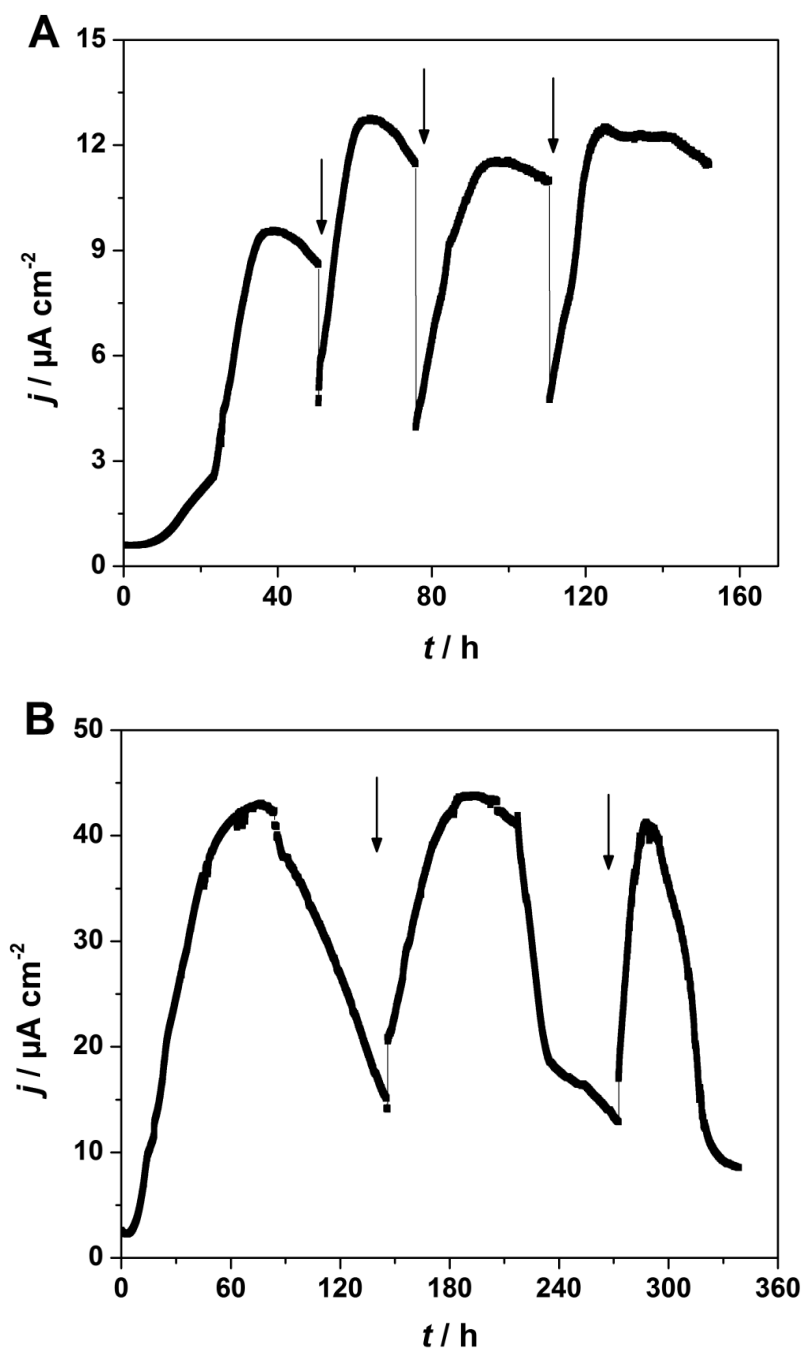


**Fig. S1** Representative CA runs showing bioelectrocatalytic current generation at A) bare electrode and B) PMA-1 in semi-batch experiments. The arrows indicate M1 medium replenishment.



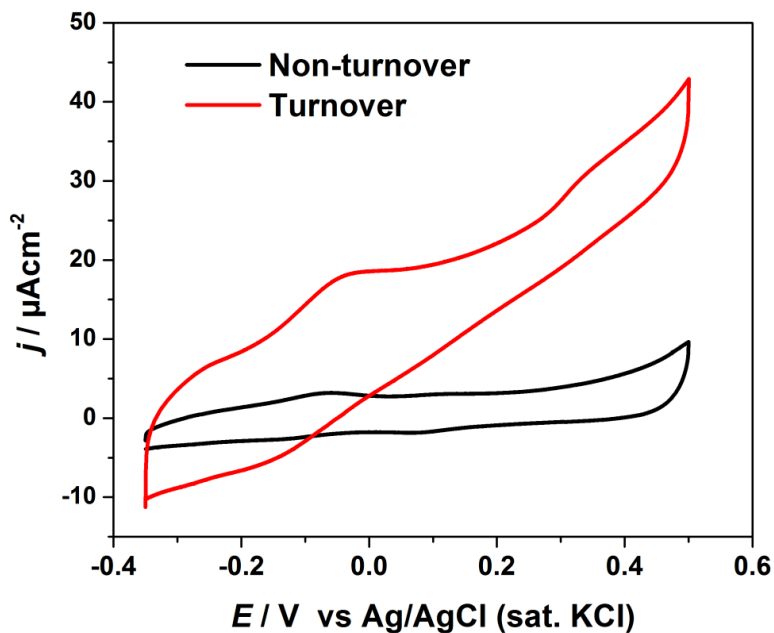


**Fig. S2** Cyclic voltammograms of *S. oneidensis* MR-1 recorded during substrate turnover and non-turnover conditions in control experiments (bare electrode). The substrate was 18 mM lactate. The scan rate was  $2 \text{ mVs}^{-1}$ .

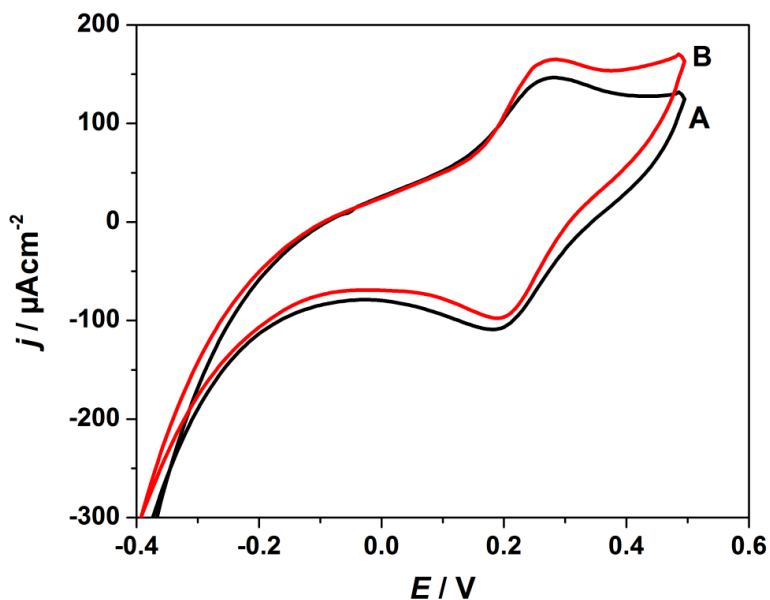


**Fig. S3** CV curves of *S. oneidensis* MR-1 with PMA-1 recorded after the second (A) and the third (B) fed batch cycles during substrate (18 mM lactate) turnover conditions. The scan rate was  $2 \text{ mVs}^{-1}$ .

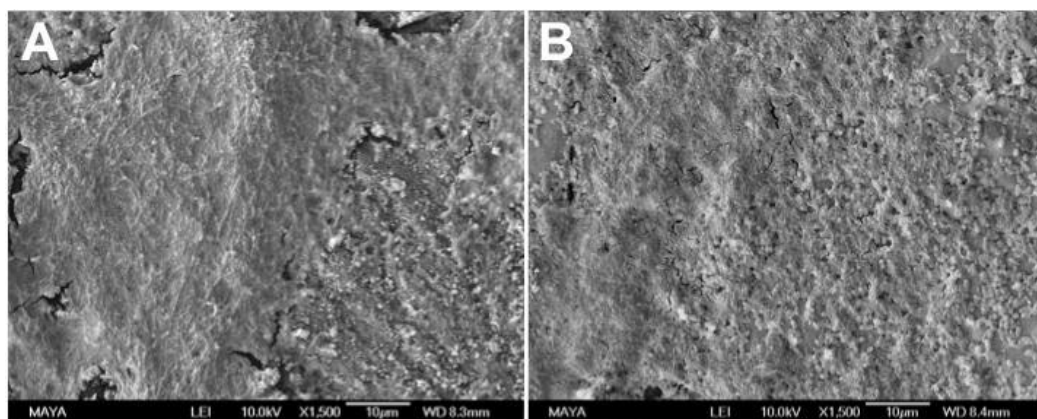


**Fig. S4** SEM images of enriched electroactive biofilms at (A) bare graphite (control) and (B) at PMA-1.

#### References:

1. F. Barrière, Y. Ferry, D. Rochefort and D. Leech, *Electrochem. Commun.*, 2004, **4**, 237-241.
2. F. Barrière, P. Kavanagh and D. Leech, *Electrochim. Acta*, 2006, **51**, 5187-5192.
3. O. Bretschger, A. Obratsova, C. A. Sturm, I. S. Chang, Y. A. Gorby, S. B. Reed, D. E. Culley, C. L. Reardon, S. Barua, M. F. Romine, J. Zhou, A. S. Beliaev, R. Bouhenni, D. Saffarini, F. Mansfeld, B.-H. Kim, J. K. Fredrickson and K. H. Nealson, *Appl. Environ. Microbiol.*, 2007, **73**, 7003-7012.
4. R. M. Atlas, *Handbook of Microbiological Media*, CRC Press LLC, New York, 3<sup>rd</sup> edn., 2004, p 2056.
5. V. Coman, T. Gustavsson, A. Finkelsteinas, C. Von Wachenfeldt, C. Hägerhäll and L. Gorton, *J. Am. Chem. Soc.*, 2009, **131**, 16171-16176.
6. J. Haladjian, P. Bianco, F. Nunzi and M. Bruschi, *Anal. Chim. Acta*, 1994, **289**, 15-20.



# Paper III



# Electrochemical Communication Between Electrodes and *Rhodobacter capsulatus* Grown in Different Metabolic Modes

Kamrul Hasan,<sup>\*[a]</sup> Kesava Vijalapuram Raghava Reddy,<sup>[a]</sup> Vera Eßmann,<sup>[b]</sup> Kamil Górecki,<sup>[a]</sup> Peter Ó Conghaile,<sup>[c]</sup> Wolfgang Schuhmann,<sup>[b]</sup> Dónal Leech,<sup>[c]</sup> Cecilia Hägerhäll,<sup>[a]</sup> and Lo Gorton<sup>\*[a]</sup>

**Abstract:** The majority of efforts on microbial and photosynthetic microbial fuel cells are both curiosity driven and made to possibly meet the future growing demand for sustainable energy. The most metabolically versatile purple bacteria *Rhodobacter capsulatus* is a potential candidate for this purpose. However, utilizing bacteria in such systems requires efficient electronic transfer communication between the microbial cells and the electrodes, which is one of the greatest challenges. Previous studies demonstrated that osmium redox polymers (ORPs) could be used for extracellular electron transfer between the cells and electrodes. Recently, heterotrophically grown *R. capsulatus* has been wired with ORP modified electrodes. Here in this communication, we report electron transfer from *R. capsulatus* grown under heterotrophic as well as

under photoheterotrophic conditions to electrodes. The cells, immobilized on bare graphite and ORP modified graphite electrodes, were excited with visible light and subsequent photosynthetic electron transfer was recorded using cyclic voltammetric and chronoamperometric measurements. Photoheterotrophically grown *R. capsulatus* cells on bare graphite generate a significant photocurrent density of  $3.46 \mu\text{A cm}^{-2}$ , whereas on an ORP modified electrode the current density increases to  $8.46 \mu\text{A cm}^{-2}$ . Furthermore, when 1 mM *p*-benzoquinone is added to the electrolyte the photocurrent density reaches  $12.25 \mu\text{A cm}^{-2}$ . Our results could have significant implications in photosynthetic energy conversion and in development of photobioelectrochemical devices.

**Keywords:** Microbial fuel cell • *Rhodobacter capsulatus* • Photosynthesis • Light • Electrodes

## 1 Introduction

One of the greatest challenges for modern society is the development of CO<sub>2</sub> free and sustainable clean energy [1]. Life as we know currently depends on photosynthesis, a process by which light energy is converted into chemical energy occurring in plants, algae, and photosynthetic bacteria [2]. Purple bacteria carry out anoxygenic photosynthesis that involves oxidation of organic carbon instead of water. Photosynthesis and cellular respiration could provide the blueprint for addressing human energy demand by converting solar energy into chemical energy [3]. Hydrogen is widely accepted as an alternative source of fossil fuels. Photosynthetic bacteria are potential candidates for bio-hydrogen production due to their high metabolic versatility and conversion efficiency [4]. *Rhodobacter sphaeroides* has been studied for hydrogen production from wastewater streams [5]. Cho et al. reported on power generation from *R. sphaeroides* in the presence of light as well as under dark conditions [6].

*Rhodobacter capsulatus* is a photosynthetic gram-negative, purple, nonsulfur prokaryotic bacterium that converts light energy into chemical energy by anoxygenic photosynthesis [7]. It is widely studied because of its high metabolic versatility [8], e.g. anoxygenic photosynthesis, fermentation, and aerobic respiration [7]. One of the remarkable characteristics of *Rhodobacter* is that it can

grow photoheterotrophically, where light serves as an energy source and organic compounds serve as carbon sources [7]. *Rhodobacter* can use a variety of substrates such as fatty acids, amino acids, sugars, as well as aromatic compounds. Moreover, it can also grow photoautotrophically in the presence of CO<sub>2</sub>/H<sub>2</sub> or CO<sub>2</sub>/H<sub>2</sub>S [9].

The photosynthetic process in *Rhodobacter* is considerably simpler compared to their eukaryotic counterparts. The photosynthetic event occurs in intracellular membranes, whereas in green plants and algae it happens in a particularly designed organelle called chloroplast [10]. *Rhodobacter* contains only one photosystem that is not

[a] K. Hasan, K. V. R. Reddy, K. Górecki, C. Hägerhäll, L. Gorton  
Department of Analytical Chemistry/Biochemistry and Structural Biology, Lund University  
P. O. Box 124, SE-22100 Lund, Sweden  
\*e-mail: Lo.Gorton@biochemistry.lu.se  
Kamrul.Hasan@biochemistry.lu.se

[b] V. Eßmann, W. Schuhmann  
Analytische Chemie – Elektroanalytik & Sensorik, Ruhr-Universität Bochum  
Universitätsstr. 150, 44780 Bochum, Germany

[c] P. Ó Conghaile, D. Leech  
School of Chemistry & Ryan Institute, National University of Ireland Galway  
University Road, Galway, Ireland

powerful enough for the photolysis of water [11]. The photosynthetic electron flow released from organic carbon (for instance acetate/malate) pumped through a number of electron carriers such as quinones, cytochrome  $c_2$  and cytochrome  $bcl$  complex (Cyt  $bc_1$ ). The energy generated from this cyclic electron transport (ET) system forms a proton motive force across the membrane that is used by ATP synthase to generate ATP [12]. In purple bacteria the photosynthetic event is not electron consuming; instead the photosynthetic pigments get relaxed while transferring electrons to the cyclic ET system [13].

In photomicrobial fuel cells (PMFCs), photosynthetic bacterial cells use sunlight to generate electrons from oxidation of organic matters, a process called photofermentation [14]. It is essential in any bioelectrochemical systems (BES) that electrons generated inside the microorganisms be transferred outside of the cells and ultimately transferred to the electrode [15]. In bioelectrochemical systems, the major route of extracellular ET from microorganisms to the electrode is carried out by monomeric artificial mediators and is therefore not compatible for use in regular continuous flow applications [15]. Instead, the use of a surface confined flexible osmium redox polymer has already been successfully used in reagentless biosensors [16], where they fulfill most of the characteristics of a ideal mediator as well as work as an immobilization matrix for the bio-components [15]. ORPs supply the system with a mediator (which does not diffuse away with time) and form a 3D immobilized matrix (hydrogel) with enzymes as well as with bacterial cells [17]. With this polymeric mediator, the ET takes place by collision between reduced ( $Os^{3+}$ ) and oxidized centers ( $Os^{2+}$ ) and efficiently competes with  $O_2$  as electron acceptor [17]. Furthermore ORPs are attractive [18], since they form a stable 3D hydrogel containing multiple layers of enzymes [19] or bacterial cells [20] with a very high local concentration of mediating functionalities. Previously such ORPs have been extensively used for electrochemical communication between a variety of bacterial cells [21] and electrodes [22].

*R. capsulatus* has been widely investigated for bio-hydrogen production [4,13,23] but few electrochemical studies [6,24] have been conducted on it. Here, we demonstrate the anodic ET between electrodes modified with ORPs and *R. capsulatus* grown heterotrophically as well as photoheterotrophically. Four different ORPs were used with different chemical structures and redox potentials ranging from  $-0.07$  V to  $+0.290$  V vs. Ag|AgCl (sat. KCl). The possibilities of using *R. capsulatus* for use in MFC as well as in PMFCs are investigated.

## 2 Experimental

### 2.1 Chemicals

Succinic acid disodium salt, malic acid sodium salt, lactic acid, ammonium chloride, glutamic acid sodium salt,

sodium acetate, MOPS buffer (3-morpholinopropane-1-sulfonic acid), potassium chloride, *p*-benzoquinone, the nyltrifluoroacetone were purchased from either Sigma-Aldrich (Munich, Germany) or Merck (Darmstadt, Germany) and were either research or analytical grade. All aqueous solutions were prepared by using water purified and deionized (18 M $\Omega$ ) with a Milli-Q system (Millipore, Bedford, MA, USA).

### 2.2 Osmium Redox Polymers (ORPs)

[Os(4,4'-dimethoxy-2,2'-bipyridine)<sub>2</sub>(poly-vinylimidazole)<sub>10</sub>Cl]<sup>+2+</sup> ([Os-DMOPVI]),  $E^{\circ} = -0.07$  V, [Os(4,4'-dimethyl-2,2'-bipyridine)<sub>2</sub>(poly-vinylimidazole)<sub>10</sub>Cl]<sup>+2+</sup> ([Os-DMPVI]) [19],  $E^{\circ} = +0.12$  V, [Os(2,2'-bipyridine)<sub>2</sub>(poly-vinylimidazole)<sub>10</sub>Cl]<sup>+2+</sup> ([Os-BPPVI]) [26],  $E^{\circ} = +0.22$  V and [Os(4,4'-dichloro-2,2'-bipyridine)<sub>2</sub>(poly-vinylimidazole)<sub>10</sub>Cl]<sup>+2+</sup> ([Os-DCPVI]) [27],  $E^{\circ} = +0.29$  V vs. Ag|AgCl (sat. KCl) were synthesized and reported previously in respective literature.

### 2.3 Measurements and Instrumentation

Cyclic voltammetry (CV) and chronoamperometry (CA) were performed using a PalmSens potentiostat (model Emstat2, Utrecht, The Netherlands) equipped with Pstrace software. A conventional three-electrode electrochemical cell was used for all experiments performed with Ag|AgCl (sat. KCl) as reference electrode, platinum wires as counter electrode and bare-graphite or polymer modified graphite as working electrodes.

The amperometric measurements with heterotrophically grown *R. capsulatus* were conducted in a flow analysis system [22b] containing an in-house made three electrode flow-through electrochemical wall-jet cell controlled with a potentiostat (Zäta Elektronik, Hög, Sweden) containing an Ag|AgCl (0.1 M KCl) as a reference electrode (Beta Sensor AB, Södra Sandby, Sweden), a platinum wire as counter electrode and graphite as working electrode. Briefly, the working electrode was press fitted into a Teflon holder and inserted into the wall-jet cell and kept at a constant distance (ca. 1 mm) from the nozzle. The electrolyte flow was maintained at 0.5 mL/min with a peristaltic pump miniplus 2 (Gilson, Villiers-le-Bel, France). The current response was recorded on a strip chart recorder (Kipp & Zonen, Delft, The Netherlands). The injector was electrically controlled with a six-port valve (Rheodyne, Cotati, CA, USA) and the injection loop volume was 50  $\mu$ L. The MOPS buffer (20 mM MOPS; 0.1 M KCl at pH 7.40) was used as electrolyte throughout the study and was degassed under vacuum prior to experiments to prevent micro-bubbles to appear in the flow system.

### 2.4 Heterotrophically Grown *R. capsulatus*

Heterotrophic growth of *R. capsulatus* means when the cells grow in the presence of oxygen and use organic

carbon both as an energy source as well as carbon source [4]. *R. capsulatus* strain ATCC 17015 was purchased from DSMZ (Deutsche Sammlung von Mikroorganismen und Zellkulturen GmbH, Braunschweig, Germany). Cells were grown and maintained on minimal peptone yeast extract medium (MPYE) [28] agar plates. A single well-isolated colony was used for the inoculum preparation and transferred to 10 mL of MPYE broth (in 50 mL baffled). Then the flasks containing cells were incubated aerobically in dark at  $30 \pm 2^\circ\text{C}$  for 20 h at 200 rpm in an orbital shaker incubator. Cells grown in MPYE medium were harvested in the early stationary phase by centrifuging the broth at  $20^\circ\text{C}$  for 10 min at 4000 rpm. Cells were then washed in MOPS buffer once and then centrifuged again as before, re-suspended in the same buffer to adjust cell density to 1 g/mL (wet weight) [29]. Harvested cells were immediately used for the electrochemical measurements. Cells were grown under strictly sterile conditions.

### 2.5 Photoheterotrophically Grown *R. capsulatus*

The heterotrophically grown *R. capsulatus* ATCC 17015 was used to grow photoheterotrophically. For inoculum preparation, a 15 mL cell broth was transferred to 50 mL of sterile Biebl and Pfennig's [30] medium (BP-medium) in a 200 mL baffled E-flask. This solution was mixed gently and equally distributed into 4 glass test tubes (30 mL) equipped with a magnetic stirring bar inside and fitted with a cotton plug. The medium containing the cells was deoxygenation by bubbling nitrogen ( $\approx 99\%$ ) for 20 min. While undergoing de-oxygenation the test tubes were connected with sterile needles to pass out oxygen and to confirm the regular flow of nitrogen. Afterward the test tubes were fitted with Para-film to prevent oxygenation that would suppress the photosynthetic activity [31] of *R. capsulatus*. The test tubes were then kept under a halogen light (28 Watt, 240 V) at a light intensity of  $10\text{ W m}^{-2}$  for 48 h in room temperature ( $20 \pm 2^\circ\text{C}$ ). By this time the density reaches  $\approx 1.8$  in optical density measurement (OD 600 nm). Cells were harvested in the similar way as those grown under heterotrophic conditions. Strict sterile conditions were maintained in the entire cell culture.

The photosynthetic processes of *R. capsulatus* were induced on the working electrodes by a 150 W 220 V fiber optic illuminator (Titan Tool Supply, Inc. Buffalo, NY, USA) with an FOI-5 light guide (Titan Tool supply Inc.) with a light intensity of  $250\text{ mW cm}^{-2}$ . The illuminator was calibrated using a light intensity meter (Techtum Lab AB, Umeå, Sweden).

To measure the photocurrent density generated by *R. capsulatus*, the response registered under light off condition was subtracted from that registered under light on condition.

### 2.6 Preparation of Working Electrodes

Graphite rods (Alfa Aesar GmbH & Co KG, Karlsruhe, Germany, AGKSP grade, ultra "F" purity, and 3.05 mm

diameter) were used as working electrodes. The end of the graphite rod was polished on a wet emery paper (Turfbak Durite, P1200), and then carefully washed in a stream of Milli-Q water. Finally the electrodes were dried at room temperature before 5  $\mu\text{L}$  of an ORP solution (10 mg/mL, in Milli-Q water) was spread onto the entire electrode ( $0.0731\text{ cm}^2$ ). Afterwards the electrode was dried at room temperature for  $\approx 10$  min and then an amount of *R. capsulatus* cells (5  $\mu\text{L}$  of heterotrophic cells or 1  $\mu\text{L}$  of photoheterotrophic cells) was spread on the surface. A dialysis membrane (Spectrum Laboratories Inc., Rancho Dominguez, CA, USA, molecular mass cut-off: 6000–8000) was used to maintain the ORPs and *R. capsulatus* (photoheterotrophic only) on the electrode surface. The dialysis membrane (presoaked in MOPS buffer solution for  $\approx 20$  min) was pressed onto the electrode and fixed tightly to the electrode with a rubber O-ring and Para-film.

All measurements were performed at room temperature and the electrolyte solution was degassed for  $\approx 10$  min before conducting any experiment. An inert atmosphere was maintained above the electrochemical cell throughout the experiment with a flow of pure nitrogen gas ( $\approx 99\%$ ). All reported data are based on three independent experiments and standard deviation was less than 10%.

## 3 Results and Discussions

### 3.1 Characterization of ORPs

We have reported previously that heterotrophically grown *R. capsulatus* was successfully wired with an osmium redox polymer, viz. Os-BPPVI [24], to establish electrochemical communication with a graphite electrode. Here we have increased the number of ORPs to four different ones, viz. Os-DMOPVI [25], Os-DMPVI [19], Os-BPPVI [26] and Os-DCPVI [27] with their formal potentials ( $E^\circ$ )  $-0.07\text{ V}$ ,  $+0.11\text{ V}$ ,  $0.22\text{ V}$  and  $+0.29\text{ V}$  vs. Ag|AgCl (sat. KCl), respectively. Besides the different  $E^\circ$  of these ORPs, they also vary in side chains-(X) [18] in their coordination sphere and subsequently their ability for extracellular ET from *R. capsulatus*. CV was used to characterize the electrochemical behavior of the ORPs (Figure 1). The CV of a bare-graphite electrode appears in Figure 1A and the redox waves of electrodes modified with the four ORPs are clearly exhibited in Figures 1B–E revealing the electroactivity of Os-DMOPVI, Os-DMPVI, Os-BPPVI, and Os-DCPVI, respectively. The  $E^\circ$ 's of these ORPs were found to be in close agreement with previously published values [25,19,26,27]. The CV of the Os-BPPVI displays a transition at 0 V vs. Ag|AgCl (sat. KCl), indicative of the presence of residual Os(2,2'-bipyridyl) $\text{Cl}_2$  starting material. The ORPs are cationic in their chemical structure and will form strong electrostatic interactions with the anionic bacterial cell membranes [22b].



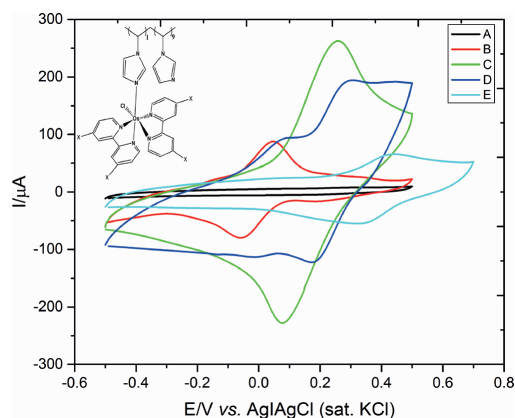


Fig. 1. Cyclic voltammograms (CVs) of (A) bare graphite electrode and electrode modified with (B) Os-DMOPVI [ $E^{\circ'} = -0.07$  V] (C) Os-DMPVI [ $E^{\circ'} = +0.11$  V] (D) Os-BPPVI [ $E^{\circ'} = +0.22$  V] (E) Os-DCPVI [ $E^{\circ'} = +0.29$  V]. Condition: 20 mM MOPS buffer 0.1 M KCl (pH 7.4), scan rate: 50  $\text{mVs}^{-1}$ . Inset: General chemical structure of these polymers, where X = OCH<sub>3</sub>, CH<sub>3</sub>, H and Cl for Os-DMOPVI, Os-DMPVI, Os-BPPVI and Os-DCPVI respectively.

### 3.2 *R. capsulatus* Cannot Communicate via DET

The direct ET (DET) is preferable in BES, since it minimizes the overpotential and simplifies the electrochemical cell design and operation [32]. Typically direct extracellular ET mechanism between bacterial cells and electrodes is restricted but few strains have shown DET properties, e.g., *Shewanella* and *Geobacter* [33]. To probe DET, *R. capsulatus* cells were immobilized on bare-graphite electrode and CA experiments were performed. However, with an applied potential of +0.350 V on the electrode there was no catalytic response when succinate was used as substrate (data not shown). The ET chain and the respiratory redox enzymes in *R. capsulatus* are deeply buried inside the thick plasma membranes [34] and do not therefore allow any significant DET.

### 3.3 Biocatalytic Current Mediated by ORPs

CA in combination with flow analysis was used to investigate any relationship between the biocatalytic current and the substrate concentration (Fig. 2) for electrodes prepared using the ORPs and *R. capsulatus*. An overpotential of +130 mV compared with the  $E^{\circ'}$ -value of the ORP was applied on the working electrode to ensure sufficient driving force for electron transfer between electrode and ORP. MOPS buffer was continuously pumped through the electrochemical cell at 0.5 mL/min. After establishment of a stable baseline response with MOPS buffer, the flow buffer was changed to also contain 0.5 mM succinate. When a stable biocatalytic response current was observed, the flow buffer was changed back

to MOBS buffer again to return to the baseline current. In the same way the biocatalytic response was recorded for all succinate concentrations.

Among the four studied ORPs, the Os-DMOPVI with the lowest  $E^{\circ'}$ -value ( $-0.07$  V) could not generate any noticeable bioelectrocatalytic current (data not shown). A possible reason behind this phenomenon could be that the  $E^{\circ'}$  of Os-DMOPVI is too low to extract any electrons from any of the participating redox components in the membrane [35]. Here it is important to mention that the reported redox potentials of the ET chain molecules varies from  $-0.52$  to  $+0.62$  V vs. Ag|AgCl (sat. KCl) [34]. The most likely membrane associated components participating in the extracellular ET chain is an outer membrane cytochrome *c* [33] with an  $E^{\circ'}$  of  $+0.05$  V vs. Ag|AgCl (sat. KCl) [36].

Maximum biocatalytic current for all ORPs reported here was obtained at 10 mM succinate. When the flow contained a higher concentration of succinate ( $> 10$  mM), the biocatalytic current decreases (data not shown). This higher succinate concentration ( $> 10$  mM), might lead to intracellular pH changes or some inhibition reaction in the bacterial cell with a consequence in a reduced biocatalytic current. A similar response vs. [succinate] was observed for wired *Bacillus subtilis* cells [22b].

The bioelectrocatalytic current density vs. [succinate] increases when changing the ORP from Os-DMPVI to Os-BPPVI (Fig. 2). In contrast when further increasing the  $E^{\circ'}$  to  $+0.29$  V using Os-DCPVI the bioelectrocatalytic current was considerably lower. A similar variation of the response for wired glucose oxidase [37] was shown previously. The difference in electroactivity of the different ORPs (see Fig. 1) may play a significant role as well as the “bulkiness” of the mediating functionality that may influence the accessibility of the ORP to interact with the redox enzymes located in the bacterial membrane.

It has been shown (Fig. 2) that Os-BPPVI ( $E^{\circ'} = +0.22$  V) compared to the other ORPs, generates a maximum bioelectrocatalytic current ( $5.05 \mu\text{A cm}^{-2}$ ). This could be because of a simple chemical structure (side chain X = H), a higher aqueous solubility and therefore greater flexibility contributing to making Os-BPPVI the best electron mediator in our experiments. Therefore further experiments reported below were conducted with Os-BPPVI.

In addition to succinate, some other substrates such as, malate, acetate, butyrate, glutamate, and glucose were also investigated (data not shown). However, none of the substrates except succinate generated a visible catalytic current. The reason behind this phenomenon is not known and a focus of future research.

### 3.4 Metabolic Viability of *R. capsulatus*

The metabolic viability of bacterial cells on the electrode surface is a critical issue since only viable cells can participate in extracellular ET [38]. The natural electron acceptor for the aerobically grown heterotrophic *R. capsula-*

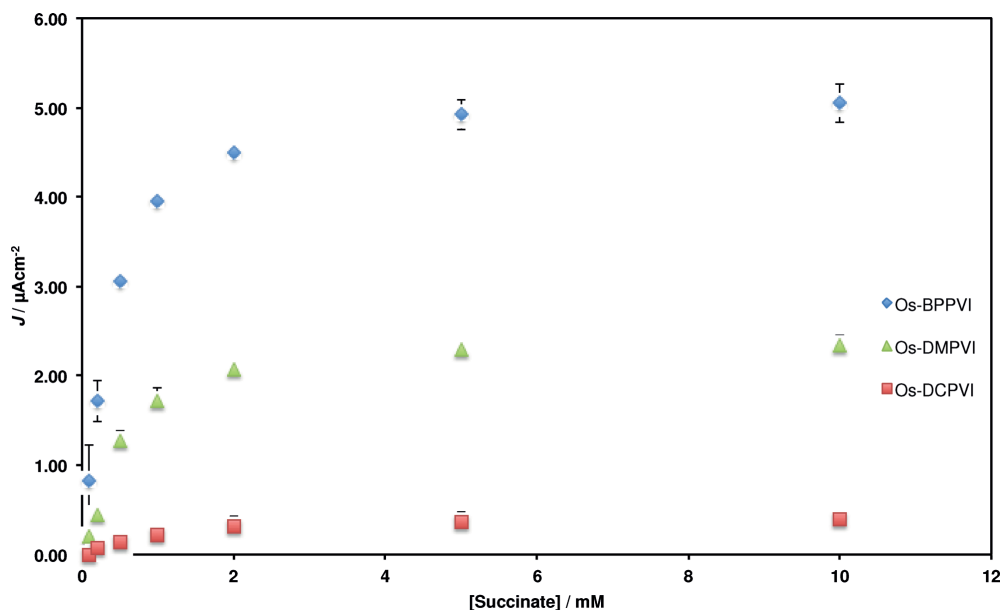


Fig. 2. Biocatalytic calibration curves (current density versus substrate concentration) obtained from *R. capsulatus* and graphite electrodes modified with different ORPs, i.e., Os-DMPVI, Os-BPPVI and Os-DCPVI. (Note: Os-DMOPVI does not generate any visible catalysis). Measurements were performed in flow analysis while using different succinate concentrations as substrate. The applied potential ( $E_{app}$ ) was +0.24 V, +0.35 V, +0.42 V vs. Ag|AgCl (sat. KCl), flow rate: 0.5 mL/min.

*tus* is  $O_2$  [7]. To investigate whether the ORPs have any adverse effect on cellular viability, the oxygen consumption of *R. capsulatus* was studied. For this 5  $\mu$ L of *R. capsulatus* solution and 5  $\mu$ L of Os-BPPVI were mixed in 1 mL of MOPS buffer and an oxygen electrode was used to determine the oxygen consumption (Fig. 3). The bacterial cells consumed oxygen regularly and within 300 min all possible oxygen available in the system was consumed. Therefore, ORPs do not have detrimental influence on cellular viability [22b]. Recently *Shewanella oneidensis* MR-1 was wired with such a polymer over a two week period and did not show any effect in their regular metabolism [39]. Other electron-mediating polymers have also been used for extracellular ET of gram-negative as well as gram-positive bacterial cells without any noticeable cytotoxicity [40].

### 3.5 Origin of Biocatalytic Current

Since succinate was used as substrate for *R. capsulatus*, we assume that the respiratory complex II (succinate/quinone oxidoreductase, EC 1.3.5.1) is the factor controlling ET. In aerobic organisms, complex II catalyzes the oxidation of succinate to fumarate in the citric acid cycle and reduces a quinone to hydroquinone in the membrane [41]. Theonoyltrifluoroacetone (TTFA) is an inhibitor for complex II and known to bind with the quinone binding

site and will consequently block the reoxidation of the reduced quinone [41].

In the flow mode with the *R. capsulatus* cells immobilized on an Os-BPPVI modified graphite electrode, a stable baseline was observed with only buffer running through the flow cell (Fig. 4). When 2 mM succinate was added to the buffer and used as substrate, a biocatalytic current density reached a value of  $4.23 \mu\text{A cm}^{-2}$  (Fig. 4). Under these conditions 1 mM TTFA was added to the flow buffer also containing 2 mM succinate and as a result the biocatalytic current decreased to baseline level within  $\approx 20$  min. Afterward when buffer containing 2 mM succinate and no TTFA was used the biocatalytic current reached only  $1.13 \mu\text{A cm}^{-2}$ . It thus appears as though TTFA reduces more than 70% of the biocatalytic current obtained when the cells were not exposed to the inhibitor compared to its non-inhibited response. It can thus be inferred that complex II is the main source of the biocatalytic current and that TTFA acts as an irreversible inhibitor.

### 3.6 Extracellular ET from *R. capsulatus* (Proposed)

The extracellular ET from heterotrophically grown *R. capsulatus* is already shown earlier [24], however, ET from photoheterotrophically grown cells are suggested here according to Scheme 1. Photosynthesis in purple

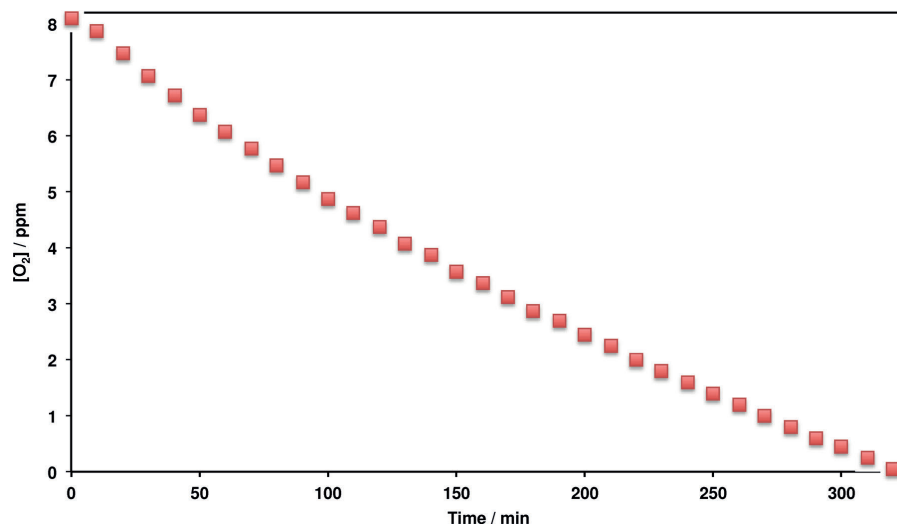


Fig. 3. The oxygen consumption of *R. capsulatus* mixed with Os-BPPVI in MOPS buffer. The experiment was conducted with Clark oxygen electrode.

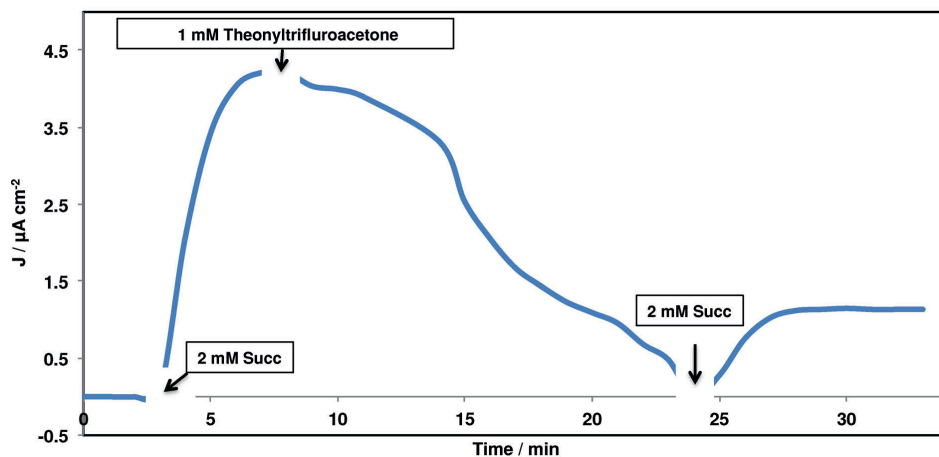
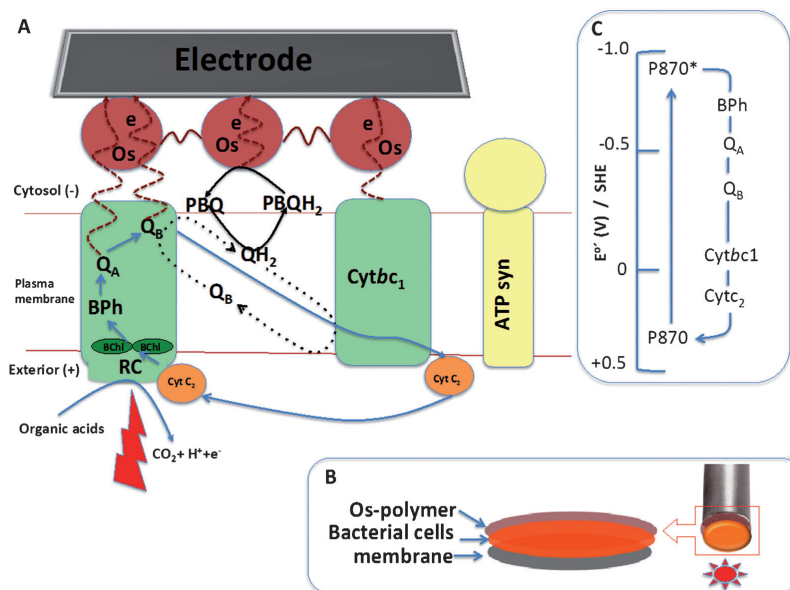


Fig. 4. The addition of an inhibitor (theonyltrifluoroacetone, TTFA) for respiratory complex II resulted in a reduced catalytic current. *R. capsulatus* was immobilized on an Os-BPPVI modified graphite electrode. The applied potential ( $E_{app}$ ) was +0.35 V and 2 mM succinate was used as a substrate.

bacteria takes place in the intracytoplasmic membrane. The core photosynthetic apparatus in *R. capsulatus* is the light harvesting complex (LH) and reaction centers (RC), where charge separation takes place [42].

The LH complex is known as P870, where P refers to pigment bacteriochlorophyll BChl a and 870 refers to the wavelength of maximum absorption. Bacterial photosynthetic ET flow is cyclic [12] and includes RC and cyto-

chrome  $bc_1$  complex (Cyt  $bc_1$ ). The main function of the RC is to produce hydroquinone (QH<sub>2</sub>) as a reducing equivalent to transfer electrons to Cyt  $bc_1$ . While light (photon) is absorbed by the BChl a (P870), the excitation energy is transferred to bacterial pheophytin (BPh). Electrons from BPh then reduce the tightly bound primary quinone (Q<sub>A</sub>) and followed by the freely associated secondary quinone (Q<sub>B</sub>) that cycles between quinone and



Scheme 1. The suggested schematic electron transfer (ET) from *R. capsulatus* (A) extracellular ET to the ORP modified electrodes; photopigment (BChl) gets excited by light (photon) and subsequent ET through a group of electron carriers, i.e. bacterial pheophytin (BPh), a pair of quinone complexes ( $Q_A$  and  $Q_B$ ), cytochrome  $bc_1$  complex (Cyt  $bc_1$ ) and finally cytochrome  $c_2$  (Cyt  $c_2$ ) followed by reaction center (RC). PBQ is assumed to oxidize the quinone pool inside the membrane and reduced to *p*-benzoquinol (PBQH<sub>2</sub>). This cyclic electron flow generates a proton gradient across the membrane and results in ATP formation by ATP synthase (ATP syn). The purple droplets indicate the osmium redox centers linked to the polymer matrix. Purple dot arrows refer to the extracellular electron flow. Blue arrow and black dot refer to the cyclic electron flow and proton translocation, (B) immobilization method of bacterial cells on ORP modified graphite electrode by using a dialysis membrane (C) the redox potential scale of purple photosynthetic bacteria based on standard hydrogen electrode (SHE).

hydroquinone states [10]. Finally a soluble cytochrome (Cyt  $c_2$ ) links the electron flow from Cyt  $bc_1$  back to the RC. This cyclic ET generates a proton gradient over the membrane and drives the synthesis of ATP from ADP [42].

### 3.7 Photosynthetic Absorption Spectra

*R. capsulatus* is considered to be the most metabolically versatile of all common known bacteria. They can grow both photoheterotrophically as well as in darkness by respiration, fermentation, or chemolithotrophy. Moreover, they can grow phototrophically in the presence of either CO<sub>2</sub> or organic compounds [7]. Among all growth conditions they prefer to grow photoheterotrophically when readily usable organic compounds are available [43]. To evaluate the photosynthetic activity of *R. capsulatus*, the photopigments were extracted according to a procedure previously published [44] and their absorption spectra were recorded (Fig. 5). As can be clearly seen (Fig. 5) the primary photopigment (BChl a) appears at 770 nm and the absorption of the other necessary secondary photopigments, i.e. carotenoids, are shown at 456 nm and 487 nm.

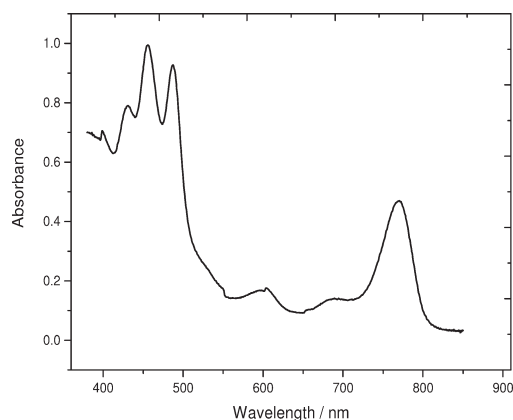


Fig. 5. The absorption spectra of photopigments extracted (in acetone: methanol, 7:2 v/v) from *R. capsulatus*. The primary photopigment, BChl a appears at 770 nm and secondary pigments at 456 nm and 487 nm.

Similar photosynthetic spectra were previously shown [44].

### 3.8 Characterization of Photocurrent by CV

Under photoheterotrophic growth conditions *R. capsulatus* uses light as energy source in the presence of organic carbon, e.g., malate [4]. It is thus also meaningful to investigate whether *R. capsulatus* can use light for photo-assisted oxidation of organic carbons for photocurrent generation. The electrochemical behavior of photoheterotrophically grown *R. capsulatus* was studied using CV in the presence of “light off” and “light on” conditions while 10 mM malate was used as substrate (Fig. 6). To investigate for any DET communication, *R. capsulatus* cells were immobilized directly onto a bare-graphite electrode without any mediator (Fig. 6). In CVA is shown a redox wave at  $\approx 0.05$  V in the absence of light and we speculate that this wave is due to the photosynthetic redox component, cytochrome  $c_2$  (Cyt  $c_2$ ) responsible for extracellular ET. When in the presence of light (CV B in Fig. 6), the oxidation peak current increases slightly and concurrently the reduction peak current decreases. This can be attributed to photo-electrooxidation of malate to form oxaloacetate is responsible for this phenomenon.

*R. capsulatus* cells were additionally immobilized on Os-BPPVI modified graphite to investigate whether the ET rate from the cells to the electrode could be enhanced compared to DET conditions in the presence of 10 mM malate (CVs B and C in Fig. 6). The redox wave of Os-BPPVI appears at +0.230 V, at a slightly higher potential than that of its  $E^{or}$  (+0.220 V). This potential shift of the

polymer is expected to be due to the interaction between the redox centers of the polymer and the bacterial cell membranes. However, in the presence of light, increases slightly compared to light off conditions. Here, it can be anticipated that the ORP with its long flexible polymer backbone and its side chains containing the redox active functionalities can reach the bacterial photosynthetic membrane and extract electrons from there. Previously, it has been reported that a similar redox polymer can wire photosystem II [45] and photosystem I [46] to electrodes and consequently generate a photocurrent in the presence of light. To investigate whether addition of a freely diffusive monomeric redox compound, 0.6 mM PBQ was added to the MOPS buffer containing 10 mM malate, when *R. capsulatus* was immobilized on Os-BPPVI modified electrode (CVs E and F in Fig. 6). In CVs E and F two well-isolated waves at +0.100 V and +0.231 V that correspond to PBQ and Os-BPPVI are observed, respectively, under light off conditions and similarly under light on conditions for which the photocurrent increases compared to light off conditions. In these CVs, it is difficult to determine the photocurrent generation quantitatively thus further experiments were undertaken using CA.

### 3.9 Quantitative Evaluation of Photocurrent

The quantitative evaluation of the photo-excited electron transfer efficiency from *R. capsulatus* to graphite electrodes was investigated with amperometric measurements by applying a constant potential. The applied potential was set to +0.35 V, more positive than that of Os-BPPVI, +0.22 V, and *p*-benzoquinone, +0.10 V, redox potentials to guarantee that the applied potential is sufficiently high for electron transfer from mediator to electrode. Light was initially turned off for 1000 s to reach a stable background baseline when 10 mM malate was introduced as substrate. Afterward light was turned on for 200 s to excite the photosynthetic events in *R. capsulatus* and to register any photocurrent generation. The photocurrent was calculated by deducting the current response under light off conditions from that of the light on conditions. No photocurrent was obtained in the absence of malate as substrate (data not shown).

The *R. capsulatus* cells were immobilized on bare-graphite electrode (curves A in Fig. 7) on Os-BPPVI modified electrodes (curves B in Fig. 7) and on Os-BPPVI modified electrodes when also 0.6 mM PBQ was used in the flow buffer (curves C in Fig. 7). In case of bare graphite electrode (curves A in Fig. 7), a stable baseline current was obtained while light was turned off. Then, light was turned on and successively the current reaches its maximum current ( $\approx 6.5 \mu\text{A cm}^{-2}$ ) with an average photocurrent of  $(6.5-1.8) 4.7 \mu\text{A cm}^{-2}$ . The average photocurrent value with bare-graphite electrode was evaluated to be  $3.7 \mu\text{A cm}^{-2}$ . This photocurrent generation can be attributed to an interaction between the graphite electrode<sup>[47]</sup> and the quinones available inside the bacterial photosynthetic membrane [42]. It has been

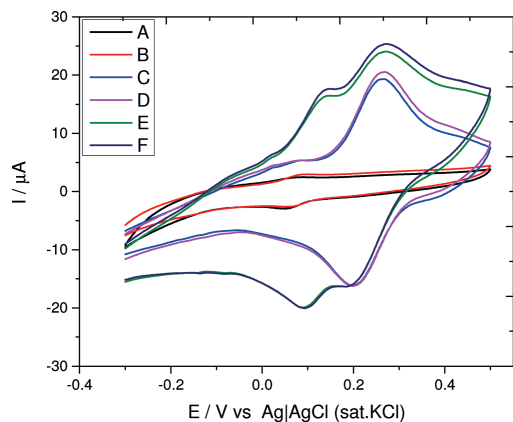


Fig. 6. The photocurrent generation from *R. capsulatus* immobilized on (A) bare graphite electrode, light off (B) bare graphite electrode, light on (C) Os-BPPVI modified graphite, light off (D) Os-BPPVI modified graphite, light on (E) Os-BPPVI modified graphite in addition to 0.6 mM PBQ, light off (F) Os-BPPVI modified graphite in addition to 0.6 mM PBQ, light on. Scan rate:  $10 \text{ mV s}^{-1}$ , substrate: 10 mM malate.

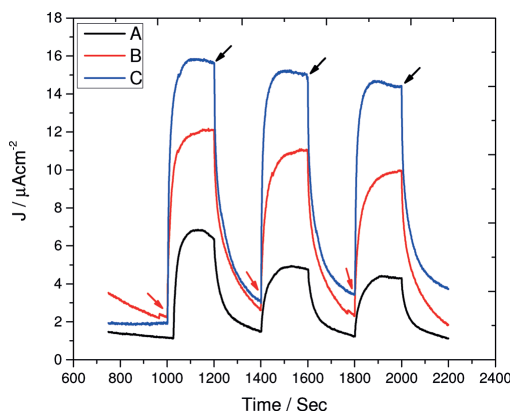


Fig. 7. The relationship of photocurrent generation when *R. capsulatus* was immobilized on (A) bare graphite electrode (B) Os-BPPVI modified graphite, (C) Os-BPPVI modified graphite in addition to 0.6 mM PBQ, applied potential ( $E_{app}$ ) was 0.35 V vs. Ag|AgCl (sat. KCl), substrate: 10 mM malate, red arrow, and black indicate light on and light off phenomenon.

reported that the plastoquinone pool in the photosynthetic ET is responsible for “direct” electrogenic activity [48].

When a Os-BPPVI modified electrode was used (curves B in Fig. 7) the photocurrent generation was enhanced to  $8.46 \mu\text{A cm}^{-2}$ . This is expected since the osmium polymer is known for ET from different redox enzymes [49] as well as from bacterial cells [20]. It can be inferred that the redox centers ( $\text{Os}^{2+/3+}$ ) in the polymer side chains can access the photosynthetic membrane, and be reduced to  $\text{Os}^{2+}$  and subsequently be electrochemically oxidized to  $\text{Os}^{3+}$  by the polarized electrode.

To improve photocurrent generation soluble PBQ was added to generate a maximum photocurrent of  $12.25 \mu\text{A cm}^{-2}$  (curves C in Fig. 7). This improvement on photocurrent density is due to higher availability of the diffusible mediator inside the membrane compared to the ORP [50]. PBQ has already been used for photocurrent generation from different photosynthetic sources such as, thylakoid membranes [51] and other photosynthetic systems [52]. Previously it has been reported that PBQ is a suitable electron acceptor for the  $\text{Q}_B$  site of the photosynthetic membrane of purple bacteria [53].

#### 4 Conclusion

In this study, we have been demonstrated that the metabolically versatile purple bacterium, *Rhodobacter capsulatus*, is a candidate for microbial fuel cells. Besides that, these bacterial cells are also explored in harnessing solar energy for photomicrobial fuel cells. This study reveals electrochemical communication between *R. capsulatus*, grown both heterotrophically as well as photoheterotrophically, and electrodes. Four different ORPs with different chemical structures and  $E^\circ$ 's have been investigat-

ed for their efficiency in extracellular ET. Among these four ORPs, Os-BPPVI with a comparatively high  $E^\circ$  value, a simple chemical structure, and a greater solubility exhibits the greatest efficiency in bioelectrocatalysis. Heterotrophically grown cells are shown to not undergo biocatalysis without the addition of an exogenous electron mediator. On the other hand photoheterotrophically grown *R. capsulatus* generates a photocurrent density of  $3.46 \mu\text{A cm}^{-2}$  without any added mediator. We speculate that the reason behind this is the membrane constituents of the bacterial cells differ when grown under different metabolic conditions. The photocurrent density was improved to reach  $8.46 \mu\text{A cm}^{-2}$  when the cells are immobilized on ORP modified electrodes and could be even further increased to  $12.25 \mu\text{A cm}^{-2}$  by addition of 0.6 mM PBQ to the electrolyte.

It is vital that the power density is improved many fold for any use in practical applications. Developing and investigating nanostructured electrodes materials that will allow near infrared light, sufficient enough for bacterial photosynthesis could improve the power density. Moreover, developing reactor designs, engineering of microorganisms for maximizing the capturing of solar energy, improved electrocatalysis, and minimizing the Ohmic resistance could improve the photocurrent density further. In addition to the improvement of power density, the long-term stability of the system will be the focus of future research.

#### Acknowledgements

The authors thank *The Swedish Research Council* (projects: 2010-5031, 2010-2013), *The Swedish Institute (SI scholarship)*, *The Nanometer Consortium at Lund University* (nmc@LU), *The European Commission* (Projects NMP4-SL-2009-229255 “3D-Nanobiodevice”, FP7-PITN-GA-2010-264772 “Chebana” and FP7-PEOPLE-2013-ITN “Bioenergy”) for financial support.

#### References

- [1] O. Kruse, J. Rupprecht, J. H. Mussgnug, G. C. Dismukes, B. Hankamer, *Photochem. Photobiol. S.* **2005**, *4*, 957–970.
- [2] X. Hu, T. Ritz, A. Damjanovic, F. Autenrieth, K. Schulten, *Q. Rev. Biophys.* **2002**, *35*, 1–62.
- [3] M. Hamburger, G. F. Moore, D. M. Kramer, D. Gust, A. L. Moore, T. A. Moore, *Chem. Soc. Rev.* **2009**, *38*, 25–35.
- [4] H. Koku, I. Eroglu, U. Gunduz, M. Yucel, L. Turker, *Int. J. Hydrogen. Energy*, **2002**, *27*, 1315–1329.
- [5] H. Zhu, T. Suzuki, A. A. Tsygankov, Y. Asada, J. Miyake, *Int. J. Hydrogen Energy*, **1999**, *24*, 305–310.
- [6] Y. K. Cho, T. J. Donohue, I. Tejedor, M. A. Anderson, K. D. McMahon, D. R. Noguera, *J. Appl. Microbiol.* **2008**, *104*, 640–650.
- [7] M. Madigan, D. Jung, in *The Purple Phototrophic Bacteria*, Vol. 28 (Eds: C. N. Hunter, F. Daldal, M. Thurnauer, J. T. Beatty), Springer, The Netherlands, **2009**, pp. 1–15.
- [8] S. J. Ferguson, J. B. Jackson, A. G. McEwan, *FEMS Microbiol. Lett.* **1987**, *46*, 117–143.

- [9] M. T. Madigan, J. M. Martinko, J. Parker, T. D. Brock, *Biology of Microorganisms*, Vol. 985, Prentice Hall, Upper Saddle River, NJ, 1997.
- [10] C. Wraight, M. Gunner, in *The Purple Phototrophic Bacteria*, Vol. 28 (Eds: C. N. Hunter, F. Daldal, M. Thurnauer, J. T. Beatty), Springer, The Netherlands, 2009, pp. 379–405.
- [11] C. N. Hunter, *The Purple Phototrophic Bacteria*, Vol. 28, Springer, Heidelberg, 2008.
- [12] A. B. Melandri, D. Zannoni, *J. Bioenerg. Biomembr.* **1978**, *10*, 109–138.
- [13] I. Akkerman, M. Janssen, J. Rocha, R. H. Wijffels, *Int. J. Hydrogen Energy* **2002**, *27*, 1195–1208.
- [14] M. Rosenbaum, U. Schröder, *Electroanalysis* **2010**, *22*, 844–855.
- [15] U. Schroder, *Phys. Chem. Chem. Phys.* **2007**, *9*, 2619–2629.
- [16] A. Heller, *Acc. Chem. Res.* **1990**, *23*, 128–134.
- [17] A. Heller, *Curr. Opin. Chem. Biol.* **2006**, *10*, 664–672.
- [18] F. Mao, N. Mano, A. Heller, *J. Am. Chem. Soc.* **2003**, *125*, 4951–4957.
- [19] T. J. Ohara, R. Rajagopalan, A. Heller, *Anal. Chem.* **1994**, *66*, 2451–2457.
- [20] K. Hasan, S. A. Patil, D. Leech, C. Hägerhäll, L. Gorton, *Biochem. Soc. T.* **2012**, *40*, 1330–1335.
- [21] J. Du, C. Catania, G. C. Bazan, *Chem. Mater.* **2013**, *26*, 686–697.
- [22] a) S. Alferov, V. Coman, T. Gustavsson, A. Reshetilov, C. von Wachenfeldt, C. Hägerhäll, L. Gorton, *Electrochim. Acta* **2009**, *54*, 4979–4984; b) V. Coman, T. Gustavsson, A. Finkelsteinas, C. Von Wachenfeldt, C. Hägerhäll, L. Gorton, *J. Am. Chem. Soc.* **2009**, *131*, 16171–16176.
- [23] a) A. A. Tsygankov, Y. Hirata, M. Miyake, Y. Asada, J. Miyake, *J. Ferment. Bioeng.* **1994**, *77*, 575–578; b) J. Gebicki, M. Modigell, M. Schumacher, J. Van Der Burg, E. Roebroek, *J. Clean. Prod.* **2010**, *18*, S36–S42.
- [24] K. Hasan, S. A. Patil, K. Go'recki, D. Leech, C. Hägerhäll, L. Gorton, *Bioelectrochemistry* **2013**, *93*, 30–36.
- [25] a) C. Taylor, G. Kenausis, I. Katakis, A. Heller, *J. Electroanal. Chem.* **1995**, *396*, 511–515; b) N. Mano, A. Heller, *J. Electrochem. Soc.* **2003**, *150*, A1136–A1138.
- [26] E. M. Kober, J. V. Caspar, B. P. Sullivan, T. J. Meyer, *Inorg. Chem.* **1988**, *27*, 4587–4598.
- [27] P. A. Jenkins, S. Boland, P. Kavanagh, D. Leech, *Bioelectrochemistry* **2009**, *76*, 162–168.
- [28] A. W. Taguchi, J. Stocker, S. Boxer, N. Woodbury, *Photosynth. Res.* **1993**, *36*, 43–58.
- [29] M. B. Hansen, S. E. Nielsen, K. Berg, *J. Immunol. Meth.* **1989**, *119*, 203–210.
- [30] H. Biebl, N. Pfennig, in *The Prokaryotes* (Eds: M. Starr, H. Stolp, H. Trüper, A. Balows, H. Schlegel), Springer, Heidelberg, **1981**, pp. 267–273.
- [31] S. Fidai, S. B. Hinchigeri, T. J. Borgford, W. R. Richards, *J. Bacteriol.* **1994**, *176*, 7244–7251.
- [32] M. T. Meredith, S. D. Minter, *Annu. Rev. Anal. Chem.*, **2012**, *5*, 157–179.
- [33] M. E. Hernandez, D. K. Newman, *CMLS, Cell. Mol. Life Sci.* **2001**, *58*, 1562–1571.
- [34] O. Schaetzle, F. Barriere, K. Baronian, *Energ. Environ. Sci.* **2008**, *1*, 607–620.
- [35] A. Heller, *Phys. Chem. Chem. Phys.* **2004**, *6*, 209–216.
- [36] K. Rabaey, W. Verstraete, *Trends Biotechnol.* **2005**, *23*, 291–298.
- [37] M. N. Zafar, X. Wang, C. Sygmund, R. Ludwig, D. Leech, L. Gorton, *Anal. Chem.* **2011**, *84*, 334–341.
- [38] K. J. Chae, M.-J. Choi, J.-W. Lee, K.-Y. Kim, I. S. Kim, *Bioresource Technol.* **2009**, *100*, 3518–3525.
- [39] S. A. Patil, K. Hasan, D. Leech, C. Hägerhäll, L. Gorton, *Chem. Commun.* **2012**, *48*, 10183–10185.
- [40] K. Nishio, R. Nakamura, X. Lin, T. Konno, K. Ishihara, S. Nakanishi, K. Hashimoto, *ChemPhysChem* **2013**, *14*, 2159–2163.
- [41] C. Hägerhäll, *Biochim. Biophys. Acta (BBA) – Bioenerg.* **1997**, *1320*, 107–141.
- [42] A. G. McEwan, *Anton. Leeuw. Int. J. G.* **1994**, *66*, 151–164.
- [43] M. T. Madigan, D. O. Jung, in *The Purple Phototrophic Bacteria*, Springer, Heidelberg, 2008, pp. 1–15.
- [44] P. Weaver, J. Wall, H. Gest, *Arch. Microbiol.* **1975**, *105*, 207–216.
- [45] A. Badura, D. Guschin, B. Esper, T. Kothe, S. Neugebauer, W. Schuhmann, M. Rögner, *Electroanalysis* **2008**, *20*, 1043–1047.
- [46] A. Badura, D. Guschin, T. Kothe, M. J. Kopczak, W. Schuhmann, M. Rögner, *Energ. Environ. Sci.* **2011**, *4*, 2435–2440.
- [47] K. F. Blurton, *Electrochim. Acta* **1973**, *18*, 869–875.
- [48] N. Sekar, Y. Umasankar, R. P. Ramasamy, *Phys. Chem. Chem. Phys.* **2014**, *16*, 7862–7871.
- [49] A. Heller, B. Feldman, in *Applications of Electrochemistry in Medicine*, Vol. 56 (Ed: M. Schlesinger), Springer US, New York, **2013**, pp. 121–187.
- [50] F. Barrière, P. Kavanagh, D. Leech, *Electrochim. Acta*, **2006**, *51*, 5187–5192.
- [51] K. Hasan, Y. Dilgin, S. C. Emek, M. Tavahodi, H. E. Åkerlund, P.-Å. Albertsson, L. Gorton, *ChemElectroChem* **2014**, *1*, 131–139.
- [52] M. Rosenbaum, Z. He, L. T. Angenent, *Curr. Opin. Biotechnol.* **2010**, *21*, 259–264.
- [53] N. R. Bowlby, C. F. Yocum, *Biochim. Biophys. Acta (BBA) – Bioenerg.* **1993**, *1144*, 271–277.

Received: August 22, 2014

Accepted: September 27, 2014

Published online: November 21, 2014

# Paper IV





# Electrochemical communication between microbial cells and electrodes via osmium redox systems

Kamrul Hasan<sup>\*1</sup>, Sunil A. Patil<sup>\*1</sup>, Dónal Leech<sup>†</sup>, Cecilia Hägerhäll<sup>\*</sup> and Lo Gorton<sup>\*2</sup>

<sup>\*</sup>Department of Biochemistry and Structural Biology, Lund University, P.O. Box 124, SE-22100 Lund, Sweden, and <sup>†</sup>School of Chemistry, National University of Ireland Galway, University Road, Galway, Ireland

## Abstract

Electrochemical communication between micro-organisms and electrodes is the integral and fundamental part of BESs (bioelectrochemical systems). The immobilization of bacterial cells on the electrode and ensuring efficient electron transfer to the electrode via a mediator are decisive features of mediated electrochemical biosensors. Notably, mediator-based systems are essential to extract electrons from the non-exoelectrogens, a major group of microbes in Nature. The advantage of using polymeric mediators over diffusible mediators led to the design of osmium redox polymers. Their successful use in enzyme-based biosensors and BFCs (biofuel cells) paved the way for exploring their use in microbial BESs. The present mini-review focuses on osmium-bound redox systems used to date in microbial BESs and their role in shuttling electrons from viable microbial cells to electrodes.

## Microbe–electrode interface

The ability of micro-organisms to transfer electrons to electrodes was first reported by Potter in 1911 [1]. After several years of negligence (with one exception [2]), research attempts during the 1980s brought this interesting technology to the public's attention [3,4]. However, this obscure field of research was later revived during the end of the 20th Century mainly because of growing concerns over the exhausting fossil fuel reserves, their detrimental effect on the environment and the demand for new sustainable energy, and attracted considerable attention thereafter [4]. The breakthroughs in natural EET (extracellular electron transfer) abilities of mineral-respiring bacteria (referred to as exoelectrogens) provided a foundation for the development of BESs (bioelectrochemical systems) such as MFCs (microbial fuel cells). MFCs operate to produce sustainable energy by diverting bioconvertible energy to electricity directly by using an anode as an insoluble electron acceptor in place of natural acceptors. In addition to electricity generation, the anode of an MFC can be used to offset the voltage required for electrical-current-driven chemical production at the cathode, referred to as microbial electrosynthesis, expanding the application range of these systems [5]. Furthermore, microbe–electrode interactions have been exploited extensively for application as electrochemical microbial sensors [6]. Regardless of the bioelectrochemical device, ET (electron

transfer) from microbes to the electrode is the most imperative and critical task that defines the theoretical limit of the energy conversion [7]. To facilitate cell–electrode communication, electrons produced during respiration exit the bacterial cell membrane either by direct physical transfer of reduced compounds or via electron hopping across the membrane using membrane-bound redox proteins [8]. In the present mini-review, we confine ourselves to discussing recent reports on EET from micro-organisms to electrodes via addition of synthetic osmium-based redox complexes and their applicability to BESs.

## Microbial EET

Microbial EET to electron acceptors other than oxygen is necessary for anaerobes, where mainly minerals containing iron and manganese oxides are reduced. By linking microbial metabolism to electrodes via EET, electrical current can be generated or consumed in BESs [9,10]. The anodic ET is based on exploitation of the necessity of living cells to dispose electrons liberated during oxidative substrate degradation. The proposed mechanisms involved in microbial ET to electrodes are illustrated in Figure 1. These are mainly classified as DET (direct electron transfer) and MET (mediated electron transfer) [7].

In DET, electrons can be transferred directly to the electrode proposed to be either via cell membrane-bound cytochromes [11,12] or via electrically conductive pili, referred to as bacterial nanowires [13–15] (as depicted in Figure 1A). DET takes place by close physical contact of the bacterial cell or any organelle of the membrane with the electrode and without involvement of a soluble redox species. The participation of cytochromes localized in the outer membrane in EET has been reported for several

**Key words:** electrochemical communication/wiring, electrode, extracellular electron transfer, microbial bioelectrochemical system, osmium redox system.

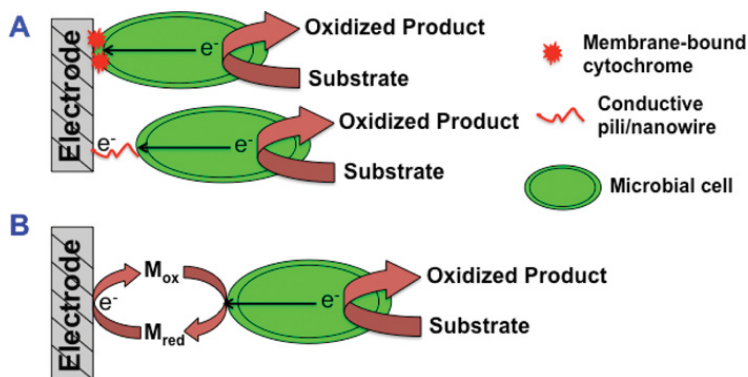
**Abbreviations used:** BES, bioelectrochemical system; CNT, carbon nanotube; DET, direct electron transfer; EET, extracellular electron transfer; ET, electron transfer; FCB2, flavocytochrome *b<sub>2</sub>*; GOx, glucose oxidase; MET, mediated electron transfer; MFC, microbial fuel cell; PQQ, pyrroloquinoline quinone; SQR, succinate:quinone reductase.

<sup>1</sup>These authors contributed equally to this paper.

<sup>2</sup>To whom correspondence should be addressed (email Lo.Gorton@biochemistry.lu.se).

**Figure 1** | Proposed mechanisms of ET from micro-organisms to the electrode

(A) DET via cell membrane-bound cytochromes and electrically conductive pili (nanowires). (B) MET via microbial or exogenous redox mediators.  $M_{ox}$  and  $M_{red}$  indicates mediator in oxidized and reduced state respectively.



iron-reducing bacteria, including *Shewanella putrefaciens* [16], *Rhodospirillum rubrum* [17,18] and several *Geobacter* species [12,17,19]. Additionally, it has been suggested that, for some bacteria such as *Geobacter sulfurreducens* and *Shewanella oneidensis* MR-1, conductive pili allow them to use a distant electron acceptor [13,15,20]. Although DET has been demonstrated for some microbes, it has limitations in terms of coulombic efficiency (the proportion of ET) and the rate of ET (i.e. the current generation) [7]. In practice, few micro-organisms are able to transfer electrons directly to the electrode. In addition, organisms possessing DET capability, such as *Geobacter* and *Shewanella* strains, are unable to utilize complex substrates and metabolize only low-molecular-mass organic acids and alcohols that consequently limits their large-scale applications in BESs [21]. Nevertheless, at the moment, DET-based BESs are the first choice for most researchers for exploration and exploitation of microbe–electrode interactions.

MET is an EET mechanism that occurs via the involvement of redox mediators (Figure 1B). These mediators can be artificial or metabolites produced by the micro-organisms [7]. Remarkably, redox mediators produced by one bacterium can also be used by other bacteria to reach the electrode [8]. Mediators are, in general, electron shuttles that can penetrate the cell membrane, gain electrons from the electron carrier within the cell, leave the cell in a reduced state and ultimately transfer electrons to the electrode. Mediators are essential for microbes that are unable to transfer electrons from the central metabolism to the outside of the cell. The advantage of using mediators in amperometric biosensors is the possibility of measurements at lower overpotential that minimizes interfering reactions contributing to the response signal and therefore increases selectivity. The EET mechanisms in microbe–electrode-based systems have been well documented in several review articles [7,22,23]. In general, most redox mediators are toxic to the bacterial cells at

higher concentrations. Therefore their concentration is kept in the micromolar range, which can constrain the overall BES performance. In addition, it is not feasible to use diffusible artificial mediators in most BESs because of requirements to continuously add them to a system. Furthermore, most freely diffusing mediators cannot compete efficiently with natural electron acceptors. To overcome problems associated with the use of diffusible mediators in enzymatic biosensors, ET to electrodes can be established by ‘wiring’ the enzyme with polycationic, water-soluble and highly flexible redox polymers bound to the electrode [24,25]. The communication between the enzyme, such as GOx (glucose oxidase) and an electrode was improved further using osmium-based redox polymers, since they possess long-term redox stability and suitable redox potential to wire GOx [25]. The use of polymeric redox mediators has proved to be convenient because of the synthetic flexibility, opening up the possibility of manipulating the formal potential, the hydrophilicity/hydrophobicity and their electron-shuttling properties [26–28]. Therefore the exploration of various osmium redox polymers has attracted increasing attention in enzyme-based BFCs and biosensors [29–34].

Development of microbial BESs and whole-cell biosensors may thus be possible through exploiting versatile bacteria that are non-exoelectrogenic, but may be wired by redox complexes. Here, the term ‘wiring’ implies that the observed current from electrochemical communication between microbe and electrode comes from the redox species incorporated in the cell membrane rather than soluble redox-active cell exudates [35].

### Osmium redox polymers

Biofilms on electrodes containing redox polymers can transform electrically insulating co-immobilized redox proteins into redox-conducting systems [26] and establish effective ET

**Table 1 | List of different micro-organisms 'wired' electrochemically with electrodes via various osmium redox systems**

Osmium system I, poly(1-vinylimidazole)<sub>12</sub>-[osmium(4,4'-dimethyl-2,2'-dipyridyl)<sub>2</sub>-Cl<sub>2</sub>]<sup>2+/+</sup>; osmium system II, poly(vinylpyridine)-[osmium-(*N,N'*-methylated-2,2'-bi-imidazole)<sub>3</sub>]<sup>2+/3+</sup>; osmium system III, [osmium(2,2'-bipyridine)<sub>2</sub>-poly(*N*-vinylimidazole)<sub>10</sub>Cl]<sup>2+/+</sup>; osmium system IV, osmium(II)bis-2,2'-bipyridine(*p*-aminomethylpyridine)chloridohexafluorophosphate; osmium system V, bis-bipyridyl osmium-complex-modified copolymer of the vinylimidazole and pent-4-enylamine; osmium system VI, bis-bipyridyl osmium-complex-modified copolymer of butyl acrylate, methyl methacrylate, acrylic acid and pyridin-4-ylmethyl acrylamide; osmium system VII, bis-bipyridyl osmium-complex-modified copolymer of butyl acrylate, dimethylaminoethyl methacrylate and imidazolylethyl acrylate. WT, wild-type strain; PPF-SWCNTs, pyrolyzed photoresist film-single-walled carbon nanotubes

BES/device	Micro-organism	Type of osmium system	Redox potential ( $E^{\circ}$ ) compared with the Ag/AgCl electrode (0.1 M KCl) (V)	Working electrode	Reference
MFC/microbial sensor	<i>G. oxydans</i> ATCC 621	I	0.140	Gold	[39]
Microbial sensor	<i>Ps. putida</i> ATCC 126633	I	0.140	Gold	[40]
	<i>Ps. fluorescens</i> DSM 6521	II	-0.195		
Microbial sensor	<i>Ps. putida</i> DSM2 50026	I	0.140	CNTs and carbon paste	[41]
MFC/microbial sensor	<i>E. coli</i> JM109 (WT)	I	0.140	Graphite	[42]
	<i>E. coli</i> JM109/pBSD 1300*	II	-0.195		
	<i>E. coli</i> JM109/pLUV 1900†				
MFC/microbial sensor	<i>B. subtilis</i> (WT)	I	0.140	Graphite and gold	[43]
	<i>B. subtilis</i> 3G18-pBSD-1200‡	II	-0.195		
MFC	<i>R. capsulatus</i> ATCC 17015 (WT)	III	0.132	Graphite and gold	[44]
	<i>R. capsulatus</i> 37b4 (capsule-lacking strain)				
Microbial biosensor	<i>P. vulgaris</i> NTC 4175	IV	0.200	PPF-SWCNTs assembled on carbon surface	[35]
MFC	<i>H. polymorpha</i> 356 (WT)	V	0.121	Graphite	[45]
	<i>H. polymorpha</i> tr1§	VI	0.061		
	<i>H. polymorpha</i> tr1§	VII	0.041		
MFC	<i>S. cerevisiae</i> NCTC 10716	IV	0.200	PPF-SWCNTs assembled on carbon surface	[46]

\*Strain overproducing the membrane anchor domain of *B. subtilis* SQR succinate:quinone reductase.

†Strain overproducing cytochrome *c*<sub>500</sub> from *B. subtilis*.

‡Strain overproducing succinate:quinone oxidoreductase (respiratory complex II).

§Genetically modified strain that overexpress FCB2.

from buried redox protein centres to electrodes. Electrostatic interactions between osmium redox polymers and the protein channel leading to the redox centre of GOx reduces the ET distance and triggers bioelectrocatalytic oxidation of glucose [36]. The redox polymers can be designed to be water-soluble, simplifying the steps required to coat electrodes with films of polymer and redox enzymes, and ensuring that the films are sufficiently hydrated to permit efficient ET throughout a three-dimensional network permitting incorporation of a large number of enzyme molecules [26]. The combination of redox polymers and enzymes with a cross-linker leads to the formation of redox hydrogels that can wire enzyme redox centres irrespective of their spatial orientation, as well as forming multilayers on electrodes that result in much higher current responses compared with monolayers [37]. Such redox hydrogels are used in amperometric biosensors for

measurement of analyte (enzyme substrate) concentrations and as enzymatic BFC anodes to increase the current density. Readers are referred to a review [37] for detailed information about redox hydrogels. Details on synthesis of osmium redox polymers are described in [28,34,37,38]. This successful application in enzymatic biosensors and BFCs has raised interest in their possible usage for wiring micro-organisms to electrodes over the last decade.

### Wiring of microbial cells to the electrode via osmium redox systems

Table 1 summarizes details of osmium redox systems used to date for wiring micro-organisms in bioelectrochemical devices. To the best of our knowledge, the first application of an osmium system for wiring intact bacterial cells

was reported by Vostiar et al. [39]. They demonstrated efficient electrochemical communication between Gram-negative *Gluconobacter oxydans* and gold electrodes with the aid of osmium redox system I having high redox potential and short side chain (see Table 1 for details). *G. oxydans* was chosen because of its known ability to produce periplasmic membrane-bound PQQ (pyrroloquinoline quinone)-containing enzymes that can efficiently oxidize a wide variety of substrates. The efficient wiring was attributed to ET between PQQ dehydrogenases and the osmium redox polymer. Thereafter, Timur et al. [40] investigated two different polymers based on system I and system II, with a lower redox potential and the longer side chain introducing increased flexibility for motion of the redox complex, to wire *Pseudomonas putida* and *Pseudomonas fluorescens* with electrodes. They found that wiring of bacterial cells with system II showed much higher substrate (catechol, phenol and glucose) sensitivity compared with that of system I. This was attributed to the good contact between the longer tethered redox complex in system II and respiratory enzymes in the *Pseudomonas* strains. A more efficient electrochemical response was subsequently reported by using CNT (carbon nanotube)-modified carbon paste electrodes containing system I to form a *Ps. putida*-based biosensor for phenol detection [41].

In relation to the improvement of bioelectrocatalytic current generation, Alferov et al. [42] investigated the use of two different cytochrome-enriched strains of the model bacterium *Escherichia coli*. Neither of the strains showed any detectable electrochemical response on electrodes because the periplasmic space and outer membrane together offer an insulating thickness of 15 nm, hampering ET out of the bacterial cell. However, in the presence of osmium redox systems, electrochemical communication between cells and electrode was facilitated. Among two different redox systems, system II showed a better current response, again postulated to be because of greater flexibility of motion of the redox complex, enhancing accessibility to the active site of redox enzymes in the inner membrane. Previously, it was assumed that it would be difficult for osmium redox systems to permeate the thick cell wall of Gram-positive bacteria, which consists of a peptidoglycan layer of a thickness of approximately 35 nm. Surprisingly, Coman et al. [43] revealed that the Gram-positive bacterium *Bacillus subtilis* can communicate with electrodes via both osmium redox system I and II. This was ascribed to the fact that the polyanionic properties of cell wall components, e.g. peptidoglycan and teichoic acids, contribute to electrostatic interactions with polycationic redox polymer systems resulting in electrochemical communication. Among two strains investigated by Coman et al. [43], the strain overproducing SQR (succinate:quinone reductase) showed better performance with succinate than the wild-type strain. Recently, Rawson et al. [35] reported that single-walled CNTs functionalized with an osmium complex (system IV) can electrochemically communicate with *Proteus vulgaris* [35], simplifying the electrochemical approach to microbial

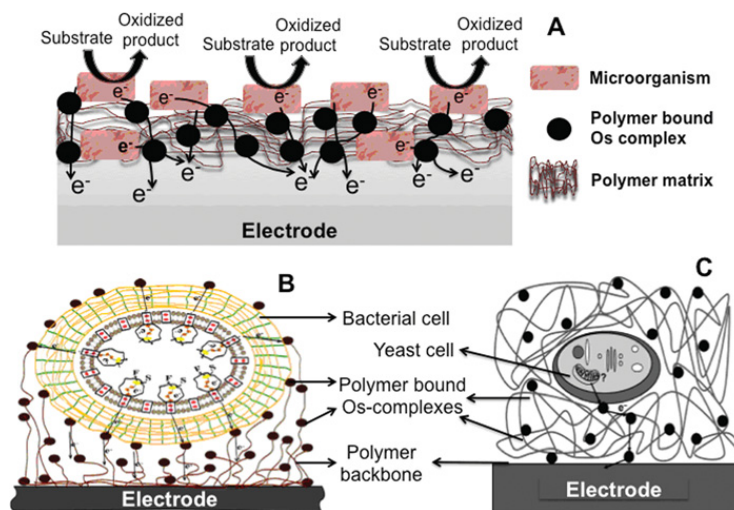
sensor development by excluding the need for soluble mediators, while providing a whole-cell biosensor system for ethanol, sodium azide and ampicillin with long-term stability. Lately, we have wired the metabolically versatile purple bacterium *Rhodobacter capsulatus* (wild-type and capsule-lacking strain) with system III to examine the applicability to BFCs and photobioelectrochemical devices [44]. The wild-type cells embedded in the osmium polymer matrix showed a greater ability to produce a significant and stable current due to succinate oxidation, compared with the capsule-lacking strain, demonstrating that the bacterial lipopolysaccharide improves the stability of the redox polymer matrix layer on the electrode.

The idea of employing yeasts as a substitute to bacteria in BESs is surfacing, since they are robust and generally non-pathogenic. With regard to their capability to metabolize a wide range of substrates and high growth rates, Shkil et al. [45] reported the electrochemical communication of *Hansenula polymorpha* with a graphite electrode, by wiring with osmium redox systems V, VI and VII. Here, genetically modified yeast cells that overexpress Fcb2 (flavocytochrome *b*<sub>2</sub>) generated more significant current with the aid of these osmium redox systems compared with that observed for the wild-type cells, highlighting that a plasma membrane redox system (Fcb2) is crucial for ET. Rawson et al. [46] recently examined ET from *Saccharomyces cerevisiae* on carbon electrodes that had been modified to introduce an osmium redox system (system IV) [46]. In this case, a stable surface-confined thin layer of osmium complex was introduced to a smooth electrode surface to facilitate ET directly from the external surface of the cell wall to the redox system, opening up queries on the capability of yeasts to 'shed' electrons to external acceptors. All of these reports highlighted that the conductive properties of osmium redox complexes promote a good electrochemical communication between electron-offering systems in the microbes and the electrode (as illustrated in Figure 2). However, the mechanisms of electron shuttling from the microbial cells to electrode via osmium polymers have not yet been thoroughly investigated and are still unclear. Predominantly, the electrical wiring of micro-organisms with electrodes is proposed to be due to the strong electrostatic interactions between the negatively charged bacterial cells and the positively charged osmium complexes bound to the polymer matrix at electrodes (Figure 2A). The close contact of the osmium-bound complexes to the cell wall or cell membrane of microbes and immobilization of the microbial cells inside the polymer matrix (Figures 2B and 2C) for electron shuttling to the electrode are proposed to be essential for efficient electrochemical communication.

In summary, studies of interactions between osmium redox systems and micro-organisms open new possibilities for basic bioelectrochemical studies, for reagentless biosensing and perhaps for the construction of more robust and improved performance MFCs. On the basis of published reports, we anticipate that the use of osmium systems (or similar redox polymers) as electron shuttles can enable the possibility of exploration of a wide range of microbial catalysts

**Figure 2** | Proposed schemes for EET from micro-organisms to electrode via osmium redox polymers

The ET occurs via sequential electrical conduit starting from the microbial cell to external osmium redox centres embedded in the polymer backbone and finally towards the electrode surface (A). Based on [44]. (B and C) Exemplary schemes that show electrical wiring of Gram-positive bacterial cell [43] and yeast cell [45] respectively to the electrode via osmium complexes.



(in particular the non-exoelectrogens) for applications as both bioanodes and biocathodes in BESs. With further investigation, we assume that the use of osmium-system-modified electrodes may simplify the design and the operational use of microbial biosensors, particularly for on-site applications. For such applications, the long-term stability of films of these systems on electrodes is among the major concerns. In addition, the relative amount of osmium complex within the system used to modify electrodes is a crucial aspect, as any excess amount might hamper the transfer of electrons from the microbes to the osmium centres. Furthermore, the introduction of cross-linkers such as poly(ethylene glycol) diglycidyl ether or methods to anchor the osmium systems to pre-treated electrodes might help to overcome stability concerns [35,46]. We have recently explored the electrode surface modification with osmium polymer and observed a boost in current generation with the well-known exoelectrogen *S. oneidensis* MR-1 at graphite electrodes using osmium system III [47]. Several advantages associated with these systems, such as ease of immobilization, high synthetic flexibility, excellent redox conductivity, possibility of forming multilayer scaffolds and strong electrostatic interactions with microbial cell surfaces, makes their use promising and opens a new horizon in microbial BES research.

## Funding

We are grateful to the European Commission [‘Chebana’ grant number FP7-PEOPLE-2010-ITN-264772], the Swedish Research

Council [grant numbers 2010-5031 and 2010-2013] and a Science Foundation Ireland Charles Parsons Energy Research Award for financial support.

## References

- Potter, M.C. (1911) Electrical effects accompanying the decomposition of organic compounds. Proc. R. Soc. London Ser. B **84**, 260–276
- Cohen, B. (1931) The bacterial culture as an electrical half-cell. J. Bacteriol. **21**, 18–19
- Bennetto, P.H. (1987) Microbes come to power. New Sci. **114**, 36–40
- Schröder, U. (2011) Discover the possibilities: microbial bioelectrochemical systems and the revival of a 100-year-old discovery. J. Solid State Electr. **15**, 1481–1486
- Rabaey, K. and Rozendal, R.A. (2010) Microbial electrosynthesis: revisiting the electrical route for microbial production. Nat. Rev. Microbiol. **8**, 706–716
- Su, L., Jia, W., Hou, C. and Lei, Y. (2011) Microbial biosensors: a review. Biosens. Bioelectron. **26**, 1788–1799
- Schröder, U. (2007) Anodic electron transfer mechanisms in microbial fuel cells and their energy efficiency. Phys. Chem. Chem. Phys. **9**, 2619–2629
- Rabaey, K. and Verstraete, W. (2005) Microbial fuel cells: novel biotechnology for energy generation. Trends Biotechnol. **23**, 291–298
- Rabaey, K., Angenent, L., Schröder, U. and Keller, J. (eds) (2010) Bioelectrochemical Systems: from Extracellular Electron Transfer to Biotechnological Application, IWA Publishing, London
- Lovley, D.R. and Nevin, K.P. (2011) A shift in the current: new applications and concepts for microbe–electrode electron exchange. Curr. Opin. Biotechnol. **22**, 441–448
- Busalmen, J.P., Esteve-Núñez, A., Berna, A. and Feliu, J.M. (2008) C-type cytochromes wire electricity-producing bacteria to electrodes. Angew. Chem. Int. Ed. **47**, 4874–4877
- Bond, D.R. and Lovley, D.R. (2003) Electricity production by *Geobacter sulfurreducens* attached to electrodes. Appl. Environ. Microbiol. **69**, 1548–1555

- 13 Gorby, Y.A., Yanina, S., McLean, J.S., Rosso, K.M., Moyles, D., Dohnalkova, A., Beveridge, T.J., Chang, I.S., Kim, B.H., Kim, K.S. et al. (2006) Electrically conductive bacterial nanowires produced by *Shewanella oneidensis* strain MR-1 and other microorganisms. *Proc. Natl. Acad. Sci. U.S.A.* **103**, 11358–11363
- 14 Richter, H., McCarthy, K., Nevin, K.P., Johnson, J.P., Rotello, V.M. and Lovley, D.R. (2008) Electricity generation by *Geobacter sulfurreducens* attached to gold electrodes. *Langmuir* **24**, 4376–4379
- 15 Reguera, G., McCarthy, K.D., Mehta, T., Nicoll, J.S., Tuominen, M.T. and Lovley, D.R. (2005) Extracellular electron transfer via microbial nanowires. *Nature* **435**, 1098–1101
- 16 Kim, H.J., Park, H.S., Hyun, M.S., Chang, I.S., Kim, M. and Kim, B.H. (2002) A mediator-less microbial fuel cell using a metal reducing bacterium, *Shewanella putrefaciens*. *Enzyme Microb. Technol.* **30**, 145–152
- 17 Tender, L.M., Reimers, C.E., Stecher, III, H.A., Holmes, D.E., Bond, D.R., Lowy, D.A., Pilobello, K., Fertig, S.J. and Lovley, D.R. (2002) Harnessing microbially generated power on the seafloor. *Nat. Biotechnol.* **20**, 821–825
- 18 Chaudhuri, S.K. and Lovley, D.R. (2003) Electricity generation by direct oxidation of glucose in mediatorless microbial fuel cells. *Nat. Biotechnol.* **21**, 1229–1232
- 19 Bond, D.R., Holmes, D.E., Tender, L.M. and Lovley, D.R. (2002) Electrode-reducing microorganisms that harvest energy from marine sediments. *Science* **295**, 483–485
- 20 Reguera, G., Nevin, K.P., Nicoll, J.S., Covalla, S.F., Woodard, T.L. and Lovley, D.R. (2006) Biofilm and nanowire production leads to increased current in *Geobacter sulfurreducens* fuel cells. *Appl. Environ. Microbiol.* **72**, 7345–7348
- 21 Pant, D., Van Bogaert, G., Diels, L. and Vanbroekhoven, K. (2010) A review of the substrates used in microbial fuel cells (MFCs) for sustainable energy production. *Bioresour. Technol.* **101**, 1533–1543
- 22 Rosenbaum, M., Aulenta, F., Villano, M. and Angenent, L.T. (2011) Cathodes as electron donors for microbial metabolism: which extracellular electron transfer mechanisms are involved? *Bioresour. Technol.* **102**, 324–333
- 23 Qiao, Y., Bao, S.-J. and Li, C.M. (2010) Electrocatalysis in microbial fuel cells: from electrode material to direct electrochemistry. *Energy Environ. Sci.* **3**, 544–553
- 24 Degani, Y. and Heller, A. (1987) Direct electrical communication between chemically modified enzymes and metal electrodes. 1. Electron transfer from glucose oxidase to metal electrodes via electron relays, bound covalently to the enzyme. *J. Phys. Chem.* **91**, 1285–1289
- 25 Heller, A. (1990) Electrical wiring of redox enzymes. *Acc. Chem. Res.* **23**, 128–134
- 26 Heller, A. (1992) Electrical connection of enzyme redox centers to electrodes. *J. Phys. Chem.* **96**, 3579–3587
- 27 Karan, H.I. (2005) Enzyme biosensors containing polymeric electron transfer systems. In *Biosensors and Modern Biospecific Analytical Techniques* (Gorton, L., ed.), pp. 131–178, Elsevier, Amsterdam
- 28 Guschin, D., Castillo, J., Dimcheva, N. and Schuhmann, W. (2010) Redox electrodeposition polymers: adaptation of the redox potential of polymer-bound Os complexes for bioanalytical applications. *Anal. Bioanal. Chem.* **398**, 1661–1673
- 29 Timur, S., Yigzaw, Y. and Gorton, L. (2006) Electrical wiring of pyranose oxidase with osmium redox polymers. *Sens. Actuators B* **113**, 684–691
- 30 Mano, N., Mao, F. and Heller, A. (2002) A miniature biofuel cell operating in a physiological buffer. *J. Am. Chem. Soc.* **124**, 12962–12963
- 31 Kavanagh, P., Boland, S., Jenkins, P. and Leech, D. (2009) Performance of a glucose/O<sub>2</sub> enzymatic biofuel cell containing a mediated *Melanocarpus albomyces* laccase cathode in a physiological buffer. *Fuel Cells* **9**, 79–84
- 32 Barriere, F., Kavanagh, P. and Leech, D. (2006) A laccase–glucose oxidase biofuel cell prototype operating in a physiological buffer. *Electrochim. Acta* **51**, 5187–5192
- 33 Zafar, M.N., Wang, X., Sygmund, C., Ludwig, R., Leech, D. and Gorton, L. (2012) Electron transfer studies with a new FAD-dependent glucose dehydrogenase and osmium polymers of different redox potentials. *Anal. Chem.* **84**, 334–341
- 34 Mao, F., Mano, N. and Heller, A. (2003) Long tethers binding redox centers to polymer backbones enhance electron transport in enzyme “wiring” hydrogels. *J. Am. Chem. Soc.* **125**, 4951–4957
- 35 Rawson, F.J., Garrett, D.J., Leech, D., Downard, A.J. and Baronian, K.H.R. (2011) Electron transfer from *Proteus vulgaris* to a covalently assembled, single walled carbon nanotube electrode functionalised with osmium bipyridine complex: application to a whole cell biosensor. *Biosens. Bioelectron.* **26**, 2383–2389
- 36 Degani, Y. and Heller, A. (1989) Electrical communication between redox centers of glucose oxidase and electrodes via electrostatically and covalently bound redox polymers. *J. Am. Chem. Soc.* **111**, 2357–2358
- 37 Heller, A. (2006) Electron-conducting redox hydrogels: design, characteristics and synthesis. *Curr. Opin. Chem. Biol.* **10**, 664–672
- 38 Boland, S. (2008) Integrating Enzymes, Electron Transfer Mediators and Mesostuctured Surfaces to Provide Bio-electroresponsive Systems. Ph.D. Thesis, National University of Ireland Galway, Galway, Ireland
- 39 Vostiar, I., Ferapontova, E.E. and Gorton, L. (2004) Electrical “wiring” of viable *Gluconobacter oxydans* cells with a flexible osmium-redox polyelectrolyte. *Electrochem. Commun.* **6**, 621–626
- 40 Timur, S., Haghghi, B., Tkac, J., Pazarlioglu, N., Telefoncu, A. and Gorton, L. (2007) Electrical wiring of *Pseudomonas putida* and *Pseudomonas fluorescens* with osmium redox polymers. *Bioelectrochemistry* **71**, 38–45
- 41 Timur, S., Anik, U., Odaci, D. and Gorton, L. (2007) Development of a microbial biosensor based on carbon nanotube (CNT) modified electrodes. *Electrochem. Commun.* **9**, 1810–1815
- 42 Alferov, S., Coman, V., Gustavsson, T., Reshetilov, A., von Wachenfeldt, C., Hägerhäll, C. and Gorton, L. (2009) Electrical communication of cytochrome enriched *Escherichia coli* JM109 cells with graphite electrodes. *Electrochim. Acta* **54**, 4979–4984
- 43 Coman, V., Gustavsson, T., Finkelsteinas, A., von Wachenfeldt, C., Hägerhäll, C. and Gorton, L. (2009) Electrical wiring of live, metabolically enhanced *Bacillus subtilis* cells with flexible osmium-redox polymers. *J. Am. Chem. Soc.* **131**, 16171–16176
- 44 Hasan, K., Patil, S.A., Görecki, K., Leech, D., Hägerhäll, C. and Gorton, L. (2012) Electrochemical communication between heterotrophically grown *Rhodobacter capsulatus* with electrodes mediated by an osmium redox polymer. *Bioelectrochemistry*, doi:10.1016/j.bioelechem.2012.05.004
- 45 Shkil, H., Schulte, A., Guschin, D.A. and Schuhmann, W. (2011) Electron transfer between genetically modified *Hansenula polymorpha* yeast cells and electrode surfaces via Os-complex modified redox polymers. *ChemPhysChem* **12**, 806–813
- 46 Rawson, F.J., Gross, A.J., Garrett, D.J., Downard, A.J. and Baronian, K.H.R. (2012) Mediated electrochemical detection of electron transfer from the outer surface of the cell wall of *Saccharomyces cerevisiae*. *Electrochem. Commun.* **15**, 85–87
- 47 Patil, S.A., Hasan, K., Leech, D., Hägerhäll, C. and Gorton, L. (2012) Improved microbial electrocatalysis with osmium polymer modified electrodes. *Chem. Commun.* **48**, 10183–10185

Received 2 May 2012  
doi:10.1042/BSI20120120

# Paper V





DOI: 10.1002/celec.201300148

EAB

# Photoelectrochemical Communication between Thylakoid Membranes and Gold Electrodes through Different Quinone Derivatives

Kamrul Hasan,<sup>[a]</sup> Yusuf Dilgin,<sup>[b]</sup> Sinan Cem Emek,<sup>[a]</sup> Mojtaba Tavahodi,<sup>[c]</sup> Hans-Erik Åkerlund,<sup>[a]</sup> Per-Åke Albertsson,<sup>[a]</sup> and Lo Gorton<sup>\*[a]</sup>

Photosynthesis is a sustainable process for the conversion of light energy into chemical energy. Thylakoids in energy-transducing photosynthetic membranes are unique in biological membranes because of their distinguished structure and composition. The quantum trapping efficiency of thylakoid membranes is appealing in photobioelectrochemical research. In this study, thylakoid membranes extracted from spinach are shown to communicate with a gold-nanoparticle-modified solid gold electrode (AuNP–Au) through a series of quinone derivatives. Among these, *para*-benzoquinone (PBQ) is found

to be the best soluble electron-transfer mediator, generating the highest photocurrent of approximately  $130 \mu\text{A cm}^{-2}$  from water oxidation under illumination. In addition, the photocurrent density is investigated as a function of applied potential, the effect of light intensity, quinone concentration, and amount of thylakoid membrane. Finally, the source of photocurrent is confirmed by using 3-(3,4-dichlorophenyl)-1,1-dimethylurea (known by its trade name, Diuron), an inhibitor of photosystem II, which decreases the total photocurrent by 50%.

## 1. Introduction

The viable production of solar fuels through photochemical energy conversion is a promising resource that can offer long-standing global energy. Nature has optimized photosynthesis, its own solar energy-conversion system, to a finely tuned molecular mechanism.<sup>[1]</sup> Photosynthesis is the sustainable, efficient, and complex process that converts light energy into chemical energy.<sup>[2]</sup> Thylakoid membranes, photosynthetic subcellular organelles, are found in cyanobacteria and in plant chloroplasts. Thylakoids contain the photosynthetic apparatus that is composed of two photosystems, photosystem I (PS I) and photosystem II (PS II), and other necessary components, such as enzymes and cofactors, as outlined in Scheme 1. The photosynthetic reaction starts from the photoexcitation of PS II by light, which results in the oxidation of water into  $\text{O}_2$ . The electrons produced from this reaction are transferred through a series of electron carriers, for example plastoquinone (PQ), cytochrome  $b_6/f$ , and plastocyanin (PC), to PS I, in which they are excited once more.<sup>[3]</sup> Excitation of PS I results in the transfer of the electrons, causes them to reduce the terminal elec-

tron-acceptor ferredoxin (Fd), and subsequently produces reduced nicotinamide adenine dinucleotide phosphate (NADPH), which is used in the Calvin cycle for fixation of  $\text{CO}_2$  to produce sugars.<sup>[4]</sup> The proton gradient, resulting from the photosynthetic reactions, is used by adenosine triphosphate (ATP) synthase to produce ATP, which is the ultimate cellular energy currency.<sup>[3]</sup> The quantum yield in the thylakoid membrane is nearly 100%, which makes it very attractive for photobioelectrochemical systems.<sup>[5]</sup>

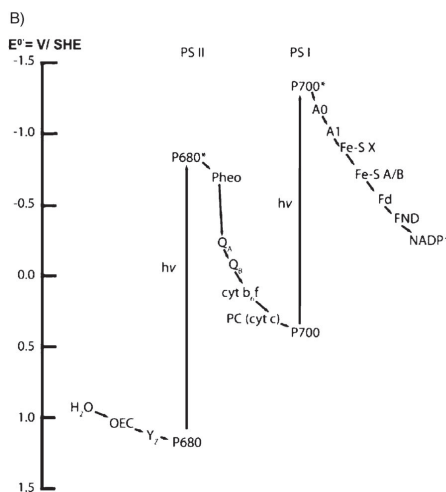
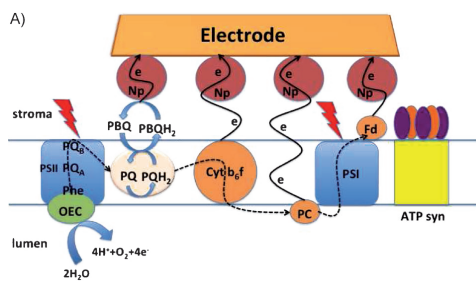
In recent years, extensive research has been focused on photoelectrochemical and artificial solar cells imitating photosynthesis for energy production.<sup>[6–10]</sup> Isolated photosynthetic reaction centers, especially PS I, have been wired to electrodes to produce hydrogen as a feasible energy source.<sup>[1, 11–13]</sup> Isolated PS I has previously been wired to a gold electrode by using an osmium-containing redox polymer and methyl viologen as a final electron acceptor, which generated a photocurrent density of  $29 \mu\text{A cm}^{-2}$ .<sup>[14]</sup> To take advantage of natural photosynthesis, several research groups have devoted their efforts on photobioelectrochemical systems that are based on chloroplasts,<sup>[15]</sup> thylakoid membranes,<sup>[16–19]</sup> photosynthetic reaction centers,<sup>[2, 20–27]</sup> and bacterial cells.<sup>[28–31]</sup> However, low electron-transfer efficiency from the photosynthetic machinery to the electrode has confined the performance of these types of systems. Isolated photosynthetic components have some benefits over the entire cell/membrane. For instance, they do not have respiration competing with the photosynthetic electron-transfer pathways and they do not require any nutrients for their growth to continue. However, they suffer from low competence because of their inadequate stability on an electrode surface. It might be that proper immobilization and good electri-

[a] K. Hasan, Dr. S. C. Emek, Prof. H.-E. Åkerlund, Prof. P.-Å. Albertsson, Prof. L. Gorton  
Biochemistry and Structural Biology, Lund University  
P.O. Box 124, SE-22100, Lund (Sweden)  
E-mail: Lo.Gorton@biochemistry.lu.se

[b] Prof. Y. Dilgin  
Science & Art Faculty, Department of Chemistry  
Çanakkale Onsekiz Mart University, Çanakkale (Turkey)

[c] M. Tavahodi  
Department of Chemistry  
Institute of Advanced Studies in Basic Sciences, Zanjan (Iran)

Supporting Information for this article is available on the WWW under <http://dx.doi.org/10.1002/celec.201300148>.



**Scheme 1.** A) Possible electron transfer from thylakoid membranes (suspended in solution) to the AuNP–Au via different proteins, for example PQ, cytochrome  $b_6f$ , plactocyanin (PC), and Fd. For simplification, other components of the thylakoid membranes are not shown. PS I and PS II refer to the photosynthetic reaction centers. B) The redox-potential scale of the different components of thylakoids is shown in V versus SHE. Key components:  $H_2O$ , oxygen evolution complex (OEC), tyrosine residue (Yz), P680, P680\*, pheo,  $PQ_A$ ,  $PQ_B$ ,  $b_6f$ , PC, P700, P700\*, chlorophyll (A0), pyloquinone (A1), the iron and iron–sulfur centers (Fe-SX and Fe-S A/B), Fd, FND NADP reductase (FND), and  $NADP^+$ .<sup>[51]</sup>

cal communication between the isolated photosynthetic reaction center and the electrode is constrained.<sup>[32]</sup> To harvest light energy, it is thermodynamically beneficial to collect electrons when the photosynthetic component is in its high-energy state, such as photoinduced PS II.<sup>[33,34]</sup> Furthermore, it is advantageous to use a photosynthetic system that is able to use water as the electron donor such as PS II instead of PS I, in which an additional electron donor is required. Attempts have been made to immobilize the PS II reaction center on the electrode surface through cytochromes<sup>[25]</sup> and nickel nitrilotriacetic acid<sup>[35]</sup> as cross linkers. All of these different methods use gold materials as the electrode, together with various immobilization procedures. PS II isolated from a thermophilic cyanobacterium has been modified on mesoporous indium–tin oxide

(ITO), and a small photocurrent density ( $1.6 \mu A cm^{-2}$ ) was documented in the absence of any redox mediator, whereas an enhanced photocurrent density was obtained in the presence of a soluble redox mediator, for example 1,4 naphthoquinone sulfonate ( $12 \mu A cm^{-2}$ ) or 2,6-dichloro-1,4-benzoquinone ( $22 \mu A cm^{-2}$ ).<sup>[21]</sup> A PS II-modified photoanode and a bilirubin oxidase/carbon-nanotube-functionalized cathode were used to construct a photobiofuel cell, which generated electricity upon illumination in the absence of any artificial mediator.<sup>[2]</sup>

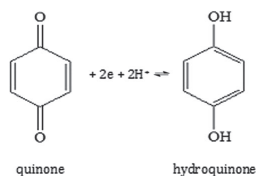
Photosynthetic membranes/organelles possess several advantages over isolated reaction centers for light harvesting applications such as long-term stability of the individual proteins embedded inside the lipid bilayer, relatively straightforward immobilization methods, and various electron-transfer conduits.<sup>[36]</sup> Therefore, the thylakoid membrane can be used as a potential candidate for photobioelectrochemical systems that can offer high stability for energy conversion and fuel production. In a study by Calkins et al.,<sup>[16]</sup> a photocurrent density as high as  $68 \mu A cm^{-2}$  was obtained by immobilizing spinach thylakoids onto multiwalled carbon nanotubes (MWCNT). Through diverse conduits of electron transfer from the thylakoids, a steady-state current density of  $38 \mu A cm^{-2}$  was documented, which is quite remarkable.<sup>[16]</sup>

In Minteer's research group, significant efforts<sup>[18]</sup> have been made to photochemically wire thylakoids, and they have shown that the thylakoids are capable of direct electron transfer (DET) with the electrode. Although it is a great effort to make this direct electrical communication, which is a desirable way of wiring in bioelectrochemistry, it suffers from a low photocurrent density response (ca.  $0.44 \mu A cm^{-2}$ ). This photocurrent density could be improved by combining a thylakoid bioanode with a laccase biocathode to construct a biosolar cell, which generated a current density of  $15.0 \mu A cm^{-2}$ .<sup>[18]</sup>

In this study, we investigate the photoelectrochemical potential of isolated thylakoid membranes kept in aqueous solution.<sup>[37]</sup> It has been reported that native thylakoids suspended in aqueous solution are more competent than their immobilized counterpart in obtaining higher anodic photocurrents.<sup>[38]</sup> Herein, a gold electrode surface is used as the working electrode, which is further modified with gold nanoparticles (AuNP–Au) to increase the surface area as well as to enhance the electron-transfer efficiency. Different quinone derivatives, varying in their chemical structures as well as in redox potentials, are studied to improve the photocurrent. In addition, other parameters are also investigated for further improvements in the photocurrent, for example light intensity, chlorophyll concentration of the thylakoids in the electrolyte surrounding the electrode, concentration of quinone derivatives, and the applied potential of the electrode. The origin of the photocurrent is confirmed by using a specific inhibitor for PS II, 3-(3,4-dichlorophenyl)-1,1-dimethylurea (known by the trade name, Diuron), which blocks the electron transfer between plastoquinone A ( $PQ_A$ ) and plastoquinone B ( $PQ_B$ ), see Scheme 1.

## 2. Results and Discussion

Initially, cyclic voltammograms (CVs) of all of the *para*-benzoquinone derivatives at 0.6 mM suspended in phosphate buffer solution (PBS) were recorded in light-off and light-on conditions. *para*-Benzoquinone (PBQ) in aqueous buffered medium shows a single ( $2e^-/2H^+$ ) reaction system,<sup>[45]</sup> which is typical of the redox couple quinone  $\leftrightarrow$  hydroquinone, as shown in Scheme 2.



**Scheme 2.** The reversible redox reaction of quinone and hydroquinone in aqueous buffer.

In Figure 1, the standard CV for PBQ (—) exhibits an anodic peak at about +141 mV, at which PBQH<sub>2</sub> is oxidized to PBQ. During the reverse potential scan; a cathodic peak appears at about +58 mV, which corresponds to the reduction of PBQ back to PBQH<sub>2</sub>. The observed midpoint potential ( $E_{1/2}$ ) of 100 mV for the quinone redox couple (PBQ/PBQH<sub>2</sub>) is close to its theoretical value.<sup>[46]</sup> The difference between the anodic and cathodic peak potentials ( $\Delta E_p = E_{pa} - E_{pc}$ , in which  $E_{pa}$  and  $E_{pc}$  represent the anodic and cathodic peak potentials, respectively) is 83 mV, a value that is higher than that expected for a dissolved reversible system.<sup>[47]</sup> In addition, the anodic ( $I_{pa}$ ) and cathodic ( $I_{pc}$ ) peak current ratio ( $I_{pa}/I_{pc}$ ) is 0.80. This suggests that the electrochemical behavior of PBQ is a quasireversible process.

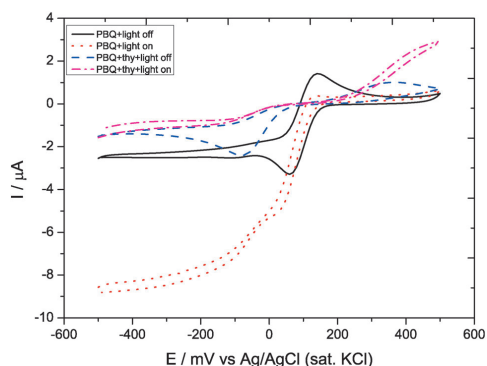


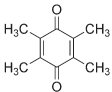
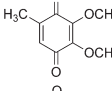
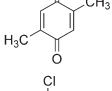
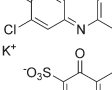
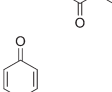
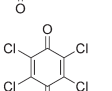
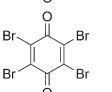
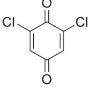
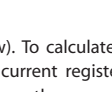
**Figure 1.** CVs of PBQ in the absence of thylakoid membranes (light-off — and light-on ·····) and in the presence of thylakoid membranes (light-off --- and light-on -·-·-). Experimental condition: PBS buffer at pH 7.0, 0.6 mM PBQ, 60  $\mu\text{g mL}^{-1}$  thylakoid (chlorophyll), scan rate: 5  $\text{mV s}^{-1}$ .

When the electrode surface was illuminated with a 150 W quartz halogen illuminator of  $680 \text{ mW cm}^{-2}$  (Figure 1 ·····), a pronounced increase in the cathodic peak current was observed, whereas the anodic peak current decreased. These phenomena can be attributed to the photoelectrochemical reduction of O<sub>2</sub> to H<sub>2</sub>O<sub>2</sub>, catalyzed by PBQH<sub>2</sub>,<sup>[48]</sup> in combination with the direct reduction of O<sub>2</sub> into water, respectively. An aliquot of thylakoid solution with a chlorophyll concentration corresponding to 60  $\mu\text{g mL}^{-1}$  was added to the PBS buffer in the presence of 0.6 mM PBQ to investigate the photoelectrochemical response from the thylakoids (Figure 1 ---). The anodic and cathodic peak potentials of PBQ shifted towards more positive and more negative directions, respectively, in the presence of thylakoids (Figure 1 ---) when the light was turned off. This can be attributed to a large and complex molecule, such as the thylakoid membrane, restricting the electron-transfer rate between the PBQ redox couple and the electrode. However, when the electrode surface was illuminated in the presence of both the thylakoid and PBQ, a greater anodic current was generated (Figure 1 -·-·-). We assume that the photocurrent is the consequence of water oxidation by the photosynthetic reaction centers embedded in the thylakoid membranes under illumination. The electron-transfer conduit of the thylakoid membrane (Scheme 1) can explain the origin of the photocurrent. In brief, PS II is excited at a wavelength of 680 nm, abstracts electrons from water, and raises the energy of the electrons to a sufficiently negative potential for reducing PQ to plastoquinol (PQH<sub>2</sub>) via pheophytin (pheo), PQ<sub>A</sub>, and PQ<sub>B</sub>. PQH<sub>2</sub> acts as a reductant for the cytochrome b<sub>6</sub>f complex that passes the electrons further to PC in the luminal side of the thylakoid membrane. PC then transfers the electrons to PS I, which is excited at 700 nm and reduces Fd in a one-electron-transfer reaction.<sup>[49]</sup>

A simplified electron-transfer conduit from the thylakoid membrane to the AuNP–Au electrode is shown in Scheme 1, in which it is suggested that photoexcited electrons from water oxidation are transferred via PQ, cytochrome, PC, and Fd. PBQ resembles PQ and is an appropriate molecule for electron transfer. PQH<sub>2</sub> is known to act as an electron donor for PBQ<sup>[50]</sup> and can, in turn, transfer these electrons to the high-potential-poised AuNP–Au electrode (Scheme 1). PBQ can also be reduced as the electrons are transferred from PQ<sub>A</sub> to PQ<sub>B</sub> (not shown in Scheme 1 for simplification).<sup>[50]</sup> The lower redox potentials of PQ<sub>A</sub>, PQ<sub>B</sub>, cytochrome b<sub>6</sub>f, and Fd in the thylakoid membrane also support their ability to reduce external electron acceptors.<sup>[51]</sup>

It can be assumed that PBQ can efficiently mediate electron transfer from the thylakoid membranes suspended in the PBS buffer to the AuNP–Au electrode (Figure 1). All of the quinone derivatives used in this work are detailed in Table 1, together with their individual chemical structures, observed  $E_{1/2}$  values, and obtained photocurrent densities ( $I$ ); in addition, the relationships of the generated photocurrent density with the different quinone derivatives are presented in Figure 2. It is important to note that the photocurrent densities given in Table 1 and Figure 2 were measured from chronoamperometry (CA) experiment in PBS buffer, and represent the optimized

**Table 1.** Chemical structure of different quinone molecules, their observed midpoint potential ( $E_{1/2}$ ), and obtained photocurrent density ( $J$ ). Experimental condition: PBS buffer at pH 7.0,  $60 \mu\text{g mL}^{-1}$  thylakoid chlorophyll,  $0.6 \text{ mM}$  quinone, light intensity =  $680 \text{ mW cm}^{-2}$ .

Quinone	Structure	$E_{1/2}$ [mV]	$J$ [ $\mu\text{A cm}^{-2}$ ]
duroquinone		-145.0	$7.0 \pm 0.1$
2,3-DMO-5-M-PBQ		-20	$31 \pm 2.16$
2,5-DM-PBQ		-15.0	$13.27 \pm 0.2$
DCIP		+23.0	$4.47 \pm 0.40$
naphthoquinone		+24.0	$20.21 \pm 0.71$
PBQ		+100	$127 \pm 4.43$
tetrachloro-PBQ		+131	$30 \pm 0.88$
tetrabromo-PBQ		+135	$23.18 \pm 0.34$
DCBQ		+150	$122 \pm 9.13$

values (see below). To calculate the actual photocurrent density, the response current registered during the light-off period was subtracted from the current registered during the light-on measurement.

Both the chemical structures as well as the redox potentials of the investigated quinones affect their efficiency to transfer charge to the electrode. For example, a methyl and a chloride group are electron-donating substituents for the quinone aromatic ring, whereas the methoxy group is an electron-accepting substituent. Satoh et al. have obtained similar results with isolated PS II,<sup>[50]</sup> and it was reported that methyl-substituted benzoquinone has a very low affinity for the  $\text{PQ}_8$  site, whereas the chlorine-substituted version has a lower affinity for the  $\text{PQ}_8$  site. Duroquinone generates very little or almost no affinity for the  $\text{PQ}_8$  site, but receives electrons from endogenous  $\text{PQH}_2$

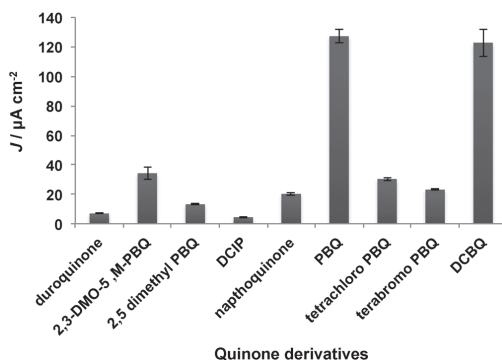


**Figure 2.** The relationship of photocurrent obtained with different quinone derivatives. Experimental condition: PBS buffer at pH 7.0,  $0.6 \text{ mM}$  PBQ,  $60 \mu\text{g mL}^{-1}$  thylakoid (chlorophyll), applied potential =  $400 \text{ mV}$ , light intensity =  $680 \text{ mW cm}^{-2}$ .

and generates a current density of only  $7.0 \pm 0.1 \mu\text{A cm}^{-2}$ . PBQ and 2,6-dichloro-PBQ, with higher redox potentials, generate similar photocurrent densities of around  $125 \mu\text{A cm}^{-2}$ . The halogenated quinones (tetrachloro-PBQ, tetrabromo-PBQ) are supposed to have a very high affinity for the  $\text{PQ}_8$  site, but, in this case, they are incompetent and do not generate high photocurrent densities because of their low solubility in the PBS buffer. 2,6-Dichloroindophenol (DCIP) and 1,2-naphthoquinone-4-sulfonic acid potassium salt (naphthoquinone), with lower redox potentials and extended aromatic ring systems, also have limited solubility, resulting in the generation of a lower photocurrent density. From the results shown in Table 1, the use of PBQ results in the highest photocurrent densities, whereas DCIP results in the lowest response; this could be attributed to their structure, solubility, and their redox potential. As a conclusion, PBQ, with the simplest structure and with a comparatively high observed redox potential ( $E_{1/2} = 100 \text{ mV}$ ), results in the highest photocurrent density and was, thus, selected for further studies as the best soluble mediator. The rest of the work, reported on below, was conducted with this mediator.

To obtain the maximum photocurrent, the effects of other parameters, including applied potential, concentration of PBQ, concentration of chlorophyll (thylakoid membrane), and light intensity, were investigated by recording CA curves. To explore the variation in photocurrent density generation as a function of the applied potential, CA measurements were recorded with various potentials applied to the electrode in the presence of PBQ only, thylakoid membrane only, and both PBQ and the thylakoid membrane together (Figure 3A). The effect of the applied potential on the photocurrent is graphically presented in Figure 3B (data extracted from Figure 3A).

As can be seen in Figures 3A and 3B, no photocurrent was observed in the presence of only the thylakoids between 0 and  $400 \text{ mV}$  (Figure 3A —). However, when applying a higher potential, a very marginal increase in the registered photocurrent was noticed. It is expected that any DET from

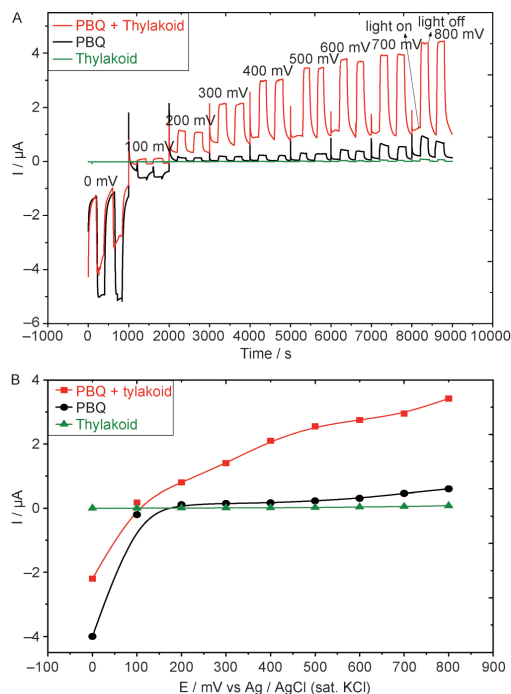


**Figure 3.** A) Photocurrent generation obtained in the presence of thylakoids only (—), PBQ only (—), and both of them together (—) at various applied potentials. The light-on and -off sign is indicated once to avoid complication, but is applicable in all other upward and downward states. For each potential, two replica of light-on/-off responses are shown. Experimental condition: PBS buffer at pH 7.0, 0.6 mM PBQ, 60  $\mu\text{g mL}^{-1}$  thylakoid (chlorophyll), applied potential = 400 mV, light intensity = 680  $\text{mW cm}^{-2}$ . B) The influence of the applied potential on the photocurrent response for thylakoid only (—), PBQ (—), and both of them together (—). Data extracted from Figure 3A.

the thylakoid membrane to the electrode surface would be constrained, owing to the deeply buried redox-active sites in this high molecular weight and complex thylakoid molecule; however, a very small photocurrent was found to be generated in a study by Ramussen et al.<sup>[18]</sup> The photocurrent generated through DET is insignificant when compared with the current obtained in the presence of PBQ, see below. In the presence of only PBQ (Figure 3A —), the formation of  $\text{H}_2\text{O}_2$  through  $\text{O}_2$  reduction was observed at a potential lower than 100 mV. At a higher potential, a faster conversion occurs between the redox couple of PBQ (Scheme 2). This behavior supports our results obtained from the CVs in the same potential region. However, the registered photocurrent at an even higher potential (> 300 mV) was slightly increased by the increased applied potential, because of an increased thermodynamic force required to oxidize  $\text{PBQH}_2$ . It could be attributed to light absorption by the PBQ molecules on the AuNP–Au electrode.<sup>[52]</sup>

A substantial photocurrent was observed in the presence of both the thylakoid and PBQ (Figure 3A —), and the generat-

ed photocurrent increased almost linearly with an increasing applied potential from 100 to 400 mV. The most likely reason for this linear behavior is thought to be because of the vast range of redox potentials involved in the participating photosynthetic components, see Scheme 1. When extrapolating the information given from ref. [51], the following redox potentials could be calculated at pH 7: +1.2 (P680), -0.85 (P680\*), +0.41 (P700), -1.32 (P700\*), -0.27 ( $\text{PQ}_\text{A}$ ), -0.1 ( $\text{PQ}_\text{B}$ ), +0.09 (cyt  $b_6/f$ ), and +0.31 (PC) V versus a standard hydrogen electrode (SHE), where P680 and P700 are the photosynthetic pigments of PS I and PS II, respectively, and \* refers to the respective excited state. At higher applied potentials, several redox components can participate in the electron-transfer event, whereas at a lower potential, only a few of them are able to be involved. Above 400 mV, the photocurrent does not increase linearly with any further increase in the applied potential. This is consistent with the redox potential of PBQ at pH 7 ( $E^\circ = 81$  mV versus a Ag/AgCl reference electrode saturated with KCl). At a higher potential, the PBQ relay units are retained in their oxidized state and, thus, the photoinduced electron transfer is accompanied by an immediate pumping of electrons from the relay units to the electrode. This vectorial electron transfer minimizes back electron-transfer reactions and leads to high photocurrents. At a potential less than 100 mV, the relay units are transformed into the reduced state that do not accept any electron transfer from the thylakoids.<sup>[2]</sup> As a result, 400 mV was selected as the optimum applied potential for further investigations.

To comprehend the effect of chlorophyll concentration in the thylakoid membrane on the photocurrent, CA experiments were recorded at various thylakoid concentrations in the presence of 0.6 mM PBQ (Figure 4A), and the results are exhibited in Figure 4B. The photocurrent increases with increasing thylakoid concentration until 120  $\mu\text{g mL}^{-1}$ . This result is expected and reasonable, because the thylakoid membrane is the source of photocurrent generation from the photoexcited oxidation of water. However, if the thylakoid membrane concentration is increased to more than 120  $\mu\text{g mL}^{-1}$ , then the photocurrent decreases drastically. We believe that very highly concentrated thylakoid membrane solutions prevent the illumination from reaching the working electrode surface, thus resulting in a considerably decreased photocurrent. We, therefore, considered that a chlorophyll concentration of the thylakoid membrane equal to 100  $\mu\text{g mL}^{-1}$  should be the optimized value.

It was also important to investigate how different concentrations of PBQ influenced the generation of the photocurrent. CA curves were recorded at various PBQ concentrations in the presence of the optimized concentration of thylakoid membrane (100  $\mu\text{g mL}^{-1}$ ) and the optimized applied potential of 400 mV was used (Figure 5A). The effect of different PBQ concentrations on the generated photocurrent is graphically displayed in Figure 5B. The photocurrent increases linearly with increasing PBQ concentrations until 0.6 mM and after this concentration, the photocurrent was found to be virtually stable, which is thought to be because the thylakoid membrane becomes saturated with PBQ at a concentration of 0.6 mM. When

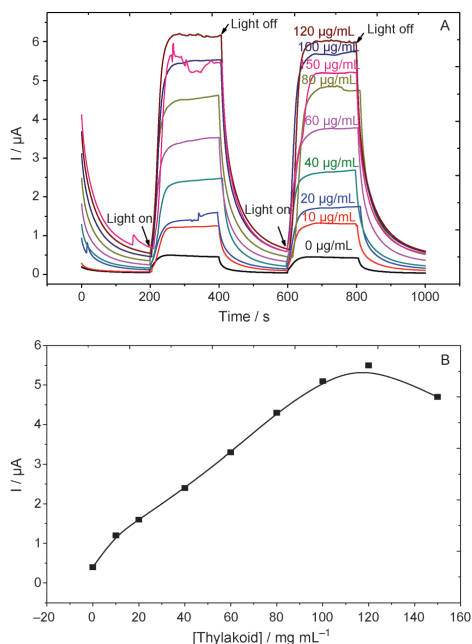


**Figure 4.** A) Relationship of photocurrent rise with thylakoid chlorophyll concentration. Experimental condition: PBS buffer at pH 7.0, 0.6 mM PBQ, applied potential = 400 mV, light intensity = 680 mW cm<sup>-2</sup>. B) The relationship of photocurrent with different thylakoid chlorophyll concentrations. Data extracted from Figure 4A.

the PBQ concentration is increased further, there are no more reducing-equivalents available to react with PBQ, and these extra PBQ molecules do not participate in electrochemical communication. Thus, the optimum PBQ concentration was selected at 0.6 mM.

The light intensity has a significant effect on the oxygenic photosynthesis of the thylakoid membrane,<sup>[53]</sup> but too high an intensity can potentially damage the photosynthetic apparatus, especially PS II.<sup>[54]</sup> Thus, it was imperative to investigate the influence of different light intensities on the generation of the photocurrent. For this purpose, CA curves were recorded at various light intensities of the 150 W halogen illuminator in the presence of the optimized chlorophyll concentration of the thylakoid membrane 100 μg mL<sup>-1</sup>, PBQ (0.6 mM) and an applied potential of +400 mV (Figure 6A). The effect of the light intensity on photocurrent generation is graphically shown in Figure 6B and, as can be realized from this figure, the photocurrent increases almost linearly with increasing light intensity. A similar relationship has been shown in a previous study, in which the thylakoid membrane was immobilized on MWCNTs.<sup>[16]</sup> Thus, the maximum light intensity of the 150 W light illuminator was fixed at 680 mW cm<sup>-2</sup> to obtain the highest possible response.

To obtain more information about the source of the generated photocurrent, one of the most widely used specific PS II in-

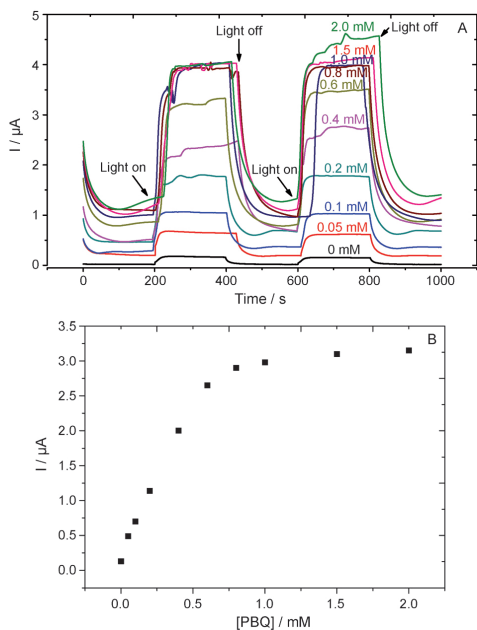


**Figure 5.** A) Correlation of photocurrent obtained from various PBQ concentrations. Experimental condition: PBS buffer at pH 7.0, 60 μg mL<sup>-1</sup> thylakoid (chlorophyll), applied potential = 400 mV, light intensity = 680 mW cm<sup>-2</sup>. B) Calibration curve of photocurrent responses with different PBQ concentrations. Data extracted from Figure 5A.

hibitors, Diuron, was used. There are two primary sites of herbicide action in the photosynthetic electron-transfer chain: the first one blocks electron transfer between the PQ<sub>B</sub> and PQ<sub>A</sub> of PS II and the other diverts the electron flow through PS I. In both cases, the herbicide encourages lipid peroxidation, which results in destruction of the membrane integrity, cellular disorganization, and phytotoxicity. The mechanism of the inhibition of PS II is known in more detail than the action of any other inhibitor.<sup>[55]</sup> It has been reported that Diuron, as a PS II inhibitor, reduces 50% of the photocurrent when added in the μM-concentration range.<sup>[56]</sup> Hence, 10 μM Diuron was added to the electrochemical cell in the presence of 10 μg mL<sup>-1</sup> thylakoids and 0.6 mM PBQ, resulting in a 50% inhibition of the total initial photocurrent (see the Supporting Information). This phenomenon was expected and reasonable, because Diuron binds with PQ<sub>B</sub> and restricts electron transfer between PQ<sub>A</sub> and PQ<sub>B</sub>.<sup>[53]</sup> This confirms that PS II is the major source of photocurrent generation.<sup>[16]</sup> But, the cause of the remaining photocurrent might be the result of electron-transfer leakage in the photosynthetic pathway, or it could be that electron transfer from the thylakoid membrane to the electrode is maintained by PQ<sub>A</sub>, which remains unaffected by Diuron.

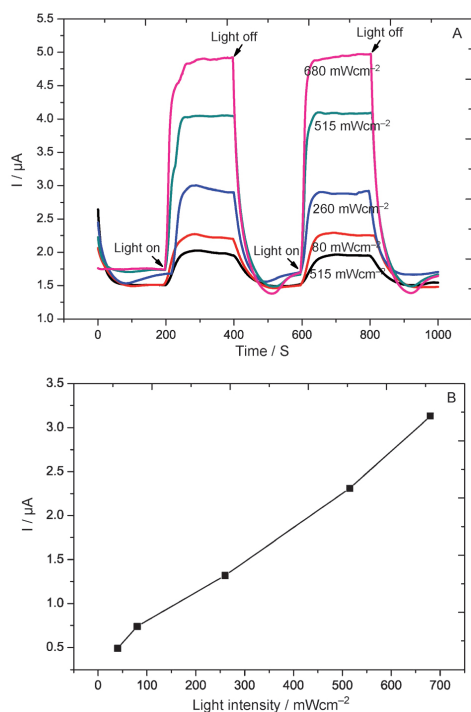


**Figure 6.** A) The effect of light intensity on photocurrent generation with various light intensities, for example 40, 80, 260, 515, and 680  $\text{mW cm}^{-2}$ . Experimental condition: PBS buffer at pH 7.0, 0.6 mM PBQ, 60  $\mu\text{g mL}^{-1}$  thylakoid (chlorophyll), applied potential = 400 mV. B) Graphical presentation of the linear relationship between light intensity and photocurrent. Data extracted from Figure 6A.

### 3. Conclusions

Thylakoid membranes were photoelectrochemically wired to AuNP–Au electrodes in the presence of a range of quinone derivatives in solution. It was observed that photocurrent generation depends on the chemical structure and redox potential of the quinone derivative used. Among these, PBQ, which has the simplest structure and the highest redox potential, was found to be the best soluble electron transfer mediator that generates the maximum photocurrent. The optimized concentration of PBQ was fixed at 0.6 mM for shuttling electrons that were generated from water oxidation under illumination. The potential applied to the working electrode had a significant influence, because the participating photosynthetic components for photocurrent generation exhibited a vast range in their redox potentials. Thus, the applied potential was optimized at 400 mV, which was sufficient to extract all the electrons generated in the photosynthetic electron-transfer pathway. As thylakoids were responsible for photoinduced water oxidation in these experiments, the chlorophyll concentration of thylakoid membrane was optimized to 100  $\mu\text{g mL}^{-1}$  for maximum photo-

current generation. In addition, the light intensity is one of the important parameters in oxygenic photosynthesis, and a light beam from a 150 W illuminator was adjusted to 680  $\text{mW cm}^{-2}$ . Although the photocurrent linearly increased with increasing light intensity, we were concerned about possible photodamage of the thylakoid membrane.

The photocurrent value that was obtained under optimized conditions was outstanding and equal to approximately 130  $\mu\text{A cm}^{-2}$ . To evaluate the origin of the photocurrent, one of the most well-known inhibitors that is known to be PS II site-specific, Diuron, was explored. Diuron inhibited 50% of the total photocurrent, confirming that PS II was the major source of electrons for the photocurrent. The outcome from this study has substantial implication for photosynthetic energy conversion, as well as photofuel production. It might be possible to boost this photocurrent value with further electrode surface modification, or by using a more elaborate 3D electrode with a suitable material. However, the stability of a thylakoid-membrane-based fuel cell suffers from practical concerns that may be overcome with suitable immobilization of the thylakoid membranes, that is, in a way in which they can stay alive in their native state of action. To keep the thylakoid membrane in its native environment, the chloroplast can also be considered for further continuation of research. Future work is likely to be focused on a possible DET pathway, from the thylakoid membrane to the electrode, to be able to omit the regular addition of a soluble mediator, which questions its application. This effort opens the possibility for green energy harvesting from a natural process that evolved from the origin of life.

### Experimental Section

Duroquinone, 2,3-dimethoxy-5-methyl-*para*-benzoquinone (2,3-DMO-5-M-PBQ), 2,5-dimethyl-1,4-benzoquinone (2,5-DM-PBQ), DCIP, naphthoquinone, PBQ, tetrachloro-PBQ, tetrabromo-PBQ, and 2,6 dichloro-1,4-benzoquinone (DCBQ) were purchased from Sigma–Aldrich, (Munich, Germany) and Merck (Darmstadt, Germany), and were of either research or analytical grade. All aqueous solutions were prepared by using water purified and deionized (18 M $\Omega$ ) with a Milli-Q system (Millipore, Bedford, MA, USA).

All electrochemical experiments were carried out by using a Compactstat Electrochemical Interface (Ivium Technologies, Eindhoven, The Netherlands). A Metrohm 827-pH lab meter (Metrohm AG, Herisau, Switzerland) was used for adjusting the pH values of the solutions. A Bandelin Sonorex RK 100H ultrasonic bath (BANDELIN electronic GmbH & Co., Berlin, Germany) was used for the cleaning procedure of the Au electrodes before they were modified with gold nanoparticles. To perform photoelectrochemical experiments, a fiber optic illuminator (FOI-150–220, 150 W and 220 V) with an FOI-5 light guide (Titan Tool Supply Inc., Buffalo, NY, USA) was used to illuminate the electrode surface. The illuminator was adjusted by using a light intensity meter (Techtum Lab AB, Umeå, Sweden).

Thylakoid membranes were extracted from leaves of spinach (*Spinacia oleracea*), as described in ref. [39], and were suspended in water to a concentration 3.2  $\text{mg mL}^{-1}$ . The chlorophyll content in the thylakoid membranes was determined according to the method described in ref. [40]. Oxygen evolution was measured with a Clark-type electrode in a medium containing phenyl-p-benzoqui-



none (0.4  $\mu\text{mol}$ ), pH 6.5 sodium phosphate buffer (70  $\mu\text{mol}$ ), NaCl (12  $\mu\text{mol}$ ), and thylakoid membrane (corresponding to 46  $\mu\text{g}$  of chlorophyll in a total volume of 2.3 mL).<sup>[37]</sup> The oxygen evolution activity was found to be 126  $\mu\text{mol O}_2 \text{ mg chlorophyll}^{-1} \text{ h}^{-1}$ , indicating the high activity of the extracted thylakoid membranes.<sup>[37]</sup>

To prepare the AuNP–Au electrode, all-gold nanoparticles (AuNP) were initially synthesized, according to the method published in refs. [41] and [42]. Briefly, branched polyethylenimine (PEI; 0.01 g; Sigma–Aldrich, USA) was completely dissolved in distilled water (100 mL) for 1 h. Then, H<sub>2</sub>AuCl<sub>4</sub> was dissolved in the aqueous PEI solution (to a concentration of 2 mM) under magnetic stirring for an additional 1 h. The mixture was stirred vigorously at room temperature for 24 h for complete reduction to occur. In this case, PEI plays the role of a mild reductant; therefore, a gradual color change, from yellow to red, was observed, indicating the formation of AuNPs. Then, the reaction mixture was dialyzed by using a membrane with a molecular-weight cutoff of 12 kDa with repeated water changes for 1 day to eliminate any unreacted chemicals.

Prior to modification, polycrystalline solid gold electrodes (BAS, West Lafayette, IL, USA), with a surface area of 0.02 cm<sup>2</sup>, were immersed into a freshly prepared Piranha solution (3:1 v/v. H<sub>2</sub>SO<sub>4</sub>/H<sub>2</sub>O<sub>2</sub>) for 3 min for chemical pretreatment, followed by rinsing with Milli-Q water. Note: Piranha solutions need to be treated with great care. Then, the Au electrodes were mechanically cleaned by polishing with an alumina slurry with a grain size of 1  $\mu\text{m}$  and then 0.1  $\mu\text{m}$  (Struers, Copenhagen, Denmark) on a polishing microcloth (Buehler, Lake Bluff, IL, USA) for 3 min. This was followed by ultrasonication in Milli-Q water for 5 min and subsequent electrochemical cleaning in 0.5 M H<sub>2</sub>SO<sub>4</sub>, which was performed by using cyclic voltammetry between  $-0.1 \text{ V}$  and  $+1.7 \text{ V}$  at a scan rate of 300  $\text{mVs}^{-1}$  for 20 cycles.<sup>[43]</sup> The electrodes were rinsed again with Milli-Q water and dried at room temperature. Then, 10  $\mu\text{L}$  of the AuNP suspension was added to the surface of the solid Au electrode (5  $\mu\text{L}$  at a time allowing the drop to dry for ca. 10 min) and dried under atmospheric conditions.

For the electrochemical measurements investigating the photoelectrochemical behavior of the thylakoid membrane in the presence of mediators, cyclic voltammetric and chronoamperometric techniques were used. Electrochemical experiments were carried out in PBS (containing 10 mM NaCl and 5 mM MgCl<sub>2</sub>)<sup>[44]</sup> at pH 7.0 using AuNP–Au as the working electrode, a platinum foil as the counter electrode, and Ag/AgCl (saturated with KCl) as a reference electrode. Electrolyte solutions were deaerated with pure argon gas for 5 min before all experiments were conducted. If not stated otherwise, all CVs were obtained between potentials of  $-0.5 \text{ V}$  and  $+0.50 \text{ V}$  with a scan rate of 5  $\text{mVs}^{-1}$ . All reported data were based on three independent experimental results and the standard deviation was less than 10%.

## Acknowledgements

The authors thank The Swedish Research Council (projects: 2010-5031, 2010-2013), The Nanometer consortium at Lund University (nmC@LU), The European Commission (projects NMP4-SL-2009-229255 "3D-Nanobiodevice", FP7-PITN-GA-2010-264772 "Chebana" and FP7-PEOPLE-2013-ITN "Bioenergy"), for financial support.

**Keywords:** gold electrode · light · photocurrent · quinone · thylakoid membranes

- [1] L. M. Utschig, N. M. Dimitrijevic, O. G. Poluektov, S. D. Chemerisov, K. L. Mulford, D. M. Tiede, *J. Phys. Chem. Lett.* **2011**, *2*, 236–241.
- [2] O. Yehezkeili, R. Tel-Vered, J. Wasserman, A. Trifonov, D. Michaeli, R. Nechushtai, I. Willner, *Nat. Commun.* **2012**, *3*, 742.
- [3] C. F. Meunier, J. C. Rooke, A. Léonard, H. Xie, B. L. Su, *Chem. Commun.* **2010**, *46*, 3843–3859.
- [4] J. A. Basham, A. A. Benson, M. Calvin, *J. Biol. Chem.* **1950**, *185*, 781–787.
- [5] C. F. Meunier, P. Van Cutsem, Y. U. Kwon, B. L. Su, *J. Mater. Chem.* **2009**, *19*, 1535–1542.
- [6] K. Kalyanasundaram, M. Graetzel, *Curr. Opin. Biotechnol.* **2010**, *21*, 298–310.
- [7] A. J. Bard, M. A. Fox, *Acc. Chem. Res.* **1995**, *28*, 141–145.
- [8] D. Gust, T. A. Moore, A. L. Moore, *Acc. Chem. Res.* **2001**, *34*, 40–48.
- [9] M. Hambourger, G. F. Moore, D. M. Kramer, D. Gust, A. L. Moore, T. A. Moore, *Chem. Soc. Rev.* **2009**, *38*, 25–35.
- [10] R. E. Blankenship, D. M. Tiede, J. Barber, G. W. Brudvig, G. Fleming, M. Ghirardi, M. R. Gunner, W. Junge, D. M. Kramer, A. Melis, T. A. Moore, C. C. Moser, D. G. Nocera, A. J. Nozik, D. R. Ort, W. W. Parson, R. C. Prince, R. T. Sayre, *Science* **2011**, *332*, 805–809.
- [11] I. J. Iwuchukwu, M. Vaughn, N. Myers, H. O'Neill, P. Frymier, B. D. Bruce, *Nat. Nanotechnol.* **2010**, *5*, 73–79.
- [12] J. F. Millsaps, B. D. Bruce, J. W. Lee, E. Greenbaum, *Photochem. Photobiol.* **2001**, *73*, 630–635.
- [13] R. A. Grimme, C. E. Lubner, D. A. Bryant, J. H. Golbeck, *J. Am. Chem. Soc.* **2008**, *130*, 6308–6309.
- [14] A. Badura, D. Guschin, T. Kothe, M. J. Kopczak, W. Schuhmann, M. Rögner, *Energy Environ. Sci.* **2011**, *4*, 2435–2440.
- [15] R. Bhardwaj, R. L. Pan, E. L. Gross, *Nature* **1981**, *289*, 396–398.
- [16] J. O. Calkins, Y. Umasankar, H. O'Neill, R. P. Ramasamy, *Energy Environ. Sci.* **2013**, *6*, 1891–1900.
- [17] K. H. Sjöholm, M. Rasmussen, S. D. Minteer, *ECS Electrochem. Lett.* **2012**, *1*, G7–G9.
- [18] M. Rasmussen, A. Shrier, S. D. Minteer, *Phys. Chem. Chem. Phys.* **2013**, *15*, 9062–9065.
- [19] K. B. Lam, E. F. Irwin, K. E. Healy, L. Lin, *Sens. Actuators B* **2006**, *117*, 480–487.
- [20] P. N. Ciesielski, A. M. Scott, C. J. Faulkner, B. J. Berron, D. E. Cliffl, G. K. Jennings, *ACS Nano* **2008**, *2*, 2465–2472.
- [21] M. Kato, T. Cardona, A. W. Rutherford, E. Reisner, *J. Am. Chem. Soc.* **2012**, *134*, 8332–8335.
- [22] A. Badura, T. Kothe, W. Schuhmann, M. Rögner, *Energy Environ. Sci.* **2011**, *4*, 3263–3274.
- [23] A. Efrati, R. Tel-Vered, D. Michaeli, R. Nechushtai, I. Willner, *Energy Environ. Sci.* **2013**, *6*, 2950–2956.
- [24] A. Badura, B. Esper, K. Ataka, C. Grunwald, C. Wöll, J. Kuhlmann, J. Heberle, M. Rögner, *Photochem. Photobiol.* **2006**, *82*, 1385–1390.
- [25] N. Lebedev, S. A. Trammell, A. Spano, E. Lukashev, I. Griva, J. Schnur, *J. Am. Chem. Soc.* **2006**, *128*, 12044–12045.
- [26] O. Yehezkeili, O. I. Wilner, R. Tel-Vered, D. Roizman-Sade, R. Nechushtai, I. Willner, *J. Phys. Chem. B* **2010**, *114*, 14383–14388.
- [27] P. N. Ciesielski, C. J. Faulkner, M. T. Irwin, J. M. Gregory, N. H. Tolk, D. E. Cliffl, G. K. Jennings, *Adv. Funct. Mater.* **2010**, *20*, 4048–4054.
- [28] A. Ptak, A. Dudkowiak, D. Frackowiak, *J. Photochem. Photobiol. A* **1998**, *115*, 63–68.
- [29] D. P. B. T. B. Strik, R. A. Timmers, M. Helder, K. J. J. Steinbusch, H. V. M. Hamelers, C. J. N. Buisman, *Trends Biotechnol.* **2011**, *29*, 41–49.
- [30] M. Rosenbaum, Z. He, L. T. Angenent, *Curr. Opin. Biotechnol.* **2010**, *21*, 259–264.
- [31] Z. Yongjin, J. Pisciotta, R. B. Billmyre, I. V. Baskakov, *Biotechnol. Bioeng.* **2009**, *104*, 939–946.
- [32] B. Esper, A. Badura, M. Rögner, *Trends Plant Sci.* **2006**, *11*, 543–549.
- [33] A. Badura, D. Guschin, B. Esper, T. Kothe, S. Neugebauer, W. Schuhmann, M. Rögner, *Electroanalysis* **2008**, *20*, 1043–1047.
- [34] M. Vittadello, M. Y. Gorbunov, D. T. Mastrogianni, L. S. Wielunski, E. L. Garfunkel, F. Guerrero, D. Kirilovsky, M. Sugiura, A. W. Rutherford, A. Safari, P. G. Falkowski, *ChemSusChem* **2010**, *3*, 471–475.
- [35] T. Noji, H. Suzuki, T. Gotoh, M. Iwai, M. Ikeuchi, T. Tomo, T. Noguchi, *J. Phys. Chem. Lett.* **2011**, *2*, 2448–2452.
- [36] E. Fuhrmann, S. Gathmann, E. Rupprecht, J. Golecki, D. Schneider, *Plant Physiol.* **2009**, *149*, 735–744.

- [37] H.-E. Åkerlund, B. Andersson, P.-Å. Albertsson, *Biochim. Biophys. Acta Bioenerg.* **1976**, *449*, 525–535.
- [38] M. Purcell, R. Carpentier, D. Bélanger, G. Fortier, *Biotechnol. Tech.* **1990**, *4*, 363–368.
- [39] E. Andreasson, P. Svensson, C. Weibull, P.-Å. Albertsson, *Biochim. Biophys. Acta Bioenerg.* **1988**, *936*, 339–350.
- [40] R. J. Porra, W. A. Thompson, P. E. Kriedemann, *Biochim. Biophys. Acta Bioenerg.* **1989**, *975*, 384–394.
- [41] W.-J. Song, J.-Z. Du, T.-M. Sun, P.-Z. Zhang, J. Wang, *Small* **2010**, *6*, 239–246.
- [42] S. Frasca, O. Rojas, J. Salewski, B. Neumann, K. Stiba, I. M. Weidinger, B. Tiersch, S. Leimkühler, J. Koetz, U. Wollenberger, *Bioelectrochemistry* **2012**, *87*, 33–41.
- [43] R. Ortiz, H. Matsumura, F. Tasca, K. Zahma, M. Samejima, K. Igarashi, R. Ludwig, L. Gorton, *Anal. Chem.* **2012**, *84*, 10315–10323.
- [44] A. Agostiano, D. C. Goetze, R. Carpentier, *Photochem. Photobiol.* **1992**, *55*, 449–455.
- [45] P. S. Guin, S. Das, P. C. Mandal, *Int. J. Electrochem.* **2011**, 816202.
- [46] M. L. Fultz, R. A. Durst, *Anal. Chim. Acta* **1982**, *140*, 1–18.
- [47] P. T. Kissinger, W. R. Heineman, *J. Chem. Educ.* **1983**, *60*, 702.
- [48] G. S. Calabrese, R. M. Buchanan, M. S. Wrighton, *J. Am. Chem. Soc.* **1982**, *104*, 5786–5788.
- [49] *Photosynthetic generators of protonmotive force*, D. G. Nicholls, S. J. Ferguson in *Bioenergetics*, 3rd ed., Academic Press, London, **2003**, pp. 157–194.
- [50] K. Satoh, M. Oh-hashi, Y. Kashino, H. Koike, *Plant Cell Physiol.* **1995**, *36*, 597–605.
- [51] I. McConnell, G. Li, G. W. Brudvig, *Chem. Biol.* **2010**, *17*, 434–447.
- [52] E. A. Braude, *J. Chem. Soc.* **1945**, 490–497.
- [53] P.-Å. Albertsson, *Trends Plant Sci.* **2001**, *6*, 349–354.
- [54] I. Vass, *Biochim. Biophys. Acta Bioenerg.* **2012**, *1817*, 209–217.
- [55] E. P. Fuerst, M. A. Norman, *Weed Sci.* **1991**, *39*, 458–464.
- [56] R. Carpentier, C. Loranger, J. e. Chartrand, M. Purcell, *Anal. Chim. Acta* **1991**, *249*, 55–60.

Received: September 4, 2013



# Paper VI



# Photocurrent Generation from Thylakoid Membranes on Osmium-Redox-Polymer-Modified Electrodes

Hassan Hamidi,<sup>[a, d]</sup> Kamrul Hasan,<sup>\*,[a]</sup> Sinan Cem Emek,<sup>[a]</sup> Yusuf Dilgin,<sup>[b]</sup> Hans-Erik Åkerlund,<sup>[a]</sup> Per-Åke Albertsson,<sup>[a]</sup> Dónal Leech,<sup>[c]</sup> and Lo Gorton<sup>\*,[a]</sup>

Thylakoid membranes (TMs) are uniquely suited for photosynthesis owing to their distinctive structure and composition. Substantial efforts have been directed towards use of isolated photosynthetic reaction centers (PRCs) for solar energy harvesting, however, few studies investigate the communication between whole TMs and electrode surfaces, due to their complex structure. Here we report on a promising approach to generate photosynthesis-derived bioelectricity upon illumination of TMs wired with an osmium-redox-polymer modified graphite electrode, and generate a photocurrent density of 42.4  $\mu\text{A cm}^{-2}$ .

All forms of life require energy, and most of the energy that organisms on earth use originates from the sun. Green plants, algae, and some bacteria capture sunlight and convert it into chemical energy with a quantum yield of nearly 100%<sup>[1]</sup> through photosynthesis, which in higher plants and algae takes place in chloroplasts. Thylakoid membranes (TMs) located within the chloroplasts and the most-abundant biological membranes in nature are the sites of the photosynthetic events.

In attempts to harvest solar energy for future energy needs, considerable efforts have been devoted towards the development of photo-bioelectrochemical cells (PBECs) based on inserting photosynthetic reaction centers (PRCs) into artificial

constructs, such as histidine-tagged<sup>[2]</sup> osmium-complex-containing redox polymers (Os-polymers) forming a hydrogel,<sup>[3]</sup> multilayer-assembled,<sup>[4]</sup> and self-assembled structures.<sup>[5]</sup> Agostiano et al. reported on photocurrent generation by depositing PSI and PSII onto platinum electrodes<sup>[6]</sup> as well as the photosynthetic Z-scheme in an electrochemical cell.<sup>[7]</sup>

Most PBEC designs have focused on isolated PRCs because of their easier electrochemical accessibility, but they usually suffer from instability, inadequate immobilization, and insufficient electrical communication.<sup>[8]</sup> On the contrary, as PRCs are buried in the complex structure of TMs a decrease in the efficiency of the electron transfer (ET) process from the TMs to the electrode is expected. Despite this difficulty, the electrical communication of TMs with electrodes has attracted substantial research efforts.<sup>[9,10]</sup> To the best of our knowledge, no successful effort in which the entire TMs were "wired" with osmium-modified polymers that eliminate the requirement to use monomeric mediators, which are not only environmentally unfriendly but also impractical, has yet been reported. Based on our recently published work on TMs,<sup>[11]</sup> we demonstrate herein that such osmium polymers can efficiently access the PRCs embedded in the TMs and shuttle electrons to an electrode surface.

In this Communication we report on the incorporation of TMs instead of isolated photosynthetic enzymes (e.g., PSI and PSII) into a PBEC. Osmium polymers of different redox potentials have been used to optimize the energy gap in the electron transfer from the PRCs to the osmium polymer and the electrode. The PBEC generates energy when illuminated and the ET efficiency was compared in terms of registered current for the following setups: (1) TMs on bare graphite; (2) TMs on graphite (TMG) in the presence of a freely diffusing mediator, ferricyanide, known to accept electrons from both PSI and PSII;<sup>[12]</sup> (3) TMG in the presence of phenyl-*p*-benzoquinone known to accept electrons only from PSII;<sup>[13]</sup> and (4) TMG modified with four different osmium polymers that span a potential window between 0.015 and 0.441 V vs. SHE. This potential window is supposed to be sufficient to connect to different photosynthetic redox complexes (PRC) in the TMs. To record and determine the photocurrent from the "wired" TMs, we used cyclic voltammetry (CV) and chronoamperometry (CA). Photocurrent density generated by TMs was measured by subtracting the light-off response from that registered under light-on conditions. Control experiments without TMs yield no photocurrent under illumination (data not shown). The proposed possible photosynthetic ET pathways from TMs to the electrode are presented in (Supporting Information, Figure S1).

[a] Dr. H. Hamidi,<sup>\*</sup> K. Hasan,<sup>\*</sup> Dr. S. C. Emek, Prof. H.-E. Åkerlund, Prof. P.-Å. Albertsson, Prof. L. Gorton  
Department of Analytical Chemistry/Biochemistry and Structural Biology  
Lund University  
P.O. Box 124, SE-221 00 Lund (Sweden)  
E-mail: kamrul.hasan@biochemistry.lu.se  
lo.gorton@biochemistry.lu.se

[b] Prof. Y. Dilgin  
Department of Chemistry, Science & Art Faculty  
Çanakkale Onsekiz Mart University  
17100, Çanakkale (Turkey)

[c] Prof. D. Leech  
School of Chemistry & Ryan Institute  
National University of Ireland Galway  
University Road, Galway (Ireland)

[d] Dr. H. Hamidi<sup>\*</sup>  
Department of Chemistry, Zanjan Branch  
Islamic Azad University  
P. O. Box 49195-467, Zanjan (Iran)

[\*] These authors contributed equally to this work.

Supporting Information for this article is available on the WWW under <http://dx.doi.org/10.1002/cssc.201403200>.

When the TMs were immobilized onto bare graphite in the absence of any mediator (setup-1) and illuminated, a very low but still detectable anodic photocurrent ( $6.8 \mu\text{A cm}^{-2}$ ) was observed due to a direct ET (DET) process between the PRCs and the electrode (Supporting Information, Figure S2) yielding a fifteen fold higher current density than what was exhibited in a previous report.<sup>[14]</sup>

To explore the best possible ET we tested photocurrent generation in the presence of two different monomeric mediators, ferricyanide (setup-2) and phenyl-*p*-benzoquinone (setup-3) (Supporting Information, Figures S3 and S4), to yield a photocurrent generation,  $51.7 \mu\text{A cm}^{-2}$  in setup-2 and  $24.9 \mu\text{A cm}^{-2}$  in setup-3, respectively. These mediators can freely diffuse through the PRCs buried in the TMs and transfer electrons to the electrode where they have better access to extract electrons.

Osmium polymers<sup>[15]</sup> have been extensively used in combination with a range of different redox enzymes. The highly cationic nature of the osmium polymers makes them strongly interact with proteins and also with whole cells that are anionic at neutral pH forming a 3D electrostatic complex, a hydrogel that allows aqueous soluble species to freely diffuse in and out. We have pioneered the use of such osmium polymers with both Gram(-)<sup>[16]</sup> but also Gram(+) bacterial cells<sup>[17]</sup> as well as with yeast cells.<sup>[18]</sup> To investigate the effect of the formal potential ( $E^{\circ}$ ) on the efficiency of ET from the PRCs to the electrode, four different Os-polymers of different structures<sup>[19]</sup> were studied: (Os-1) poly(vinylpyridine)-[Os(N,N'-methylated-2,2'-biimidazole)<sub>3</sub>]<sup>+2+</sup>,  $E^{\circ} = 15 \text{ mV vs. SHE}$ ; (Os-2) [Os(4,4'-dimethoxy-2,2'-bipyridine)<sub>2</sub>(polyvinylimidazole)<sub>10</sub>Cl]<sup>+2+</sup>,  $E^{\circ} = 140 \text{ mV vs. SHE}$ ; (Os-3) [Os(4,4'-dimethyl-2,2'-bipyridine)<sub>2</sub>(polyvinylimidazole)<sub>10</sub>Cl]<sup>+2+</sup>,  $E^{\circ} = 309 \text{ mV vs. SHE}$ ; and (Os-4) [Os(2,2'-bipyridine)<sub>2</sub>(polyvinylimidazole)<sub>10</sub>Cl]<sup>+2+</sup>,  $E^{\circ} = 441 \text{ mV vs. SHE}$ .

Figure 1A shows two CVs of TMs wired with the co-deposited osmium polymer of the highest  $E^{\circ}$ -value (0.441 V vs. SHE, Os-4), on a graphite electrode in PBS (setup-4). One pair of redox peaks is observed for Os-4 with a  $E^{\circ}$  value (taken as the mean value of the anodic,  $E_{\text{pa}}$  and cathodic peak,  $E_{\text{pc}}$ , potentials) equal to 0.441 V vs. SHE, in agreement with previously published work.<sup>[20]</sup> Upon illumination, the anodic current increases and the cathodic current decreases concomitantly, which confirms that the bound  $\text{Os}^{3+}$  moieties can accept electrons released during the photosynthetic process and shuttle them from the TMs to the electrode. In contrast, no noticeable current change was observed in CVs of Os-4 alone, without TMs, on the electrode under otherwise equal conditions (Supporting Information, Figure S5). Figure 1B shows the generation of a photocurrent density for TMs wired with Os-4 upon illumination applying a constant potential of +0.7 V vs. SHE. In the absence of illumination a background current density of approximately  $12.8 \mu\text{A cm}^{-2}$  was registered. When illuminated initially with a light intensity of  $6800 \text{ W m}^{-2}$  the current density rapidly increased to reach a maximum value of  $55.2 \mu\text{A cm}^{-2}$ .

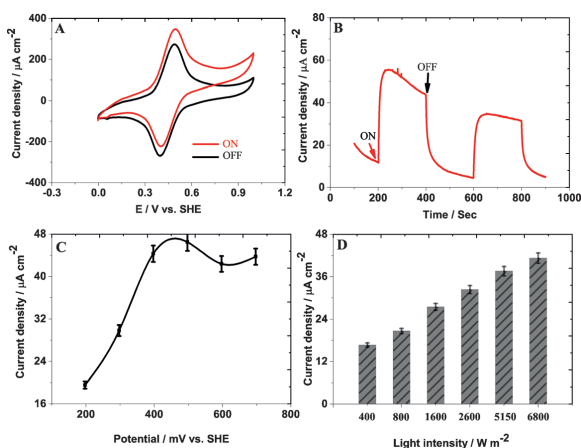


**Figure 1.** The photocurrent generation from TMs and osmium-polymer-modified electrode (setup-4). (A) CVs of TMs immobilized graphite electrode modified with Os-4 in the absence (black line) and presence of illumination (red line) at an intensity of  $6800 \text{ W m}^{-2}$ ; scan rate  $0.01 \text{ V s}^{-1}$ . (B) CAs of the same electrode upon a cyclic 'ON-OFF' illumination at the same light intensity. (C) Dependence of the photocurrent on  $E_{\text{app}}$ , resulting from chronoamperometric studies, (D) Dependence of the photocurrent on intensity of the incident light. Electrolyte: 10 mM phosphate buffer, 10 mM NaCl, 5 mM  $\text{MgCl}_2$  at pH 7.0 (PBS).

The net increase of  $42.4 \mu\text{A cm}^{-2}$  ( $55.2 - 12.8 \mu\text{A cm}^{-2}$ ) indicates a high efficiency of ET between the TMs and the electrode comparable to when using the monomeric mediators. As can be seen in Figure 1B, the initial photocurrent density decreases somewhat during illumination due to a partial photo-destruction of the TMs ascribed to the photo-induced damage of TMs,<sup>[21]</sup> which is clearly revealed in Figure S6 (Supporting Information).

In order to investigate the influence of the  $E^{\circ}$ -value of the osmium polymer on the ET that in turn can be correlated with different components of the TMs, the results obtained with Os-4 were compared to those obtained with equally prepared electrodes but using the other three Os-polymers, that is, Os-1, Os-2, Os-3 (Supporting Information, Figure S7). The photocurrent density increases with  $E^{\circ}$  of the osmium polymers and was found to be 0.3 (Os-1), 9.3 (Os-2), 31.5 (Os-3), and  $42.4 \mu\text{A cm}^{-2}$  (Os-4). It can thus be concluded that the osmium polymer with the highest  $E^{\circ}$  is the most efficient in transferring electrons to the electrodes. Table S1 (Supporting Information) shows the photocurrent density obtained for the various electron mediators used in different setups.

To the source of the photocurrent, an inhibitor (a herbicide, diuron (1,1-dimethyl, 3-(3',4'-dichlorophenyl) urea) known for its selective action on PSII was used, since its mechanism of action is well understood compared with that of other herbicides.<sup>[22]</sup> Diuron blocks the electron transfer between plastoquinone molecules in PSII that induce lipid peroxidation and consequently results in cellular disorientation and phytotoxicity.<sup>[22]</sup> The photocurrent generation from TMs was substantially inhibited by diuron.<sup>[9b]</sup> Hence, diuron was introduced into the solu-

tion to a concentration of 0.2 mM (in setup-4 with Os-4), while recording the photocurrent upon illumination (Supporting Information, Figure S8). Addition of 0.2 mM diuron results in a 50% decrease in photocurrent compared to the non-inhibited system, which confirms the major source of photocurrent is PSII as diuron binds tightly to the  $Q_B$ -sites of PSII, making them non-reducible and as a consequence in a blocked photosynthetic ET.

The effect of the applied potential ( $E_{app}$ ) on photocurrent density on Os-4 polymer modified TMs (setup-4) is displayed in Figure 1C. As the  $E_{app}$  is stepwise made more positive, the current density increases until  $E_{app}$  coincides with the  $E^{ox}$ -value of Os-4 polymer. At more positive potentials ( $E_{app} > 0.5$  V vs. SHE), most of the osmium moieties are in the active  $Os^{3+}$  form and thus the photocurrent density levels off to a relatively constant value.

The influence of irradiation intensity to the photocurrent density was further investigated in setup-4. The results are shown in Figure 1D showing increased light intensity from  $400\text{ W m}^{-2}$  to  $6800\text{ W m}^{-2}$ . The standard deviation of photocurrent values in Figure 1C and D could arise from electrode preparation and during illumination. However, the quantum yield decreases from 0.09% to 0.01% with increased intensity from  $400\text{ W m}^{-2}$  to  $6800\text{ W m}^{-2}$  (Supporting Information, Figure S9). Since the quantum efficiency of photosynthesis is nearly 100%, the ET from the TMs to the osmium polymer followed by the electrode could limit the quantum yield. At saturated light intensity, the photocurrent recorded (setup-4 with Os-4) to  $42.4\text{ }\mu\text{A cm}^{-2}$  that is equivalent to  $3.1\text{ }\mu\text{A}$  (electrode surface area =  $0.0731\text{ cm}^2$ ). This photocurrent ( $3.1\text{ }\mu\text{A}$ ) corresponds to  $36\text{ }\mu\text{mol e}^- (\text{mg chlorophyll})^{-1}\text{ h}^{-1}$  since TMs contain  $3.2\text{ }\mu\text{g mL}^{-1}$  chlorophyll.

When using a Clark electrode to follow the production of molecular oxygen with an equivalent amount of TMs in solution, an oxygen evolution of  $126\text{ }\mu\text{mol O}_2 (\text{mg chlorophyll})^{-1}\text{ h}^{-1}$  (comparable to  $504\text{ }\mu\text{mol e}^- (\text{mg chlorophyll})^{-1}\text{ h}^{-1}$ ) was revealed. We assume that illuminating the TMs, when free in the solution and measuring the evolution of molecular oxygen, is the more efficient system compared when being immobilized onto the osmium-polymer-modified electrode. When comparing the photowired system (setup-4 with Os-4) with the Clark electrode system, an efficiency of 7.2% can be calculated (the equation used for efficiency measurement is shown in Supporting Information). The photocurrent generation reported here is in the similar range of an earlier study by Agostino et al.<sup>[9b]</sup> though they vary with different experimental parameters. Although the efficiency of harvesting sunlight is low but it can be improved by engineering electrode materials, for example, highly conductive and 3-dimensional (3D) electrode materials, developing better immobilization methods and the quest for a superior mediator will be the focus of future work. In addition the stability of this system remains to be examined.

This study demonstrates the photoelectrochemical activity of immobilized thylakoid membranes on osmium-polymer-modified electrodes. The osmium polymer with the highest  $E^{ox}$  value,  $[Os(\text{bpy})_2(\text{PVI})_{10}\text{Cl}]^{+/2+}$ , Os-4 can act as an electron acceptor from TMs and generate a current density of

$42.4\text{ }\mu\text{A cm}^{-2}$ . The photocurrent is, by addition of an inhibitor, diuron, confirmed to originate from PSII. The findings have implications for photosynthetic energy conversion and photofuel production, and are also applicable to studies on other light-sensitive devices. The present work, based on bio-hybrid energy conversion from thylakoid membranes, could open a new horizon for green and sustainable energy conversion.

## Experimental Section

Cyclic voltammetry (CV) and chronoamperometry (CA) were performed using a PalmSens potentiostat (model EmStat2, Utrecht, The Netherlands) equipped with PSTrace software with a conventional three-electrode set-up, in which a modified graphite electrode, an Ag|AgCl (sat. KCl) electrode (+0.197 V vs. SHE) and a platinum foil served as the working, reference, and auxiliary electrodes respectively. 10 mM phosphate buffer including 10 mM NaCl, 5 mM  $\text{MgCl}_2$ , at pH 7 (PBS) was used as the electrolyte in all these studies. All measurements were performed at room temperature and electrolyte solution was degassed with pure argon gas for at least 10 min before any experiment. All reported data were based on three independent experimental results and the standard deviation was less than 10%. Currents with an origin other than from photosynthetic phenomena were subtracted in all chronoamperometric data, by running controlled experiments without thylakoid membranes. The scan rate in CV experiments was maintained at  $0.01\text{ V s}^{-1}$  if not stated otherwise. A fiber optic illuminator (150 W 220 V) providing white visible light was used to induce the photosynthesis. The light intensity considered for photosynthesis was between 400–700 nm, known as photosynthetic active region (PAR).

## Acknowledgements

The authors thank the European Commission (Erasmus Mundus, EMIIY Acation II programme and "BIOENERGY" FP7-PEOPLE-2013-ITN-607793), Science Foundation Ireland (Charles Parsons Energy Research Award) and The Swedish Research Council (2010-5031, 2010-2013, 2014-5908) for financial support. We thank Dr. Domhnall MacAodha and Dr. Peter Ó Conghaile (NUI, Galway) for synthesis of the osmium polymers.

**Keywords:** electrodes • osmium • photosynthesis • redoxpolymers • thylakoid membranes

- [1] S. Berry, B. Rumberg, *Bioelectrochemistry* **2001**, *53*, 35–53.
- [2] a) A. Badura, B. Esper, K. Ataka, C. Grunwald, C. Wöll, J. Kuhlmann, J. Heberle, M. Rögner, *Photochem. Photobiol.* **2006**, *82*, 1385–1390; b) M. Vitadello, M. Y. Gorbunov, D. T. Mastrogianni, L. S. Wielunski, E. L. Garfunkel, F. Guerrero, D. Kirilovsky, M. Sugiura, A. W. Rutherford, A. Safari, P. G. Falkowski, *ChemSusChem* **2010**, *3*, 471–475.
- [3] a) A. Badura, D. Guschin, T. Kothe, M. J. Kopczak, W. Schuhmann, M. Rögner, *Energy Environ. Sci.* **2011**, *4*, 2435–2440; b) A. Badura, D. Guschin, B. Esper, T. Kothe, S. Neugebauer, W. Schuhmann, M. Rögner, *Electroanalysis* **2008**, *20*, 1043–1047.
- [4] L. Frollov, O. Wilner, C. Carmeli, I. Carmeli, *Adv. Mater.* **2008**, *20*, 263–266.
- [5] N. Terasaki, N. Yamamoto, T. Hiraga, Y. Yamanoi, T. Yonezawa, H. Nishihara, T. Ohmori, M. Sakai, M. Fujii, A. Tohri, M. Iwai, Y. Inoue, S. Yoneyama, M. Minakata, I. Enami, *Angew. Chem. Int. Ed.* **2009**, *48*, 1585–1587; *Angew. Chem.* **2009**, *121*, 1613–1615.



- [6] A. Agostiano, A. Ceglie, M. D. Monica, *Bioelectrochem. Bioenergy* **1984**, *12*, 499–507.
- [7] A. Agostiano, F. K. Fong, *Bioelectrochem. Bioenergy* **1987**, *17*, 325–337.
- [8] B. Esper, A. Badura, M. Rögner, *Trends Plant Sci.* **2006**, *11*, 543–549.
- [9] a) J. O. Calkins, Y. Umasankar, H. O'Neill, R. P. Ramasamy, *Energy Environ. Sci.* **2013**, *6*, 1891–1900; b) A. Agostiano, D. C. Goetze, R. Carpentier, *Photochem. Photobiol.* **1992**, *55*, 449–455.
- [10] a) M. Rasmussen, S. D. Minter, *Anal. Methods* **2013**, *5*, 1140–1144; b) M. Rasmussen, A. Shrier, S. D. Minter, *Phys. Chem. Chem. Phys.* **2013**, *15*, 9062–9065.
- [11] K. Hasan, Y. Dilgin, S. C. Emek, M. Tavahodi, H.-E. Åkerlund, P.-Å. Albertsson, L. Gorton, *ChemElectroChem* **2014**, *1*, 131–139.
- [12] M. Mimeault, R. Carpentier, *Enzyme Microb. Technol.* **1988**, *10*, 691–694.
- [13] H.-E. Åkerlund, C. Jansson, B. Andersson, *Biochim. Biophys. Acta Bioenerg.* **1982**, *681*, 1–10.
- [14] M. Rasmussen, S. D. Minter, *Electrochim. Acta* **2014**, *126*, 68–73.
- [15] a) A. Heller, *Curr. Opin. Chem. Biol.* **2006**, *10*, 664–672; b) A. Heller, B. Feldman, *Chem. Rev.* **2008**, *108*, 2482–2505; c) A. Heller, B. Feldman in *Applications of Electrochemistry in Medicine*, Vol. 56 (Ed.: M. Schlesinger), Springer US, **2013**, pp. 121–187.
- [16] a) I. Vostiar, E. E. Ferapontova, L. Gorton, *Electrochem. Commun.* **2004**, *6*, 621–626; b) S. Timur, B. Haghighi, J. Tkac, N. Pazarlioglu, A. Telefoncu, L. Gorton, *Bioelectrochemistry* **2007**, *71*, 38–45; c) S. Timur, U. Anik, D. Odaci, L. Gorton, *Electrochem. Commun.* **2007**, *9*, 1810–1815; d) S. Alferov, V. Coman, T. Gustavsson, A. Reshetilov, C. von Wachenfeldt, C. Hägerhäll, L. Gorton, *Electrochim. Acta* **2009**, *54*, 4979–4984; e) S. A. Patil, K. Hasan, D. Leech, C. Hägerhäll, L. Gorton, *Chem. Commun.* **2012**, *48*, 10183–10185; f) K. Hasan, S. A. Patil, K. Görecki, D. Leech, C. Hägerhäll, L. Gorton, *Bioelectrochemistry* **2013**, *93*, 30–36; g) K. Hasan, K. V. R. Reddy, V. Elßmann, K. Görecki, P. Ó. Conghaile, W. Schuhmann, D. Leech, C. Hägerhäll, L. Gorton, *Electroanalysis* **2015**, *27*, 118–127; h) K. Hasan, H. B. Yildiz, E. Sperling, P. O'Conghaile, M. A. Packer, D. Leech, C. Hägerhäll, L. Gorton, *Phys. Chem. Chem. Phys.* **2014**, *16*, 24676–24680.
- [17] a) V. Coman, T. Gustavsson, A. Finkelsteinas, C. von Wachenfeldt, C. Hägerhäll, L. Gorton, *J. Am. Chem. Soc.* **2009**, *131*, 16171–16176; b) K. Hasan, S. A. Patil, D. Leech, C. Hägerhäll, L. Gorton, *Biochem. Soc. Trans.* **2012**, *40*, 1330–1335.
- [18] A. Heiskanen, V. Coman, N. Kostasheva, D. Sabourin, N. Haslett, K. Baronian, L. Gorton, M. Dufva, J. Emnéus, *Anal. Bioanal. Chem.* **2013**, *405*, 3847–3858.
- [19] M. N. Zafar, F. Tasca, S. Boland, M. Kujawa, I. Patel, C. K. Peterbauer, D. Leech, L. Gorton, *Bioelectrochemistry* **2010**, *80*, 38–42.
- [20] M. N. Zafar, X. Wang, C. Sygmund, R. Ludwig, D. Leech, L. Gorton, *Anal. Chem.* **2012**, *84*, 334–341.
- [21] a) A. Melis, *Trends Plant Sci.* **1999**, *4*, 130–135; b) I. Vass, *Biochim. Biophys. Acta Bioenerg.* **2012**, *1817*, 209–217.
- [22] E. P. Fuerst, M. A. Norman, *Weed Sci.* **1991**, *39*, 458–464.

Received: October 29, 2014

Revised: December 5, 2014

Published online on February 20, 2015

## Supporting Information

### **Photocurrent Generation from Thylakoid Membranes on Osmium-Redox-Polymer-Modified Electrodes**

Hassan Hamidi,<sup>[a, d]</sup> Kamrul Hasan,<sup>\*[a]</sup> Sinan Cem Emek,<sup>[a]</sup> Yusuf Dilgin,<sup>[b]</sup> Hans-Erik Åkerlund,<sup>[a]</sup> Per-Åke Albertsson,<sup>[a]</sup> Dónal Leech,<sup>[c]</sup> and Lo Gorton<sup>\*[a]</sup>

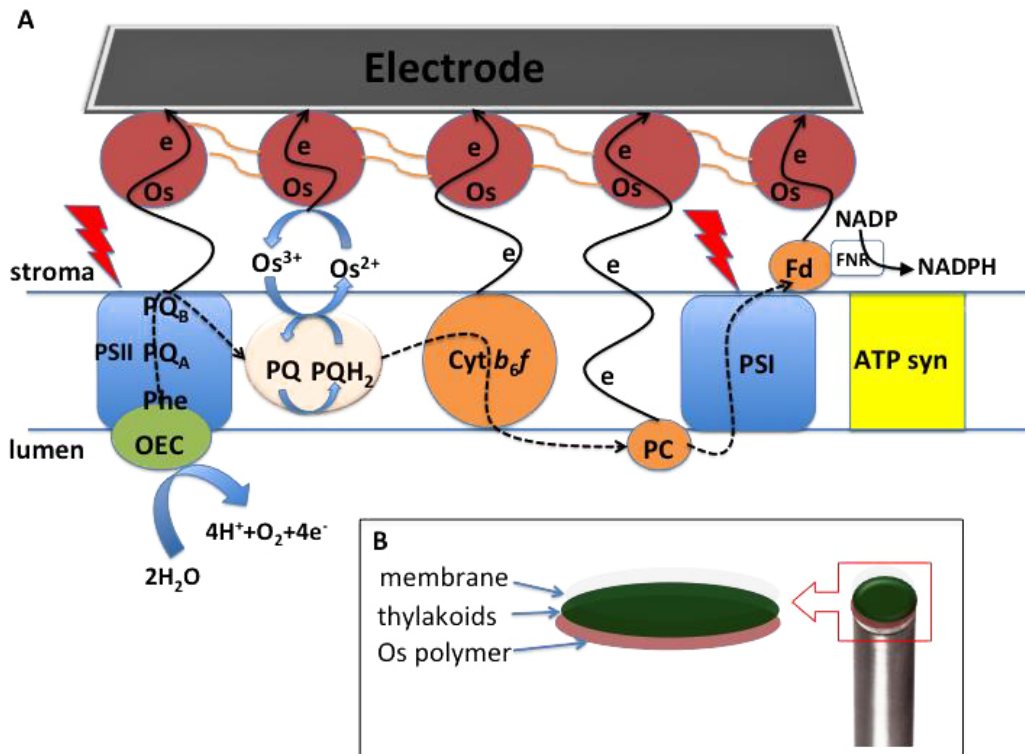
cssc\_201403200\_sm\_miscellaneous\_information.pdf



### Photosynthetic electron transfer (PET)

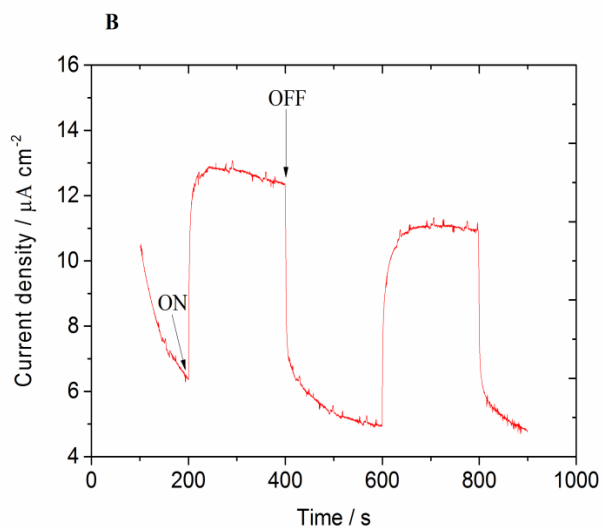
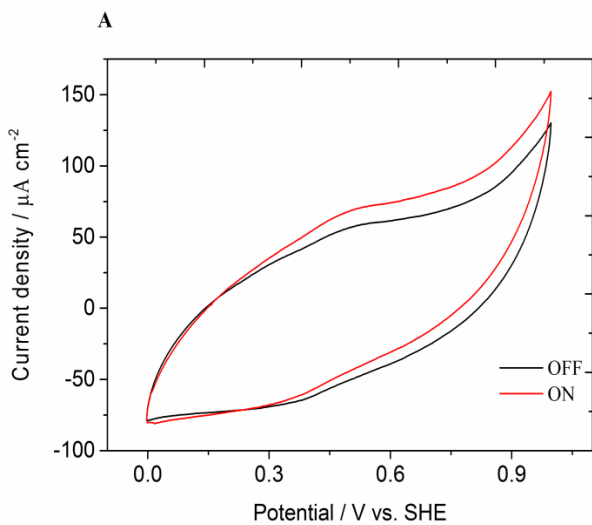
The photosynthetic electron transport chain (PETC) of the thylakoid membranes (TMs) from higher plants and green algae consists of the three protein complexes (Supplementary Fig. 1); i.e., photosystems I and II (PSI and PSII) and the cytochrome  $b_6f$  complex (Cyt  $b_6f$ ), as well as two electron carriers, plastoquinone (PQ) and plastocyanin (PC). PQ connects PSII with Cyt  $b_6f$  followed by PC that link Cyt  $b_6f$  with PSI<sup>[1]</sup> (Supplementary Fig.1).

The photoexcitation of PSII (P680 to P680\*) results in ET to pheophytin (Phe) and followed by the PQA and PQB. Afterwards electrons are transferred to reduce PQ to plastoquinol (PQH<sub>2</sub>) via two successive one-electron reactions, which, through a series of ET processes, regenerates PSII<sup>[2]</sup>. The oxidized oxygen-evolving complex, OEC (Mn<sub>4</sub>Ca cluster) within PSII oxidizes water to molecular oxygen, while regenerating the PSII center<sup>[3]</sup>. Photoexcitation of PSI (P700 to P700\*) leads to an ET to ferredoxin (Fd) and subsequently to ferredoxin NADP reductase (FNR) that eventually produces nicotinamide adenine dinucleotide phosphate (NADPH) that in turn is used to reduce CO<sub>2</sub> to sugars in the light independent reactions of photosynthesis. The proton gradient generated over the membrane is used by ATP synthase (ATP syn) to produce ATP, the cellular energy<sup>[4]</sup>.



### Supplementary Figure 1.

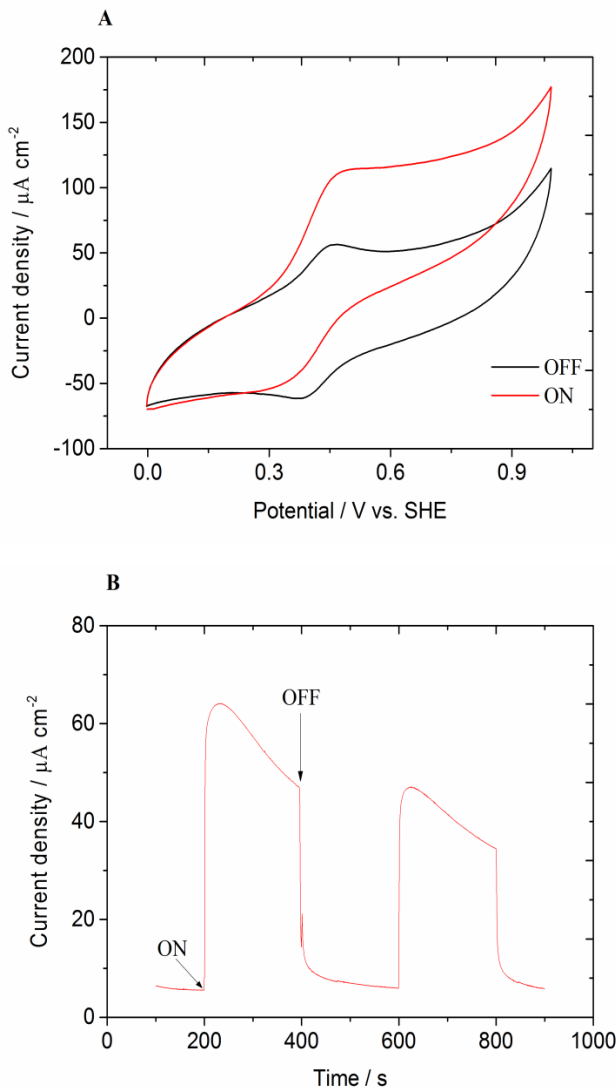
Proposed photosynthetic ET from TMs to the electrode and electrode preparation. (A) A scheme showing possible ET from TMs (immobilized on the electrode surface) to the Os-polymer modified electrode via different proteins. OEC, Phe, PQA, PQB, PQ, PQH<sub>2</sub>, Cyt  $b_6f$ , PC, ATP syn represent regular symbols in photosynthesis and are explained in the text. Purple circles symbolize osmium redox centers that are connected through the polymer backbones. (B) Illustration of preparation of the Os-polymer modified electrode with TMs immobilized with the aid of a permselective membrane.



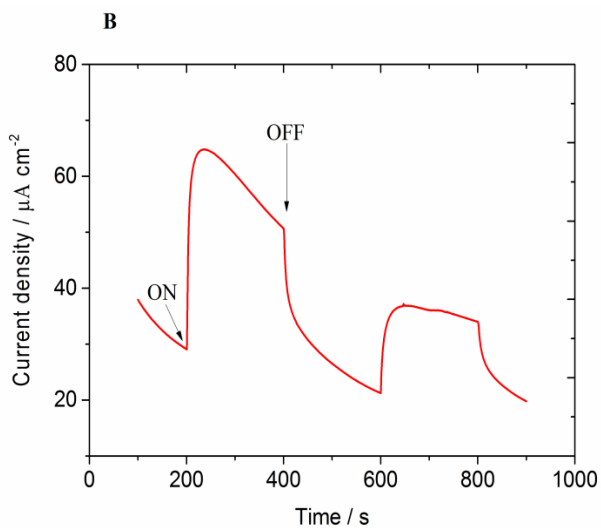
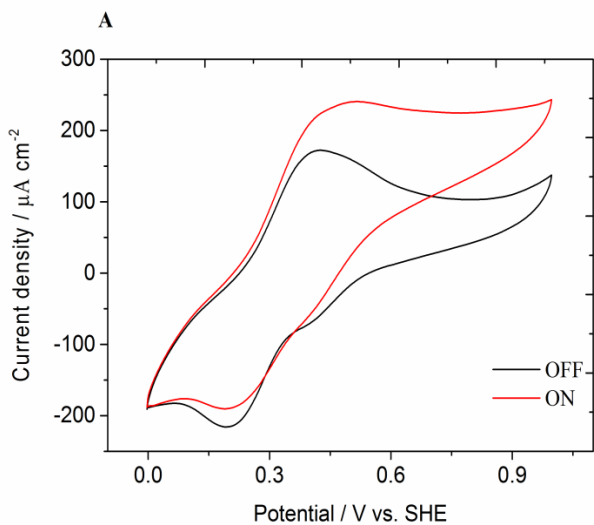
**Supplementary Figure 2.** Direct electron transfer (DET) from TMs to a bare graphite electrode (A) CVs of TMs immobilized on bare graphite electrode in the absence (black line) and presence of illumination (red line) at a light intensity of  $6800 \text{ Wm}^{-2}$  in PBS. (B) CA of the same electrode upon a cyclic 'ON-OFF' illumination at the same light intensity;  $E_{\text{app}} = 0.7 \text{ V vs. SHE}$ .

### ET via monomeric electron mediators

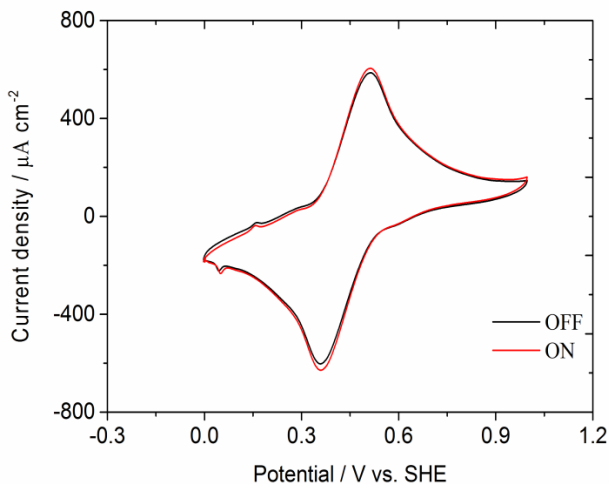
Ferricyanide (standard redox potential at pH 7.0,  $E^{\circ} = +0.420$  V vs. SHE) known as a soluble mediator used in setup-2 and generates a photocurrent of  $51.7 \mu\text{A cm}^{-2}$  (Supplementary Fig. 3) that is sevenfold higher than that observed in the absence of mediator (DET). With phenyl-*p*-benzoquinone, with a slightly lower  $E^{\circ}$ -value ( $+0.298$  V vs. SHE) than that of ferricyanide, a photocurrent density of  $24.9 \mu\text{A cm}^{-2}$  (setup-3) (Supplementary Fig. 4) was generated, which is around 50% less than that obtained in setup-2. The ET via benzoquinone is proposed to be a result of its binding affinity to the  $\text{PQ}_A$  and  $\text{PQ}_B$ -sites inside the TMs<sup>[5]</sup>.



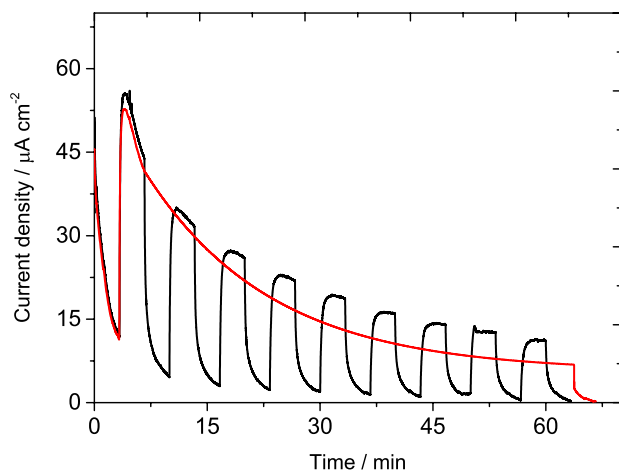
**Supplementary Figure 3.** ET from TMs to electrode via a soluble monomeric mediator, ferricyanide, in setup-2. (A) CVs of a TMs modified graphite electrode (TMG) in the absence (black line) and presence of illumination at a light intensity of  $6800 \text{ Wm}^{-2}$  (red line) in PBS containing  $0.5 \text{ mM}$  ferricyanide; (B) CAs of the same electrode upon a cyclic 'ON-OFF' illumination at a same light intensity;  $E_{\text{app}} = 0.7 \text{ V}$  vs. SHE.



**Supplementary Figure 4.** ET from TMs to an electrode via a soluble monomeric mediator, phenyl-*p*-benzoquinone, in setup-3. (A) CVs of TMs modified graphite electrode (TMG) in the absence (black line) and presence of illumination at a light intensity of  $6800 \text{ Wm}^{-2}$  (red line) in PBS containing 0.5 mM phenyl-*p*-benzoquinone (B) CAs of the same electrode upon a cyclic 'ON-OFF' illumination at the same light intensity;  $E_{\text{app}} = 0.7 \text{ V vs. SHE}$ .



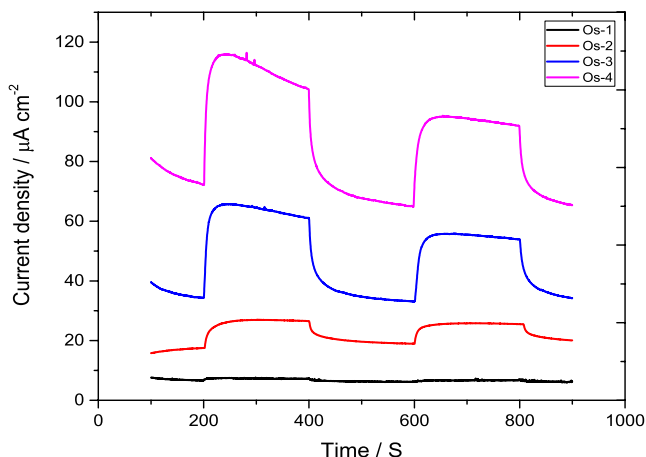
**Supplementary Figure 5.** Cyclic voltammograms (CVs) of Os-4 polymer on a graphite electrode.  $\text{Os}(\text{bpy})_2(\text{PVI})_{10}\text{CJ}^{+/2+}$  immobilized on a graphite electrode in the absence (black line) and presence of illumination (red line) at a light intensity of  $6800 \text{ W m}^{-2}$ . Electrolyte: PBS buffer; scan rate  $0.01 \text{ V s}^{-1}$ .



**Supplementary Figure 6.** The decay of photocurrent. Chronoamperograms (CA) of TMG modified with Os-4 polymer electrode upon a cyclic 'ON-OFF' illumination (black) and continuous illumination (red) at a light intensity of  $6800 \text{ W m}^{-2}$ . Electrolyte: PBS buffer, Applied potential,  $E_{\text{app}}=0.7 \text{ V vs. SHE}$ .

The continuous decay of photocurrent in cyclic 'ON-OFF' as well as in uninterrupted illumination for one hour is exhibited in Supplementary Fig. 6. The regular decay of the photocurrent is attributed to photo-oxidative damage of PSII since PSII is exposed to reactive oxygen species, ROS, that will lower the rate of photosynthesis. The rate of photo-damage in oxygenic photosynthesis depends on the intensity of the incident light. More particularly, at a very high light intensity ( $\gg$ saturated light for photosynthesis, when the light intensity is not the rate limiting factor for photosynthesis)  $\text{PQ}_A$  in PSII remains reduced, which will obstruct or slow down the forward ET resulting in that the excitation energy is not used anymore and dissipates via a non-assimilatory process. This situation produces an imbalance between the ratio of light-energy absorption and utilization; a phenomenon known as photo-inhibition of photosynthesis<sup>[6]</sup>.



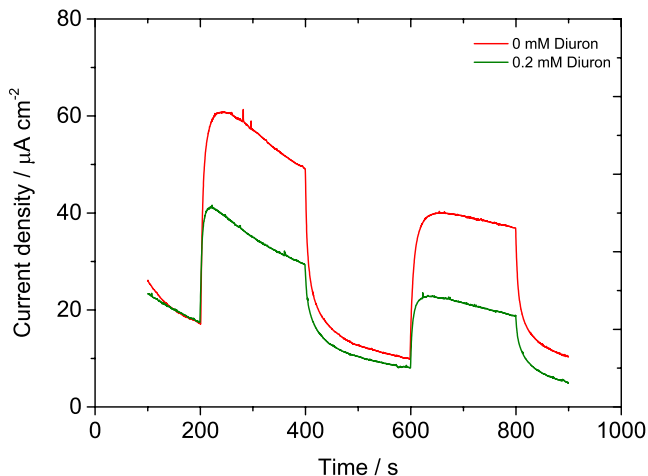


**Supplementary Figure 7.** Variation of photocurrent generation using the four different Os-polymers ( Os-1, Os-2, Os-3 and Os-4). Chronoamperograms (CAs) of the graphite electrode modified with thylakoid membranes and Os-1 (black;  $E^{\circ} = 15$  mV vs. SHE), Os-2 (red;  $E^{\circ} = 140$  mV vs. SHE), Os-3 (blue;  $E^{\circ} = 309$  mV vs. SHE), and Os-4 (pink;  $E^{\circ} = 440$  mV vs. SHE) upon a cyclic 'ON-OFF' illumination at a light intensity of  $6800 \text{ Wm}^{-2}$ . Note the polymers are: Poly(vinylpyridine)-[Os(N,N'-methylated-2,2'-biimidazole)<sub>3</sub>]<sup>+1/2+</sup> (**Os-1**), (Os(4,4'-dimethoxy-2,2'-bipyridine)<sub>2</sub>(polvinylimidazole, PVI)Cl)<sup>+1/2+</sup> (**Os-2**), [Os(4,4'-dimethyl-2,2'-bipyridine)<sub>2</sub>(PVI)Cl]<sup>+1/2+</sup> (**Os-3**), [Os(2,2'-bipyridine)<sub>2</sub>(PVI)Cl]<sup>+1/2+</sup> (**Os-4**). Electrolyte: PBS. The applied potential was 0.7 V vs. SHE.

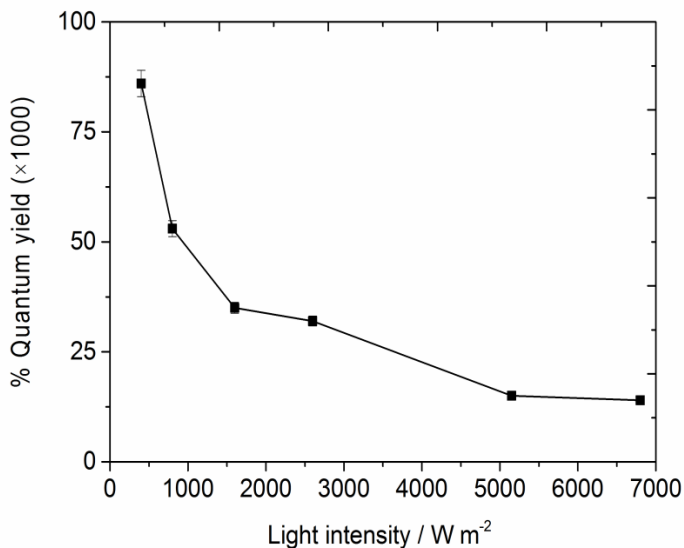
In order to assess the mechanism by which electrons are transferred from the photosystem to the Os-polymers, we now discuss the relative characteristics of the different components of our wired photosystem. The approximate  $E^{\circ}$  values at pH 7.0 of the participating redox complexes in the TMs are +1.2 (P680), -0.85 (P680\*), +0.41 (P700), -1.32 (P700\*), -0.27 (PQ<sub>A</sub>), -0.1 (PQ<sub>B</sub>), +0.09 (Cyt *b<sub>6</sub>f*) and +0.31 (PC) V vs. SHE, which have been extrapolated from reference<sup>[7]</sup>. P680\*, P700\*, PQ<sub>A</sub>, PQ<sub>B</sub>, PQ and Cyt *b<sub>6</sub>f* should have a reduction potential sufficient to provide electrons to the Os-polymers. The short lifetime of P700\* and P680\* makes it unlikely that the Os-polymers could compete with the natural electron acceptors. The negligible magnitude of photocurrent registered when using (Os-1) that has a lower redox potential compared to other Os-polymers, also suggests that PSI is unlikely to act as redox donors in this system. Reduced plastoquinone (PQH<sub>2</sub>), on the other hand, has a long lifetime, is mobile in the membrane, and occurs in multiple copies per PETC<sup>[8]</sup>. It is therefore likely that PQH<sub>2</sub> (PQ<sub>A</sub> is bound to the PSII site while PQ<sub>B</sub> could be either in free or bound form) was the main electron donor to the Os-polymers. Redox components of the Cyt *b<sub>6</sub>f* complex and PC could also contribute<sup>[7]</sup>.

**Supplementary Table 1:** Summary of photocurrent generation from TMs mediated by different electron mediators as well as direct photocurrent (no mediator). In all cases TMs (5  $\mu\text{L}$ ) were immobilized on the graphite electrode. In case of no mediator, TMs were immobilized on a bare graphite electrode. The other graphite electrodes were modified with 1  $\mu\text{L}$  of Os-polymers. The light intensity was  $6800 \text{ Wm}^{-2}$  from a fiber optic illuminator.

Setup	Electron mediator	Formal potential / $E^{\circ}$ vs SHE	Applied potential / $E_{\text{app}}$ vs SHE	Photocurrent density / $\mu\text{A cm}^{-2}$
1	No mediator		0.7	6.8
2	Ferricyanide (0.5 mM)	0.417	0.7	51.7
3	Phenyl- <i>p</i> -benzoquinone (0.5 mM)	0.31	0.7	24.9
4	Os-1	0.015	0.7	0.3
4	Os-2	0.14	0.7	9.3
4	Os-3	0.309	0.7	31.5
4	<b>Os-4</b>	<b>0.441</b>	<b>0.7</b>	<b>42.4</b>

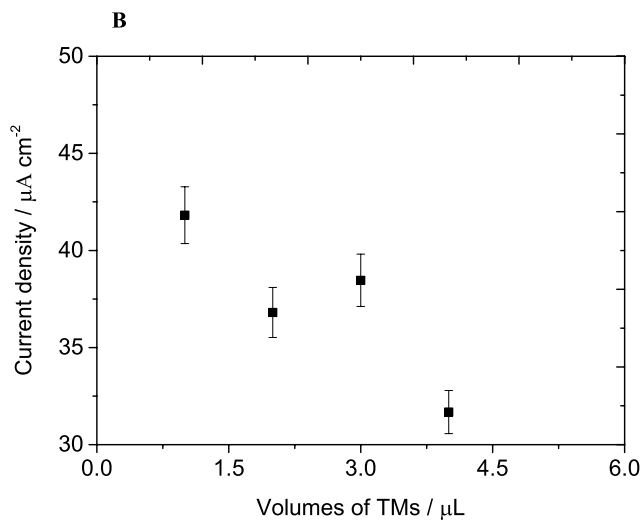
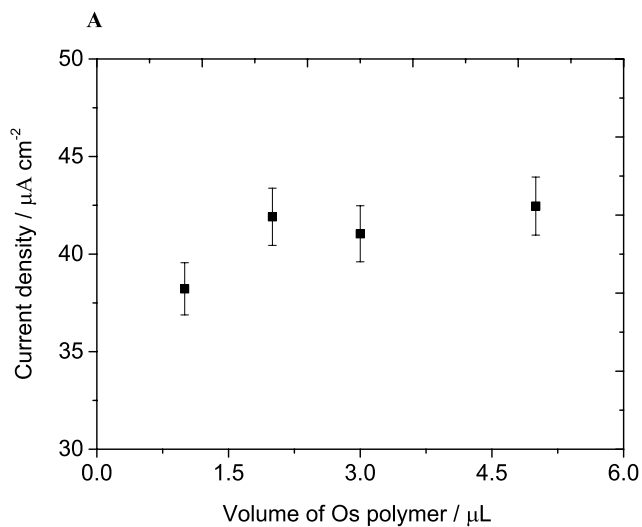


**Supplementary Figure 8.** Inhibition of photocurrent. CAs of TMs immobilized on Os-4 modified graphite electrode upon a cyclic 'ON-OFF' illumination at a light intensity of  $6800 \text{ W m}^{-2}$ , in PBS in the absence (red) and presence (green) of 0.2 mM diuron;  $E_{\text{app}} = 0.7 \text{ V}$  vs. SHE.



**Supplementary Figure 9.** The quantum yields of photocurrent harvesting at different light intensities (data collected from Fig. 1 D). Photocurrent registered while TMs were immobilized on Os-4 polymer modified electrodes upon illumination at different light intensities in PBS,  $E_{\text{app}} = 0.7 \text{ V}$  vs. SHE. (Quantum yield defined as the ratio of the number of incident photons and electrons taken up by the electrode mediated by TMs)

The quantum yields (QY)<sup>[9]</sup> were calculated by using the following equation,  $\text{QY} = \frac{J/F}{I \times f}$   
 Where J is current density on the electrode surface in  $\mu\text{A m}^{-2}$ ; F is the Faraday constant; I is the light irradiance in  $\text{W m}^{-2}$ ; f is average conversion factor between irradiance and photon flux density in the spectral region used ( $5 \mu\text{mol W}^{-1}\text{s}^{-1}$ ).



**Supplementary Figure 10.** The variation of photocurrent density with (A) volume of Os-4 solution [1  $\mu\text{L}$  of TMs were immobilized on the electrode] (B) volume of TMs solution [5  $\mu\text{L}$  of Os-4 was immobilized on the electrode]. Data were collected from chronoamperometric experiments in PBS,  $E_{\text{app}} = 0.7 \text{ V vs. SHE}$ .

## **Supplementary Experimental**

### Chemicals

Diuron [(1,1-dimethyl, 3-(3',4'-dichlorophenyl) urea)], sodium phosphate and sodium hydrogen phosphate, magnesium chloride, and sodium chloride were purchased from Sigma-Aldrich Chemicals (Stein, Germany). Water was purified in a Milli-Q water purification system (Millipore, Bedford, MA, USA).

### Thylakoid membrane preparation

Thylakoid membranes were isolated from spinach (*Spinacia oleracea*) as described in reference<sup>[10]</sup> and the chlorophyll content was determined according to a published procedure<sup>[11]</sup>.

### Modification of electrodes

Graphite rods (Alfa Aesar GmbH & Co KG, Karlsruhe, Germany, AGKSP grade, ultra "F" purity, and 3.05 mm diameter) were used to prepare the working electrodes. The end of the graphite rod was polished on fine emery SiC paper (Turfbak Durite, P1200), carefully washed with Milli-Q water, and finally dried, before 5  $\mu\text{L}$  of an Os-polymer solution (10 mg mL<sup>-1</sup> in Milli-Q water) was spread onto the entire active surface of the electrode (0.0731 cm<sup>2</sup>). The electrode was dried at room temperature for 10-15 min and then 1  $\mu\text{L}$  of the thylakoid membrane solution (3.2 mg mL<sup>-1</sup> chlorophyll) was spread onto the surface. Before use, a dialysis membrane (Spectrum Laboratories Inc., Rancho Dominguez, CA, USA, molecular mass cut-off: 6000–8000) was used to maintain the Os-polymers and thylakoid membranes on the electrode surface. The dialysis membrane (pre-soaked in buffer) was pressed onto the electrode and fixed tightly to the electrode with a rubber O-ring and Para-film. Note that the amounts of Os polymer (5  $\mu\text{L}$ ) and thylakoid membranes (1  $\mu\text{L}$ ) used were the optimized values. The variations of photocurrent with the amount of Os-polymer and thylakoid membranes are shown in Supplementary information, Fig. 9.

### Oxygen evolution

Oxygen evolution was measured polarographically with a Clark-type electrode in a medium containing 0.4  $\mu\text{mol}$  of phenyl-*p*-benzoquinone, 70  $\mu\text{mol}$  of sodium phosphate buffer (pH 6.5), 12  $\mu\text{mol}$  of NaCl, and an amount of thylakoid membrane corresponding to 46  $\mu\text{g}$  of chlorophyll, in a total volume of 2.3 mL<sup>[12]</sup>. The value of oxygen evolution activity was 126  $\mu\text{mol O}_2$  (mg chlorophyll)<sup>-1</sup> h<sup>-1</sup>.

Photosynthetic processes were induced on the working electrodes by a 150 W 220 V fiber optic illuminator (Titan Tool Supply, Inc. Buffalo, NY, USA). The illuminator was calibrated using a light intensity meter (Tehtum Lab AB, Umeå, Sweden).

### Reference:

- [1] S. Berry, B. Rumberg, *Bioelectrochemistry* **2001**, 53, 35-53.
- [2] A. Badura, T. Kothe, W. Schuhmann, M. Rogner, *Energ. Environ. Sci.* **2011**, 4, 3263-3274.
- [3] J. Yano, J. Kern, K. Sauer, M. J. Latimer, Y. Pushkar, J. Biesiadka, B. Loll, W. Saenger, J. Messinger, A. Zouni, V. K. Yachandra, *Science*. **2006**, 314, 821-825.
- [4] O. Yehezkeili, R. Tel-Vered, J. Wasserman, A. Trifonov, D. Michaeli, R. Nechushtai, I. Willner, *Nat. Commun.* **2012**, 3, 742
- [5] G. Renger, B. Hanssum, H. Gleiter, H. Koike, Y. Inoue, *BBA-Bioenergetics*. **1988**, 936, 435-446.
- [6] A. Melis, *Trend Plant Sci.* **1999**, 4, 130-135.
- [7] I. McConnell, G. Li, G. W. Brudvig, *Chem. Biol.* **2010**, 17, 434-447.
- [8] J. Kruk, S. Karpinski, *BBA-Bioenergetics*. **2006**, 1757, 1669-1675.
- [9] J. B. Skillman, *J. Exp. Bot.* **2008**, 59, 1647-1661.
- [10] E. Andreasson, P. Svensson, C. Weibull, P. A. Albertsson, *Biochim. Biophys. Acta.* **1988**, 936, 339-350.
- [11] R. J. Porra, W. A. Thompson, P. E. Kriedemann, *Biochim. Biophys. Acta.* **1989**, 975, 384-394.
- [12] H. E. Akerlund, B. Andersson, P. A. Albertsson, *Biochim. Biophys. Acta.* **1976**, 449, 525-535.



# Paper VII





Cite this: *Phys. Chem. Chem. Phys.*,  
2014, **16**, 24676

Received 24th September 2014,  
Accepted 30th September 2014

DOI: 10.1039/c4cp04307c

www.rsc.org/pccp

## Photo-electrochemical communication between cyanobacteria (*Leptolyngbia* sp.) and osmium redox polymer modified electrodes†

Kamrul Hasan,<sup>a</sup> Huseyin Bekir Yildiz,<sup>b</sup> Eva Sperling,<sup>a</sup> Peter Ó Conghaile,<sup>c</sup>  
Michael A. Packer,<sup>d</sup> Dónal Leech,<sup>c</sup> Cecilia Hägerhäll<sup>a</sup> and Lo Gorton<sup>\*a,3</sup>

Photosynthetic microbial fuel cells (PMFCs) are an emerging technology for renewable solar energy conversion. Major efforts have been made to explore the electrogenic activity of cyanobacteria, mostly using practically unsustainable reagents. Here we report on photocurrent generation ( $\approx 8.64 \mu\text{A cm}^{-2}$ ) from cyanobacteria immobilized on electrodes modified with an efficient electron mediator, an  $\text{Os}^{2+/3+}$  redox polymer. Upon addition of ferricyanide to the electrolyte, cyanobacteria generate the maximum current density of  $\approx 48.2 \mu\text{A cm}^{-2}$ .

Photosynthetic microbial fuel cells (PMFCs) are an emerging prospective technology for  $\text{CO}_2$  free renewable solar energy production and rely on photosynthesis for generation of electricity.<sup>1</sup> Cyanobacteria account for 20–30% of global photosynthetic productivity and convert solar energy into chemical energy.<sup>2</sup> They contain both respiratory and photosynthetic systems in their thylakoid membranes unlike higher plants and algae and any excess electrons generated in photosynthesis can be shared with the respiratory system.<sup>3</sup> Moreover, cyanobacteria have their own mechanism to prevent photo-damage at high light intensity and are able to survive under different environmental conditions, e.g., at irregular levels of  $\text{CO}_2$ , diverse light exposure, and dryness,<sup>4</sup> which is supposed to give them a long stability in PMFCs.<sup>5</sup> Therefore cyanobacteria have the practical potential to harness solar energy in a versatile global area.

Studies have revealed that cyanobacteria may be exploited in photo-bioelectrochemical cells *via* direct electron transfer (DET) with electrodes.<sup>2,6</sup> They have been explored for biofuel

generation<sup>7</sup> as well as heavy metal remediation.<sup>8</sup> Cyanobacteria have greater advantages over metal reducing bacteria, since external organic carbon sources are not needed for electricity generation.<sup>2</sup> Energy generation from isolated photosynthetic reaction centers, photosystem I (PSI), photosystem II (PSII), and thylakoids require complex isolation and immobilization techniques resulting in short-term stability that limits their use in applications.<sup>5</sup> Reports demonstrated different cyanobacteria in PMFCs, e.g. *Anabaena* sp.,<sup>9</sup> *Synechococcus* sp.<sup>10</sup> and *Synechocystis* sp.,<sup>11</sup> and mostly using artificial redox mediators to carry out the extracellular electron transfer from the cells to the electrode. However, the use of environmentally unfriendly, unsustainable and practically unfeasible artificial mediators in PMFCs limits their practical application currently.<sup>6</sup> In contrast, flexible osmium redox polymers (ORPs) have already been very successfully used in enzyme based reagentless biosensors,<sup>12</sup> where they fulfil the requirements of both supplying the system with a mediator (that does not diffuse away with time) and also forming a 3-D immobilization matrix (a hydrogel) for the enzyme. Besides that polymeric mediators draw attention due to their efficient shuttling properties, stable adsorption on the electrode surface and the possibility to form multiple layers of enzymes<sup>13</sup> as well as bacterial cells.<sup>14,15</sup>

Here we report on the electrochemical communication of *Lyptolyngbia* sp. (CYN82)<sup>16</sup> using an ORP modified graphite electrode. Cyclic voltammetry (CV) and chronoamperometry (CA) measurements have been used to record the photocurrent generation. To the best of our knowledge, this is the first time PMFCs with such a polymeric mediator have been reported. To measure the photocurrent density generated by cyanobacteria, the response registered under light off conditions is subtracted from that registered under light on conditions. All potentials mentioned here are referred to  $\text{Ag|AgCl}$  (sat. KCl) if not stated otherwise.

Cyanobacteria convert  $\text{H}_2\text{O}$  and  $\text{CO}_2$  to glucose by photosynthesis and under dark conditions they consume glucose for survival. They can generate electricity from both the photosynthetic and the respiratory machinery that provide the foundation of PMFCs if these electrons are collected.<sup>17</sup>

<sup>a</sup> Department of Analytical Chemistry/Biochemistry and Structural Biology, Lund University, P.O. Box 124, SE-22100 Lund, Sweden.

E-mail: Lo.Gorton@biochemistry.lu.se, Kamrul.Hasan@biochemistry.lu.se

<sup>b</sup> Department of Materials Science and Nanotechnology Engineering, KTO Karatay University, 42020 Konya, Turkey

<sup>c</sup> School of Chemistry, National University of Ireland Galway, University Road, Galway, Ireland

<sup>d</sup> Cawthron Institute, Private Bag 2, Nelson, New Zealand

† Electronic supplementary information (ESI) available. See DOI: 10.1039/c4cp04307c



To investigate the presence of photosynthetic pigment inside CYN82, absorbance measurements of the extracted photosynthetic dye were made and it was confirmed that the most essential photosynthetic pigment responsible for current generation,<sup>18</sup> chlorophyll *a*, appeared at a wavelength of 665 nm. In addition other necessary pigments such as chlorophyll *b* and carotenoids were visible in the spectrum at  $\approx 400$  nm (ESI,† Fig. S1). The appearance of these pigments at their particular wavelengths confirms the necessary photosynthetic activity of CYN82.<sup>19</sup>

DET between the cells and electrodes may be preferable over mediated electron transfer (MET) for power generation, since it minimizes the over-potential in bio-electrochemical systems and simplifies the electrochemical cell design and operation. We investigated whether CYN82 can communicate with a solid bare graphite electrode directly without any mediator. It has been revealed that DET of cyanobacteria<sup>5</sup> is feasible *via* their naturally produced nanowires, proposed to be similar to that reported for metal reducing bacteria.<sup>20</sup> To investigate for the possibility for DET, CYN82 cells were adsorbed on a bare graphite electrode and illuminated with a fibre optic light source with a light intensity of  $44 \text{ mW cm}^{-2}$  (a light intensity where photosynthesis is no longer limited by light) and only pure electrolyte was present as an electron donor (Fig. 1).

It was shown (Fig. 1) that when the CYN82 cells were illuminated they generated a photocurrent of  $1.30 \text{ } \mu\text{A cm}^{-2}$  evaluated as the difference in registered current density between situations “light on” and “light off” ( $6.85\text{--}5.70 \text{ } \mu\text{A cm}^{-2}$ ). We anticipate interactions between oxygen containing functional groups on the surface of the graphite<sup>21</sup> and quinones present in the photosynthetic electron transfer chain (PETC) of CYN82. Previously it was reported that the plastoquinone pool in PETC is responsible for the direct electrogenic activity between the cells and the electrode.<sup>5</sup> The reason for current generation was attributed to photo-electrolysis of water by the PETC inside the CYN82 cells.

In contrast, when the light was turned off the photocurrent decreased, since in the absence of light no water-splitting can

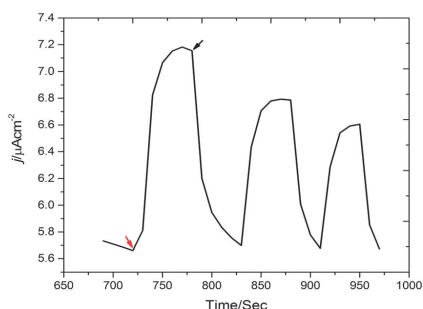


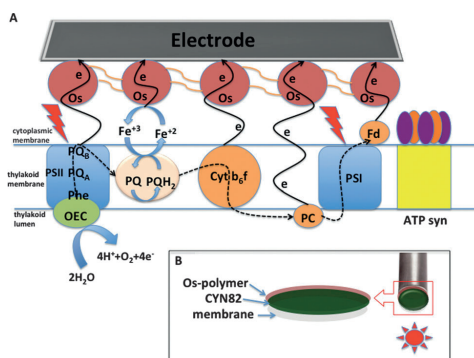
**Fig. 1** DET between CYN82 (9.5  $\mu\text{g}$ , wet weight) and a bare-graphite electrode. Electrolyte: 10 mM phosphate buffer at pH 7.0, 10 mM NaCl and 5 mM  $\text{MgCl}_2$ , applied potential: 350 mV vs.  $\text{Ag|AgCl}$  (sat. KCl), light intensity:  $44 \text{ mW cm}^{-2}$ , black and red arrows stand for light off and on, respectively.

occur, which is the origin of the electrons that can be transferred to the electrode surface through the PETC (Fig. 1). It is proposed here that PETC in the CYN82 cells is responsible for the photocurrent generation. Control experiments with unmodified graphite electrodes yielded no photocurrent when illuminated.

To improve the photocurrent density we investigated four different cationic ORP<sup>14,22</sup> (ESI,† Fig. S2) denoted Os-A, Os-B, Os-C and Os-D, having different ligands to the metal center resulting in a range of redox potentials ( $E^\circ$ ) from  $-0.07$  (Os-A),  $0.12$  (Os-B),  $0.22$  (Os-C) and  $0.35 \text{ V}$  (Os-D) vs.  $\text{Ag|AgCl}$  (sat. KCl). This potential window covers a large part of the potential range of PETC and therefore it is possible to extract electrons generated from PETC of the CYN82 cells at various positions. The approximate  $E^\circ$  of the participating redox complexes in the PETC are  $+1.0$  (P680),  $-1.05$  (P680\*),  $+0.21$  (P700),  $-1.52$  (P700\*),  $-0.47$  (PQ<sub>A</sub>),  $-0.3$  (PQ<sub>B</sub>),  $-0.11$  (Cyt *b<sub>6</sub>f*) and  $+0.11$  (PC) v vs.  $\text{Ag|AgCl}$  (sat. KCl).<sup>23</sup>

In Scheme 1 the possible electron transfer sites are presented. Recently, Os-C was successfully used to “wire” heterotrophically grown *Rhodobacter capsulatus* cells,<sup>24</sup> where it forms a 3-D hydrogel through electrostatic interactions between the cationic ORP and the anionic bacterial cell membrane precipitating onto the electrode surface. A similar interaction is expected to take place between the ORP and the CYN82 cells.

Photocurrent generation with Os-A, Os-B, Os-C, and Os-D exhibited  $1.32$ ,  $4.24$ ,  $8.64$  and  $6.33 \text{ } \mu\text{A cm}^{-2}$  (Fig. 2). The photocurrent increases linearly with an increased  $E^\circ$  of ORP except for Os-D. It is expected that when increasing the  $E^\circ$  a higher photocurrent is to be exhibited as the thermodynamic driving force is increased for donation of electrons to the ORP. However, variation in accessibility of the redox complex to the electron-donating site



**Scheme 1** (A) Schematic potential electron transfer sites of cyanobacterial cells immobilized on a graphite electrode *via* different redox complexes in the PETC e.g., PSII, plastoquinone (PQ), cytochrome *b<sub>6</sub>f* (Cyt *b<sub>6</sub>f*), plastocyanin (PC), PSI, and ferridoxin (Fd). OEC, Phe, PQ<sub>A</sub>, PQ<sub>B</sub>, PQH<sub>2</sub> and ATP syn represent oxygen evolving complex, pheophytin, plastoquinone A, plastoquinone B, plastoquinol and ATP synthase respectively. PSI and PSII refer to the photosynthetic reaction centres and their respective pigments are P680 (P680\*) and P700 (P700\*), where \* signifies the excited state. (B) The immobilization of cyanobacteria on an ORP modified graphite electrode surface and illumination approach.

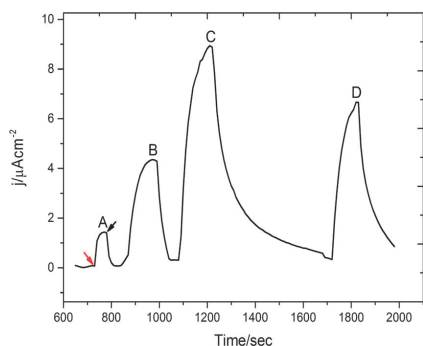


Fig. 2 Comparison of background corrected (light off conditions) photocurrent generation mediated with (A) Os-A, (B) Os-B, (C) Os-C and (D) Os-D; the  $E^{o'}$  of Os-A, Os-B, Os-C and Os-D was  $-0.07$ ,  $0.12$ ,  $0.22$  and  $0.35$  V vs. Ag/AgCl, respectively, applied potential:  $+130$  mV  $> E^{o'}$  of each ORP, electrolyte:  $10$  mM phosphate buffer at pH  $7.0$ ,  $10$  mM NaCl and  $5$  mM  $MgCl_2$ , light intensity:  $44$   $mW\ cm^{-2}$ , black and red arrows stand for light off and on respectively. The results of four different experiments with the four different ORPs have been combined in this figure.

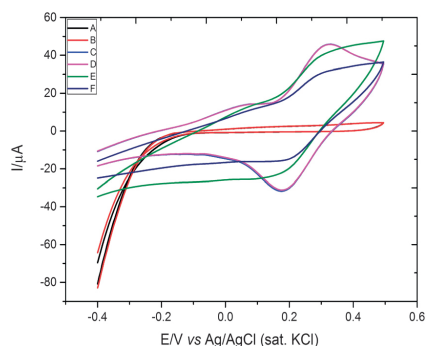


Fig. 3 CVs of a (A) bare graphite electrode with light off, (B) bare graphite electrode with light on, (C) Os-C modified electrode with light off, (D) Os-C modified electrode with light on, (E) CYN82 immobilized on Os-C modified electrode with light on, (F) CYN82 immobilized on Os-C modified electrode with light off, applied potential:  $350$  mV vs. Ag/AgCl (sat. KCl), light intensity:  $44$   $mW\ cm^{-2}$ . Electrolyte:  $10$  mM phosphate buffer at pH  $7.0$ ,  $10$  mM NaCl, and  $5$  mM  $MgCl_2$ .

in the PETC should also be of importance. The lower  $E^{o'}$  values of P680\*, P700\*, PQ<sub>A</sub>, PQ<sub>B</sub>, PQ, and Cyt *b<sub>6</sub>f* compared to the  $E^{o'}$  values of the ORPs indicate that they should be able to donate electrons to the ORP. Control experiments with the ORPs but with the absence of cells revealed no photocurrent when illuminated.

However, the short lifetime of P700\* and P680\* makes them unlikely to be possible electron donors to ORP rather than for the natural electron acceptors in the electron transfer pathway of the photosystems. The increase in photocurrent generation from Os-A to Os-C indicates that  $E^{o'}$  of the ORP plays an important role in accepting electrons from PETC. Reduced plastoquinone (PQH<sub>2</sub>), known for having a long life time and predominant presence in PETC,<sup>25</sup> makes it a good electron donor, whereas Cyt *b<sub>6</sub>f* and PC could also be used. Here, Os-C generates the highest photocurrent ( $8.64$   $\mu A\ cm^{-2}$ ) possibly because of better the combination of accessibility to the PETC in the lipid bilayer membrane, higher  $E^{o'}$ , and greater solubility.<sup>13</sup> Therefore, the rest of the experiments were conducted with this polymer.

The concentration of CYN82 on the electrode surface was optimized and it was found that  $9.5$   $\mu g$  (wet weight) shows the highest photocurrent (ESI,† Fig. S3). When the concentration increased ( $> 9.5$   $\mu g$ ) the photocurrent goes down, possibly due to the formation of too thick a cell layer, where light does not reach through the entire layer of cells. Therefore, all the experiments presented here were conducted with this optimized concentration.

To investigate the effect of illumination CVs were recorded for bare, Os-C and CYN82 with Os-C modified electrodes. There is an insignificant influence of light either on the bare graphite electrode (Fig. 3A and B) or on the Os-C polymer modified electrode (Fig. 3C and D). The  $E^{o'}$  of Os-C is, from the CV,  $0.22$  V in agreement with the previously determined value.<sup>26</sup>

When CYN82 cells were immobilized on Os-C modified electrodes and in the absence of light (Fig. 3F), the intensity of both the anodic and the cathodic peak currents goes down since the CYN82 cells retard the redox response of the osmium redox centers of Os-C due to the strong electrostatic interactions. A similar change in response was observed for electrodes modified with redox polymers with and without different kinds of bacterial cells.<sup>14</sup>

The most significant response was observed for electrodes modified with both CYN82 cells in combination with Os-C when illuminated (Fig. 3E) as the anodic and cathodic current increases. The Os<sup>2+/3+</sup> redox centres in the polymer matrix are reduced by available electrons from photo-electrolysis of the electrolyte and re-oxidized at the electrode surface polarized at a higher potential ( $E_{app} > E^{o'}$  of Os-C). It can be assumed from these CVs that the Os<sup>3+</sup> moieties can easily accept electrons produced during the photosynthetic event and shuttle them to the electrode.

The influence of light intensity on the generation of photocurrent was investigated and the results are shown in ESI,† Fig. S4. Studies showed that the light intensity has a significant influence on the photosynthetic carbon reduction cycle, however, too much light may destroy the photosynthetic apparatus, especially that of PSII.<sup>27</sup> It is known that the light intensity to saturate photosynthesis is obtained for a light intensity of  $25$   $mW\ cm^{-2}$ . In our experiments the photocurrent increases from  $2.32$  to  $9.21$   $\mu A\ cm^{-2}$  when increasing the light intensity from  $44$  to  $680$   $mW\ cm^{-2}$ . A similar response was observed for thylakoid membranes isolated from spinach.<sup>28</sup> This is attributed to the fact that while the light intensity increases, a larger portion of the plastoquinone pool in PETC gets reduced by the electrons available from photolysis of the electrolyte and will become oxidized at the electrode resulting in a higher photocurrent. To avoid any kind of photo-damage of the photosynthetic machinery of the CYN82 cells, it was decided to conduct all the experiments at  $44$   $mW\ cm^{-2}$ .

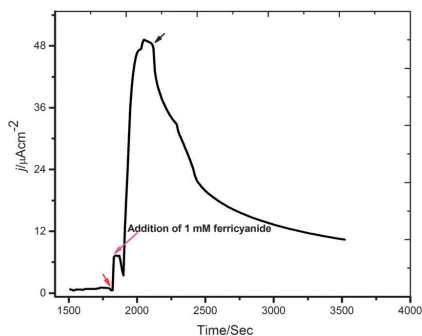


Fig. 4 Improvement of photocurrent generation with a double mediator. The figure shows background corrected (light off conditions) current density. CYN82 immobilized on Os-C modified electrode, [ferricyanide]: 1 mM, applied potential: 350 mV vs. Ag/AgCl (sat. KCl), light intensity: 44 mW cm<sup>-2</sup>. Electrolyte: 10 mM phosphate buffer at pH 7.0, 10 mM NaCl, and 5 mM MgCl<sub>2</sub>, black and red arrow stands for light off and on respectively.

Ferricyanide is known to mediate electron transfer from multiple photosynthetic reaction centers to electrodes and can diffuse easily through the cell membranes and is a suitable choice because of its low inherent photo activity compared to any quinone derivatives that are also commonly used as mediators.<sup>18</sup> To explore the effect of ferricyanide on the photocurrent, it was added to the electrolyte while the CYN82 cells were immobilized on the surface of a bare graphite electrode. The results show that CYN82 cells generated 5.92  $\mu\text{A cm}^{-2}$  in the presence of 1.0 mM ferricyanide when the light was turned on (ESI,† Fig. S5).

To boost up the generation of the photocurrent, one soluble (ferricyanide) and one polymeric mediator (Os-C) were used together. Ferricyanide is known to be an efficient electron acceptor for both PSI and PSII,<sup>29</sup> and Os-C is known to exhibit efficient electron transfer properties with bacterial cells.<sup>14</sup> When the CYN82 cells were immobilized on the Os-C modified electrode, the photocurrent upon addition of 1 mM ferricyanide increased from 6.74 to 48.15  $\mu\text{A cm}^{-2}$  (Fig. 4).

The reason can be attributed to the low molecular weight ferricyanide having higher diffusing capability into the membrane than the Os-C polymer and results in more efficient electron transfer from the cells to the electrode. A similar increase in response was demonstrated when the cyanobacterial cells were treated with another soluble mediator *p*-benzoquinone.<sup>5</sup> A higher catalytic response is also observed for *Saccharomyces cerevisiae* cells when using a double mediator system.<sup>30</sup> Control experiments with ferricyanide in solution and with bare graphite exhibited no significant photocurrent when illuminated.

The source of photocurrent generation is of great importance to discover, and especially, which particular photosynthetic pigment is responsible for donating electrons to the ORP. Among all photosynthetic inhibitors, diuron is the most widely used and known particularly for inhibiting PSII, blocking the electron transfer from PSII to plastoquinone (PQ) by binding with either PQ<sub>A</sub> or PQ<sub>B</sub>. When diuron binds with PQ<sub>B</sub> the electron

transfer is shut down entirely, whereas binding with PQ<sub>A</sub> it slows down the electron transfer rate.<sup>31</sup> The effect of inhibition by diuron at different concentrations as well as comparison with non-inhibited photocurrent is displayed in ESI,† Fig. S6. When the concentration of diuron was increased gradually from 0 mM to 0.4 mM, the photocurrent generation went down from 8.52 to 1.20  $\mu\text{A cm}^{-2}$  and at 0.5 mM, more than 90% of the original photocurrent is inhibited. It can be inferred from this phenomenon that diuron binds with PQ<sub>B</sub>. A reasonable suggestion is thus that photo-electrolysis of the electrolyte by PSII is the major source of photocurrent in this entire system.

## Conclusions

In this work both direct and mediated electrogenic activity of cyanobacterial cells have been confirmed as the source of photocurrent. Of the four investigated ORPs, Os-C yields a significant photocurrent generation of 8.64  $\mu\text{A cm}^{-2}$ , possibly because of a combination of a high  $E^{o'}$ , a greater accessibility to the membrane of the cyanobacterial cells, and a better solubility. When ferricyanide was added to the electrolyte in combination with the ORP the photocurrent reaches a maximum of 48.15  $\mu\text{A cm}^{-2}$ . We believe this observation has substantial implication for future photosynthetic solar energy conversion. No optimization of the electrode with any conductive nanomaterials and engineering of the cyanobacterium has been attempted to enhance the photocurrent density. However, for further progress of power generation future work should focus on the use of three-dimensional electrode material, greater design of the electrochemical cell, and an improved immobilization technique. An understanding of the photosynthetic light harvesting complex on the molecular level and a detailed investigation of its electron transfer mechanism would be useful to reveal nature's own finely tuned energy generation process.

## Acknowledgements

The authors thank The Swedish Research Council (projects: 2010-5031, 2010-2013), The Nanometer consortium at Lund University (nmc@LU), The European Commission (projects NMP4-SL-2009-229255 "3D-Nanobiodevice", FP7-PITN-GA-2010-264772 "Chebana" and FP7-PEOPLE-2013-ITN "Bioenergy"), Federation of European Biochemical Societies, FEBS and New Zealand Ministry of Innovation, Business and Enterprise (PROJ-13838-NMTS-LVL) for financial support.

## Notes and references

- A. J. McCormick, P. Bombelli, A. M. Scott, A. J. Philips, A. G. Smith, A. C. Fisher and C. J. Howe, *Energy Environ. Sci.*, 2011, 4, 4699–4709.
- J. M. Pisciotta, Y. Zou and I. V. Baskakov, *PLoS One*, 2010, 5, e10821.
- W. F. J. Vermaas, *eLS*, John Wiley & Sons, Ltd, Chichester, 2001, 10.1038/npg.els.0001670.

- 4 W. Adams III, C. R. Zarter, K. Mueh, V. E. Amiard and B. Demmig-Adams, in *Photoprotection, Photoinhibition, Gene Regulation, and Environment*, ed. B. Demmig-Adams, W. Adams, III and A. Mattoo, Springer, Netherlands, 2006, ch. 5, vol. 21, pp. 49–64.
- 5 N. Sekar, Y. Umasankar and R. P. Ramasamy, *Phys. Chem. Chem. Phys.*, 2014, **16**, 7862–7871.
- 6 M. Rosenbaum, Z. He and L. T. Angenent, *Curr. Opin. Biotechnol.*, 2010, **21**, 259–264.
- 7 O. Kruse, J. Rupperecht, J. H. Mussgnug, G. C. Dismukes and B. Hankamer, *Photochem. Photobiol. Sci.*, 2005, **4**, 957–970.
- 8 C. F. Meunier, J. C. Rooke, A. Léonard, H. Xie and B. L. Su, *Chem. Commun.*, 2010, **46**, 3843–3859.
- 9 K. Tanaka, R. Tamamushi and T. Ogawa, *J. Chem. Technol. Biotechnol.*, 1985, **35**, 191–197.
- 10 T. Yagishita, T. Horigome and K. Tanaka, *J. Chem. Technol. Biotechnol.*, 1993, **56**, 393–399.
- 11 Y. Zou, J. Pisciotto, R. B. Billmyre and I. V. Baskakov, *Biotechnol. Bioeng.*, 2009, **104**, 939–946.
- 12 A. Heller, *Acc. Chem. Res.*, 1990, **23**, 128–134.
- 13 A. Heller, *Curr. Opin. Chem. Biol.*, 2006, **10**, 664–672.
- 14 K. Hasan, S. A. Patil, D. Leech, C. Hägerhäll and L. Gorton, *Biochem. Soc. Trans.*, 2012, **40**, 1330–1335.
- 15 V. Coman, T. Gustavsson, A. Finkelsteinas, C. Von Wachenfeldt, C. Hägerhäll and L. Gorton, *J. Am. Chem. Soc.*, 2009, **131**, 16171–16176.
- 16 V. M. Luimstra, S. J. Kennedy, J. Güttler, S. A. Wood, D. E. Williams and M. A. Packer, *J. Appl. Phycol.*, 2013, 1–9.
- 17 T. Moriuchi, M. Keisuke and Y. Furukawa, *Int. J. Precis. Eng. Man.*, 2008, **9**, 23–27.
- 18 J. O. Calkins, Y. Umasankar, H. O'Neill and R. P. Ramasamy, *Energy Environ. Sci.*, 2013, **6**, 1891–1900.
- 19 J. Pisciotto, Y. Zou and I. Baskakov, *Appl. Microbiol. Biotechnol.*, 2011, **91**, 377–385.
- 20 Y. A. Gorby, S. Yanina, J. S. McLean, K. M. Rosso, D. Moyles, A. Dohnalkova, T. J. Beveridge, I. S. Chang, B. H. Kim, K. S. Kim, D. E. Culley, S. B. Reed, M. F. Romine, D. A. Saffarini, E. A. Hill, L. Shi, D. A. Elias, D. W. Kennedy, G. Pinchuk, K. Watanabe, S. Ishii, B. Logan, K. H. Nealson and J. K. Fredrickson, *Proc. Natl. Acad. Sci. U. S. A.*, 2006, **103**, 11358–11363.
- 21 K. F. Blurton, *Electrochim. Acta*, 1973, **18**, 869–875.
- 22 J. Du, C. Catania and G. C. Bazan, *Chem. Mater.*, 2013, **26**, 686–697.
- 23 I. McConnell, G. Li and G. W. Brudvig, *Chem. Biol.*, 2010, **17**, 434–447.
- 24 K. Hasan, S. A. Patil, K. Go'recki, D. Leech, C. Hägerhäll and L. Gorton, *Bioelectrochemistry*, 2013, **93**, 30–36.
- 25 J. Kruk and S. Karpinski, *Biochim. Biophys. Acta, Bioenerg.*, 2006, **1757**, 1669–1675.
- 26 M. N. Zafar, F. Tasca, S. Boland, M. Kujawa, I. Patel, C. K. Peterbauer, D. Leech and L. Gorton, *Bioelectrochemistry*, 2010, **80**, 38–42.
- 27 I. Vass, *Biochim. Biophys. Acta, Bioenerg.*, 2012, **1817**, 209–217.
- 28 K. Hasan, Y. Dilgin, S. C. Emek, M. Tavahodi, H.-E. Åkerlund, P.-Å. Albertsson and L. Gorton, *ChemElectroChem*, 2014, **1**, 131–139.
- 29 M. Mimeault and R. Carpentier, *Enzyme Microb. Technol.*, 1988, **10**, 691–694.
- 30 A. Heiskanen, V. Coman, N. Kostasheva, D. Sabourin, N. Haslett, K. Baronian, L. Gorton, M. Dufva and J. Emnéus, *Anal. Bioanal. Chem.*, 2013, **405**, 3847–3858.
- 31 B. D. Hsu, J. Y. Lee and R. L. Pan, *Biochem. Biophys. Res. Commun.*, 1986, **141**, 682–688, DOI: 10.1016/S0006-291X(86)80226-1.



COMMUNICATION

**Photo-electrochemical communication between cyanobacteria (*Leptolyngbia* sp.) and osmium redox polymer modified electrodes**

Cite this: DOI: 10.1039/x0xx00000x

Received 00th January 2012,  
Accepted 00th January 2012

DOI: 10.1039/x0xx00000x

www.rsc.org/

Kamrul Hasan<sup>\*a</sup>, Huseyin Bekir Yildiz<sup>b</sup>, Eva Sperling<sup>a</sup>, Peter Ó Conghaile<sup>c</sup>, Michael A. Packer<sup>d</sup>, Dónal Leech<sup>c</sup>, Cecilia Hägerhäll<sup>a</sup>, Lo Gorton<sup>\*a</sup>

**Electronic Supplementary Information (ESI):**

Chemicals

Diuron [(1,1-dimethyl, 3-(3', 4'-dichlorophenyl) urea)], sodium phosphate dibasic, and sodium phosphate monobasic, magnesium chloride, sodium chloride and potassium hexacyanoferrate (III) were purchased from Sigma-Aldrich (Munich, Germany) and Merck (Darmstadt, Germany) and were of either research or analytical grade. All aqueous solutions were prepared by using water purified and deionized (18 MΩ) with a Milli-Q system (Millipore, Bedford, MA, USA).

Osmium redox polymer

[Os(4,4'-dimethoxy-2,2'-bipyridine)<sub>2</sub>(poly-vinylimidazole)<sub>10</sub>Cl]<sup>2+/+</sup>, E<sup>o'</sup> = -70 mV vs. Ag|AgCl (3 M KCl) Os-A<sup>1,2</sup>, [Os(4,4'-dimethyl-2,2'-bipyridine)<sub>2</sub>(poly-vinylimidazole)<sub>10</sub>Cl]<sup>2+/+</sup>, E<sup>o'</sup> = 120 mV vs. Ag|AgCl (3 M KCl) Os-B<sup>3</sup>, [Os(2,2'-bipyridine)<sub>2</sub>(poly-vinylimidazole)<sub>10</sub>Cl]<sup>2+/+</sup>, E<sup>o'</sup> = 220 mV vs. Ag|AgCl (3 M KCl) Os-C<sup>4</sup> and [Os(4,4'-dichloro-2,2'-bipyridine)<sub>2</sub>(PVI)<sub>10</sub>Cl]<sup>2+/+</sup>, E<sup>o'</sup> = 350 mV vs. Ag|AgCl (3 M KCl), Os-D<sup>2,5</sup> were synthesized and reported as described previously in the literature.

Measurements and instrumentation

All electrochemical experiments (cyclic voltammetry, CV and chronoamperometry, CA) were carried out using a PalmSens potentiostat (model Emstat<sup>2</sup>, Palm Instruments BV, Utrecht, The Netherlands) equipped with PStace software with a conventional three electrode configuration; a Ag|AgCl (sat. KCl) (Sensortechnik, Meinsberg, Germany), a bare/polymer modified graphite (active surface area A = 0.0731 cm<sup>2</sup>) and platinum foil served as the reference, working and counter electrodes, respectively. A Metrohm 827-pH lab meter (Metrohm AG, Herisau, Switzerland) was used for setting the pH values of the solutions. In order to perform photo-electrochemical experiments, a fibre optic illuminator FOI-150-220 (150 W and 220 V) with FOI-5 Light Guide (Titan Tool Supply Inc., Buffalo, NY, USA) was used to illuminate the electrode surface. The illuminator was adjusted using a light intensity meter (Tehtum Lab AB, Umeå, Sweden). To excite the photosynthetic activity of CYN82, a light intensity of 44 mWcm<sup>-2</sup> was used. Phosphate buffer (5 mM NaH<sub>2</sub>PO<sub>4</sub>, 5 mM Na<sub>2</sub>HPO<sub>4</sub>, 10 mM NaCl, 5 mM MgCl<sub>2</sub>, at pH 7.0) was used as an electrolyte in all these studies. The electrolyte solutions were

degassed with pure argon for  $\approx 10$  min before measurements, which were performed at room temperature. All reported data were based on three independent experimental replicas. All potential mentioned in this manuscript is according to Ag|AgCl (sat. KCl) as a reference electrode.

#### Modification of working electrode

Graphite rods (Alfa Aesar GmbH & Co KG, Karlsruhe, Germany, AGKSP grade, ultra "F" purity, and 3.05 mm diameter) were used for making the working electrodes. The end of the graphite rod was polished on fine emery SiC paper (Turbak Durite, P1200), carefully washed with Milli-Q water, and finally dried. Then an aliquot of 5  $\mu\text{L}$  of an ORP solution (10 mg  $\text{mL}^{-1}$  in Milli-Q water) was spread onto the entire active surface of the electrode (0.0731  $\text{cm}^2$ ). Afterwards the electrode was dried at room temperature for 10 to 15 min and then 9.5  $\mu\text{g}$  of CYN82 was spread onto the surface. Before use, a dialysis membrane (Spectrum Laboratories Inc., Rancho Dominguez, CA, USA, molecular mass cut-off: 6000–8000) was used to keep the ORP and CYN82 on the electrode surface. The dialysis membrane (pre-soaked in phosphate buffer at pH 7.0) was pressed onto the electrode and fixed tightly with a rubber O-ring and Para film. Note that the amount of ORP (5  $\mu\text{L}$ ) and CYN82 bacteria (9.5  $\mu\text{g}$ ) are the optimized standards.

#### CYN82 growth condition and inoculum preparation

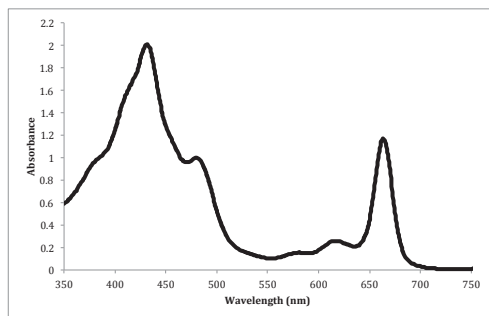
The cyanobacterium investigated in this work is *Leptolyngbia* sp. CYN826 and was collected from the Cawthron Institute Collection Culture of Microalgae (CICCM), New Zealand. The growth and culture condition of CYN82 reported by Luimstra et al<sup>6</sup>. In brief a low ionic strength MLA medium was used as growth medium and a light source of 40  $\mu\text{mol photons m}^{-2} \text{s}^{-1}$  from a white cool fluorescent lamp was arranged over the culture with a regime of 12:12 light and dark. The culture growth was maintained at room temperature ( $\approx 21^\circ \text{C}$ ). To harvest the CYN82, the cells were centrifuged at 4000 rpm for 10 min at  $20^\circ \text{C}$  and

later on washed with electrolyte and centrifuged again at the same condition. Finally, the CYN82 cells were re-suspended in the same electrolyte to adjust the concentration at 1 g/ml and used immediately for electrochemical measurements. MLA is a complex growth medium that is comprised of  $\text{NaNO}_3$  (2.00 mM),  $\text{NaHCO}_3$  (2.019 mM),  $\text{MgSO}_4 \cdot 7\text{H}_2\text{O}$  (200.43  $\mu\text{M}$ ),  $\text{CaCl}_2 \cdot 2\text{H}_2\text{O}$  (200  $\mu\text{M}$ ),  $\text{K}_2\text{HPO}_4$  (199.77  $\mu\text{M}$ ),  $\text{NaEDTA}$  (11.7  $\mu\text{M}$ ),  $\text{H}_2\text{SeO}_3$  (10.00  $\mu\text{M}$ ),  $\text{H}_3\text{BO}_3$  (39.95  $\mu\text{M}$ ),  $\text{MnCl}_2 \cdot 4\text{H}_2\text{O}$  (18.19  $\mu\text{M}$ ),  $\text{FeCl}_3 \cdot 6\text{H}_2\text{O}$  (5.85  $\mu\text{M}$ ),  $\text{CuSO}_4 \cdot 5\text{H}_2\text{O}$  (40.1  $\mu\text{M}$ ),  $\text{ZnSO}_4 \cdot 7\text{H}_2\text{O}$  (76.5  $\mu\text{M}$ ),  $\text{CoCl}_2 \cdot 6\text{H}_2\text{O}$  (79.86  $\mu\text{M}$ ),  $\text{Na}_2\text{MoO}_4 \cdot 2\text{H}_2\text{O}$  (24.8  $\mu\text{M}$ ), biotin (0.05  $\mu\text{g/L}$ ), vitamin  $\text{B}_{12}$  (0.05  $\mu\text{g/L}$ ), and thiamine  $\text{HCl}$  (100  $\mu\text{g/L}$ )<sup>7</sup>.

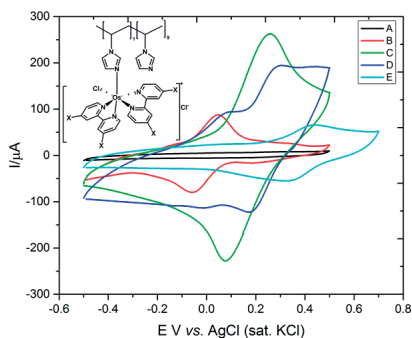
#### Photosynthetic dye extraction

For chlorophyll extraction the cells were spun down for 5 min at 4000 rpm and 5 mL of a 7:2 acetone/methanol solution was added to the pellet. The mixture was then incubated over night under slow shaking. The green supernatant was then either added into an extractor or the spectrum was immediately determined with a spectrophotometer.

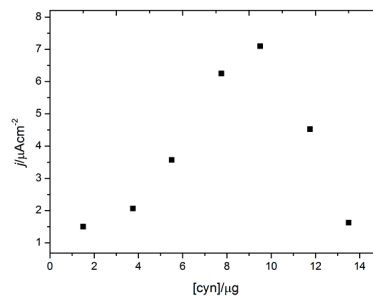
## Supplementary figure



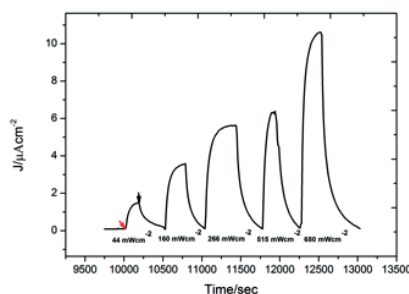
**Supplementary Figure 1.** Absorbance spectrum of CYN82. Photosynthetic pigment extracted from *Lyptolyngbia* sp. (CYN82). The distinguished peak of chlorophyll a appears at 665 nm wavelengths and chlorophyll b, carotenoid at 400 nm.



**Supplementary Figure 2.** The cyclic voltammograms (CVs) of graphite electrode modified with different osmium redox polymers (ORP); (A) bare graphite electrode; (B) Os-A; (C) Os-B; (D) Os-C; (E) Os-D. Inset shows the general chemical structure of osmium redox polymer, where Os-A ( $X = \text{OCH}_3$ ), Os-B ( $X = \text{CH}_3$ ), Os-C ( $X = \text{H}$ ) and Os-D ( $X = \text{Cl}$ ).



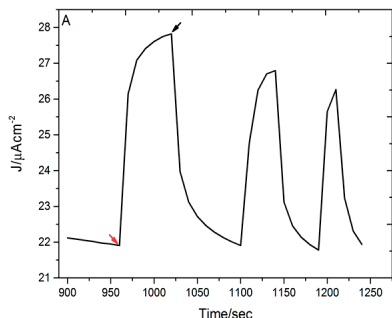
**Supplementary Figure 3.** The optimization of CYN82 concentration over Os-C polymer modified electrode, CYN82 concentration varied from 1.50, 3.75, 5.50, 7.75, 9.50, 11.75 and 13.50  $\mu\text{g}$  and optimized concentration fixed at 9.50  $\mu\text{g}$ , applied potential: 350 mV vs Ag|AgCl (sat. KCl), electrolyte: 10 mM phosphate buffer at pH 7.0, 10 mM NaCl and 5 mM  $\text{MgCl}_2$ , light intensity: 44  $\text{mWcm}^{-2}$ .



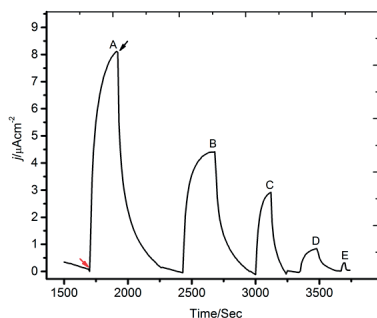
**Supplementary Figure 4.** The effect of light intensity on photocurrent generation. The figure shows background corrected (light off conditions) current density. The light intensity raises from 44, 160, 266, 515 and 680  $\text{mWcm}^{-2}$  that results photocurrent increases in 2.32, 3.87, 5.46, 6.00 and 9.21  $\mu\text{Acm}^{-2}$ . CYN82 (1.50  $\mu\text{g}$ ) immobilized on Os-C modified electrode, applied potential: 350 mV vs Ag|AgCl (sat. KCl), electrolyte: 10 mM phosphate buffer at pH 7.0, 10 mM NaCl and 5 mM  $\text{MgCl}_2$ , light intensity: 44  $\text{mWcm}^{-2}$ , black and



red arrow stand for light off and on phenomena and valid to all curves.



**Supplementary Figure 5.** Photocurrent generation from ferricyanide (1 mM) mediated electron transfer. CYN82 (9.50 μg) immobilized on bare graphite electrode, applied potential: 350 mV vs Ag|AgCl (sat. KCl), electrolyte: 10 mM phosphate buffer at pH 7.0, 10 mM NaCl and 5 mM MgCl<sub>2</sub>, light intensity: 44 mWcm<sup>-2</sup>, black and red arrow stand for light off and on phenomena and valid to all curves.



**Supplementary Figure 6.** The inhibition of photocurrent by diuron, a specific inhibitor for photosystem II. The figure shows background corrected (light off conditions) current density. The diuron concentration increases from 0.2, 0.3, 0.4 and 0.5 mM and consequences of photocurrent down to 4.78, 3.27, 1.20 and 0.65 μAcm<sup>-2</sup>, while

non-inhibited photocurrent was 8.52 μAcm<sup>-2</sup>. CYN82 (9.50 μg) immobilized on Os-C modified electrode, applied potential: 350 mV vs. Ag|AgCl (sat. KCl), electrolyte: 10 mM phosphate buffer at pH 7.0, 10 mM NaCl and 5 mM MgCl<sub>2</sub>, light intensity: 44 mWcm<sup>-2</sup>, black and red arrow stand for light off and on phenomena and valid to all curves.

### ESI References

1. C. Taylor, G. Kenausis, I. Katakis and A. Heller, *J. Electroanal. Chem.*, 1995, **396**, 511-515.
2. N. Mano and A. Heller, *J. Electrochem. Soc.*, 2003, **150**, A1136-A1138.
3. T. J. Ohara, R. Rajagopalan and A. Heller, *Anal. Chem.*, 1994, **66**, 2451-2457.
4. E. M. Kober, J. V. Caspar, B. P. Sullivan and T. J. Meyer, *J. Inorg. Chem.*, 1988, **27**, 4587-4598.
5. P. A. Jenkins, S. Boland, P. Kavanagh and D. Leech, *Bioelectrochemistry*, 2009, **76**, 162-168.
6. V. Luimstra, S.-J. Kennedy, J. Güttler, S. Wood, D. Williams and M. Packer, *J. Appl. Phycol.*, 2013, DOI: 10.1007/s10811-013-0051-2, 1-9.
7. C. S. Bolch and S. Blackburn, *J. Appl. Phycol.*, 1996, **8**, 5-13.

# Paper VIII



# Photoelectrochemical Wiring of *Paulschulzia pseudovolvox* (Algae) to Osmium Polymer Modified Electrodes for Harnessing Solar Energy

Kamrul Hasan,\* Emre Çevik, Eva Sperling, Michael A. Packer, Dónal Leech, and Lo Gorton\*

Studies on biological photovoltaics based on intact organisms are challenging and in most cases include diffusing mediators to facilitate electrochemical communication with electrodes. However, using such mediators is impractical. Instead, surface confined Os-polymers have been successfully used in electrochemical studies including oxidoreductases and bacterial cells but not with algae. Photoelectrogenic activity of a green alga, *Paulschulzia pseudovolvox*, immobilized on graphite or Os-polymer modified graphite is demonstrated. Direct electron transfer is revealed, when no mediator is added, between algae and electrodes with electrons emerging from photolysis of water via the cells to the electrode exhibiting a photocurrent density of  $0.02 \mu\text{A cm}^{-2}$ . Os-polymers with different redox potentials and structures are used to optimize the energy gap between the photosynthetic complexes of the cells and the Os-polymers and those of greater solubility, better accessibility with membranes, and relatively higher potentials yielded a photocurrent density of  $0.44 \mu\text{A cm}^{-2}$ . When benzoquinone is included to the electrolyte, the photocurrent density reaches  $6.97 \mu\text{A cm}^{-2}$ . The photocurrent density is improved to  $11.50 \mu\text{A cm}^{-2}$ , when the cells are protected from reactive oxygen species when either superoxide dismutase or catalase is added. When adding an inhibitor specific for photosystem II, diuron, the photocurrent is decreased by 50%.

## 1. Introduction

The global primary energy resource, fossil fuels, are diminishing and their concurrent combustion greatly contributes to global climate change via the greenhouse effect.<sup>[1]</sup> The detrimental effect of  $\text{CO}_2$  emission to the atmosphere from fossil fuel combustion demands a carbon neutral energy production.<sup>[2]</sup> Solar energy is a vast sustainable energy source, where the amount of solar energy arriving to the earth in 1 h is more than that of the entire annual human energy consumption.<sup>[2]</sup> Biological photovoltaics (BPVs)<sup>[3]</sup> could be a potential energy generating technology that can use sunlight to produce electrical energy in a carbon neutral fashion. BPVs are similar to microbial fuel cells (MFCs), where photosynthetic microorganisms use sunlight for photolysis of water and provide electrons to the systems.<sup>[4,5]</sup> In ordinary MFCs, a regular supply of an electron donor, most often an organic compound, is required, whereas in BPVs water can be the only electron donor using sunlight for hydrolysis.<sup>[4]</sup> Photosynthetic microorgan-

isms in BPVs are self-sustainable, inexpensive to culture, stored metabolites inside the cells can generate power even in dark conditions and make them a greater promise over the typical voltaic cell.<sup>[6]</sup>

A variety of photosynthetic organisms can be used in BPVs,<sup>[7]</sup> e.g., purple bacteria,<sup>[8]</sup> cyanobacteria,<sup>[6,9]</sup> but eukaryotic algae are preferable, since they can be used to feed heterotrophic bacteria in a conventional MFC, while grown in a mixed culture.<sup>[10]</sup> Moreover, autotrophic organisms could be used to produce hydrogen as an alternative source of fuel.<sup>[6]</sup>

The electron transfer (ET) from photolysis of water to the electrode in BPVs is complicated, since photosynthesis in algae occurs in the chloroplasts, a sub-cellular organelle insulated by a thick cell wall. The photosynthetic energy is lost while ET occurs from one carrier to another in a long photosynthetic pathway. Instead, the ET processes are simpler in the individual isolated photosystems, i.e., photosystem I and II (PSI and PS II), however, they require extensive extraction and purification processes, suffer from long-term instability

K. Hasan, E. Sperling, Prof. L. Gorton  
Department of Analytical Chemistry/Biochemistry  
and Structural Biology  
Lund University  
P. O. Box 124, SE-22100 Lund, Sweden  
E-mail: Kamrul.Hasan@biochemistry.lu.se;  
Lo.Gorton@biochemistry.lu.se

E. Çevik  
Department of Genetics and Bioengineering  
Fatih University  
B. Cekmece, Istanbul 34500, Turkey

Dr. M. A. Packer  
Cawthron Institute  
Private Bag 2, Nelson, New Zealand

Prof. D. Leech  
School of Chemistry  
National University of Ireland Galway  
University Road, Galway, Ireland

DOI: 10.1002/aenm.201501100



and inadequate immobilization on electrode surfaces.<sup>[10]</sup> Nevertheless, the entire intact organisms containing the photosynthetic machinery are considered as better candidates compared with isolated chloroplasts, thylakoid membranes or photosystems, since the intact cells are easy to grow, self-sustainable and any deposited intracellular metabolites could generate power during the dark period. However, intact organisms in BPVs also suffer from intrinsic metabolic losses in the cells and make intracellular competition for energy to survive that makes them less efficient on a short-term basis compared with isolated photosystems. These inefficiencies need to be overcome to make such devices viable for practical and commercial applications.<sup>[10]</sup>

Since the rate of direct ET from viable phototrophic organisms to electrodes is insufficient, most studies of BPV also include a monomeric exogenous electron transfer mediator that can freely diffuse into the membranes housing the photosynthetic machinery and pick up charge and then transfer the charge to the electrode. Examples of such commonly used mediators in BPVs are, e.g., 2-hydroxy-1,4-naphthoquinone (HNQ)<sup>[11,12]</sup> and 2,6-dimethyl-1,4-benzoquinone (DMBQ).<sup>[13]</sup> Besides that, the majority of such studies were conducted with prokaryotic cyanobacteria, e.g., *Anabaena variabilis*<sup>[11]</sup> and *Synechocystis* sp.<sup>[13]</sup> In cyanobacteria, photosynthesis takes place in thylakoids inside the inner cell membrane, whereas in green algae, this event occurs in chloroplasts surrounded by complex cellular membranes and the cell wall. This would mean that the electron exit via the photosynthetic redox complexes (PRCs) of prokaryotic cyanobacteria should in principle be comparatively easier than those of their eukaryotic counterparts.<sup>[6]</sup>

The greatest benefit of using the above-mentioned exogenous mediators is the simplicity while selecting microorganisms as well as electrode materials. However, the inevitability of regular and continuous addition of these mediators makes them technologically unfeasible, environmentally unfriendly, practically incompatible<sup>[6]</sup> and maybe harmful for cells.<sup>[14]</sup> Instead, surface confined flexible osmium containing redox polymers (Os-polymers) have already been successfully used as efficient mediators in enzymatic biosensors, providing electron conduits between enzyme active sites and electrode surfaces.<sup>[15]</sup> Most of the characteristics of an ideal electron transfer mediator<sup>[16]</sup> are accomplished by Os-polymers, viz., the mediating functionality is strongly bound on side chains of an aqueous soluble highly flexible polymeric backbone (and will thus not diffuse away) making the mediator accessible to reach both redox active sites of enzymes as well as of biological membranes. The cationic nature of the Os-polymer allows it to form very strong electrostatic interactions with proteins and whole cells (most of which are negatively charged at neutral pH) and will thus also serve as an immobilization matrix for the bio-components that will together with the Os-polymer precipitate forming a hydrogel on the electrode surface, guaranteeing a very high local concentration of both mediating functionality and biological component. Os-polymers supply the systems including bacterial cells,<sup>[17–19]</sup> with high concentrations of stable mediating functionalities; form a 3D hydrogel<sup>[20]</sup> containing multiple layers of enzymes/cells,<sup>[21]</sup> in which substrates and products can easily diffuse in and out. Recently, Os-polymers were studied as electron

conduits between photosynthetic organisms (*Rhodospirillum rubrum*<sup>[22]</sup> and *Leptolyngbya* sp.<sup>[23]</sup>) and electrode surfaces. There are other examples, where different polymers have been used to facilitate electrochemical communication between photosynthetic systems and electrodes, e.g., Zou et al., reported enhanced electron extraction from photosynthetic biofilms via an electrically conductive polymer, polypyrrole,<sup>[24]</sup> Rosenbaum et al., reported photocurrent generation and hydrogen production by immobilizing a green algae, *Chlamydomonas reinhardtii*, on a polymer, e.g., poly(2,3,5,6-tetrafluoroaniline) or poly(2-fluoroaniline) coated platinum mesh electrodes,<sup>[25]</sup> and Logan and co-workers have studied the bioelectricity production by employing two different microalgae, i.e., *Chlorella vulgaris* and *Ulva lactuca*.<sup>[26]</sup>

Algae are aquatic photosynthetic organisms and are responsible for 50% of the overall photosynthesis and CO<sub>2</sub> fixation. The photosynthetic processes in higher plants and algae are similar.<sup>[27]</sup> Recently, algae were also considered as a competent source of biodiesel production due to their efficient light absorption and conversion into chemical energy.<sup>[28]</sup> *Paulschulzia pseudovolvox* (*P. pseudovolvox*) is a multicellular<sup>[29]</sup> eukaryotic green algae. The strain used in this work is strongly benthic and has demonstrated greater electrogenic activity<sup>[30]</sup> than a panel of prokaryotic cyanobacteria under identical conditions. The extracellular ET (EET) from *P. pseudovolvox* is assumed to be challenging, since the photosynthetic membranes in the chloroplasts are presumably insulated by the cellular environment.<sup>[30]</sup>

Here we report on the photoelectrogenic activity of *P. pseudovolvox* for harnessing solar energy. The direct ET (DET), in the sense that no mediator was deliberately added, from photolysis of water via *P. pseudovolvox* to the bare-graphite electrode is revealed. To improve the electrochemical communication, a variety of electron transfer mediators including soluble and polymeric mediators are used. Ferricyanide (FeCN) and benzoquinone (BQ) are used as soluble mediators and a series of Os-polymers are used as surface adsorbed polymeric mediators to give Os-polymer modified electrodes. The system was further modified with either of two enzymes, i.e., superoxide dismutase (SOD) or catalase (CAT), or their combination to protect the photosynthetic apparatus of *P. pseudovolvox* from reactive oxygen species (ROS) produced from electron leakage during photosynthesis.<sup>[31]</sup> Two photosynthetic inhibitors, i.e., diuron and paraquat, are used to confirm the source of electrons for photocurrent generation.

### 1.1. Schematic ET from *P. pseudovolvox* to the Os-Polymer Modified Electrode

In microalgae, photosynthesis occurs inside the thylakoid membranes of chloroplasts like in higher plants. The photosynthetic ET chain (PETC) consists of three major protein complexes,<sup>[32]</sup> i.e., photosystem I (PSI), photosystem II (PSII), and cytochrome *b<sub>6</sub>f* complex (Cyt *b<sub>6</sub>f*) (Scheme 1). The light absorption by the photosynthetic pigments of PSII (P680) raises their energetic level in a higher state (P680\*). The excited pigments get relaxed by taking electrons from water oxidation by the oxygen evolving complex (OEC) and leads to the formation

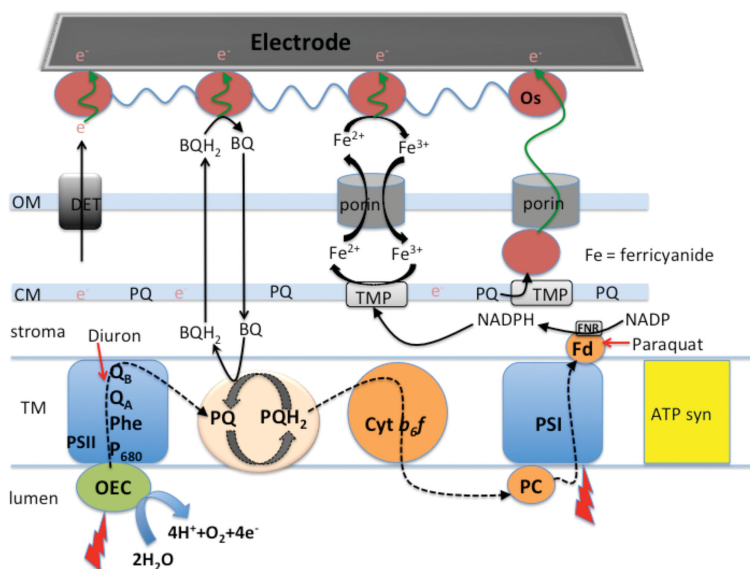
of molecular oxygen,  $O_2$ . The photoexcited electrons are then transferred via a series of electron carriers, viz., pheophytin (phe), quinone A ( $Q_A$ ), quinone B ( $Q_B$ ), and subsequently reduce plastoquinone (PQ) to plastoquinol ( $PQH_2$ ) by two consecutive two-electron reduction steps. Next, the electrons are transferred to PSI via Cyt  $b_6/f$  and plastocyanin (PC). Similarly, the light absorption by PSI excites their photosynthetic pigments and transfers these electrons eventually to ferredoxin (Fd). The liberated electrons are subsequently used to make the reduced form of nicotinamide adenine dinucleotide phosphate (NADPH) via ferredoxin-NADP reductase (FNR). In aerobic photosynthesis, NADPH is used to reduce atmospheric  $CO_2$  to make carbohydrates, i.e., sugar in a light independent reaction. In addition to these electron transfer reactions, PETC generates a proton gradient across the thylakoid membrane, which in turn is used by the adenosine triphosphate synthase (ATPsyn) to make ATP, the ultimate cellular energy.<sup>[6]</sup>

## 2. Results and Discussion

The photosynthetic viability of the *P. pseudovulvax* cells was determined by the absorbance spectrum measurements<sup>[33]</sup> of the photosynthetic pigments extracted from the cells (Figure S1, Supporting Information). A DET-based reaction between the cells and the electrode can provide for a higher

power output due to direct electrical contact between the cells and the electrodes compared a mediated system, where energy losses are expected because of the energy gap between the cells and the mediator.<sup>[34]</sup> In addition to that, DET minimizes the over-potential losses and simplifies the electrochemical cell design and operation compared to mediated systems.<sup>[35]</sup> *P. pseudovulvax* cells were absorbed on a bare-graphite electrode and illuminated to investigate for the possibility of DET (Figure 1). The electrolyte,  $10 \times 10^{-3}$  M potassium phosphate buffer with addition of  $10 \times 10^{-3}$  M NaCl and  $5 \times 10^{-3}$  M  $MgCl_2$  at pH 7.0 (PBS buffer) was used as electron donor. In the cyclic voltammetries (CVs) (Figure 1A) the anodic current signal increases somewhat during the “light on” (red line, b) compared to its counterpart during “light off” conditions (black line, a). In the control experiment (Figure S2, Supporting Information) it is shown that illumination does not have any noticeable response on a bare-graphite electrode.

To determine the photocurrent generation quantitatively, CA experiments were recorded by applying a potential of +0.35 V (Figure 1B). To obtain a stable baseline, the *P. pseudovulvax* cell modified electrodes were kept on “light off” conditions for 200 s followed by “light on” for 100 s for three identical cycles. These electrodes generate a photocurrent density of  $0.02 \mu A cm^{-2}$ , compared to the negligible alteration in current for the bare graphite electrode during the cycle. Previously, it was reported that the PQ pool in the PETC of cyanobacteria are



**Scheme 1.** The electrons from PETC enter the PQ pool in thylakoid membranes and exit via NADPH. Lipid soluble electron mediators, e.g., benzoquinone (BQ) can diffuse through the outer membranes (OM) and cytoplasmic membranes (CM). Non-lipid soluble electron mediators e.g., ferricyanide (FeCN) and Os-polymers can pass through the nonspecific porin of OM and be reduced by the transmembrane proteins (TMPs) of CM. Electrons could also be transferred to the electrode via pili or nanowires without any mediator, a process called direct ET (DET).<sup>[10]</sup> Detailed membrane components and proton pumps are not shown for simplicity. Black dotted arrows show the internal ET conduit in PETC. Red arrows show the photosynthetic inhibition points by diuron and paraquat, respectively. Purple circles symbolize the redox centers of Os-polymers linked with their backbone. Wavy green arrows show the EET to the electrode. All symbols represent the typical signs in photosynthesis and are given in detail and explained in the text.

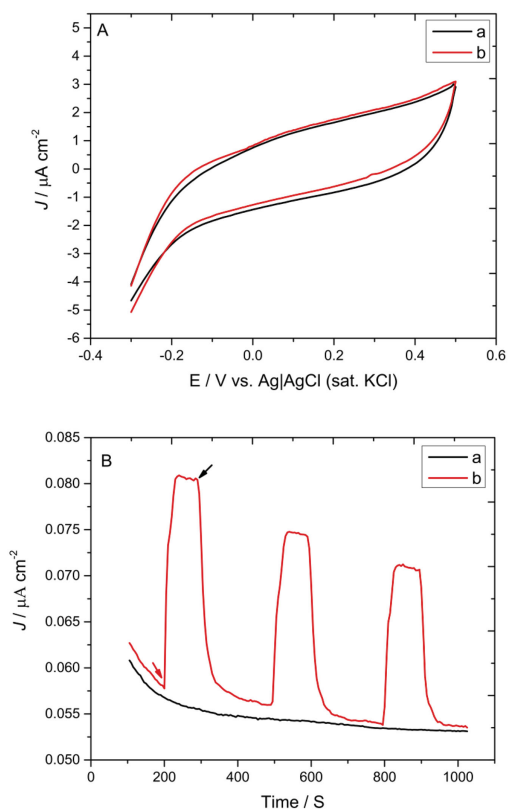


**Figure 1.** A) The CVs of *P. pseudovulvox* (4  $\mu\text{L}$ , 1  $\text{mg mL}^{-1}$ ) modified bare graphite electrodes in “light off” (black line, a) and “light on” (red line, b) conditions. Light intensity: 44  $\text{mW cm}^{-2}$ . Electrolyte:  $10 \times 10^{-3}$  M phosphate buffer,  $10 \times 10^{-3}$  M NaCl,  $5 \times 10^{-3}$  M  $\text{MgCl}_2$  at pH 7.0, scan rate: 0.01  $\text{Vs}^{-1}$ . B) The CAs of bare graphite electrode (black line, a) and *P. pseudovulvox* (4  $\mu\text{L}$ , 1  $\text{mg mL}^{-1}$ ) modified electrodes (red line, b). Black and red arrows indicate the “light off” and “light on” condition. Applied potential: 0.35 V versus Ag|AgCl (sat. KCl), light intensity: 44  $\text{mW cm}^{-2}$ . Electrolyte:  $10 \times 10^{-3}$  M phosphate buffer,  $10 \times 10^{-3}$  M NaCl,  $5 \times 10^{-3}$  M  $\text{MgCl}_2$  at pH 7.0, scan rate: 0.01  $\text{Vs}^{-1}$ .

responsible for DET.<sup>[36]</sup> A similar mediator-less DET response has been observed with green alga on transparent conductive anodes<sup>[4]</sup> and cyanobacteria on carbon cloth,<sup>[37]</sup> on graphite,<sup>[23]</sup> and a polymer coated anode.<sup>[24]</sup> The results suggest that PETC of the *P. pseudovulvox* cells generates a photocurrent by transferring electrons from the photolysis of water to the electrode.

Although DET is considered as a better process, the rate of ET from the organisms to the electrode is usually very low.<sup>[16]</sup> To seek to improve adsorption on the electrode and the rate of ET, surface confined Os-polymers<sup>[18]</sup> were used. Graphite electrodes were modified with 5  $\mu\text{L}$  of  $[\text{Os}(2,2'\text{-bipyridine})_2(\text{polyvinylimidazole})_{10}\text{Cl}]^{+/2+}$ , (Os-(bpy)PVI) (1:9) ( $E^{\circ} = +0.22$  V)<sup>[38]</sup> and CVs were recorded in the presence and absence of

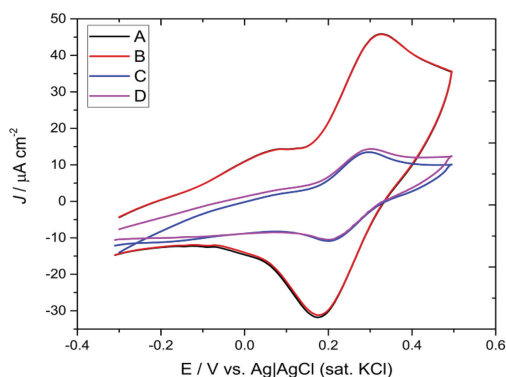


**Figure 2.** The CVs of (Os-(bpy)PVI) (1:9) modified graphite electrode in the A) absence and B) presence of light, CVs of *P. pseudovulvox* (4  $\mu\text{L}$ , 1  $\text{mg mL}^{-1}$ ) immobilized on (Os-(bpy)PVI) (1:9) modified electrode in the C) absence and D) presence of light. Light intensity: 44  $\text{mW cm}^{-2}$ . Electrolyte:  $10 \times 10^{-3}$  M phosphate buffer,  $10 \times 10^{-3}$  M NaCl,  $5 \times 10^{-3}$  M  $\text{MgCl}_2$  at pH 7.0, scan rate: 0.01  $\text{Vs}^{-1}$ .

illumination (Figure 2). A pair of redox peaks with a formal potential ( $E^{\circ}$ ) of 0.22 V versus Ag|AgCl (sat. KCl) is observed in the absence of illumination, in close agreement with previous reports on this polymer.<sup>[38]</sup> In the presence of light, the electrochemical behavior of (Os-(bpy)PVI) (1:9) goes down (Figure 2B). When the *P. pseudovulvox* cells were retained with the Os-polymer at the electrode, the peak currents are much lower than those for the electrode with Os-polymer alone (Figure 2C). It can be attributed to that the cationic Os-polymer forms strong electrostatic interactions with the anionic cell membrane of the *P. pseudovulvox* cells and subsequently retards the flexibility and mobility of the redox centers ( $\text{Os}^{+/2+}$ ) of the Os-polymer to freely interact with each other decreasing the rate of the electron “hopping.” Previously, a similar change in response was observed with both *Rhodobacter capsulatus*<sup>[22]</sup> and cyanobacteria on Os-polymer modified graphite electrodes.<sup>[23]</sup> The most significant response was observed while the *P. pseudovulvox* cell modified electrode was illuminated and showed an increased anodic peak current (Figure 2D). Here it can be assumed that the Os-polymer with its flexible backbone and redox functionalities can communicate with the thylakoid membranes inside the chloroplasts of the *P. pseudovulvox* cells and extract electrons from photolysis of water. Previously it was shown that Os-polymers can communicate with entire thylakoid membranes<sup>[39]</sup> as well as with isolated photosystem I<sup>[40]</sup> and photosystem II.<sup>[41]</sup>

There is a clear qualitative evidence of photocurrent generation in the CVs shown in Figure 2D. However, to be able to quantitatively register the photocurrent, CA measurements are a better choice. Thus, CAs were conducted on *P. pseudovulvox* cells immobilized on (Os-(bpy)PVI) (1:9) modified electrodes by applying a fixed potential at 0.35 V, which is substantially higher than the  $E^{\circ}$  of (Os-(bpy)PVI) (1:9), and it can therefore be secured that the ET from the PETC of the *P. pseudovulvox* cells to (Os-(bpy)PVI) (1:9) and subsequently to the electrode is not limited by the  $E_{\text{app}}$ . In the registered CAs, see Figure 3, it is revealed that illuminating electrodes modified with only

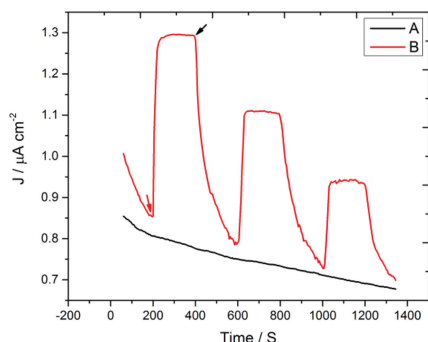


**Figure 3.** The CAs of (Os-(bpy)PVI) (1:9) modified electrode in the a) absence and b) presence of *P. pseudovulvox* (4  $\mu\text{L}$ , 1  $\text{mg mL}^{-1}$ ). Black and red arrows indicate the “light off” and “light on” condition. Applied potential: 0.35 V versus Ag/AgCl (sat. KCl), light intensity: 44  $\text{mW cm}^{-2}$ . Electrolyte:  $10 \times 10^{-3}$  M phosphate buffer,  $10 \times 10^{-3}$  M NaCl,  $5 \times 10^{-3}$  M  $\text{MgCl}_2$  at pH 7.0.

(Os-(bpy)PVI) (1:9) show very small photocurrents (Figure 3, black line, a). Instead, the background current density for the *P. pseudovulvox* cells immobilized on (Os-(bpy)PVI) (1:9) modified electrodes at “light off” conditions is 0.85  $\mu\text{A cm}^{-2}$  and at “light on” conditions, the photocurrent density reaches up to 1.29  $\mu\text{A cm}^{-2}$  (first cycle). The net photocurrent density for the first cycle is 0.44  $\mu\text{A cm}^{-2}$  (1.29–0.85  $\mu\text{A cm}^{-2}$ ), i.e., more than twofold higher than that of the DET-based system (Figure 1B). This response is four orders of magnitude higher than that of a similar investigation with *P. pseudovulvox* on carbon fiber threads coated with polypyrrole.<sup>[30]</sup> In the second and third cycles, the photocurrent density gradually decreases to 0.32 and 0.21  $\mu\text{A cm}^{-2}$ . The gradual decay of the photocurrent density is expected to be due to the imbalance between the utilization of excitation energy during photosynthesis and in the assimilatory process in the light independent reaction, a process called photoinhibition.<sup>[42]</sup> More particularly, at a high light intensity ( $\gg$  saturated photosynthetic light intensity,  $\approx 30 \text{ mW cm}^{-2}$ ), PSII inside the PETC is exposed to reactive oxygen species (ROS),<sup>[31]</sup> due to electron leakage, which causes photooxidative damage to the cells with consequences in a lower photosynthetic rate.<sup>[43]</sup> To optimize the energy gap between the used mediator and the PRCs inside the PETC of the *P. pseudovulvox* cells, a series of Os-polymers with different  $E^\circ$  values and chemical structures were investigated. The  $E^\circ$  of the Os-polymers span a potential window between –0.059 and +0.29 V versus Ag/AgCl (sat. KCl) and are expected to connect to different PRCs. The used Os-polymers are [Os(4,4'-dimethoxy-2,2'-bipyridine)<sub>2</sub>(poly-vinylimidazole)<sub>10</sub>Cl]<sup>+/2+</sup>,  $E^\circ = -0.059$  V (Os-(dmobpy)PVI (1:9));<sup>[44]</sup> [Os(4,4'-dimethyl-2,2'-bipyridine)<sub>2</sub>(poly-vinylimidazole)<sub>10</sub>Cl]<sup>+/2+</sup>,  $E^\circ = +0.11$  V (Os-(dmbpy)PVI (1:9));<sup>[21]</sup> [Os(2,2'-bipyridine)<sub>2</sub>(poly-vinylimidazole)<sub>10</sub>Cl]<sup>+/2+</sup>,  $E^\circ = +0.22$  V (Os-(bpy)PVI(1:9));<sup>[38]</sup> [Os(4,4'-dimethyl-2,2'-bipyridine)<sub>2</sub>(PVI)<sub>12</sub>Cl]<sup>+/2+</sup>,  $E^\circ = +0.244$  V (Os-(bpy)PVI) (1:11);<sup>[45]</sup> [Os(4,4'-dichloro-2,2'-bipyridine)<sub>2</sub>(PVI)<sub>10</sub>Cl]<sup>+/2+</sup>,  $E^\circ = +0.29$  V (Os-(dcbpy)PVI) (1:9).<sup>[46]</sup> These Os-polymers have the ability to adjust their  $E^\circ$  value by the coordinating ligands and the

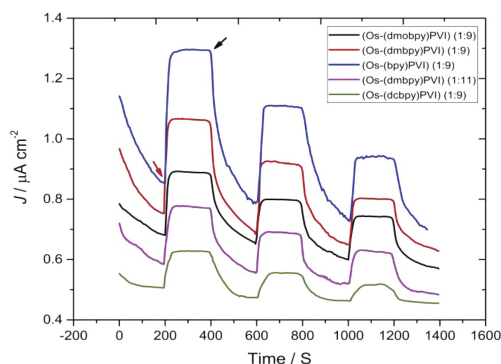


**Figure 4.** The CAs of *P. pseudovulvox* immobilized on electrode modified with different Os-polymers, Os-(dmobpy)PVI (1:9) ( $E^\circ = -0.059$  V), Os-(dmbpy)PVI (1:9) ( $E^\circ = +0.11$  V), Os-(bpy)PVI (1:9) ( $E^\circ = +0.22$  V), Os-(bpy)PVI (1:11) ( $E^\circ = +0.244$  V), Os-(dcbpy)PVI (1:9) ( $E^\circ = +0.29$  V). Black and red arrows indicate the “light off” and “light on” condition. Applied potential: 0.35 V versus Ag/AgCl (sat. KCl), light intensity: 44  $\text{mW cm}^{-2}$ . Electrolyte:  $10 \times 10^{-3}$  M phosphate buffer,  $10 \times 10^{-3}$  M NaCl,  $5 \times 10^{-3}$  M  $\text{MgCl}_2$  at pH 7.0.

relative stability of the polymer complexes and hydrogel characteristics of the polymer-modified biofilms allow rapid mass and charge transfer, thus generating a significant catalytic current response in earlier reports.<sup>[47,48]</sup>

In CAs (Figure 4) it is shown that the photocurrent density increases with an increased  $E^\circ$  of the Os-polymer, i.e., from 0.17  $\mu\text{A cm}^{-2}$  obtained with (Os-(dmobpy)PVI) (1:9),  $E^\circ = -0.059$  V) to 0.23  $\mu\text{A cm}^{-2}$  with (Os-(dmobpy)PVI) (1:9)  $E^\circ = +0.11$  V), and further to 0.30  $\mu\text{A cm}^{-2}$  with (Os-(bpy)PVI)(1:9)  $E^\circ = +0.22$  V). However, when the Os-polymers of an even higher  $E^\circ$  ( $>0.22$  V) are used the photocurrent density drops down significantly to 0.06  $\mu\text{A cm}^{-2}$  for (Os-(bpy)PVI) (1:11)  $E^\circ = +0.24$  V) and even further down to 0.05  $\mu\text{A cm}^{-2}$  for (Os-(dcbpy)PVI (1:9),  $E^\circ = +0.29$  V). Thus a maximum photocurrent density of 0.30  $\mu\text{A cm}^{-2}$  was recorded with polymer (Os-(bpy)PVI)(1:9), presumably because of a combined effect of several properties of this Os-polymer: its greater aqueous solubility, less bulky mediator structure yielding a better accessibility to reach the redox sites in the membranes of the *P. pseudovulvox* cells in combination with a relatively high  $E^\circ$ . A similar response versus  $E^\circ$ -profile was seen for thylakoid membranes from spinach (*Spinacia oleracea*) immobilized on graphite electrode modified using different Os-polymers.<sup>[39]</sup>

The estimated  $E^\circ$  values at neutral pH of the major components of the electron transport chain versus Ag/AgCl (sat. KCl) at pH 7.0 of the PRCs are +1.0 V (P680), –1.05 V (P680\*), +0.21 V (P700), –1.5 V (P700\*), –0.47 V (Q<sub>A</sub>), –0.3 V (Q<sub>B</sub>), –0.11 V (Cyt b<sub>6</sub>f), and +0.11 V (PC) and are all estimated from a previous study.<sup>[49]</sup> If the  $E^\circ$ 's of the PRCs and the Os-polymers are compared, it demonstrates that the majority of the PRCs have a reduction potential sufficiently more negative to provide electrons to any of the Os-polymers. Although the short lifetime of P680\* and P700\* are unlikely to deliver electrons, since the Os-polymers are anticipated not to compete with the natural



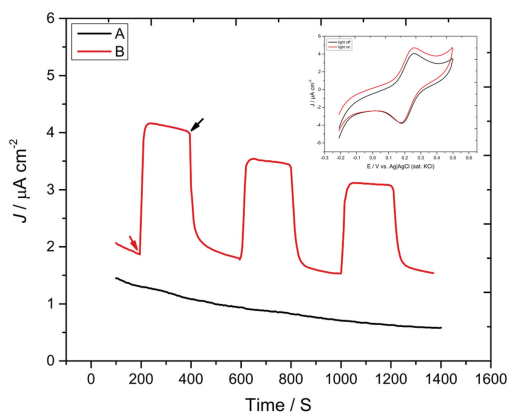


**Figure 5.** The CAs of *P. pseudovolvax* immobilized on electrode in the presence of  $0.5 \times 10^{-3}$  M ferricyanide (FeCN). Inset shows the CVs of electrode upon equal condition in the absence and presence of illumination. The typical  $E^{\circ}$  of FeCN is exhibited at +0.224 V. Black and red arrows indicate the “light off” and “light on” condition. Applied potential: 0.35 V versus Ag|AgCl (sat. KCl), light intensity:  $44 \text{ mW cm}^{-2}$ . Electrolyte:  $10 \times 10^{-3}$  M phosphate buffer,  $10 \times 10^{-3}$  M NaCl,  $5 \times 10^{-3}$  M  $\text{MgCl}_2$  at pH 7.0, scan rate:  $0.01 \text{ Vs}^{-1}$ .

electron acceptors. Instead,  $\text{PQH}_2$  in the PETC either in free or bound form is more likely to donate electrons. Besides that,  $\text{PQH}_2$  is present in several copies for each PETC and their long lifetime helps them to be a suitable electron donor.<sup>[50]</sup>

To investigate whether it is possible to further improve the ET rate from the PETC of the *P. pseudovolvax* cells to the electrode, a small freely diffusing mediator,  $0.5 \times 10^{-3}$  M ferricyanide (FeCN), was added to the PBS buffer. FeCN is a suitable choice because of its minimal photoactivity<sup>[51]</sup> and it is known to extract electrons from both PSI and PSII<sup>[52]</sup> in photosynthetic membranes.<sup>[53]</sup> In the presence of FeCN, see **Figure 5**, redline B, the photocurrent density reaches  $1.82 \mu\text{A cm}^{-2}$  that is ninefold higher compared to the DET response ( $0.02 \mu\text{A cm}^{-2}$ ). A similar increase in response enhanced by FeCN was observed earlier for thylakoid membranes.<sup>[53]</sup> However, when the electrode was not modified with *P. pseudovolvax* cells, FeCN alone does not have any considerable influence on any photocurrent upon illumination (**Figure 5** black line A). This behavior supports the schematic ET pathway suggested in Scheme 1 that FeCN is reduced by some unidentified trans-membrane proteins (TMPs)<sup>[4]</sup> inside the CM and is then successively transported to and oxidized at the electrode. The inset in **Figure 5** shows the CVs of the photocurrent density mediated by FeCN via *P. pseudovolvax* in “light off” (black line) and “light on” (red line) conditions. It is evident that the anodic current increases under “light on” conditions compared to “light off” conditions. The distinct redox waves centered around the  $E^{\circ}$  at +0.224 V indicate the  $E^{\circ}$  of FeCN. These results suggest that FeCN can mediate the electrogenic activity of *P. pseudovolvax* cells via the unknown TMPs inside the PETC. Since hydrophilic FeCN is anticipated not to be able to reach the cytoplasmic membrane (CM)<sup>[10]</sup> of *P. pseudovolvax*, the more lipophilic benzoquinone

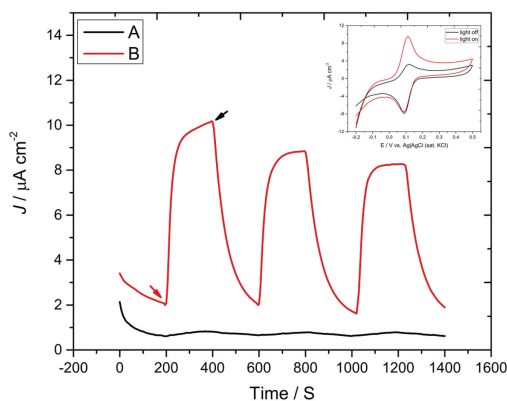


**Figure 6.** The CAs of *P. pseudovolvax* immobilized on electrode in the presence of  $0.5 \times 10^{-3}$  M benzoquinone (BQ). Inset shows the CVs of electrode upon equal condition in the absence and presence of illumination. The typical  $E^{\circ}$  of BQ is exhibited at +0.124 V. Black and red arrows indicate the “light off” and “light on” condition. Applied potential: 0.35 V versus Ag|AgCl (sat. KCl), light intensity:  $44 \text{ mW cm}^{-2}$ . Electrolyte:  $10 \times 10^{-3}$  M phosphate buffer,  $10 \times 10^{-3}$  M NaCl,  $5 \times 10^{-3}$  M  $\text{MgCl}_2$  at pH 7.0, scan rate:  $0.01 \text{ Vs}^{-1}$ .

(BQ) was used for an expected greater accessibility inside the membrane. BQ resembles PQ located in the PETC and the respiratory electron transfer chain (RETC) and links these two ET systems.<sup>[54,55]</sup> BQ is a suitable electron acceptor for  $\text{PQH}_2$ ,  $\text{Q}_B$ , and possibly also for  $\text{Q}_A$ .<sup>[56]</sup> It is shown (**Figure 6**, red line B) that, in the presence of BQ, the *P. pseudovolvax* cells generate a significant photocurrent density of  $7.10 \mu\text{A cm}^{-2}$  that is four times higher than that of the ET mediated by FeCN. In the control experiments, BQ itself (without *P. pseudovolvax* cells) does not have any noticeable effect from illumination (**Figure 6**, black line A). Earlier it was reported that photocurrent generation depends on the concentration of BQ ( $<2 \times 10^{-3}$  M).<sup>[57]</sup> However, to reduce the inhibiting activity from a higher concentration of BQ, the experiment was conducted at a concentration of BQ of  $0.5 \times 10^{-3}$  M. The inset in **Figure 6** shows the CVs of the *P. pseudovolvax* cells immobilized on the electrode in the presence of BQ under “light off” and “light on” conditions. The distinct peaks at +0.124 V indicate the  $E^{\circ}$  of BQ. The anodic peak increases significantly under illumination compared to its nonilluminated system. The experimental data suggest that BQ, having an aromatic structure can diffuse through the outer membranes (OM) and the CM of the thylakoid membranes of the *P. pseudovolvax* cells and thereby extract electrons from the PETC. Previously, BQ was studied as a good exogenous electron transfer mediator for *Synechococcus* sp.<sup>[58]</sup>

It is critical to compare on the one side these soluble redox mediators, i.e., BQ, FeCN, with the nondiffusible Os-polymers to investigate whether they have any combined influence on the EET. Thus a series of different combined electron mediating systems were examined for their ability to “harvest” as high as possible light energy to electricity. These various systems were: (I)  $0.5 \times 10^{-3}$  M BQ, (II)  $0.5 \times 10^{-3}$  M FeCN, (III)  $0.5 \times 10^{-3}$  M BQ +  $0.5 \times 10^{-3}$  M FeCN, (IV)  $0.5 \times 10^{-3}$  M BQ +  $0.5 \times 10^{-3}$  M FeCN + (Os)-(bpy)

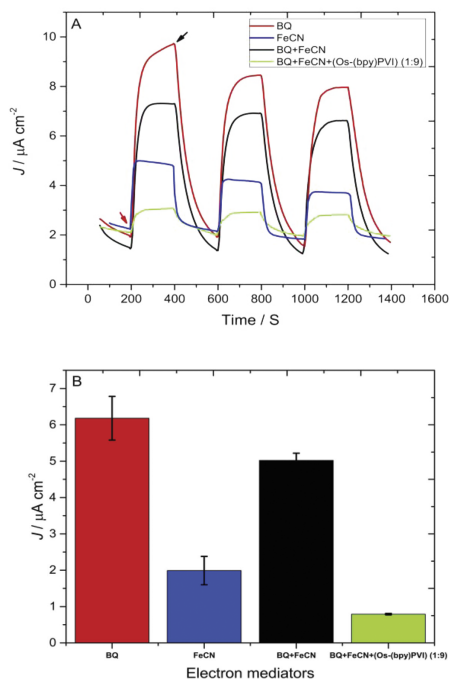


**Figure 7.** A) The comparison of photocurrent density by *P. pseudovulvox* mediated via different electron transfer mediators, benzoquinone (BQ), ferricyanide (FeCN), BQ in addition with FeCN and BQ in addition with FeCN with (Os-(bpy)PVI) (1:9) modified electrode. B) The presentation of photocurrent density in these different systems [data collected from Figure 9 A]. Black and red arrows indicate the “light off” and “light on” condition. Applied potential: 0.35 V versus Ag|AgCl (sat. KCl), light intensity: 44 mW cm<sup>-2</sup>. Electrolyte: 10 × 10<sup>-3</sup> M phosphate buffer, 10 × 10<sup>-3</sup> M NaCl, 5 × 10<sup>-3</sup> M MgCl<sub>2</sub> at pH 7.0.

PVI)(1:9) (Figure 7A). The photocurrent densities for these systems are presented in Figure 7B. In all mediating systems, the *P. pseudovulvox* cells are immobilized on bare graphite electrodes (I, II, and III) or on (Os-(bpy)PVI)(1:9) polymer modified electrodes (IV). The photocurrent densities recorded in these systems I, II, III, and IV were 6.97, 1.82, 5.02, and 0.79 μA cm<sup>-2</sup>. These results propose that while BQ itself as electron mediator provides the maximum photocurrent density of 6.97 μA cm<sup>-2</sup>, because of its greatest diffusing ability through the photosynthetic membranes. In contrast, the photocurrent density generated by FeCN was maximally 1.82 μA cm<sup>-2</sup>. This is anticipated since FeCN cannot reach the CM of the thylakoid membranes and can only extract electrons from the TMPs. The use of the Os-polymer alone (see above), (Os-(bpy)PVI) (1:9), yielded a current density of 1.29 μA cm<sup>-2</sup>, which is in the vicinity of what FeCN can accomplish. This might be expected if one considers that both FeCN and the Os-polymer can be looked upon as hydrophilic mediators that cannot really reach all those crucial locations in the membrane, which are accessible for the much more hydrophobic BQ. Thus these results in a way resemble

**Table 1.** Photocurrent density obtained with different mediators and combinations of mediators. The *P. pseudovulvox* cells were immobilized on bare-graphite or Os-polymer modified graphite electrodes. 5 μL of Os-polymers, i.e., (Os-(dmobpy)PVI) (1:9), (Os-(dmbpy)PVI) (1:9), (Os-(bpy)PVI) (1:9), (Os-(bpy)PVI) (1:11), and (Os-(dcbpy)PVI) (1:9) are immobilized on the electrode surface. 0.5 × 10<sup>-3</sup> M FeCN and BQ were dissolved in PBS buffer. Data are based on three independent experimental replicas (n = 3). Applied potential: 0.35 V versus Ag|AgCl (sat. KCl), light intensity: 44 mW cm<sup>-2</sup>. Electrolyte: 10 × 10<sup>-3</sup> M phosphate buffer with 10 × 10<sup>-3</sup> M NaCl and 5 × 10<sup>-3</sup> M MgCl<sub>2</sub> at pH 7.0.

No.	Electron mediator	Photocurrent [μA cm <sup>-2</sup> ]
1	No mediator/DET	0.02 ± 0.002
2	(Os-(dmobpy)PVI) (1:9)	0.17 ± 0.03
3	(Os-(dmbpy)PVI) (1:9)	0.23 ± 0.08
4	(Os-(bpy)PVI) (1:9)	0.36 ± 0.08
5	(Os-(bpy)PVI) (1:11)	0.06 ± 0.01
6	(Os-(dcbpy)PVI) (1:9)	0.05 ± 0.01
7	Ferricyanide (FeCN)	1.82 ± 0.40
8	Benzoquinone (BQ)	6.97 ± 0.64
9	BQ + FeCN	5.02 ± 0.20
10	BQ + FeCN + (Os-(bpy)PVI) (1:9)	0.79 ± 0.02

those of a previously studied system, where a double mediator system, composed of menadiene and an Os-polymer, demonstrated improved bioelectrochemical communication with *Saccharomyces cerevisiae* cells. The hydrophobic menadiene enters the yeast cells and is reduced and then the Os-polymer in turn reoxidises reduced menadiene at the cell wall and transfers the charge to the electrode.<sup>[59]</sup>

The most remarkable results are obtained when BQ and FeCN were included together in the electrolyte and the photocurrent density was documented to be 5.02 μA cm<sup>-2</sup>. The lower photocurrent density compared to the system when BQ was present alone can be due to their dissimilar E<sup>o</sup> values and ET properties of BQ and FeCN. When all the three types of electron mediators (IV) are present, the least photocurrent density is obtained, i.e., 0.8 μA cm<sup>-2</sup>. The most probable reason for this restricted response might be due to the different ET properties of these mediators and there might be competition among these mediators for the electron extraction from different PRCs. In the last two systems mixing FeCN with BQ or mixing FeCN and BQ with an Os-polymer possibly results in some short circuiting of the system as the current density so drastically decreases. A comparison of the photocurrent density including standard deviation values obtained from the different electron transfer mediators and the various combinations of mediators are presented in Table 1.

In visible light (400–700 nm), the PETC and protein environments are destroyed by reactive oxygen species (ROS),<sup>[42]</sup> formed by electron leakage from PSII to O<sub>2</sub>. ROS include singlet oxygen (<sup>1</sup>O<sub>2</sub>), superoxide (O<sub>2</sub><sup>-</sup>), hydroxyl radicals (OH) and hydrogen peroxide (H<sub>2</sub>O<sub>2</sub>). Among them <sup>1</sup>O<sub>2</sub> and OH are the most reactive species and cause lipid peroxidation and consequently in cell death.<sup>[60]</sup> In contrast, H<sub>2</sub>O<sub>2</sub> is less harmful but is highly diffusible through the cellular membranes and causes

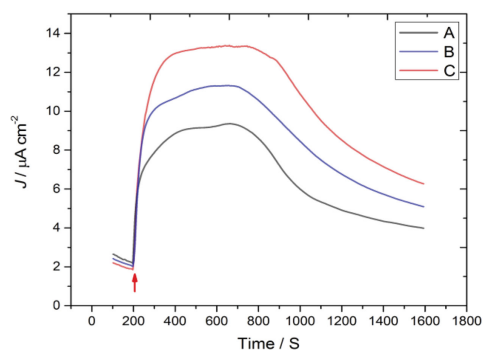


**Figure 8.** The effect of addition of enzymes catalyzing the destruction of reactive oxygen species (ROS) on photocurrent, e.g., A) no added enzyme present (control), B) catalase (CAT), C) superoxide dismutase (SOD). *P. pseudovolvax* immobilized on bare graphite electrode in the presence of  $0.5 \times 10^{-3}$  M benzoquinone. CAT catalyzes the disproportionation of  $\text{H}_2\text{O}_2$  into water ( $\text{H}_2\text{O}$ ) and molecular oxygen ( $\text{O}_2$ ) and SOD catalyzes the conversion of superoxide radicals ( $\text{O}_2^-$ ) into molecular oxygen ( $\text{O}_2$ ) and hydrogen peroxide ( $\text{H}_2\text{O}_2$ ). Red arrow indicates the "light on" condition. Applied potential: 0.35 V versus Ag/AgCl (sat. KCl), light intensity:  $44 \text{ mW cm}^{-2}$ . Electrolyte:  $10 \times 10^{-3}$  M phosphate buffer,  $10 \times 10^{-3}$  M NaCl,  $5 \times 10^{-3}$  M  $\text{MgCl}_2$  at pH 7.

cell damage.<sup>[60]</sup> Superoxide dismutase (SOD; EC 1.15.1.1) catalyzes the conversion of the superoxide radicals ( $\text{O}_2^-$ ) into oxygen ( $\text{O}_2$ ) and hydrogen peroxide ( $\text{H}_2\text{O}_2$ ) that is less harmful than the radicals. Catalase (CAT; EC 1.11.1.6) disproportionates  $\text{H}_2\text{O}_2$  into  $\text{H}_2\text{O}$  and  $\text{O}_2$  without consuming cellular reducing equivalents.<sup>[31]</sup> SOD and CAT were investigated for their protection of the photosynthetic apparatus of the *P. pseudovolvax* cells from ROS. For those experiments aliquots of 3  $\mu\text{L}$  of SOD ( $1 \text{ mg mL}^{-1}$ ) or CAT ( $1 \text{ mg mL}^{-1}$ ) were immobilized on the *P. pseudovolvax* modified electrodes. It is shown that under illumination and in the presence of  $0.5 \times 10^{-3}$  M BQ, the photocurrent density generated by *P. pseudovolvax* is  $6.8 \mu\text{A cm}^{-2}$  (Figure 8A) similar to that in Figure 6B. In the presence of CAT or SOD the photocurrent density increases to  $9.35 \mu\text{A cm}^{-2}$  (Figure 8B) and  $11.50 \mu\text{A cm}^{-2}$  (Figure 8C). The increase in photocurrent density caused by the addition of CAT or SOD is 35% and 70%, respectively, compared to the control system, where neither was present (Figure 8A). Minter and co-workers have previously shown improved photocurrent generation from thylakoid membranes in the presence of CAT.<sup>[61]</sup> The reason for an increased photocurrent density could be attributed to the neutralizing influence from SOD or CAT on ROS. These results indicate that  $\text{O}_2^-$  is more destructive for the photosynthetic apparatus of the *P. pseudovolvax* cells than that of  $\text{H}_2\text{O}_2$ . Although the photocurrent density increases with SOD and CAT, however, within 23 min (1400 s) a substantial amount of photocurrent density still drops down. It might be that the short lifetime<sup>[62]</sup> of SOD and CAT could not protect the *P. pseudovolvax* cells from ROS for a prolonged time. The enhancement in photocurrent density with CAT or SOD is presented in Table 2.

In order to further investigate the source of photocurrent, two photosynthetic inhibitors, i.e., diuron [3-(3',4'-dichlorophenyl)-1,1-dimethyl urea] and paraquat (*N,N'*-dimethyl-4,4'-bipyridinium dichloride) were used. Diuron and paraquat are well-known

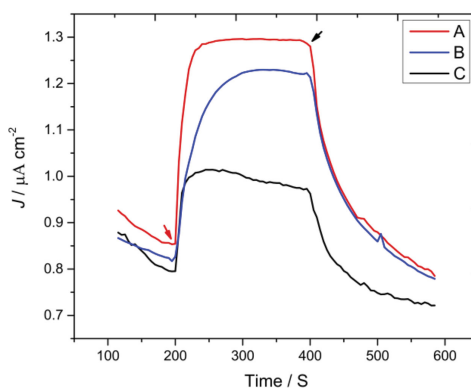


**Figure 9.** The comparison of photocurrent density of a noninhibiting system A) with two inhibitors, e.g., B)  $0.2 \times 10^{-3}$  M paraquat C)  $0.2 \times 10^{-3}$  M diuron. *P. pseudovolvax* is immobilized on (Os-(bpy)PVI) (1:9) modified electrode. Black and red arrows indicate the "light off" and "light on" condition. Applied potential: 0.35 V versus Ag/AgCl (sat. KCl), light intensity:  $44 \text{ mW cm}^{-2}$ . Electrolyte:  $10 \times 10^{-3}$  M phosphate buffer,  $10 \times 10^{-3}$  M NaCl,  $5 \times 10^{-3}$  M  $\text{MgCl}_2$  at pH 7.0.

inhibitors for PSII and PSI, respectively.<sup>[63]</sup> Diuron irreversibly blocks the ET between  $\text{Q}_A$  and  $\text{Q}_B$  in PSII and prevents the electron flow to the plastoquinone pool<sup>[64]</sup> (Scheme 1). In contrast, paraquat competes with Fd (Scheme 1) for electrons and transfers them to molecular oxygen ( $\text{O}_2$ ) to form ROS, and results in lipid peroxidation.<sup>[64]</sup> The photocurrent density of a noninhibiting system is compared with those two inhibitors (Figure 9).  $4 \mu\text{L}$  of a *P. pseudovolvax* cell containing solution was immobilized onto an (Os-(bpy)PVI)(1:9) modified electrode surface. The photocurrent density for the noninhibiting system was  $0.44 \mu\text{A cm}^{-2}$  (Figure 9A), whereas in the presence of  $0.2 \times 10^{-3}$  M diuron in PBS buffer, 50% of the photocurrent density was inhibited and reached  $0.22 \mu\text{A cm}^{-2}$  (Figure 9C). Based on these results, it is assumed that the binding of diuron with  $\text{Q}_B$  makes it then non-reducible and results in a blocked photosynthetic ET. Previously it has been reported that photocurrent generation from cyanobacteria is substantially inhibited by diuron.<sup>[58,65]</sup> The residual current could be attributed either from the respiratory electron transfer system<sup>[66]</sup> or that (Os-(bpy)PVI)(1:9) mediates electrons

**Table 2.** Improved photocurrent density in the presence of a ROS neutralizer, catalase (CAT), or superoxide dismutase (SOD). In the control system,  $4 \mu\text{L}$  of *P. pseudovolvax* cells is immobilized on bare-graphite electrodes in the presence of  $0.5 \times 10^{-3}$  M BQ in PBS buffer. To improve the photocurrent density  $3 \mu\text{L}$  of SOD or CAT is immobilized on the *P. pseudovolvax* cell modified electrode. Applied potential: 0.35 V versus Ag/AgCl (sat. KCl), light intensity:  $44 \text{ mW cm}^{-2}$ . Electrolyte:  $10 \times 10^{-3}$  M phosphate buffer with  $10 \times 10^{-3}$  M NaCl and  $5 \times 10^{-3}$  M  $\text{MgCl}_2$  at pH 7.

No.	ROS neutralizer	Photocurrent [ $\mu\text{A}^{-1} \text{cm}^{-2}$ ]	% increase
1	Control (A)	6.80	
2	CAT (B)	9.35	30%
3	SOD (C)	11.50	70%

**Table 3.** Inhibition of photocurrent density by  $0.2 \times 10^{-3}$  M diuron or paraquat. 4  $\mu\text{L}$  of *P. pseudovolvax* cells was immobilized on (Os-(bpy)PVI)(1:9) modified graphite electrodes. Diuron, the PSII inhibitor could inhibit 50% of photocurrent generated in the noninhibited system. In contrast paraquat, the PSI inhibitor, did not inhibit any photocurrent. Applied potential: 0.35 V versus Ag|AgCl (sat. KCl), light intensity:  $44 \text{ mW cm}^{-2}$ . Electrolyte:  $10 \times 10^{-3}$  M phosphate buffer,  $10 \times 10^{-3}$  M NaCl,  $5 \times 10^{-3}$  M  $\text{MgCl}_2$  at pH 7.0.

No	Inhibitor	Photocurrent [ $\mu\text{A}^{-1} \text{cm}^{-2}$ ]	% of inhibition
1	No inhibitor	0.44	
2	Diuron	0.22	50%
3	Paraquat	0.44	0%

from the  $Q_A$  site. When  $0.2 \times 10^{-3}$  M paraquat was included in the PBS buffer, the photocurrent density was not inhibited (Figure 8B), although the background current level is changed. Earlier a similar response was observed with thylakoid membranes and paraquat.<sup>[51]</sup> It can be attributed that (Os-(bpy)PVI)(1:9) mediates electrons only from the PSII site. Apart from that, paraquat could also shuttle electrons from PSI to molecular oxygen or to the electrode surface. These results suggest the major source of photocurrent is from PSII, the site of photolysis of water. The photocurrent density inhibited with either diuron or paraquat is compared with the noninhibited system and is presented in Table 3.

### 3. Conclusions

This study demonstrates the photoelectrogenic activity of a eukaryotic green alga, *P. pseudovolvax*, immobilized on graphite electrodes. The photoexcited ET from photolysis of water via *P. pseudovolvax* is revealed on bare-graphite electrodes and the photocurrent density is documented at  $0.02 \mu\text{A cm}^{-2}$ . To optimize the energy gap among the PRCs, a series of Os-polymer varying in  $E^\circ$  values and chemical structures were used. A maximum photocurrent density of  $0.44 \mu\text{A cm}^{-2}$  was attained with (Os-(bpy)PVI)(1:9) having a greater solubility, an enhanced accessibility in the photosynthetic membranes, and a relatively high  $E^\circ$  of 0.22 V. The photocurrent density was improved to  $6.97 \mu\text{A cm}^{-2}$  by including BQ, which has a greater diffusivity inside the cellular membranes. However, a combination of mediators, i.e., FeCN, BQ and (Os-(bpy)PVI)(1:9) having dissimilar  $E^\circ$  values and ET properties, generates a low photocurrent density of  $0.79 \mu\text{A cm}^{-2}$ . The photocurrent density was further improved to  $11.50 \mu\text{A cm}^{-2}$  by using SOD that neutralizes the superoxide radicals responsible for cellular damage. The origin of photocurrent is confirmed to PSII by using diuron, an inhibitor that blocks the ET between quinone molecules ( $Q_A$  and  $Q_B$ ) in PSII.

These findings have significant implication on sustainable eco-friendly photosynthetic energy conversion, power remote instruments, portable electronics devices, and photofuel production. However, to explore this system for the rising energy need, the power output is required to be improved with several orders of magnitude. The key features for further developments could be the photosynthetic electron exit to the

cellular exterior and their long-term viability in the system. A superior electrode material by maximizing surface area and minimizing the distance between cells and the electrode could improve the ET rate and thus improve the performance. A 3D entrapment of cells was reported to improve their cellular activity and viability for a few months.<sup>[67]</sup> Currently, we are focusing on the photoelectrochemical study of algae on 3D electrodes. In addition to that a deeper understanding of photosynthesis in Nature is essential to make BPVs compatible with conventional solar powered devices. Engineering photosynthetic biomaterial could be approached to increase the sunlight absorption range and enhanced electrons excretion and thereby a substantial improvements of BPVs. As a final comment it can be stated that this work can also be looked upon as a work in the greater context on how to be able to establish electrochemical communication between living cells and electrodes.<sup>[18,68]</sup>

### 4. Experimental Section

#### Maintenances of *P. pseudovolvax* Growth and Inoculum Preparation:

The alga, *P. pseudovolvax* was isolated from an environmental sample from Lake Tikitapu, New Zealand and its growth conditions have been previously reported.<sup>[30]</sup> In brief, a low ionic strength MLA<sup>[69]</sup> growth medium was used with a white cool fluorescent lamp providing a light intensity of  $\approx 10 \text{ W m}^{-2}$  on a 12:12 h light and dark regime. The growth culture was maintained in 100 mL clear polystyrene bottles (VWR, Stockholm, Sweden) at room temperature ( $20 \pm 2^\circ\text{C}$ ). For experiments the *P. pseudovolvax* cells were harvested by centrifugation at 4000 rpm for 10 min at  $20^\circ\text{C}$ . The cells were washed with  $10 \times 10^{-3}$  M phosphate buffer at pH 7.0 and centrifuged again under the same condition. Finally, the cells were resuspended in the same buffer adjusting the cell density to  $1 \text{ mg mL}^{-1}$  (wet weight) and then immediately used for electrochemical measurements.

For inoculum preparation, a dense clot of *P. pseudovolvax* cells was transferred to 60 mL of MLA medium contained in 100 mL polystyrene bottles tightly closed with a cover. A fresh thick green mass of cells appears in the bottle within  $\approx 2$  weeks.

**Measurements and Instrumentation:** All electrochemical measurements, i.e., cyclic voltammetry (CV) and chronoamperometry (CA) were carried out using a PalmSens potentiostat (model Emstat<sup>3</sup>, Palm Instruments BV, Utrecht, The Netherlands) equipped with PSTrace software. A conventional three-electrode<sup>[70]</sup> configuration was used, i.e., an Ag|AgCl(sat. KCl) reference (Sensortechnik, Meinsberg, Germany), a bare-graphite or an Os-polymer modified graphite electrode (active surface area,  $A = 0.0731 \text{ cm}^2$ ) as the working electrode, and a platinum foil as counter electrode.

The working electrode surface was illuminated by a fiber optic illuminator FOI-150-220 (150 W and 220 V) with a FOI-5 light guide (Titan Tool Supply Inc., Buffalo, NY, USA). The illuminator light intensity was adjusted by a light meter (Techtum Lab AB, Umeå, Sweden). A light intensity of  $44 \text{ mW cm}^{-2}$  was used to excite the photosynthetic activity of the *P. pseudovolvax* cells. In all experiments, a  $10 \times 10^{-3}$  M phosphate buffer including  $10 \times 10^{-3}$  M NaCl and  $5 \times 10^{-3}$  M  $\text{MgCl}_2$  at pH 7.0 (PBS buffer) was used as electrolyte. The pH of the electrolyte solutions was measured with a Metrohm 827-pH lab meter (Metrohm AG, Herisau, Switzerland). The electrolyte solutions were degassed with pure argon for  $\approx 10$  min before conducting the experiments.

In CV measurements, a scan rate of  $0.01 \text{ Vs}^{-1}$  was used if not stated otherwise. In CA measurements, the applied potential ( $E_{\text{app}}$ ) was fixed at  $+0.35 \text{ V}$  versus Ag|AgCl(sat.) KCl, i.e., a potential much higher than the  $E^\circ$  of any of the used mediators, to generate a photocurrent independently. All experiments were conducted at room temperature ( $20 \pm 2^\circ\text{C}$ ). All data reported here are based on three independent

experimental replicas. All potential values (V) mentioned here are according to Ag|AgCl (sat. KCl) as reference electrode (+197 mV vs SHE).

**Working Electrode Preparation:** Graphite rods (Alfa Aesar GmbH & Co KG., Karlsruhe, Germany, AGKSP grade, ultra "F" purity and 3.05 mm diameter) were used to prepare working electrodes. The end of the graphite rod was polished on fine emery SiC paper (Turfbak Durite, P1200) and carefully washed with Milli-Q water and dried. Then, an aliquot of 5  $\mu\text{L}$  of an Os-polymer solution (5 mg mL<sup>-1</sup> in Milli-Q water) was spread onto the entire active surface of the electrode and allowed to dry for  $\approx 10$  min and then 4  $\mu\text{L}$  of a *P. pseudovolvax* solution (1 mg mL<sup>-1</sup>) was spread onto the surface. A dialysis membrane (Spectrum Laboratory Inc., Rancho Dominguez, CA, USA, molecular mass cut-off: 6000–8000) was used to retain the Os-polymers and *P. pseudovolvax* cells on the electrode. The dialysis membrane was presoaked in PBS buffer for  $\approx 10$  min before pressed onto the electrode and tightly fixed with a rubber O-ring and Parafilm. Note that, the amounts of Os-polymers (5  $\mu\text{L}$ ) and *P. pseudovolvax* (4  $\mu\text{L}$ , 1 mg mL<sup>-1</sup>) are the optimized values (data not shown).

## Supporting Information

Supporting Information is available from the Wiley Online Library or from the author.

## Acknowledgements

The authors thank The Swedish Research Council (Project Nos. 2010–2013, 2010–5031, and 2014–5908), The European Commission (Erasmus Mundus, EMIIY Action II program and "BIOENERGY" FP7-PEOPLE-2013-ITN-607793), Science Foundation Ireland (Charles Parsons Energy Research Award), and New Zealand Ministry of Innovation, Business and Enterprise (PROJ-13838-NMTS-LVL) for financial support. The authors thank Dr. Domhnall MacAodha and Dr. Peter Ó Conghaile (NUI, Galway) for synthesis of the Os-polymers.

Received: June 4, 2015

Revised: July 1, 2015

Published online:

- [1] O. Kruse, J. Rupprecht, J. H. Mussnug, G. C. Dismukes, B. Hankamer, *Photochem. Photobiol. Sci.* **2005**, *4*, 957.
- [2] N. S. Lewis, D. G. Nocera, *Proc. Natl. Acad. Sci. USA* **2006**, *103*, 15729.
- [3] Z. Yongjin, J. Pisciotta, R. B. Billmyre, I. V. Baskakov, *Biotechnol. Bioeng.* **2009**, *104*, 939.
- [4] A. J. McCormick, P. Bombelli, A. M. Scott, A. J. Philips, A. G. Smith, A. C. Fisher, C. J. Howe, *Energy Environ. Sci.* **2011**, *4*, 4699.
- [5] Y. Zhang, J. S. Noori, I. Angelidakis, *Energy Environ. Sci.* **2011**, *4*, 4340.
- [6] M. Rosenbaum, U. Schröder, *Electroanalysis* **2010**, *22*, 844.
- [7] A. J. McCormick, P. Bombelli, R. W. Bradley, R. Thorne, T. Wenzel, C. J. Howe, *Energy Environ. Sci.* **2015**, *8*, 1092.
- [8] Y. K. Cho, T. J. Donohue, I. Tejedor, M. A. Anderson, K. D. McMahon, D. R. Noguera, *J. Appl. Microbiol.* **2008**, *104*, 640.
- [9] M. Rosenbaum, Z. He, L. T. Angenent, *Curr. Opin. Biotechnol.* **2010**, *21*, 259.
- [10] R. W. Bradley, P. Bombelli, S. J. L. Rowden, C. J. Howe, *Biochem. Soc. Trans.* **2012**, *40*, 1302.
- [11] K. Tanaka, R. Tamamushi, T. Ogawa, *J. Chem. Technol. Biotechnol.* **1985**, *35*, 191.
- [12] a) T. Yagishita, S. Sawayama, K. Tsukahara, T. Ogi, *J. Biosci. Bioeng.* **1999**, *88*, 210; b) T. Yagishita, S. Sawayama, K. I. Tsukahara, T. Ogi, *Sol. Energy* **1997**, *61*, 347.
- [13] S. Tsujimura, A. Wadano, K. Kano, T. Ikeda, *Enzym. Microb. Technol.* **2001**, *29*, 225.
- [14] R. W. Bradley, P. Bombelli, D. J. Lea-Smith, C. J. Howe, *Phys. Chem. Chem. Phys.* **2013**, *15*, 13611.
- [15] A. Heller, *Acc. Chem. Res.* **1990**, *23*, 128.
- [16] U. Schröder, *Phys. Chem. Chem. Phys.* **2007**, *9*, 2619.
- [17] K. Hasan, S. A. Patil, D. Leech, C. Hägerhäll, L. Gorton, *Biochem. Soc. Trans.* **2012**, *40*, 1330.
- [18] J. Du, C. Catania, G. C. Bazan, *Chem. Mater.* **2013**, *26*, 686.
- [19] H. Shkil, A. Schulte, D. A. Guschin, W. Schuhmann, *ChemPhysChem* **2011**, *12*, 806.
- [20] A. Heller, *Curr. Opin. Chem. Biol.* **2006**, *10*, 664.
- [21] T. J. Ohara, R. Rajagopalan, A. Heller, *Anal. Chem.* **1994**, *66*, 2451.
- [22] K. Hasan, K. V. R. Reddy, V. Eßmann, K. Górecki, P. Ó Conghaile, W. Schuhmann, D. Leech, C. Hägerhäll, L. Gorton, *Electroanalysis* **2015**, *27*, 118.
- [23] K. Hasan, H. B. Yildiz, E. Sperling, P. Ó Conghaile, M. A. Packer, D. Leech, C. Hägerhäll, L. Gorton, *Phys. Chem. Chem. Phys.* **2014**, *16*, 24676.
- [24] Y. Zou, J. Pisciotta, R. B. Billmyre, I. V. Baskakov, *Biotechnol. Bioeng.* **2009**, *104*, 939.
- [25] M. Rosenbaum, U. Schröder, F. Scholz, *Appl. Microbiol. Biotechnol.* **2005**, *68*, 753.
- [26] S. B. Velasquez-Orta, T. P. Curtis, B. E. Logan, *Biotechnol. Bioeng.* **2009**, *103*, 1068.
- [27] N. Sekar, R. P. Ramasamy, *J. Photochem. Photobiol. C: Photochem. Rev.* **2015**, *22*, 19.
- [28] J. V. Moroney, R. A. Ynalvez, *Algal Photosynthesis, eLS*, John Wiley & Sons, Ltd, Chichester, West Sussex, England **2009**.
- [29] M. D. Herron, J. D. Hackett, F. O. Aylward, R. E. Michod, *Proc. Natl. Acad. Sci. USA* **2009**, *106*, 3254.
- [30] V. Luimstra, S.-J. Kennedy, J. Güttler, S. Wood, D. Williams, M. A. Packer, *J. Appl. Physiol.* **2014**, *26*, 15.
- [31] N. Mallick, F. H. Mohn, *J. Plant. Physiol.* **2000**, *157*, 183.
- [32] S. Berry, B. Rumberg, *Bioelectrochemistry* **2001**, *53*, 35.
- [33] J. Pisciotta, Y. Zou, I. Baskakov, *Appl. Microbiol. Biotechnol.* **2011**, *91*, 377.
- [34] G. Reguera, K. D. McCarthy, T. Mehta, J. S. Nicoll, M. T. Tuominen, D. R. Lovley, *Nature* **2005**, *435*, 1098.
- [35] B. E. Logan, B. Hamelers, R. Rozendal, U. Schröder, J. Keller, S. Freguia, P. Aelterman, W. Verstraete, K. Rabaey, *Environ. Sci. Technol.* **2006**, *40*, 5181.
- [36] N. Sekar, Y. Umasankar, R. P. Ramasamy, *Phys. Chem. Chem. Phys.* **2014**, *16*, 7862.
- [37] A. Cereda, A. Hitchcock, M. D. Symes, L. Cronin, T. S. Bibby, A. K. Jones, *PLoS ONE* **2014**, *9*, e91484.
- [38] E. M. Kober, J. V. Caspar, B. P. Sullivan, T. J. Meyer, *Inorg. Chem.* **1988**, *27*, 4587.
- [39] H. Hamidi, K. Hasan, S. C. Emek, Y. Dilgin, H.-E. Åkerlund, P.-Å. Albertsson, D. Leech, L. Gorton, *ChemSusChem* **2015**, *6*, 990.
- [40] A. Badura, D. Guschin, T. Kothe, M. J. Kocpczak, W. Schuhmann, M. Rögner, *Energy Environ. Sci.* **2011**, *4*, 2435.
- [41] A. Badura, D. Guschin, B. Esper, T. Kothe, S. Neugebauer, W. Schuhmann, M. Rögner, *Electroanalysis* **2008**, *20*, 1043.
- [42] T. Roach, A. K. Krieger-Liszka, *Curr. Prot. Pep. Sci.* **2014**, *15*, 351.
- [43] A. Melis, *Trend. Plant. Sci.* **1999**, *4*, 130.
- [44] a) C. Taylor, G. Kenausis, I. Katakis, A. Heller, *J. Electroanal. Chem.* **1995**, *396*, 511; b) N. Mano, A. Heller, *J. Electrochem. Soc.* **2003**, *150*, A1136.
- [45] A. Heller, *J. Phys. Chem.* **1992**, *96*, 3579.
- [46] P. A. Jenkins, S. Boland, P. Kavanagh, D. Leech, *Bioelectrochemistry* **2009**, *76*, 162.
- [47] a) D. MacAodha, M. L. Ferrer, P. Ó Conghaile, P. Kavanagh, D. Leech, *Phys. Chem. Chem. Phys.* **2012**, *14*, 14667; b) A. PrévotEAU, N. Mano, *Electrochim. Acta* **2013**, *112*, 318.

- [48] I. Osadebe, D. Leech, *ChemElectroChem* **2014**, *1*, 1988.
- [49] I. McConnell, G. Li, G. W. Brudvig, *Chem. Biol.* **2010**, *17*, 434.
- [50] J. Kruk, S. Karpinski, *Biochim. Biophys. Acta, Bioenergy* **2006**, 1757, 1669.
- [51] J. O. Calkins, Y. Umasankar, H. O'Neill, R. P. Ramasamy, *Energy Environ. Sci.* **2013**, *6*, 1891.
- [52] M. Mimeault, R. Carpentier, *Enzyme Microb. Technol.* **1988**, *10*, 691.
- [53] R. Carpentier, S. Lemieux, M. Mimeault, M. Purcell, D. C. Goetze, *Bioelectrochem. Bioenerg.* **1989**, *22*, 391.
- [54] M. Hirano, K. Satoh, S. Katoh, *Photosynth. Res.* **1980**, *1*, 149.
- [55] M. Paumann, G. Regelsberger, C. Obinger, G. A. Peschek, *Biochim. Biophys. Acta, Bioenergy* **2005**, 1707, 231.
- [56] K. Satoh, M. Oh-hashii, Y. Kashino, H. Koike, *Plant. Cell. Physiol.* **1995**, *36*, 597.
- [57] Y. Yu, F. Zuo, C.-Z. Li, *Electrochim. Acta* **2013**, *113*, 603.
- [58] M. Torimura, A. Miki, A. Wadano, K. Kano, T. Ikeda, *J. Electroanal. Chem.* **2001**, 496, 21.
- [59] A. Heiskanen, V. Coman, N. Kostashe, D. Sabourin, N. Haslett, K. Baronian, L. Gorton, M. Dufva, J. Emnéus, *Anal. Bioanal. Chem.* **2013**, *405*, 3847.
- [60] I. Vass, *Biochim. Biophys. Acta, Bioenergy* **2012**, 1817, 209.
- [61] K. H. Sjöholm, M. Rasmussen, S. D. Minteer, *ECS Electrochem. Lett.* **2012**, *1*, G7.
- [62] P. C. Heinrich, M. Müller, L. Graeve, *Löffler/Petrides Biochemie und Pathobiochemie*, Springer-Verlag, Berlin **2014**.
- [63] E. P. Fuerst, M. A. Norman, *Weed Sci.* **1991**, *39*, 458.
- [64] B. D. Hsu, J.-Y. Lee, R. L. Pan, *Biochem. Biophys. Res. Commun.* **1986**, *141*, 682.
- [65] J. M. Pisciotta, Y. Zou, I. V. Baskakov, *PLoS ONE* **2010**, *5*, e10821.
- [66] P. Bombelli, R. W. Bradley, A. M. Scott, A. J. Philips, A. J. McCormick, S. M. Cruz, A. Anderson, K. Yunus, D. S. Bendall, P. J. Cameron, J. M. Davies, A. G. Smith, C. J. Howe, A. C. Fisher, *Energy Environ. Sci.* **2011**, *4*, 4690.
- [67] J. C. Harper, T. L. Edwards, T. Savage, S. Harbaugh, N. Kelley-Loughnane, M. O. Stone, C. J. Brinker, S. M. Brozik, *Small* **2012**, *8*, 2613.
- [68] J. H. Collier, M. Mrksich, *Proc. Natl. Acad. Sci. USA* **2006**, *103*, 2021.
- [69] C. J. S. Bolch, S. I. Blackburn, *J. Appl. Phycol.* **1996**, *8*, 5.
- [70] M. Rimboud, D. Pocaznoi, B. Erable, A. Bergel, *Phys. Chem. Chem. Phys.* **2014**, *16*, 16349.



# ADVANCED ENERGY MATERIALS

## Supporting Information

for *Adv. Energy Mater.*, DOI: 10.1002/aenm.201501100

Photoelectrochemical Wiring of *Paulschulzia pseudovolvox*  
(Algae) to Osmium Polymer Modified Electrodes for  
Harnessing Solar Energy

*Kamrul Hasan, \* Emre Çevik, Eva Sperling, Michael A. Packer,  
Dónal Leech, and Lo Gorton\**





# Photo-electrochemical wiring of *Paulschulzia pseudovolvox* (algae) to osmium polymer modified electrodes for harnessing solar energy

Kamrul Hasan<sup>\*a</sup>, Emre Çevik<sup>b</sup>, Eva Sperling<sup>a</sup>, Michael A. Packer<sup>c</sup>, Dónal Leech<sup>d</sup>, Lo Gorton<sup>\*a</sup>

<sup>a</sup> Department of Analytical Chemistry/Biochemistry and Structural Biology, Lund University, P.O. Box 124, SE-22100 Lund, Sweden.

<sup>b</sup> Department of Genetics and bioengineering, Faculty of Engineering, Fatih University, B. Cekmece, Istanbul 34500, Turkey.

<sup>c</sup> Cawthron Institute, Private Bag 2, Nelson, New Zealand.

<sup>d</sup> School of Chemistry, National University of Ireland Galway, University Road, Galway, Ireland.

Corresponding author:

Kamrul.Hasan@biochemistry.lu.se

Lo.Gorton@biochemistry.lu.se

## Experimental

### Chemicals

Diuron [(1,1-dimethyl, 3-(3', 4'-dichlorophenyl) urea)], paraquat, superoxide dismutase, sodium phosphate dibasic, and sodium phosphate monobasic, magnesium chloride, sodium chloride, potassium hexacyanoferrate (III) and *p*-benzoquinone were purchased from either Sigma-Aldrich (Munich, Germany) or Merck (Darmstadt, Germany) and were of either research or analytical grade. All aqueous solutions were prepared by using water purified and deionized (18 MΩ) with a Mili-Q system (Millipore, Bedford, MA, USA).

### Chlorophyll extraction

The photosynthetic pigments, i.e., chlorophyll was isolated according to previously published method<sup>1</sup>. The *P. pseudovolvox* cells were centrifuged at 4000 rpm 5 min and 5 mL of acetone: methanol (7:2) was added to the pellet. Then the mixture was incubated at room temperature over night under slow shaking. The spectrum of supernatant was determined with an orbital spectrophotometer.

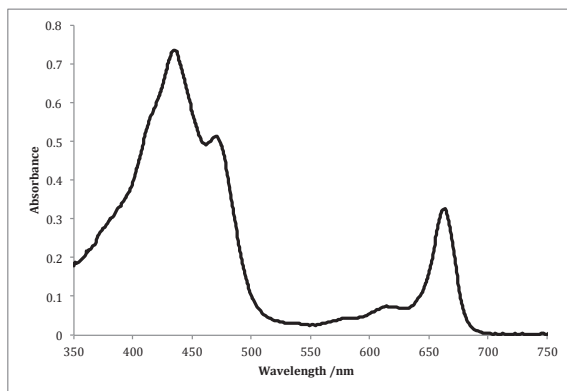


Fig. S1 The absorbance measurements of photosynthetic pigments extracted from *P. pseudovolvox*. The most essential pigments, i.e., chlorophyll a and secondary pigments, i.e., chlorophyll b is appeared in their particular wavelength at 665 nm and ≈400 nm.

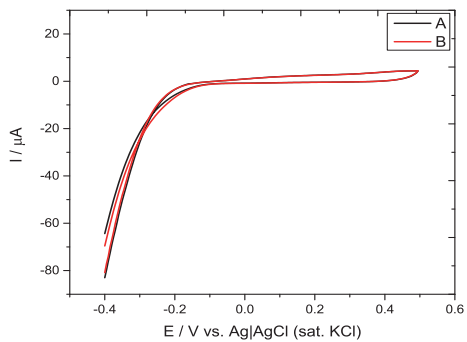


Fig. S2 The CVs of bare-graphite electrode in the absence (black line A) and presence illumination (red line B). Light intensity:  $44 \text{ mW cm}^{-2}$ . Electrolyte: 10 mM phosphate buffer, 10 mM NaCl, 5 mM  $\text{MgCl}_2$  at pH 7.0, scan rate:  $0.01 \text{ VS}^{-1}$ .

Reference:

1. P. Weaver, J. Wall and H. Gest, *Arch. Microbiol.*, 1975, **105**, 207.

# Paper IX



# Comparison of photocurrent generation by cyanobacteria and algae to harness sunlight

Kamrul Hasan<sup>1\*</sup>, Valentina Grippo<sup>1</sup>, Eva Sperling<sup>1</sup>, Michael A. Packer<sup>2</sup>, Dónal Leech<sup>3</sup>, Lo Gorton<sup>1\*</sup>

<sup>1</sup>Department of Analytical Chemistry/Biochemistry and Structural Biology, Lund University, P.O. Box 124, SE-221 00 Lund, Sweden

<sup>2</sup>Cawthron Institute, Private Bag 2, Nelson, New Zealand

<sup>3</sup>School of Chemistry & Ryan Institute, National University of Ireland Galway, University Road, Galway, Ireland

\*Corresponding author:

E-mail: Lo.Gorton@biochemistry.lu.se, Kamrul.Hasan@biochemistry.lu.se

Supplementary information available

## Abstract

Biological photovoltaics (BPVs) are emerging as a potential sustainable energy generating technology to convert solar energy into electrical energy. Although a great variety of photosynthetic biomaterials were studied in BPVs, however, cyanobacteria are possibly considered as a superior candidate because of their simpler physiology. To facilitate the extracellular electron transfer (EET) from cyanobacteria to electrodes is the greatest challenge to be able to improve the performance of BPVs. However, a systematic study comparing the photo-excited EET from these organisms is not reported on yet. Here we report on a comparison of photocurrent density generated by benthic cyanobacteria, i.e., *Leptolyngbya* sp. (CYN65) (CYN82), *Chroococcales* sp. (CYN67) and a eukaryotic alga, i.e., *Paulschulzia pseudovolvox* (UKE). CYN65, CYN82 and UKE are from New Zealand and CYN67 are from Antarctica. We demonstrate the EET mediated by three different electron transfer (ET) mediating systems on graphite electrodes. These are as follows (I) [Os(2,2'-(bipyridine)<sub>2</sub>(polyvinylimidazole)<sub>10</sub>Cl]<sup>+2+</sup> (1:9) [Os-(bpy)PVI] (II) p-benzoquinone (PBQ) (III) [Os-(bpy)PVI] together with PBQ. The maximum photocurrent density of 47.17  $\mu\text{A cm}^{-2}$  is obtained from CYN67 mediated by [Os-(bpy)PVI] together with PBQ.

## Introduction

The global energy demand is increasing regularly due to the increased population growth and economic development. The primary energy resources are depleting and their combustion detrimentally contributes to the global climate change. The supply of a cost-effective sustainable eco-friendly energy generation is one of the greatest challenges in the 21<sup>st</sup> century<sup>1</sup>. Solar energy is the most abundant and the most exploitable sustainable energy resource among others. However, the technology available to convert solar energy into electrical power denoted photovoltaics are highly expensive and their efficiency is limited due to the inherent chemical structure and composition of these materials<sup>2</sup>. Biological photovoltaics (BPVs)<sup>3</sup>, also referred to as photosynthetic microbial fuel cells (PMFC)<sup>4</sup>, are recently emerging as an energy generating technology, where photosynthetic biomaterials are used to convert solar energy into electrical energy. In a typical ordinary microbial fuel cell (MFC) inorganic compounds or organic carbons acting as electrons donors are a prerequisite for function, whereas in BPVs photosynthetic organisms can use water as the sole electron donor<sup>3</sup>.

Photosynthetic materials in BPVs are inexpensive, easy to maintain and their stored respiratory metabolites could be used to generate power around the clock<sup>4a</sup>. The quantum efficiency of charge separation in photosynthesis is nearly 100%, whereas the internal quantum efficiency of silicon based photovoltaics is around 34%. Photosynthetic organisms in BPVs can reduce atmospheric CO<sub>2</sub> during the light independent reaction that is yet to be achieved by any of the non-biological photovoltaics designed so far. These facts give BPVs a greater promise over conventional photovoltaics<sup>2,5</sup>.

In BPVs electrons are generated from the oxidation of water by photosynthetic materials. A great variety of photosynthetic materials, e.g., isolated photosynthetic membranes<sup>6</sup>(thylakoid membranes), photosystems<sup>7</sup>, and chloroplasts<sup>8</sup> have been investigated in BPVs. The sub-cellular materials can efficiently transfer electrons to electrodes in BPVs. However, they require long extraction and purification processes and are incapable to self-sustainment for a long period<sup>5</sup>. Instead intact photosynthetic organisms are self-sustainable and can self-repair in diverse environmental conditions<sup>3</sup>. Therefore, a diverse range of photosynthetic organisms are exploited in BPVs<sup>9</sup> including purple bacteria<sup>10</sup>, prokaryotic cyanobacteria<sup>11</sup>, and eukaryotic algae<sup>12</sup>. Purple bacteria are less preferable in BPVs, since they require providing with organic substrates as electron donors<sup>3</sup>.

Cyanobacteria and algae are desirable candidates in BPVs, since they can oxidize water as the sole electron donor. Although these organisms appeared on earth a time long ago, however, they are not adapted for EET to electrodes in BPVs<sup>2</sup>. Algae are eukaryotic organisms, where photosynthesis occurs in an isolated

organelle, chloroplast that is insulated by thick membranes. Thus delivering photoenergized electrons from algae to electrodes is presumably difficult<sup>13</sup>.

Instead cyanobacteria are prokaryotic organisms and their physiology is simpler and requires low energy compared to algae. In cyanobacteria photosynthesis occurs in thylakoid membranes (TMs) located inside the cellular membrane system. The photosynthetic electron transfer chain (PETC) and respiratory electron transfer chain (RETC) in cyanobacteria can communicate through soluble charge carriers that can diffuse between and coexist in the TMs and the cytoplasmic membranes<sup>14</sup>. This unique characteristic gives them the possibility to handle excess electrons<sup>15</sup> and results in their ability to survive in almost all environments on earth<sup>16</sup>. Thus cyanobacteria are considered as a superior photosynthetic candidate in BPVs<sup>5</sup>. However, the EET from cyanobacteria to electrodes is the greatest challenge<sup>16</sup> to improve the performance of BPVs.

Most of the studies of BPVs were conducted on planktonic cyanobacterial species<sup>3</sup> including *Synechocystis* sp.<sup>11, 17</sup>, *Spirulina* sp.<sup>18</sup>, and *Anabena* sp.<sup>19</sup>. Benthic organisms, however, are assumed to be more electrogenic than planktonic species<sup>20</sup>, since they can inherently interact with a surface. Nevertheless, a systematic study comparing photo-excited EET from benthic cyanobacteria and algae is yet to be reported.

Here we report on a comparison of photocurrent density generated by benthic cyanobacteria and alga from New Zealand and Antarctica. The investigated prokaryotic cyanobacterial species are two different *Leptolyngbya* sp. denoted CYN65 and CYN82, one *Chroococcales* sp. denoted CYN67 and one eukaryotic alga, *Paulschulzia pseudovolvox* denoted UKE. Both CYN65 and CYN82 are under the same genera, however, CYN65 is from Antarctica and CYN82 is from New Zealand. We have demonstrated the photo-excited EET from these organisms mediated by three different of ET-mediating systems on graphite electrodes. These are (I) [Os(2,2'-(bipyridine)<sub>2</sub>(polyvinylimidazole)<sub>10</sub>Cl]<sup>+2+</sup> (1:9) (formal potential, E<sup>0'</sup>= 0.22 V [Os-(bpy)PVI]<sup>21</sup>, (II) *p*-benzoquinone (PBQ, E<sup>0'</sup>= 0.081 V), and (III) [Os-(bpy)PVI] together with PBQ. All potential values reported here are versus the Ag|AgCl (sat. KCl) as reference electrode. All reported data documented are based on three experimental replica (n = 3) and all measurements were conducted at room temperature (20 ±2 °C).

## Results and discussion

The photosynthetic viability of CYN65, CYN67, CYN82 and UKE are determined by measuring the absorption spectra of the photosynthetic pigments extracted from these cells<sup>22</sup> (Figure S1. Supplementary information).



The direct electron transfer (DET) from microorganisms to electrode is preferable, since it allows a high coulombic efficiency, minimizes the overpotential losses and simplifies the design and operation of the bioelectrochemical cell<sup>23</sup>. However, the electrical power output generated from a purely DET based system is relatively low compared to a mediated electron transfer (MET) based system<sup>24</sup>. The DET-based photocurrent densities reported for *Leptolyngbya* sp.<sup>25</sup> and *Paulschulzia pseudovolvox*<sup>26</sup> were 1.30  $\mu\text{A cm}^{-2}$  and 0.02  $\mu\text{A cm}^{-2}$ , respectively. The enhanced DET-based photocurrent density of 3.0  $\mu\text{A cm}^{-2}$  was obtained for *Synechocystis* PCC-6803 on carbon paint<sup>27</sup>. Moreover the photocurrent was further improved to 9.3  $\mu\text{A cm}^{-2}$  via *Synechococcus* sp. on surface modified highly conductive electrode materials<sup>4b</sup>.

To obtain more improved photocurrent densities we have investigated different ET-mediating systems including I, II, and III. Osmium redox polymers have already been successfully used in different BESs for their efficient surface confined polymeric ET properties and their documented ability to “wire”, i.e., facilitate electrochemical communication, between both many redox enzyme and viable bacterial cells and electrodes. In addition osmium redox polymers are known to work as a immobilization matrix for biomaterials on electrode surface<sup>28</sup>. Cyclic voltammetry (CVs) and chronoamperometry (CA) were executed to record the photocurrent. The electrochemical “wiring” of *Leptolyngbya* sp.<sup>25</sup> and *Paulschulzia pseudovolvox*<sup>26</sup> on [Os-(bpy)PVI] modified graphite electrodes was reported earlier. An aliquot of 5  $\mu\text{L}$  of a [Os-(bpy)PVI] solution was drop coated on a graphite electrode to give a polymer modified electrode. CYN67 (3 mg, wet weight) was immobilized on the surface of the modified electrode surface. In the presence of CYN67, the  $E^{0'}$  of [Os-(bpy)PVI] shifted from 0.22 V to 0.25 V (Fig. 1 A). It was anticipated since the large amount of intact organisms restrict the ET between the [Os-(bpy)PVI] and the electrode. In the presence of illumination the anodic peak current increases slightly (Fig. 1 B).

These results suggest that [Os-(bpy)PVI] can communicate with the PETC of CYN67 and extract electrons from photolysis of water. Previously a similar redox polymer was used for the photoelectrochemical communication of isolated photosystem II<sup>7c</sup> and TMs from spinach<sup>29</sup>. In earlier work Os based polymers were shown to somehow reach the cytosolic membrane of both gram (-) and (+) bacterial cells and extract electrons from trans-membranes proteins<sup>26, 30</sup>. In control experiments [Os-(bpy)PVI] modified electrodes in the absence of CYN67 does not show any detectable photocurrent during illumination indicating the biological source of current (Fig. 2 A).

Previously a lipid soluble ET-mediator such as PBQ was used for its greater accessibility through the complex membrane systems including outer and inner cell membranes<sup>3,31</sup>. CYN67 cells were immobilized on a bare-graphite electrode and 0.5 mM PBQ was dissolved in the electrolyte. Like [Os-(bpy)PVI] the  $E^{0'}$  of PBQ is also shifted towards a more positive voltage from 0.081 V to 0.11 V. It is ascribed to the large amount of cyanobacteria on the electrode constrained ET between PBQ and electrode (Fig. 1C). A shift of  $E^{0'}$  towards positive direction indicates either pH change or the reduced form experience difficulties to be oxidized since the interaction of reduced form with biomaterials is stronger than that of oxidized form. In the presence of illumination the anodic peak current increases notably and concomitantly the cathodic peak current decreases (Fig. 1C). This result suggests that PBQ can efficiently communicate with the cells and accept electrons possibly through its documented ability to diffuse through the outer and inner membranes onto the TMs, which in turn is exhibited in an enhanced photo-induced EET from CYN67. PBQ resembles structurally the naturally occurring plastoquinone (PQ) molecules, shared in both PETC and RETC<sup>14</sup> and can thus be considered an efficient electron acceptor. PBQ was shown to extract a large portion of the electrons from photolysis of water mediated by *Synechococcus* sp.<sup>32</sup>. In control experiments PBQ in the absence of CYN67 does not show any noticeable effect of illumination (Fig. 2) in close agreement with our previous observation<sup>26</sup>.

It seems essential to combine both a lipid soluble ET mediator (PBQ) and a non-lipid polymeric ET mediator ([Os-(bpy)PVI]) to investigate whether both mediators together could have a substantial beneficial effect on photo-excited EET. The redox waves of PBQ appeared centered at 0.01 V and those of [Os-(bpy)PVI] around 0.25 V. The positive shifts in  $E^{0'}$  values of both mediators are due to the specific interactions of these mediators with the microenvironment at the electrode surface (Fig. 1E). In the presence of illumination the anodic peak currents of both mediators increase and concurrently the cathodic ones decrease (Fig. 1F). The increase in anodic peak currents is noticeably greater compared to the situation when these mediators are used separately (Figs. 1B and 1D). These photocurrent responses are exciting and it can be proposed that both mediators used together could have some sorts of collective effect on the photo-excited EET from cyanobacteria. A similar response was observed with *Saccharomyces cerevisiae* when menadione (vitamin K<sub>3</sub>) was used as a lipid soluble mediator in combination with an osmium based polymer similar to the one used in this investigation<sup>33</sup>.

The results exhibited in Fig. 1 indicate that both [Os-(bpy)PVI] and PBQ can extract electrons from photolysis of water performed by CYN67. However, to evaluate the quantitative performance of these mediators on the photocurrent generation chronoamperometry (CA) is a better choice. Thus CAs were recorded

for graphite electrodes modified with different ET-mediating systems in the absence and presence of CYN67. The applied potential ( $E_{app}$ ) was higher than the  $E^{0'}$  of the used mediators to remove any influence of the kinetics of the reoxidation of the reduced form of the mediator on the photocurrent response and it was set to 0.40 V. To obtain a stable baseline before illumination of the electrode surfaces, the system was kept in 'light off conditions' for  $\approx 1000$  s followed by 'light on' and 'light off' each for 300 s and three identical subsequent cycles were recorded.

The results showed that all the ET-mediating systems in the absence of CYN67 cells will not yield any photocurrent when illuminated (Figs. 2A, 2C, 2E). In the presence of CYN67 cells, system I reveals a very small photocurrent density on illumination, i.e.,  $1.76 \mu\text{A cm}^{-2}$  (Fig. 2B). In comparison the photocurrent densities recorded system II and III were  $31.34 \mu\text{A cm}^{-2}$  and  $41.17 \mu\text{A cm}^{-2}$ , respectively, i.e., a difference in around  $10 \mu\text{A cm}^{-2}$ , a value which in turn should be compared with that obtained for system I. The high value of standard deviation on photocurrent density is the result of the difficulties in the reproducibility in electrode preparation and illumination. The gradual deterioration of the photocurrent density (Figs. 2D and 2F) is a common observation in these kinds of studies<sup>6a, 11</sup> and attributed to photoinhibition<sup>34</sup> of primarily photosystem II caused by the formation of reactive oxygen species. What is also noteworthy is that the registered high background current density shown in Figs. 2D and 2F could be attributed to respiration of the carbohydrate reservoir such as glycogen<sup>35</sup>. A comparison of the photocurrent density obtained from CYN67 with the three different ET-mediating systems are presented in Fig. 3 and also summarized in Table 1.

To compare the different electrogenic activities of CYN65, CYN67, CYN82 and UKE we studied the results that were obtained using the three ET-mediating systems I, II, III with all the four different photosynthetic cells. Optimized amounts of the respective cells were immobilized on graphite electrodes and CA experiments identical to those shown in Fig. 2 were performed. A comparison of the photocurrent densities obtained with these cells using the three different ET-mediating systems is presented in Fig. 3. As shown the photocurrent densities obtained for the three prokaryotic CYN65, CYN67, CYN82 are higher than obtained of UKE when using ET-mediating systems II and III but not for system I (Os polymer alone). Previously cyanobacteria was shown for greater electrogenic activity compared to algae in a mediator-less BPVs<sup>4b</sup>.

The greater photocurrent density generated by CYN65, CYN67 and CYN82 could be attributed to the site of photosynthetic apparatus inside the cells. In cyanobacterial photosynthesis occurs in the TMs inside the membrane and the EET is simpler. Instead in algae photosynthesis takes place in a separate sub-

cellular organelle, the chloroplast, that is surrounded by a complex cellular exterior. The EET from chloroplasts is restricted due to its insulated multi cell wall lipid composition. A maximum photocurrent density of  $47.17 \mu\text{A cm}^{-2}$  is documented with *Chroococcales* sp. (CYN67) mediated by [Os-(bpy)PVI] in combination with PBQ and presented in Fig. 2. Although CYN65 and CYN82 belong to the same cyanobacterial genera (*Leptolyngbya*), however, the photocurrent generation from these two organisms varied in different ET-mediating systems. The most probable reason could be their physiological changes developed in Antarctica and New Zealand, the two dissimilar places. A deep understanding of CYN67 is required to explain their outperformance on photocurrent density. The physiological properties and benthic characteristics of CYN67 could be of interest for further investigation.

## Conclusion

Here we demonstrate that cyanobacteria act as a superior photosynthetic candidate in BPVs compared with a eukaryotic counterpart, algae. A double ET-mediating system composed of a lipid soluble mediator, PBQ and a non-lipid soluble mediator,  $[\text{Os}(2,2'-(\text{bipyridine})_2(\text{polyvinylimidazole})_{10}\text{Cl}]^{+2+}$  is shown for enhanced photo-excited EET. Although lipophilic artificial mediators are suspected to be toxic in BPVs<sup>31</sup>, however, a system based on vitamin K3 mediated photocurrent generation from cyanobacteria did not reveal any toxicity caused by this mediator. Instead the current generation from the photosynthetic and respiratory ET-chains from cyanobacteria was considered as an energetic burden<sup>35</sup>. A detailed understanding of the photosynthetic and respiratory ET-mechanisms in cyanobacterial is required to improve their electrogenic activity and to develop new-engineered strains for superior EET. These findings could have significant implications in photosynthetic energy conversion and photofuel production.

## Acknowledgements

The authors thank The Swedish Research Council (projects: 2010-2013, 2010-5031, 2014-5908), The European Commission (Erasmus Mundus, EMIY Action II program and “BIOENERGY” FP7-PEOPLE-2013-ITN-607793), The Science Foundation Ireland (Charles Parsons Energy Research Award) and New Zealand Ministry of Innovation, Business and Enterprise (PROJ-13838-NMTS-LVL) for financial support. We thank Dr. Domhnall MacAodha and Dr. Peter ÓConghaile (NUI, Galway) for synthesis of the Os-polymers.

## References

1. O. Kruse, J. Rupprecht, J. H. Mussgnug, G. C. Dismukes and B. Hankamer, *Photochemical and Photobiological Sciences*, 2005, **4**, 957.
2. N. Sekar and R. P. Ramasamy, *Electrochemical Society Interface*, 2015, **24**, 67.
3. A. J. McCormick, P. Bombelli, R. W. Bradley, R. Thorne, T. Wenzel and C. J. Howe, *Energy & Environmental Science*, 2015, **8**, 1092.
4. (a) M. Rosenbaum, Z. He and L. T. Angenent, *Current Opinion in Biotechnology*, 2010, **21**, 259; (b) A. J. McCormick, P. Bombelli, A. M. Scott, A. J. Philips, A. G. Smith, A. C. Fisher and C. J. Howe, *Energy & Environmental Science*, 2011, **4**, 4699.
5. N. Sekar and R. P. Ramasamy, *Journal of Photochemistry and Photobiology C: Photochemistry Reviews*, 2015, **22**, 19.
6. (a) J. O. Calkins, Y. Umasankar, H. O'Neill and R. P. Ramasamy, *Energy & Environmental Science*, 2013, **6**, 1891; (b) R. Carpentier, S. Lemieux, M. Mimeault, M. Purcell and D. C. Goetze, *Bioelectrochemistry and Bioenergetics*, 1989, **22**, 391; (c) M. Rasmussen and S. D. Minteer, *Electrochimica Acta*, 2013, **126**, 68; (d) K. B. Lam, E. F. Irwin, K. E. Healy and L. Lin, *Sensors and Actuators, B: Chemical*, 2006, **117**, 480.
7. (a) O. Yehezkeili, R. Tel-Vered, J. Wasserman, A. Trifonov, D. Michaeli, R. Nechushtai and I. Willner, *Nature Communications*, 2012, **3**, 742; (b) A. Mershin, K. Matsumoto, L. Kaiser, D. Yu, M. Vaughn, M. K. Nazeeruddin, B. D. Bruce, M. Graetzel and S. Zhang, *Scientific Reports*, 2012, **2**, DOI: 10.1038/srep00234; (c) A. Badura, D. Guschin, B. Esper, T. Kothe, S. Neugebauer, W. Schuhmann and M. Rögner, *Electroanalysis*, 2008, **20**, 1043.
8. E. Greenbaum, *Journal of Physical Chemistry*, 1990, **94**, 6151.
9. C. F. Meunier, J. C. Rooke, A. Léonard, H. Xie and B. L. Su, *Chemical Communications*, 2010, **46**, 3843.
10. K. Hasan, K. V. R. Reddy, V. Eßmann, K. Górecki, P. Ó. Conghaile, W. Schuhmann, D. Leech, C. Hägerhäll and L. Gorton, *Electroanalysis*, 2015, **27**, 118.
11. J. M. Pisciotta, Y. Zou and I. V. Baskakov, *PLoS ONE*, 2010, **5**, e10821.
12. Y. Yuan, Q. Chen, S. Zhou, L. Zhuang and P. Hu, *Journal of Hazardous Materials*, 2011, **187**, 591.
13. V. Luimstra, S.-J. Kennedy, J. Güttler, S. Wood, D. Williams and M. Packer, *Journal of Applied Phycology*, 2014, **26**, 15.
14. W. F. J. Vermaas, in *eLS*, John Wiley & Sons Ltd., Chichester, 2001.
15. J. M. Pisciotta, Y. Zou and I. V. Baskakov, *Applied Microbiology and Biotechnology*, 2011, **91**, 377.
16. D. J. Lea-Smith, P. Bombelli, R. Vasudevan and C. J. Howe, *Biochimica et Biophysica Acta (BBA)-Bioenergetics*, <http://dx.doi.org/10.1016/j.bbabi.2015.10.007>.

17. T. Yagishita, T. Horigome and K. Tanaka, *Journal of Chemical Technology & Biotechnology*, 1993, **56**, 393.
18. C.-C. Fu, T.-C. Hung, W.-T. Wu, T.-C. Wen and C.-H. Su, *Biochemical Engineering Journal*, 2010, **52**, 175.
19. K. Tanaka, R. Tamamushi and T. Ogawa, *Journal of Chemical Technology and Biotechnology*, 1985, **35**, 191.
20. D. Esson, S. A. Wood and M. A. Packer, *AMB express*, 2011, **1**, 19.
21. E. M. Kober, J. V. Caspar, B. P. Sullivan and T. J. Meyer, *Inorganic Chemistry*, 1988, **27**, 4587.
22. R. J. Porra, in *Discoveries in Photosynthesis*, Springer, Dordrecht, 2005, pp. 633-640.
23. B. E. Logan, B. Hamelers, R. Rozendal, U. Schröder, J. Keller, S. Freguia, P. Aelterman, W. Verstraete and K. Rabaey, *Environmental Science & Technology*, 2006, **40**, 5181.
24. U. Schröder, *Physical Chemistry Chemical Physics*, 2007, **9**, 2619.
25. K. Hasan, H. B. Yildiz, E. Sperling, P. Ó. Conghaile, M. A. Packer, D. Leech, C. Hägerhäll and L. Gorton, *Physical Chemistry Chemical Physics*, 2014, **16**, 24676.
26. K. Hasan, E. Çevik, E. Sperling, M. A. Packer, D. Leech and L. Gorton, *Advanced Energy Materials*, 2015, DOI: 10.1002/aenm.201501100.
27. Y. Zou, J. Pisciotta, R. B. Billmyre and I. V. Baskakov, *Biotechnology and Bioengineering*, 2009, **104**, 939.
28. (a) K. Hasan, S. A. Patil, D. Leech, C. Hägerhäll and L. Gorton, *Biochemical Society Transactions*, 2012, **40**, 1330; (b) A. Heller, *Current Opinion in Chemical Biology*, 2006, **10**, 664.
29. H. Hamidi, K. Hasan, S. C. Emek, Y. Dilgin, H.-E. Åkerlund, P.-Å. Albertsson, D. Leech and L. Gorton, *ChemSusChem*, 2015, **8**, 990.
30. V. Coman, T. Gustavsson, A. Finkelsteinas, C. Von Wachenfeldt, C. Hägerhäll and L. Gorton, *Journal of the American Chemical Society*, 2009, **131**, 16171.
31. R. W. Bradley, P. Bombelli, S. J. L. Rowden and C. J. Howe, *Biochemical Society Transactions*, 2012, **40**, 1302.
32. M. Torimura, A. Miki, A. Wadano, K. Kano and T. Ikeda, *Journal of Electroanalytical Chemistry*, 2001, **496**, 21.
33. A. Heiskanen, V. Coman, N. Kostesha, D. Sabourin, N. Haslett, K. Baronian, L. Gorton, M. Dufva and J. Emnéus, *Analytical and Bioanalytical Chemistry*, 2013, **405**, 3847.
34. T. Roach and A. K. Krieger-Liszkay, *Current Protein & Peptide Science*, 2014, **15**, 351.
35. X. H. Xie, E. L. Li and Z. Kang Tang, *Journal of Chemical Technology and Biotechnology*, 2011, **86**, 109.

### Table and legend

Table 1. A comparison of photocurrent density generated by CYN65, CYN67, CYN82, and UKE using the three different ET- mediating systems, (I) [Os(2,2'-(bipyridine)<sub>2</sub>(polyvinylimidazole)<sub>10</sub>Cl]<sup>+1/2+</sup> (1:9) (formal potential, E<sup>0</sup>'= 0.22 V [Os-(bpy)PVI], (II) p-benzoquinone (PBQ, E<sup>0</sup>'= 0.081 V), and (III) [Os-(bpy)PVI] together with PBQ. 5  $\mu$ L of an [Os(2,2'-(bipyridine)<sub>2</sub>(polyvinylimidazole)<sub>10</sub>Cl]<sup>+1/2+</sup> (1:9) was drop coated on the electrode surface and 0.5 mM of PBQ was dissolved in the electrolyte. An adjusted amount of CYN65 (1.2 mg) and CYN67 (3 mg), CYN82 (9.5  $\mu$ g) and UKE (4  $\mu$ L, 1 g mL<sup>-1</sup>), respectively, was immobilized on the graphite electrode surface. Data were collected from Fig. 2 and identical CA experiments performed for CYN65, CYN82 and UKE. Applied potential: 0.40 V vs. Ag|AgCl (sat. KCl), light intensity: 40 mW cm<sup>-2</sup>, Electrolyte: 10 mM phosphate buffer at pH 7.0 including 10 mM NaCl and 5 mM MgCl<sub>2</sub>. Data reported here are based on three independent experimental replica (n = 3).

Cyanobacteria / Alga →	CYN65		CYN67		CYN82		UKE	
	J/ $\mu$ A cm <sup>-2</sup>	STDE V	J/ $\mu$ A cm <sup>-2</sup>	STDE V	J/ $\mu$ A cm <sup>-2</sup>	STDE V	J/ $\mu$ A cm <sup>-2</sup>	STDEV
[Os-(bpy)PVI]	0.64	0.39	1.76	0.09	0.38	0.06	1.54	0.44
PBQ	18.00	4.97	31.45	9.65	29.48	2.67	9.92	5.58
[Os(bpy)PVI] +PBQ	24.02	2.50	47.17	13.33	22.87	3.06	5.76	1.05

STDEV stands for standard deviation

## Figures legends

**Figure 1.** CVs of *Chroococcales* sp. (CYN67) (3 mg, wet weight) on graphite electrode modified with different ET-mediating system (I) [Os-(bpy)PVI], (II) 0.5 mM PBQ, (III) [Os-(bpy)PVI] in combination with 0.5 mM PBQ. A 5  $\mu$ L of [Os(2,2'-(bipyridine)<sub>2</sub>(polyvinylimidazole)<sub>10</sub>Cl)]<sup>+1/2+</sup> (1:9) was drop coated on electrode surface and 0.5 mM PBQ was dissolved in the electrolyte. Light intensity: 40 mW cm<sup>-2</sup>, Electrolyte: 10 mM phosphate buffer at pH 7.0 including 10 mM NaCl and 5 mM MgCl<sub>2</sub>, scan rate: 10 mVs<sup>-1</sup>.

**Figure 2.** The CAs of graphite electrode modified with different ET-mediating system in the absence and presence of *Chroococcales* sp. (CYN67) (3 mg, wet weight) (A) [Os-(bpy)PVI] modified graphite electrode without CYN67 (B) [Os-(bpy)PVI] modified graphite electrode with CYN67 (C) PBQ with CYN67 (D) PBQ without CYN67 (E) [Os-(bpy)PVI] modified graphite electrode in addition with 0.5 mM PBQ dissolved in the electrolyte without CYN67 (F) [Os-(bpy)PVI] modified graphite electrode in addition with 0.5 mM PBQ dissolved in the electrolyte with CYN67. Red and black arrows indicate 'light on' and 'light off' condition. Applied potential: 0.40 V vs. Ag|AgCl (sat. KCl), light intensity: 40 mW cm<sup>-2</sup>, Electrolyte: 10 mM phosphate buffer at pH 7.0 including 10 mM NaCl and 5 mM MgCl<sub>2</sub>.

**Figure 3.** The comparison of photocurrent density generated by CYN65, CYN67, CYN82, and UKE at different ET-mediating systems, e.g., (I) [Os-(bpy)PVI] (II) PBQ (III) [Os-(bpy)PVI] together with PBQ. 5  $\mu$ L of [Os-(bpy)PVI] was drop coated on electrode and 0.5 mM of PBQ was dissolved in electrolyte. The adjusted amount of CYN65 (1.2 mg) and CYN67 (3 mg), CYN82 (9.5  $\mu$ g) and UKE (4  $\mu$ L, 1 g mL<sup>-1</sup>) were immobilized on graphite electrode surface. Data were collected from Fig. 2 and identical CA experiments performed on CYN65, CYN82 and UKE. Applied potential: 0.40 V vs. Ag|AgCl (sat. KCl), light intensity: 40 mW cm<sup>-2</sup>, Electrolyte: 10 mM phosphate buffer at pH 7.0 including 10 mM NaCl and 5 mM MgCl<sub>2</sub>. Data reported here are based on three independent experimental replica (n = 3).



Figure 1

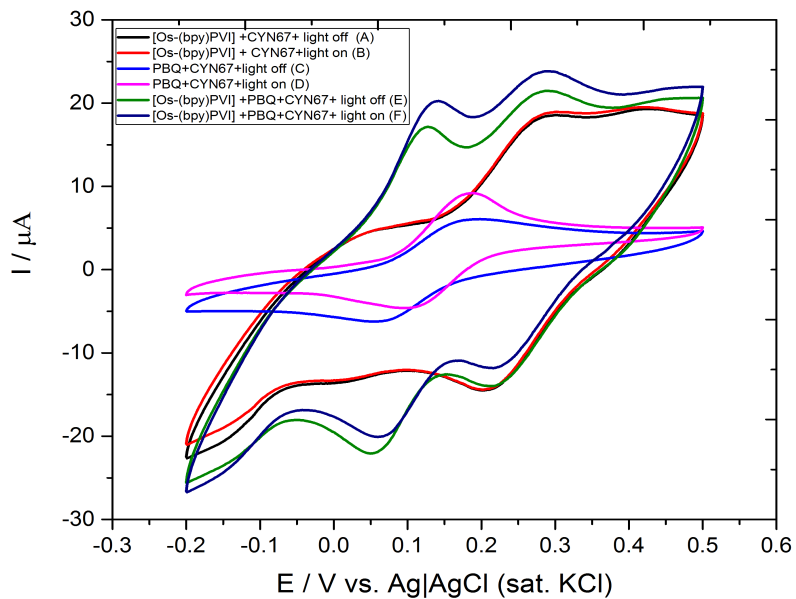


Figure 2

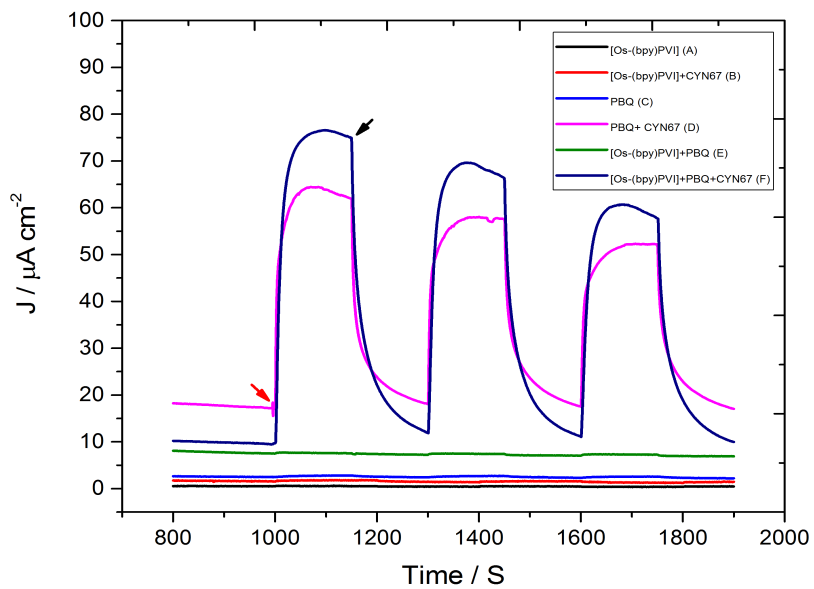
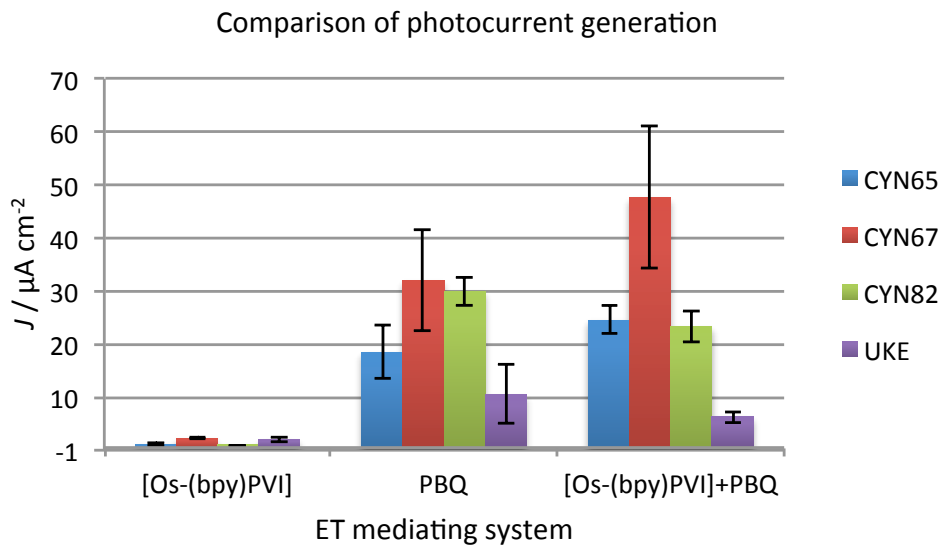


Figure 3



## Chemicals

Acetone, diuron [1,1-dimethyl, 3-(3'4'-dichlorophenyl)-urea], ethanol, magnesium chloride, methanol, *p*-benzoquinone (PBQ), sodium chloride, sodium phosphate monobasic, sodium phosphate dibasic were bought from either Sigma-Aldrich (Munich, Germany) and or Merck (Darmstadt, Germany). These chemicals were of either analytical or research grade. Aqueous solutions were prepared by using water purified and deionized (18 M $\Omega$ ) with a Milli-Q system (Millipore, Bedford, MA; USA). The synthesis and preparation of [Os(2,2'-(bipyridine)<sub>2</sub>(polyvinylimidazole)<sub>10</sub>Cl]<sup>+2+</sup> (1:9) ( $E^0 = 0.22$  V vs. Ag|AgCl (sat. KCl) [Os-(bpy)PVI] was reported earlier<sup>1</sup>. The [Os-(bpy)PVI] was dissolved in Milli-Q water at a concentration of 10 mg mL<sup>-1</sup>.

## Maintenance of the growth culture of cyanobacteria and alga and preparation of their inocula

The benthic cyanobacteria and algae were collected from Cawthron Institute Collection Culture of Microalgae (CICCM), Nelson, New Zealand. The prokaryotic cyanobacterial species of *Leptolyngbya* sp. was collected from different places, e.g., Antarctica (CYN65) and New Zealand (CYN82). The other cyanobacterial species *Chroococcales* sp. (CYN67) was collected from Antarctica. The eukaryotic alga *Paulschulzia pseudovolvox* (UKE) was collected from an environmental sample from Lake Tikitapu, New Zealand. The growth conditions of CYN65, CYN67, CYN82 and UKE were reported earlier<sup>2</sup>.

In briefly they were grown in a low ionic strength MLA<sup>3</sup> growth medium arranged with a white fluorescent lamp providing a light intensity of 10 Wm<sup>-2</sup> on a 12:12 h light and dark regime. MLA is nutritionally a poor growth medium for heterotrophic organisms and we did not observe any outperforming bacterial biomass. The CYN65, CYN67, CYN82 and UKE were grown in 100 mL clear polystyrene wide mouth bottles (VWR, Stockholm, Sweden) for  $\approx$  three weeks at room temperature (20  $\pm$  2  $^{\circ}$ C).

To harvest CYN65, CYN67, CYN82 and UKE, the cells were transferred to 50 mL Eppendorf-tube and centrifuged at 4000 rpm for 15 min at 20  $^{\circ}$ C and washed with 10 mM phosphate buffer at pH 7.0 including 10 mM NaCl and 5 mM MgCl<sub>2</sub> at pH 7.0 (PBS buffer). Cells were centrifuged again under the same condition. CYN82 and UKE were re-suspended in PBS buffer to adjust the concentration of 1 g mL<sup>-1</sup> (wet weight) and immediately used for the electrochemical experiments. CYN65 and CYN67 cells were densely coagulated together and an analytical scale (ICA AB, Gislaved, Sweden) was used to measure the optimized amount of cells. The adjusted amount of CYN65 and CYN67 and CYN82 immobilized onto the

electrode surface was 1.2 mg, 3 mg and 9.5  $\mu\text{g}$  (wet weight) respectively. The adjusted volume of CYN82 immobilized on the electrode surface was 4  $\mu\text{L}$  ( $1\text{ g mL}^{-1}$ ).

For preparation of the inoculum, a dense clot of CYN65, CYN67, CYN82 and UKE cells were transferred to 60 mL of MLA growth medium contained in 100 mL clear polystyrene wide mouth bottles (VWR, Stockholm, Sweden) closed with cover. A fresh green thick mass of cells appeared in the bottle within 2-3 weeks.

MLA<sup>3</sup> is a complex growth medium comprising  $\text{NaNO}_3$  (2.00 mM),  $\text{NaHCO}_3$  (2.02 mM),  $\text{MgSO}_4 \cdot 7\text{H}_2\text{O}$  (200.43  $\mu\text{M}$ ),  $\text{CaCl}_2 \cdot 2\text{H}_2\text{O}$  (200.00  $\mu\text{M}$ ),  $\text{K}_2\text{HPO}_4$  (199.77  $\mu\text{M}$ ),  $\text{NaEDTA}$  (11.70  $\mu\text{M}$ ),  $\text{H}_2\text{SeO}_3$  (10.00  $\mu\text{M}$ ),  $\text{H}_3\text{BO}_3$  (39.95  $\mu\text{M}$ ),  $\text{MnCl}_2 \cdot 4\text{H}_2\text{O}$  (18.19  $\mu\text{M}$ ),  $\text{FeCl}_3 \cdot 6\text{H}_2\text{O}$  (5.85  $\mu\text{M}$ ),  $\text{CuSO}_4 \cdot 5\text{H}_2\text{O}$  (40.10  $\mu\text{M}$ ),  $\text{ZnSO}_4 \cdot 7\text{H}_2\text{O}$  (76.50  $\mu\text{M}$ ),  $\text{CoCl}_2 \cdot 6\text{H}_2\text{O}$  (79.86  $\mu\text{M}$ ),  $\text{Na}_2\text{MoO}_4 \cdot 2\text{H}_2\text{O}$  (24.80  $\mu\text{M}$ ), biotin (0.05  $\mu\text{g/L}$ ), vitamin B12 (0.05  $\mu\text{g/L}$ ) and thiamine HCl (100.00  $\mu\text{g/L}$ ).

### Working electrode preparation

Spectrographic graphite rods (Alfa Aesar GmbH & Co Kg., Karlsruhe, Germany, AGKSP grade, ultra 'F' purity and 3.05 mm diameter) were used as working electrodes. The end of the graphite rod was polished on the fine emery SiC paper (Turbak Durite, P1200) and cautiously washed with Milli-Q water and allowed to dry at room temperature. The procedure of working electrode preparation was reported previously<sup>4</sup>. For [Os-(bpy)PVI] modified electrode, an aliquot of 5  $\mu\text{L}$  of a solution of [Os-(bpy)PVI] ( $10\text{ mg mL}^{-1}$  in Milli-Q water) was spread onto the active surface ( $A = 0.0731\text{ cm}^2$ ) and allowed to dry for  $\approx 10\text{ min}$ . The optimized amount of CYN65 (1 mg), CYN67 (3 mg), CYN82 (9.5  $\mu\text{g}$ , wet weight) and UKE (4  $\mu\text{L}$ ,  $1\text{ g mL}^{-1}$ ) were immobilized on the electrode surface and allowed to dry for  $\approx 10\text{ min}$ .

### Measurements and instrumentations

The procedure of electrochemical measurements, i.e., cyclic voltammetry (CV) and chronoamperometry (CA) were demonstrated earlier<sup>4,5</sup>. A regular three-electrode arrangement, i.e., Ag|AgCl (sat. KCl) (Sensortechnik, Meinsberg, Germany) as reference electrode, bare graphite or [Os-(bpy)PVI] modified graphite electrode as working electrode and a platinum foil as counter electrode was used.

A fiber optic illuminator FOI-150-220 (150 W and 220 V) with a FOI-5 light guide (Titan Tool Supply Inc., Buffalo, NY, USA) was used to illuminate the working electrode. A light intensity of  $40\text{ mW cm}^{-2}$  was used to excite the photosynthetic activity of the CYN65, CYN67, CYN82 and UKE cells immobilized onto the electrode surface. In all measurements PBS buffer was used as electrolyte. In CV experiments  $10\text{ mV s}^{-1}$  was used if not stated otherwise. In

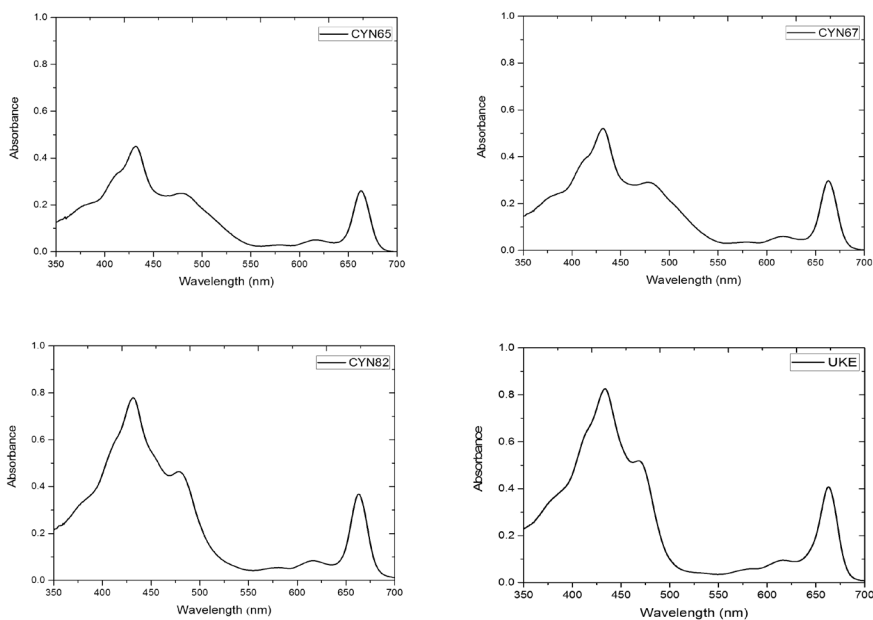
CA experiments the applied potential ( $E_{ap}$ ) was set at 0.4 V, a potential greater than redox potential ( $E^{0'}$ ) of any used electron transfer mediators. All potential values (V) reported here are based on Ag|AgCl (sat. KCl) as reference electrode (0.197 V vs SHE). All experiments were executed at room temperature.

### **Extraction of photosynthetic pigments**

The determination of chlorophyll is important due to their fundamental role in photosynthesis. For chlorophyll extraction<sup>6</sup>, cells including a 5 mL solution of acetone: methanol (8:2) was incubated for 24 h. The greenish supernatants were separated from the pellets by centrifugation at 4000 rpm for 5 min at 20 °C. The absorption spectrum of supernatant was determined with an orbital spectrometer by scanning from 800 nm to 300 nm. The absorption spectra of the photosynthetic pigments extracted from the cells are presented in Fig S1.

## Figure and legend

Fig S1. Absorption spectra of the photosynthetic pigments of CYN65, CYN67, CYN82 and UKE extracted in acetone:methanol (8:2) solvent. The primary pigments, i.e., chlorophyll a appear at their distinguished wavelength at 665 nm and secondary pigments such as chlorophyll b and carotinoids appear at 400 nm to 500 nm.



## References

1. (a) E. M. Kober, J. V. Caspar, B. P. Sullivan and T. J. Meyer, *Inorganic Chemistry*, 1988, **27**, 4587; (b) A. Heller, *Current Opinion in Chemical Biology*, 2006, **10**, 664.
2. V. Luimstra, S.-J. Kennedy, J. Güttler, S. Wood, D. Williams and M. Packer, *Journal of Applied Phycology*, 2014, **26**, 15.
3. C. S. Bolch and S. Blackburn, *Journal of Applied Phycology*, 1996, **8**, 5.
4. K. Hasan, E. Çevik, E. Sperling, M. A. Packer, D. Leech and L. Gorton, *Advanced Energy Materials*, 2015, DOI: 10.1002/aenm.201501100.
5. K. Hasan, H. B. Yildiz, E. Sperling, P. Ó.Conghaile, M. A. Packer, D. Leech, C. Hägerhäll and L. Gorton, *Physical Chemistry Chemical Physics*, 2014, **16**, 24676.
6. R. J. Porra, in *Discoveries in Photosynthesis*, Springer, Dordrecht, 2005, pp. 633-640.



Kamrul Hasan was born in Narsingdi, a northeast district of the capital city of Bangladesh. He received a Bachelor of Science in Biotechnology and Genetic Engineering at Khulna University, Bangladesh. In 2008, Kamrul moved to Sweden for higher education in Biotechnology and in 2010 he received a Master of Science at Lund University.

In 2011 he joined as a PhD student in Professor Lo Gorton's Bioelectrochemistry research group at the Analytical Chemistry Department of the Chemistry Institute at Lund University. His research interest focused on Bioelectrochemical Systems, Microbial Biosensors, Microbial Fuel Cells, and Biological Photovoltaics. The extracellular electron transfer from biomaterials to electrode surfaces is one of the greatest challenges in these systems and this thesis is focused on it.

The global energy consumption is increasing regularly while the primary energy sources, fossil fuels, are decreasing substantially. A secured supply of a cost effective sustainable clean energy production is one of the greatest challenges in the 21st century. The amount of solar energy radiating from the sun to the earth in one hour is greater than the entire annual global energy demand. Biological photovoltaic is emerging as a potential energy generating technology to harness energy. Kamrul is greatly interested in this very exciting research field.

